LEABHARLANN CHOLÁISTE NA TRÍONÓIDE, BAILE ÁTHA CLIATH | TRINITY COLLEGE LIBRARY DUBLIN
Ollscoil Átha Cliath | The University of Dublin

Terms and Conditions of Use of Digitised Theses from Trinity College Library Dublin

Copyright statement

All material supplied by Trinity College Library is protected by copyright (under the Copyright and Related Rights Act, 2000 as amended) and other relevant Intellectual Property Rights. By accessing and using a Digitised Thesis from Trinity College Library you acknowledge that all Intellectual Property Rights in any Works supplied are the sole and exclusive property of the copyright and/or other IPR holder. Specific copyright holders may not be explicitly identified. Use of materials from other sources within a thesis should not be construed as a claim over them.

A non-exclusive, non-transferable licence is hereby granted to those using or reproducing, in whole or in part, the material for valid purposes, providing the copyright owners are acknowledged using the normal conventions. Where specific permission to use material is required, this is identified and such permission must be sought from the copyright holder or agency cited.

Liability statement

By using a Digitised Thesis, I accept that Trinity College Dublin bears no legal responsibility for the accuracy, legality or comprehensiveness of materials contained within the thesis, and that Trinity College Dublin accepts no liability for indirect, consequential, or incidental, damages or losses arising from use of the thesis for whatever reason. Information located in a thesis may be subject to specific use constraints, details of which may not be explicitly described. It is the responsibility of potential and actual users to be aware of such constraints and to abide by them. By making use of material from a digitised thesis, you accept these copyright and disclaimer provisions. Where it is brought to the attention of Trinity College Library that there may be a breach of copyright or other restraint, it is the policy to withdraw or take down access to a thesis while the issue is being resolved.

Access Agreement

By using a Digitised Thesis from Trinity College Library you are bound by the following Terms & Conditions. Please read them carefully.

I have read and I understand the following statement: All material supplied via a Digitised Thesis from Trinity College Library is protected by copyright and other intellectual property rights, and duplication or sale of all or part of any of a thesis is not permitted, except that material may be duplicated by you for your research use or for educational purposes in electronic or print form providing the copyright owners are acknowledged using the normal conventions. You must obtain permission for any other use. Electronic or print copies may not be offered, whether for sale or otherwise to anyone. This copy has been supplied on the understanding that it is copyright material and that no quotation from the thesis may be published without proper acknowledgement.

The Design, Synthesis and Biological Evaluation of Novel Barbiturate-based MMP inhibitors.

Jun Wang M.Sc.

A thesis presented to the University of Dublin for the degree of Doctor of Philosophy
in Pharmaceutical Chemistry



Based on research carried out under the supervision of
John Gilmer B.A. (Mod), Ph.D.
Marek Radomski PhD, M.D.

at

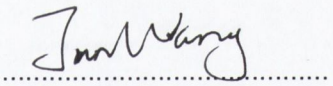
The School of Pharmacy and Pharmaceutical Sciences,
Trinity College,
Dublin.

2010

TRINITY COLLEGE
23 AUG 2012
LIBRARY DUBLIN
Thesis 9549

DECLARATION

This thesis has not been submitted as an exercise for a degree at any other University. The work described is entirely my own work except where duly acknowledged. I agree that the library may lend or copy the thesis upon request



Jun Wang

Dedicated to my wife, Xiaofen Xiong, for her love and devotion

Abstract

Matrix metalloproteinases (MMPs) are a group of Zn-dependent endopeptidases that participate in many diseases. Two MMPs, MMP-2 and MMP-9, which are especially associated with inflammatory diseases and tumor metastasis have been considered as promising target for arthritis, stroke, IBD, various pulmonary disorders and cancer.

A great number of MMP inhibitors have been reported and are classified into different groups based on their structure, including hydroxamates, carboxylates, and thiols. Although some of these compounds exhibit great potency on inhibition of MMPs, their clinical trial results are disappointed due to lack of selectivity. Recently, appropriate C-5 substituted barbiturates have been found to show MMP inhibitory effects. Since barbiturates have been used as sedatives and hypnotics for decades and have well established clinical history, the MMP inhibitors we prepared were based on the structure of barbiturate.

The two substituents on C-5 on the barbiturate ring can fit into the S1′ and S2′ pocket of MMPs and improve the binding affinity. Phenoxyphenyl groups and homopiperazine ring were found to fit well into S1′ and S2′ pocket, respectively, resulting in nanomole IC_{50} values on both MMP-2 and MMP-9. Therefore, a series of compounds were synthesized with phenoxyphenyl group and homopiperazine ring on the C-5 position. In order to achieve selectivity between MMP-2 and MMP-9, these inhibitors had various subgroups attached to homopiperazine to target the differences in the S2′ pocket of two proteins, where MMP-2 has Ile222 and MMP-9 has Met422. Compound **82** was the most selective inhibitor with 9-fold selectivity for MMP-9 over MMP-2. Although the docking results of these compounds were disappointing, they could tell the orientations of these inhibitors in the proteins which were useful for explanation of selectivity and potency. In addition, these compounds also inhibited Caco-2 cell invasion through matrigel membranes.

The large molecular barbiturates (Chapter 4), which are unable to undergo absorption and therefore be confined to the intestinal tract, were prepared based on conjugate of a hydrophobic UDCA or formation of dimers. These compounds were stable in the duodenal fluid for a couple of hours and had abilities to inhibit gelatinase activities and Caco-2 cell invasion.

Hybrid drugs were designed in which R-ONO_2, a nitric oxide releasing group was incorporated into the barbiturate inhibitor type. These retained the ability to inhibit the gelatinases. They inhibit Caco-2 invasiveness, produced nitric oxide metabolites and caused cancer cell death. They merit further study as potential chemotherapeutics.

Acknowledgements

I would like to express my sincerest gratitude to Dr. John Gilmer for giving me the opportunity to undertake this project, for his constant guidance, support and advice throughout the duration of this project. I would also like to thank Prof. Marek Radomski for guidance and support during last four years.

I would like to thank Dr. Carlos Medina and Dr. Maria Jose Santos-Martinez for their great helpfulness, assistance, and advice throughout the duration of this project.

I would especially like to thank my parents, my brother, and my beloved wife for everything they have given me for last 31 years. I can safely say that I could not have done this without your support, advice, encouragement, and love.

I would like to thank Dr. John O'Brien and Dr. Martin Feenzey, Department of Chemistry, TCD, for performing NMR and HRMS analysis respectively. I would like to thank to Dr. Shona Harmon for helps in cell works and proof reading. Many thanks to Dr. John Wash and Orla Wood for provide the plate reader.

A special thank to Dr. Ruchika Sharma for helping, chatting, proof reading and, of course, beautiful singing during last four years! I would also like to thank Bill, Tao, and Yvonne for proof reading.

I would like to thank the technical staff in the teaching lab, especially Ray, for all their assistance and support. I would also thank all the postgrads I have worked with over the last few year, including, Juan, Paul, Niamh, Ferenc, Mike, Patrick, Orla, Aneta, Jose, and Joanna.

Finally I wish express my special thanks to my Chinese friends in Dublin, including, Bo, Shengbao, Shu, Wei, Ming, Long, Quan, Feng, Chao, Yu and Sisi, for all the support, fun and help.

Table of Contents

	Page No.
Title Page	i
Declaration	ii
Abstract	iv
Acknowledgements	v
Table of Contents	vi
Table of Figures	x
Table of Tables	xiv
Table of Schemes	xv
Abbreviations	xvi

CHAPTER 1 AN INTRODUCTION OF MATRIX METALLOPROTEINASES AND THEIR INHIBITORS

1.1	Introduction	2
1.2	Structure of MMPs	4
	1.2.1 Propeptide domain	4
	1.2.2 Catalytic domain	5
	1.2.3 Hinge Region	5
	1.2.4 Hemopexin domain	6
1.3	Regulation of MMPs	7
	1.3.1 Transcriptional regulation	7
	1.3.2 Activation of MMPs	8
	1.3.3 Endogenous Inhibitors	10
1.4	Functions of MMPs	12
	1.4.1 Collagenases	12
	1.4.2 Gelatinases	14
	1.4.3 Stromelysins	16
	1.4.4 Matrilysins	18
	1.4.5 Membrane-type MMPs	19
	1.4.6 Other MMPs	20
1.5	Pathological roles of Gelatinases	21
	1.5.1 Cancer and metastasis	22

1.5.2 Cardiovascular diseases 23
1.5.3 Inflammatory bowel disease 25
1.6 Differences between MMP-2 and MMP-9 27
1.7 MMP inhibitors 29
1.7.1 Hydroxamic acids 29
1.7.2 Carboxylates 39
1.7.3 Thiols 42
1.7.4 Clinical trials of MMP inhibitors 47
1.8 Aims and objective 50
1.8.1 aims 50
1.8.2 objectives 50

CHAPTER 2 SYNTHESIS OF NOVEL PIPERAZINE- AND HOMOPIPERAZINE-BASED BARBITURATES

2.1 Introduction 53
2.1.1 Barbiturates as sedatives and hypnotics 53
2.1.2 MMP inhibition and barbiturates 58
2.2 Synthesis of phenyl, benzyloxyphenyl, and phenoxyphenyl substituted barbiturate-based inhibitors 72
2.2.1 Synthesis of phenyl substituted barbiturate derivatives 72
2.2.2 Synthesis of benzyloxyphenyl substituted barbiturate derivatives 77
2.2.3 Synthesis of phenoxyphenyl substituted barbiturate derivatives 79
2.3 Evaluation of gelatinases inhibition of phenyl, benzyloxyphenyl, and phenoxyphenyl substituted barbiturate-based compounds 83
2.4 Evaluation of piperazine- and homopiperazine-based phenoxyphenyl substituted barbiturate inhibitors 93
2.4.1 Preparation of piperazine- and homopiperazine-based barbiturate inhibitors 93
2.4.2 Structure-Activity Relationships 96
2.5 Conclusion 103

CHAPTER 3 OPTIMIZING HOMOPIPERAZINE-BASED MMP INHIBITORS FOR GELATINASE SELECTIVITY

3.1 Introduction 106
3.2 Preparation of substituted homopiperazine-based MMP inhibitors 109

3.3 Structure-Activity relationships of substituted homopiperazine-based barbiturates 111
3.4 Docking of 5-homopiperazine substituted barbiturates 120
3.5 Inhibition of cancer cells invasiveness 133
3.5.1 Backgroud 133
3.5.2 Assessment of invasion inhibition by selected homopiperazine-based barbiturates 134
3.6 Gelatinase inhibition of carboxylic acids 140
3.7 Conclusion 144

CHAPTER 4 **SYNTHESIS OF LARGE MOLECULAR MMP INHIBITORS FOR INTESTINAL DISEASES**

4.1 Introduction 147
4.2 Inhibition of Protein Dimers 151
4.3 Synthesis of a UDCA conjugate of homopiperazine-based barbiturate and formation of dimers 155
4.4 Biological activities of colon targeting compounds 157
4.4.1 Evaluation of gelatinase inhibition 157
4.4.2 Inhibition of Caco-2 cell invasiveness 161
4.5 Stability Studies of the large molecular barbiturates 166
4.6 Conclusion 171

CHAPTER 5 PREPARATION AND EVALUATION OF BARBITURATE-BASED NITRATES

5.1 Introduction 174
5.1.1 Chemistry of Nitric Oxide 174
5.1.2 Biological functions of nitric oxide 174
5.2 Synthesis and evaluation of nitric oxide released gelatinase inhibitors 180
5.2.1 Synthesis 180
5.2.2 Gelatinase inhibition of phenoxyphenyl barbiturate-based nitrates 183
5.3 Inhibition of cell invasion of nitrates of gelatinase inhibitors 188
5.4 Nitric oxide release of the barbiturate-based nitrates 192
5.5 Nitric oxide and expression of gelatinases 197
5.6 Cytotoxicity of the barbiturate-based nitrates 201
5.7 Conclusion 206

CHAPTER 6 EXPERIMENTAL

6.1 Chemistry 209

6.1.1 General methods 209

6.1.2 Synthesis 209

6.2 Biological Methods 274

6.2.1. Cell culture 274

6.2.2 Gelatinases secretion 274

6.2.3 Zymography 274

6.2.4 MMP-2 and MMP-9 Fluorogenic Assay 275

6.2.5 Invasion assay 275

6.2.6 Griess assay 276

6.2.7 MTT assay 277

6.3 Molecular modelling 277

6.4 Stability studies 278

REFERENCES 279

Table of Figures

Figure 1.1	*Histogram on publications of MMPs and MMPs*	3
Figure 1.2	*3D domain structure of MMPs*	4
Figure 1.3	*The six pockets around the active zinc*	5
Figure 1.4	*Domain structure of the matrix metalloproteinases*	7
Figure 1.5	*Mechanism of ProMMP activation*	10
Figure 1.6	*Structure of the complex of the catalytic domain of MT1-MMP with TIMP-2*	12
Figure 1.7	*A hydroxamate-based inhibitor binding with MMP-3*	30
Figure 1.8	*Binding of phosphonamide-based inhibitors to MMPs*	31
Figure 1.9	*The interaction of MMP-12 with CGS 27023A*	36
Figure 1.10	*The inhibition of cellular TNF-α release by marimastat*	38
Figure 1.11	*Picture of a caboxylate compound binding with MMP-13*	39
Figure 1.12	*The IC50 values of a carboxylate-based MMP inhibitor*	42
Figure 1.13	*The binding of a thiol compound with MMP-8*	43
Figure 1.14	*The binding of MAG-182 with MMP-14*	45
Figure 1.15	*The structure overlay of MMP-2 and MMP-9 with residues*	49
Figure 1.16	*The design of gelatinase selective inhibitors*	50
Figure 1.17	*The design of nitrate MMP inhibitors*	51
Figure 2.1	*Examples of sedatives and hypnotic substituted barbiturates*	54
Figure 2.2	*Tautomerisation of barbituric acid*	56
Figure 2.3	*Ionization of substituted barbituric acids*	56
Figure 2.4	*The first reported barbiturate-based MMP inhibitors*	59
Figure 2.5	*The binding of barbiturates with MMP-8*	60
Figure 2.6	*A picture of interaction of a substituted barbiturate with MMP-9*	61
Figure 2.7	*The mechanism of dimethyl 2-phenylmalonate formation*	74
Figure 2.8	*The ^{1}H NMR spectrum of compound **3***	75
Figure 2.9	*The ^{1}H NMR spectrum of compound **3***	76
Figure 2.10	*The mechanism of bromination of phenyl barbiturate*	76
Figure 2.11	*The mechanism of reactions of barbiturates and piperazines*	77
Figure 2.12	*The mechanism of formation of methyl 2-(4-benzyloxyphenyl) acetate*	78
Figure 2.13	*Unsuccessful reactions for synthesizing the diaryl ether*	82
Figure 2.14	*The possible mechanism of synthesis of methyl 2-(4-phenoxyphenyl) acetate*	82

Figure 2.15 *Picture of a zymography of PMA treated HT1080 cells* 84

Figure 2.16 *Picture of a zymography of PMA treated HT1080 cells incubated with synthesised inhibitors* 85

Figure 2.17 *Pictures of compounds (**12** and **13**) docking with a 'Connolly' surfaces on MMP-2* 90

Figure 2.18 *Pictures of compounds (**26** and **39**) docking with Gaussian Contact surface on MMP-2* 92

Figure 2.19 *The competitions between NH group on piperazine ring and NH group on barbiturate ring when reacting with acid chlorides* 95

Figure 2.20 *The curves for compounds **55** in GraphPad Prism® 4 for calculation of IC_{50} values of MMP-2 and MMP-9* 97

Figure 2.21 *Pictures of compounds (**42** and **36**) docking with a 'Connolly' surface on MMP-2* 102

Figure 3.1 *IC_{50} values of a sulphonamide-based MMP inhibitors* 106

Figure 3.2 *The interaction of a hydroxamic acid with MMP-3* 107

Figure 3.3 *A picture of a substituted carboxylic acid in MMP-3* 107

Figure 3.4 *Strategy for improving gelatinase selectivity by acyl substitution on the distal N of the homopiperazine substituted barbiturate scaffold* 108

Figure 3.5 *Pictures of compounds (**59** and **60**) docking with a 'Connolly' surfaces on MMP-2* 117

Figure 3.6 *Pictures of **82** docked with 'Connolly' surfaces on MMP-2 and MMP-9* 118

Figure 3.7 *A picture of **82** docking into MMP-9* 119

Figure 3.8 *Pictures of compound **78** docking with 'Connolly' surfaces on MMP-2 and MMP-9* 120

Figure 3.9 *Linear regression of experimental binding energies of synthesized homopiperazine-based barbiturates on MMP-2 and MMP-9 with computer calculated binding energies* 123

Figure 3.10 *Pictures of **84** docked with a 'Connolly' surface on MMP-2 and MMP-9* 131

Figure 3.11 *Microscope pictures of a negative control insert and a positive control insert* 135

Figure 3.12 *Invasion assays results for selected compounds* 136

Figure 3.13 *Microscope images from invasion assays **36*** 137

Figure 3.14 *Microscope images from invasion assays with **65**, **74**, **80**, and **82*** 139

Figure 4.1 *The role of MMP-9 in intestinal inflammation* 148

Figure 4.2 *Pharmacological approaches for treatment of IBD* 150

Figure 4.3 *chemical structure of the small molecule TNF-α inhibitor* 152

Figure 4.4 *Potent dimer inhibitors of HIV-1 protease* 152

Figure 4.5 *IC_{50} values of hydroxamic acid dimers* 154

Figure 4.6 *Example curves for **90** generated using GraphPad Prism® 4 for estimating IC_{50} values of MMP-2 and MMP-9* 157

Figure 4.7 *Pictures of Compounds (**90** and **93**) docking with a 'Connolly' surfaces on MMP-9* 160

Figure 4.8 *Microscope images of invasion assays with **90** and **93*** 161

Figure 4.9 *Inhibition of Caco-2 cell invasion by UDCA conjugate and dimer analogs* 162

Figure 4.10 *Representative pictures of invasion assay results of compounds **93** and **94*** 163

Figure 4.11 *The linearity of MMP-2 and MMP-9 IC_{50} values of the test compounds with the inhibition of invasion of Caco-2 cells* 165

Figure 4.12 *Overlaid chromatograms of the peaks for **90** in the duodenal juice* 169

Figure 4.13 *Overlaid chromatograms of the peaks for **93** in the duodenal juice* 169

Figure 4.14 *Progress curves for P1 and P2 peaks of **93** in duodenal juice preparation at 37°C.* 170

Figure 5.1 *The common methods for the preparation of nitric oxide* 174

Figure 5.2 *NO-sGC-cGMP signaling in a blood vessel* 176

Figure 5.3 *Examples of drug-type nitrates that have been entered clinical trials* 180

Figure 5.4 *Two common methods for preparation of nitrates* 180

Figure 5.5 *Sigmoid curves for **112** generated in GraphPad Prism® 4 for calculation of IC_{50} values of MMP-2 and MMP-9* 184

Figure 5.6 *Modelling pictures of compounds(**109** and **111**) docking with a 'Connolly' surfaces on MMP-9* 187

Figure 5.7 *Microscope images from invasion assay with selected nitrate hybrids.* 189

Figure 5.8 *Inhibition of Caco-2 cell invasion of the barbiturate-based nitrates* 190

Figure 5.9 *The linearity of MMP-9 IC_{50} values with inhibition of invasion of Caco-2 cells* 192

Figure 5.10 *The metabolism of nitric oxide in mammalian organisms* 193

Figure 5.11 *Chemical reactions involved in Griess test for measurement nitrite* 194

Figure 5.12 *The relationships between absorbance and the concentration of nitrite and nitrates* 195

Figure 5.13 *An image of a zymograph of PMA and barbiturate-based nitrate treated HT1080 cell supernatants* 198

Figure 5.14 *The MMP-2 and MMP-9 activities of supernatants of HT1080 cells treated with PMA and barbiturate-based nitrates* 199

Figure 5.15 *A picture of zymography of a phenanthroline loaded gel* 200

Figure 5.16 *Enzymatic cleavage of MTT by mitochondrial enzymes* 201

Figure 5.17 *Caco-2 cell survival incubated with relative to Log Concentration in the presence of the barbiturate-based nitrates for 1 and 24 h* 203

Figure 5.18 *HT1080 cell survival incubated with relative to Log Concentration in the presence of the barbiturate-based nitrates for 1 and 24 h* 204

Table of Tables

Table 1.1	*List of phosphonamide-based hydroxamaic acid inhibitors*	32
Table 1.2	*Sulphonamide-based inhibitors of MMPs*	34
Table 1.3	*Sccinate-based MMP inhibitors*	37
Table 1.4	*Carboxlates inhibitors of MMPs*	40
Table 1.5	*Thiol-based MMP inhibitors*	44
Table 1.6	*Ki values of mercaptosulphide inhibitors*	46
Table 2.1	*IC_{50} values of the first synthesized barbiturate-based MMP inhibitors*	59
Table 2.2	*MMP inhibition of published barbiturate derivatives*	63
Table 2.3	*The inhibition by phenyl substituted compounds at 10 μM estimated using zymography (**5–13**)*	86
Table 2.4	*The inhibition by benzyloxyphenyl substituted compounds determined by zymography at 10 μM (**19–27**)*	87
Table 2.5	*The inhibition by phenoxyphenyl substituted compounds determined by zymography at 0.5 μM (**32–40**)*	88
Table 2.6	*IC50 values of piperazine substituted compounds*	98
Table 2.7	*The IC_{50} values of homopiperazine substituted compounds*	99
Table 3.1	*IC_{50} values of substituted homopiperazine-based Barbiturates (**57–82**)*	112
Table 3.2	*Docking and experimental results of homopiperazine-based barbiturates (**57–82**)*	122
Table 3.3	*Prediction of binding affinity of potential homopiperazine-based barbiturates with MMP-2 and MMP-9*	125
Table 3.4	*IC_{50} values of the screened homopiperazine-based barbiturates*	129
Table 3.5	*The inhibition of MMP-2 and MMP-9 activities by small carboxylic acids at 10 μM*	141
Table 4.1	*IC_{50} values of the high molecular weight barbiturates*	158
Table 4.2	*All the tested compounds' abilities of inhibition of invasion of Caco-2 cells at 100 nM and their IC_{50} values*	164
Table 4.3	*The reverse phase HPLC gradient method for the stability study of compounds **90** and **93***	167
Table 5.1	*IC_{50} values of phenoxyphenyl barbiturate-based nitrates*	185
Table 5.2	*The IC_{50} values of three barbiturate-based nitrates and their percentage of inhibition of cell invasion*	191
Table 5.3	*Concentration of nitrite and nitrate in the homopiperazine-based nitrates treated Caco-2 cells*	196

Table of Schemes

Scheme 2.1 *Preparation of barbituric acid by malonic ester* 56

Scheme 2.2 *Forming barbituric acid by malonyl dichloride* 57

Scheme 2.3 *Preparation of amobarbital* 57

Scheme 2.4 *Preparation of allobarbital barbiturate* 58

Scheme 2.5 *Preparation of a spiro barbiturate-based inhibitor* 70

Scheme 2.6 *Preparation of piperazine substituted barbiturate-based MMP inhibitors* 71

Scheme 2.7 *Preparation of phenyl substituted barbiturate derivatives* 73

Scheme 2.8 *Preparation of benzyloxyphenyl substituted barbiturate derivatives* 79

Scheme 2.9 *Preparation of phenoxyphenyl substituted barbiturate derivatives* 81

Scheme 2.10 *Preparation of piperazine- and homopiperazine-based phenoxyphenyl substituted barbiturate derivatives* 94

Scheme 3.1 *Preparation of substituted homopiperazine-based barbiturates* 110

Scheme 3.2 *Preparation of **82** by DCC coupling* 111

Scheme 3.3 *The preparation of the screened homopiperazine-based barbiturates by coupling with the carboxylic acids* 129

Scheme 4.1 *Preparation of UDCA coupled homopiperazine-based barbiturate* 155

Scheme 4.2 *Preparation of the dimers* 156

Scheme 5.1 *Preparation of nitrate using alcohols* 182

Scheme 5.2 *Preparation of phenoxyphenyl barbiturate-based nitrates* 183

Abbreviations

(Q)SAR	(Quantitative) structure-activity relationship
AMPA	4-Aminophenyl mercuric acetate
AP-1	Activator protein-1
Arg	Arginine
ASA	aminosalicylates
BOC	*tert*-Butyl carbonyl protecting group
CD	Crohn's diseases
cGMP	Cyclic guanosine monophosphate
CNS	Central nervous system
DCC	Dicyclohexylcarbodiimide
DCM	Dichloromethane
DMAP	Dimethyl amiopyridine
DMEM	Dulbecco's modified Eagle's medium
DMF	*N,N*-dimethylformamide
DMSO	Dimethyl sulfoxide
DNA	Deoxyribonucleic acid
DPBS	Dulbecoo's phosphate buffered Saline
ECM	Extracellular matrix
EDRF	endothelium-derived relaxing factor
EDTA	ethylelediamine tetraacetic acid
EMEM	Eagle's minimal essential medium
eNOS	Endothelial nitric oxide synthases
Et_3N	Triethylamine
FBS	Fetal bovine serum
FCS	Fetal calf serum
GPCR	G protein-coupled receptors
GPI	Glycosylphosphatidylinositol
HGF	Hepatocyte growth factor
GTP	Ganosine triphophate
His	Histidine
HIV	Human immunodeficiency virus
HPLC	High performance liquid
HRMS	High resolution mass spectroscopy
IBD	Inflammatory bowel disease

IC_{50}	The half maximal inhibitory concentration
IL	Interleukin
Ile	Isoleucine
iNOS	Inducible nitric oxide synthases
IR	Infra-Red
K_i	Inhibition constant
Leu	Leucine
LGA	Lamarckian genetic algorithm
LIF	Leukemia inhibitor factor
L-NAME	N-nitro-L-arginine methyl ester
LPS	lipopolysaccharide
m.p.	Melting point
MeOH	Methanol
Met	Methionine
mg	Milligramme
ml	Milliliter
MMP	Matrix metalloproteinase
MT-MMP	Membrane-type matrix metalloproteinase
MTT	3(4,5-dimethylthiazol-2-yl)-2,5-dipenyltetrazolium) bromide
NED	*N*-1-(naphtyl)ethylenediamine
nm	Nanometer
NMR	Nuclear magnetic resonance
nNOS	neuronal Nitric oxide synthases
NO	Nitric oxide
NOR	Nitric oxide donor
NOS	Nitric oxide synthases
pdb	Protein database bank
PEA3	Polyomavirus enhancer A-binding protein-3 site
PMA	2-*O*-tetradecanoylphorbol-13-acetate
ppm	Parts per million
RMSD	Root mean square deviation
SDS-PAGE	Sodium dedecyl sulfate polyacrylamide gel electrophoresis
sGC	soluble Guanylate cyclase
SULF	sulfanilamide
TACE	TNF-α converting enzyme

THF	Tetrahydrofuran
TIMP	Tissue inhibitors of metalloproteinases
TLC	Trinitrobenzene sulfonic acid
TNBS	Thin layer chromatography
TNF	Tumor necrosis factor
TSP	Thrombospondin
UC	ulcerative colitis
UDCA	Ursodeoxycholic acid
UV	Ultra-Violet
ZBG	zinc-binding group
µg	microgramme
µM	Micromolar

Chapter 1

An introduction of matrix metalloproteinase and their inhibitors

1.1 Introduction

Matrix metalloproteinases (MMPs) are a family of zinc endopeptidases with the ability to degrade the membranes. The functions of MMPs are very complex. They play central roles in morphogenesis, wound healing, tissue repair, cellular migration, skeletal formation, inflammation major protein component of extracellular matrix (ECM) and basement formation, periodontal, asthma, rheumatic, arthritis, cardiovascular, angiogenesis, metastasis and cancer (Stamenkovic 2000; Close 2001; Parks and Shapiro 2001; Egeblad and Werb 2002; Galis and Khatri 2002; Spinale 2002; Curry TE Jr and KG 2003; kelly and Jarjour 2003; Visse and Nagasee 2003; Burrage, Kimbriee et al. 2006; Deryugina and Quigley 2006; Malemud 2006; Hu, Van den Steen et al. 2007). The discovery of the MMP family can be traced to 1962 when the first collagen degrading activity was observed during metamorphosis in tadpoles (Gross and Lapiere 1962). They discovered that in order for a tadpole to become a frog, it needed to generate collagenase in order to digest the matrix (Gross and Lapiere 1962). This was the first time a MMP had been mentioned in a scientific paper.

Twenty-four different vertebrate MMPs have been identified so far. MMPs are also found in Hydra, sea urchin and Arabidopsis (Lepage and Gache 1990; Maidement, Moore et al. 1999; Leontovich, Zhang et al. 2000). MMPs can be subdivided into six groups based on substrate specificity, domain organization and sequence similarity. The six groups of MMPs are collagenases (MMP-1, MMP-8, MMP-13 and MMP-18); gelatinases (MMP-2 and MMP-9); stromelysins (MMP-3 and MMP-10); matrilysins (MMP-7 and MMP-26); membrane-type MMPs (MMP-14, MMP-15, MMP-16, MMP-17, MMP-24, and MMP-25); and other MMPs (MMP-11, MMP-12, MMP-19, MMP-20, MMP-21, MMP-22, MMP-23, MMP-28).

Matrix metalloproteinases are excreted by a variety of host cells including macrophages, fibroblasts and bone, epithelial and endothelial cells. The enzymes are expressed as zymogens which are activated by other proteolytic enzymes (e.g.

plasmin, serine proteases etc.). Under normal circumstances the expression of MMPs is tightly regulated at the level of transcription, activation of the precursor zymogens, interaction with specific ECM components, and inhibition by endogenous inhibitors (Sternlicht and Werb 2001; Visse and Nagasee 2003). In pathological conditions the equilibrium between MMP activity and regulation is shifted toward increased MMP activity leading to tissue degradation. The activity of MMPs can be inhibited by general protease inhibitors, e.g. angiogenesis inhibitor thrombospondin-1 (TSP-1), α2-macroglobulin, and reversion-inducing cysteine-rich protein with Dazal motifs (Egeblad and Werb 2002). Tissue inhibitors of metalloproteinases (TIMPs) are specific endogenous inhibitors regulating the local activities of MMPs. Four TIMPs have been identified in vertebrates: TIMP-1, TIMP-2, TIMP-3 and TIMP-4.

Since the discovery of first MMP, there have been over 18,000 papers on the subject to 2008 on Pubmed. Over 26,400 publications on MMPs are found on SciFinder Scholar (2006 Edition) from 1987 to 2006 which includes 500 publications on MMPs-(Q)SAR [(quantitative) structure-activity relationships] (Fig. 1.1). The figure shows the huge increases of interest in MMPs. MMPs have now been considered as promising target for many diseases.

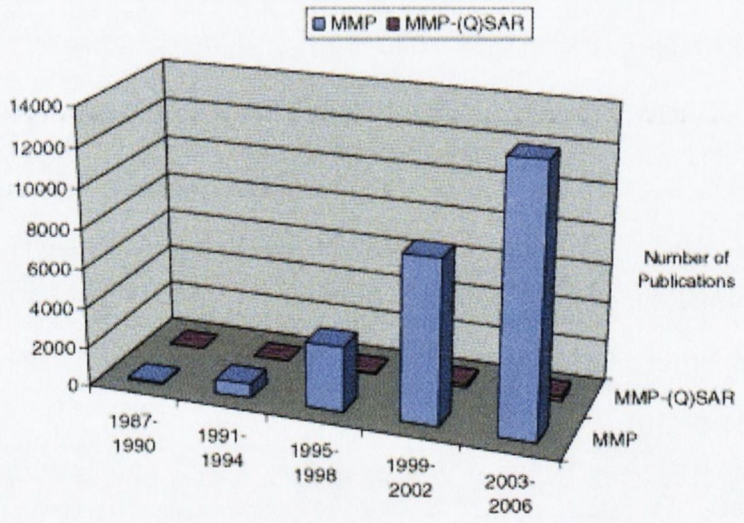


Figure 1.1. *Histogram on publications of MMPs and MMPs-(Q)SAR from 1987-1996(Verma and Hansch 2007)*

1.2 Structure of MMPs

In general, MMPs consist of four domains: an N-terminal prodomain, a catalytic domain, a hinge region and a hemopexin domain (Fig. 1.2), which are either secreted from the cell or anchored to the plasma membrane (Visse and Nagasee 2003).

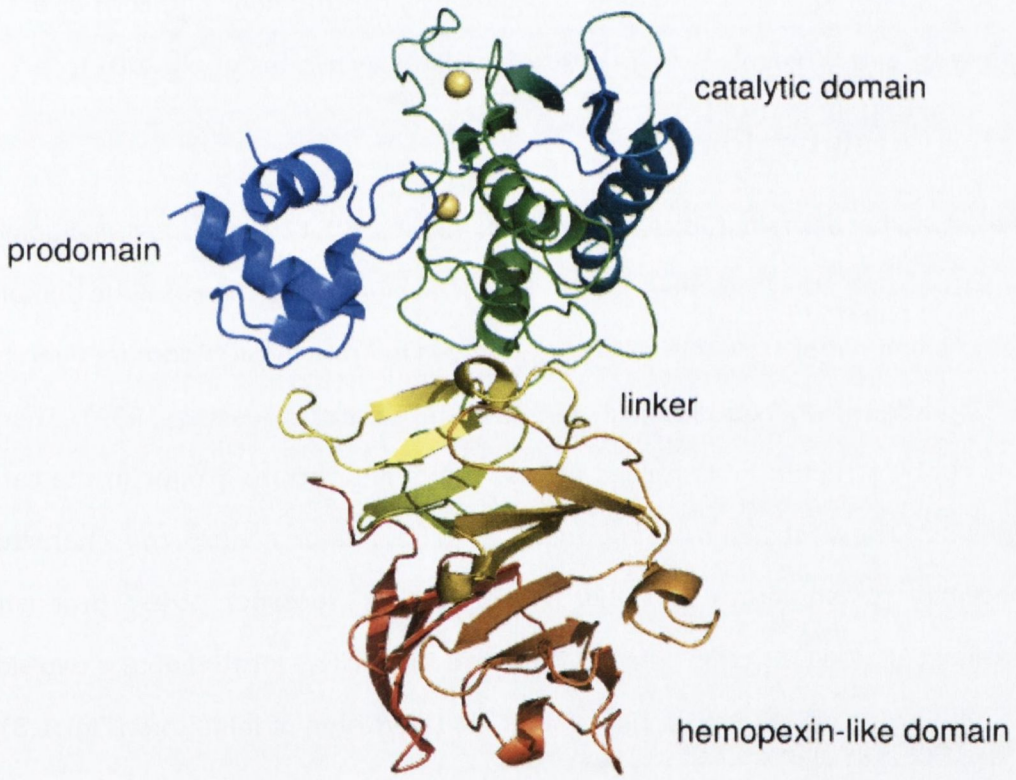


Figure 1.2. *3D domain structure of MMP-1. The picture was generated by the programme PyMOL® based on the crystal structures of MMP-1 (pdb code 1su3).*

1.2.1 Propeptide domain

The propeptide domain is about 80 amino acids large containing a unique PRCG(V/N)PD sequence (Van Wart and Birkedal-Hansen 1990; Visse and Nagasee 2003). Most MMPs contains the cysteine switch motif (PRCGXPD) in the propeptide which is responsible for the latency of the zymogen form (proMMP) except for MMP-23. In the pro-MMPs, the catalytic zinc in the active site is linked to the

conserved cysteine residue prohibiting the activity of the MMPs. The water-zinc interaction (called the cysteine switch) disrupts the cysteine-zinc interaction to activate the MMPs (Springman, Angleton et al. 1990; Van Wart and Birkedal-Hansen 1990). Two common methods used to achieve the activation of MMPs *in vitro* are organomercurial treatment with 4-aminophenyl mercuric acetate (AMPA) or proteolysis (Klein, Vellenga et al. 2004). The AMPA method results in a permanent disruption of the cysteine-zinc interaction, whereas the cysteine residue in propeptide domain is removed in proteolysis (Springman, Angleton et al. 1990; Van Wart and Birkedal-Hansen 1990; Brandstetter, Grams et al. 2001).

1.2.2 Catalytic domain

The catalytic domain typically contains about 160-170 residues, including the structural zinc atom and sites for binding of calcium ions. The catalytic domain has a zinc-binding motif (HEXGHXXGXXH) involved in proteolysis (Fridman, Fuerst et al. 1992; Morgunova, Tuuttila et al. 1999; Nagasee and Woessner 1999). There are only subtle structural differences among the five substrate groups in the catalytic domains. These structural differences are thought to control the characteristic specificity for substrate of MMPs (Nagasee and Woessner 1999; Brandstetter, Grams et al. 2001). In this domain, there are six pockets located on the two sides of the active zinc which are very important for the design of inhibitors (Fig. 1.3).

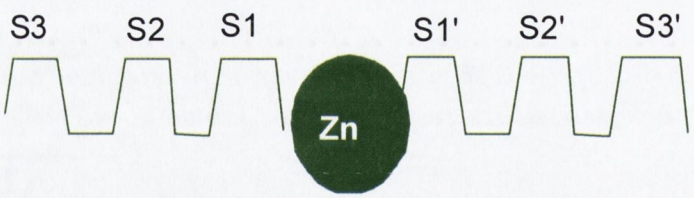


Figure 1.3. *The six pockets around the active zinc.*

1.2.3 Hinge Region

In MMPs the catalytic domain is followed by a linker region usually referred to as the hinge region. This region plays critical roles in the stability of enzyme. It is important for the degradation of complex substrates such as fibrillar collagen by

collagenases which require the concerted action of the catalytic and the hemopexin domain (Chung, Dinakarpandian et al. 2004). Recent studies showed the contribution of the hinge region to collagen binding and unwinding and its breakdown (Tam, Moore et al. 2004). The hinge region is rich in proline residues and varies in length. The collagenolytic activity of MMP-8 was dramatically reduced with the replacement of proline with alanine, indicating that the presence of a right linker structure is important for collagenolysis (Knauper, Docherty et al. 1997).

1.2.4 Hemopexin domain

The hemopexin domain of about 200 residues consists of a four blade propeller structure with a disc like structure in the middle (Fig. 1.2), containing a calcium ion stabilized by a disulfide bond and contributes to substrate specificity and to interaction with endogenous inhibitors (Morgunova, Tuuttila et al. 1999; Overall and Lopez-Otin 2002). Most MMPs contain this domain except for MMP-7,-26 and -23, but it has no effect for catalytic activity. For example, the hemopexin-like domain of MMP-12 is lost shortly after activation, but it this does not affect elastin degradation activity (Faber, Groom et al. 1995). However, substrate recognition and substrate specificity may be greatly impacted by hemopexin domain. In the investigation into the subfamily of collagenase, the ability of processing triple-helical collagen is critically dependent on the hemopexin domain (Murphy, Allan et al. 1992). The hexmopexin domain only cleaves gelatin-like peptides but does not process collagen. This domain also assists to the binding of TIMP. In the case of gelatinases, there is binding of TIMP to the domain even when the enzyme are in their zymogen form

Besides the four domains, some MMPs contain other structural features (Fig. 1.4): Signal peptide: furin-cleavage site insert, fibronectin-like domain, and membrane insertion extension.

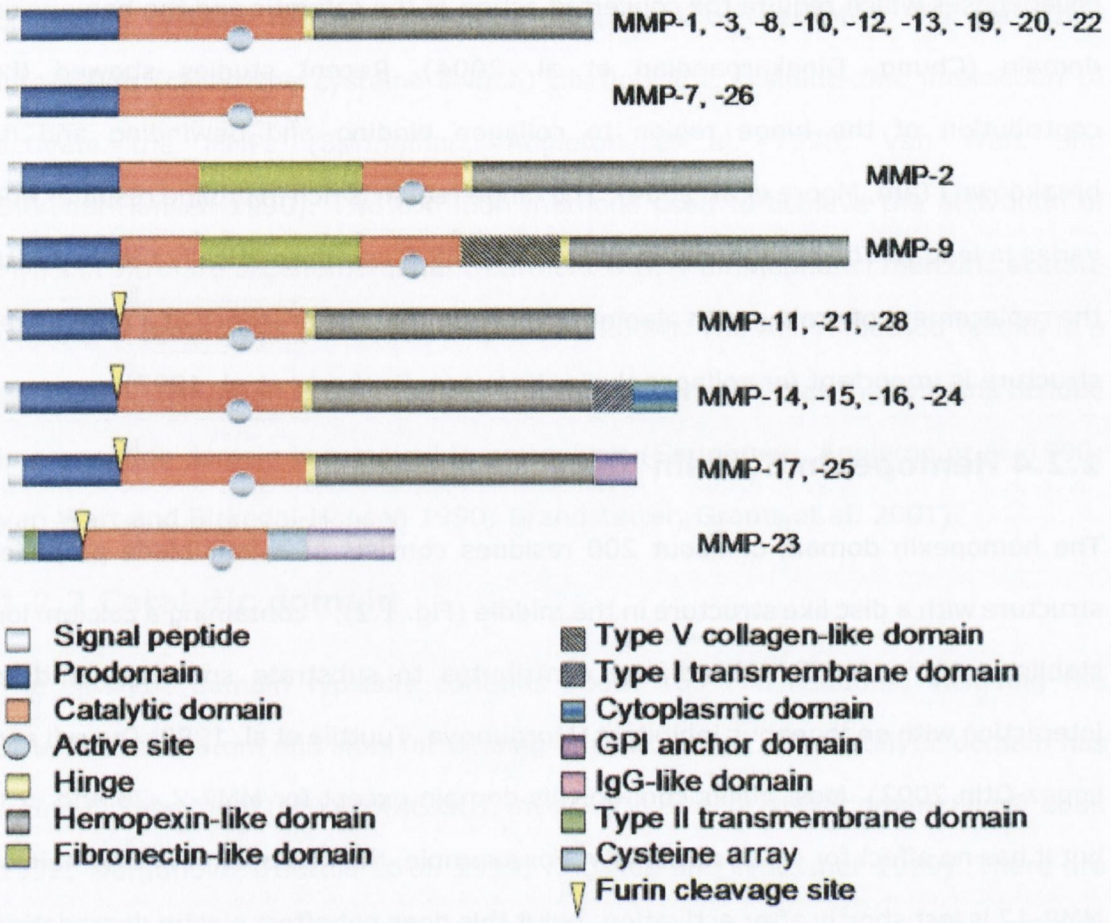


Figure. 1.4. *Domain structure of the matrix metalloproteinases (adapted from (Lemaitre and D'Armiento 2006))*

1.3 Regulation of MMPs

Since MMPs play important roles in both physiological and pathological conditions, it is necessary to understand the mechanism of regulation of MMP expression. As for all secreted proteinases, the catalytic activity of MMPs is generally regulated by three ways: transcriptional control, proenzyme activation, and endogenous inhibitors.

1.3.1 Transcriptional regulation

Much evidence indicates that MMPs are precisely regulated at the transcriptional level. In the normal conditions, the MMP expression is at low level and can be stimulated by growth factor, hormones, and cytokines. In diseases, e.g. cancer, MMP gene expression is induced several types of cells such as epithelia tumor cells

and stromal fibroblasts. Analysis of the promoter regions from several MMP genes appeared to provide insights into the mechanisms that regulate their expression. Activator protein-1 (AP-1) is the first cis-element MMP promoter that induces MMP-1 expression (Angel, Baumann et al. 1987). Besides, several MMP promoters have been reported to appear in a variety of function of cis-element such as polyomavirus enhancer A-binding protein-3 site (PEA3), β-catenin/Tcf-4, and NF-κB. The MMP promoters can be divided into three groups based on the composition of cis-elements. The first group promoters (including MMP-1, -3, -7, -9, -10, -12, -13, -19, and -26) contain TATA boxes at around −30 bp and AP-1 site at around −70 bp. The second promoter also contain TATA boxes, but without an AP-1 site, including MMP-8, -11, and -21. The MMP promoters in the last group have neither TATA box nor AP-1 sites, including MMP-2, -14 and -28). MMP gene expression is subject to changes in the amount and activity of the corresponding *trans*-activators with the presence of the AP-1 sites, either alone or in cooperation with PEA3 (Benbow and Brinckerhoff 1997; Westermarck and Kähäri 1999). Some DNA polymorphisms derived from nucleoside insertions, substitutions, or microsatelite instability have been found in a number of MMP promoters that regulate gene expression by altering interaction between cis-elements and transcription factors (Ye 2000). Finally, epigenetic regulation is also associated with MMP gene regulation. It has been reported that hypomethylation, a mechanism of epigenetic regulation, is regulatory for MMP expression (Chicoine, Estève et al. 2002; Couillard, Demers et al. 2006).

1.3.2 Activation of MMPs

Like most proteolytic enzymes, MMPs are synthesized as inactive proenzymes. Thus, activation of these zymogens is another important step in the regulation of MMP activity. One of the unique properties of MMPs is that proMMPs are not only activated by proteinases, but also by chemical agents, such as N-ethylmaleimide, 4-aminophenylmercuric acetate (APMA), SDS, oxidized glutathione, and reactive oxygen species (NO_2, ONO_2^-) (Woessner and Nagase 2000) (Fig. 1.5). Heat treatment and low pH acid can also cause activation. These chemical agents most

likely activate MMPs through the cysteine switch mechanism. The proMMPs have a highly conserved cysteine residue in the proform enzyme prodomain interacting with the zinc ion of the catalytic site, which keeps the proenzyme in a catalytically inactive state. During the activation, the zinc-cysteine interaction is broken and the cysteine reacts with SH reagents, preventing the reassociation of cysteine and zinc ions and leaving the active site exposed (Woessner and Nagase 2000). Research on MMP-3 activation with APMA has shown that the cleavage initially occurs within the propeptide and the rest of the propetpide is subsequently removed by intermolecular reaction of the generated intermediates (Okada, Harris et al. 1988; Nagase, Enghild et al. 1990). In this mechanism, the prodomain is either cleaved by agents or autolytic cleavage (Ra and Parks 2007).

Most proMMPs are activated extracellularly except for MMP-11, -23, -28 and six MT-MMPs which can be activated intracellularly by furin (Visse and Nagase 2003). This is because these enzymes contain a furin recognition sequence at the C-terminal end of the peptide, which serves as a target for proprotein convertases or furins (Ra and Parks 2007).

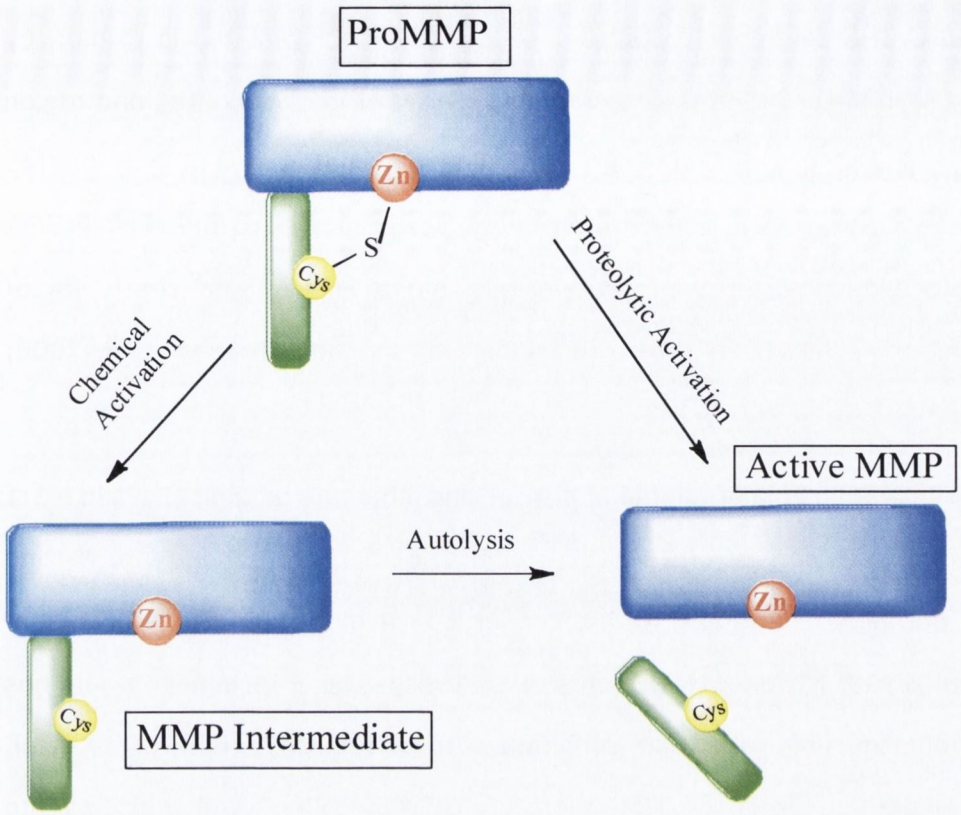


Figure 1.5. *Mechanism of ProMMP activation. The proMMP is maintained by the thiol-zinc bond between cysteine (yellow) in the prodmain (green) and the active zinc (red) in the catalytic domain (blue). The inactive proMMP can be activated by non-proteolytic and proteolytic agents. Chemical agents, such as APMA, can break the interaction of thiol-zinc resulting in partial activation of proMMP. Then the prodomain is removed by autolysis to gain the full activity. The proteolytic activation is involved in furin and other proteinases which cleave the thiol constraint and remove the propeptide.*

ProMMPs can also be activated by a number of MMPs which have the ability to cleave the prodomain of other MMP zymogens (Nagase 1997). It has been reported that proMMP-13 can be activated by MMP-3 and MT1-MMP (Knäuper, Will et al. 1996; Knauper, Lopez-Otin et al. 1996). Apart from activation of procollagenase-3, MT1-MMP can also activate proMMP-2 and proMMP-9 (Murphy, Stanton et al. 1999).

1.3.3 Endogenous Inhibitors

The activity of MMPs can also be regulated by a number of endogenous inhibitors. Some of these inhibitors are general proteinase inhibitors e.g. α2-macroglobulin. α2-Macroglobulin has shown inhibitory effects on most proteinases includingMMP-1, human MMP-2, rabbit MMP-3, and human and mouse MMP-12 (Woessner and

Nagase 2000). The binding of a proteinase with α2-macroglobulin is formed by trapping the proteinase within the macroglobulin after proteolysis of the bait region which triggers large changes in α2-macroglobulin conformation resulting in the trap (Barrett 1981). Furthermore, other proteins have been reported to inhibit MMPs. For example, procollagen C-terminal proteinase inhibits MMP-2 and tissue factor pathway inhibitor-2 has been shown to inhibit MMPs (Mott, Thomas et al. 2000; Herman, Sukhova et al. 2001).

TIMPs, different with α2-macroglobulin, are specific inhibitors binding MMPs in a 1:1 stoichiometry. TIMPs consist of 184-189 amino acids and are divided into N- and C-terminal domains containing three conserved disulfide bonds (Williamson, Marston et al. 1990; Murphy, Houbrechts et al. 1991). The N-terminal domain has folds as a separate unit with MMP inhibitory activity (Murphy, Houbrechts et al. 1991). The overall shape of the TIMP molecule is "wedge-like", which inserts into the active site of MMP in a manner like that of the substrate. The interaction of TIMP-2 and MT1-MMP is shown in the Fig. 1.6, where the residues in the N-terminal region bind in the catalytic site and the active zinc (Fernandez-Catalan, Bode et al. 1998). The four TIMPs inhibit all MMPs tested so far, but TIMP-1 is a poor inhibitor for MMP-19 and MT1-MMP, MT3-MMP, MT5-MMP (Lee, Rapti et al. 2003). Apart from inhibiting MMPs, TIMP-3 also blocks the activity of ADAMs (ADAM-10, -12, and -17) and ADAMTSs (ADAMTS-1, -4, and -5) (Amour, Knight et al. 2000; Kashiwagi, Tortorella et al. 2001; Nagase, Visse et al. 2006). Recent studies have shown that TIMP-3 is a better inhibitor of ADAM-17 and aggrecanases than MMPs (Visse and Nagase 2003). TIMP-3 deficient mice have shown faster apoptosis of mammary epithelia cells after weaning and lung emphysema-like alveolar damage, whereas TIMP-1 and TIMP-2 knockout mice do not exhibit obvious abnormalities, suggesting that TIMP-3 is important for regulation of MMP activities *in vivo* (Fata, Leco et al. 2001; Leco, Waterhouse et al. 2001). In addition, other TIMPs have important biological functions. For example, local expression of TIMP-1 prevents aortic aneurism, degradation and rupture in a rat model and adenovius-mediated

overexpression of TIMP-1 showed a reduction in the lesion in a mouse model of atherosclerosis. All these studies together demonstrate the potential application of TIMPs as endogenous inhibitors.

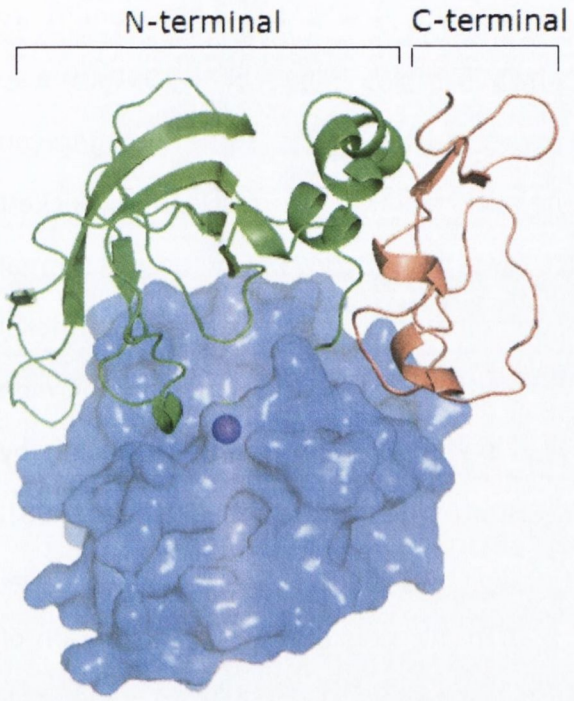


Figure 1.6. *Structure of the complex of the catalytic domain of MT1-MMP with TIMP-2 (PDB code: 1bqq), prepared by Pymol®. TIMP-2 is shown as a ribbon diagram. It has N-terminal (green) and C-terminal (red). The MT1-MMP catalytic domain is shown as a transparent surface (blue). The N-terminal slots into the active-site cleft and binding with zinc (purple).*

1.4 Functions of MMPs

1.4.1 Collagenases

Interstitial collagenase or collagenase-1 (MMP-1), neutrophil collagenase or collagenase-2 (MMP-8), and collagenase-3 (MMP-13) are included in this group. The fourth type of vertebrate collagenase (MMP-18) has been found only from *Xenopus laevis* (Stolow, Bauzon et al. 1996). The key feature of these proteases is their unique ability to cleave the major fibrillar collagens I II III in their very resistant triple-helical domain at neutral pH and producing fragments that are three-fourth

N-terminal and one-fourth C-terminal of the intact molecule (Jeffrey, William et al. 1998).

The first vertebrate MMP-1 was purified from human fibroblast cells as a pair of approximate 52-kDa zymogens (Stricklin, Bauer et al. 1977). It has a higher affinity for type III collagen compared to types I and II (Jeffrey, William et al. 1998). It also degrades the other substrates including perlean, activates cytokines and aggrecan such as interleukin (IL-1) β and tumour necrosis factor (TNF)-α. (Gearing, Beckett et al. 1994; Schonbeck, Mach et al. 1998). MMP-1 is produced by numerous normal cells, such as: stromal macrophages, endothelial cells, fibroblasts, and epithelial cells, as well as by tumors indicating this collagenase is associated with a wide variety of roles in biology. MMP-1 plays a beneficial role in wound healing by facilitating cell migration during re-epithelialization (Pilcher, Sudbeck et al. 1998). The degradation of type III collagen, a vital structural element of the alveolar walls, caused by the transgenic expressing MMP-1 in mice resulted in the disruption of lung structure and emphysema (D'Armiento, Dalal et al. 1992; Shiomi, Okada et al. 2003). MMP-1 expression is found in the lungs of patients with emphysema, but not normal lungs (Imai, Dalal et al. 2001). All these together strongly suggest that MMP-1 plays important roles in the development of emphysema. In addition, MMP-1 is involved in many other diseases such as breast cancer, heart diseases (Kim, Dalal et al. 2000; Boire, Covic et al. 2005).

MMP-8, collagenase-2, is generally released by neutrophils in inflammatory diseases and cleaves all three types of collagen (Jeffrey, William et al. 1998). It is identical in size and is considerably glycosylated (Jeffrey, William et al. 1998). The molecular weight of fully glycosylated proenzyme form MMP-8 is approximately 60 kDa (Jeffrey, William et al. 1998). MMP-8 knockout mice have prevented neutrophil infiltration resulting in significant lower lethal hepatitis, suggesting its important role in liver diseases. Collagenase-2 expression has been detected in mice postpartum uterus, in macrophages, and in the endothelium of atheroma, where it

could contribute to tissue remodelling and inflammation (Balbin, Fueyo et al. 1998; Herman, Sukhova et al. 2001).

Collagenase-3 (MMP-13), identified by Freije *et al.* in 1994, has stronger catalytic efficiency on type II collagen than type I and type III (Freije, Diez-Itza et al. 1994; Jeffrey, William et al. 1998). It also has the ability to cleave a broad range of substrates such as fibronectin, elastin, proteoglycans, and laminin (Knauper, Lopez-Otin et al. 1996). MMP-13 plays crucial roles in rheumatoid arthritis and osteoarthritis due to its ability to degrade aggrecan and collagens (Takahashi, Kimura et al. 2008). It is considered the most important collagenase for the cleavage of collagen within the cartilage due to its higher degrading efficiency on type II collagen over type I and III collagens (knauper, Will et al. 1996; Mitchell, Magna et al. 1996). MMP-13 is a key contributor for the skeletal remodelling in postnatal tissues (Ståhle-Bäckdahl, Sandstedt et al. 1997). MMP-13 knockout mice have acute defects in growth plate cartilage, a delay in endochondra ossification, and formation and vascularization of primary ossification centres indicating its importance in skeletal development (Inada, Wang et al. 2004).

1.4.2 Gelatinases

Gelatinases include 72-kDa gelatinase A (MMP-2) and 92-kDa gelatinase-B (MMP-9). These enzymes readily digest denatured collagens or gelatins. In addition, they degrade cytokines, various collagens, and growth factors, and modify chemokines (Opedenakker, Van den Steen et al. 2001). Gelatinases have additional three repeats of fibronectin-like gelatin-binding domains in the catalytic domain binding to gelatin, collagens, and laminin (Allan, Docherty et al. 1995).

MMP-2 or gelatinase A digests types IV, V, VII, and X collagen, laminin, fibronectin, elastin, and several chemokines, and plays important roles in cell migration, inflammation, and metastasis (Yu, Murphy et al. 1998). It is released by many cell types and can activate proMMP-1 and proMMP-2. Like most MMPs, gelatinase A is secreted in a latent form and must be activated extracellularly. However, unlike

most other matrixins, proMMP-2 is normally found selectively interacting with the endogenous inhibitor TIMP-2 (Yu, Murphy et al. 1998). While generally active MMPs are inhibited by TIMPs binding to the active site. In human platelets, MMP-2 is expressed during aggregation induced by collagen and thrombin and its release can positively affect platelet aggregation (Yu, Murphy et al. 1998). Recent research shows MMP-2 regulates platelet activation and aggregation through the binding of C-terminal hemopexin-like domain with integrin $\alpha_{IIb}\beta_3$ (CHOI, JEON et al. 2008). Platelets play a central role in tumour metastasis. Cancer cells have shown the ability to aggregate platelets which correlates with the metastatic potential of tumour cells (Jurasz, Alonso-Escolan et al. 2004). Therefore inhibition of MMP-2 expression in platelets aggregation may result in prevention of metastasis.

Gelatinase B or MMP-9 contains a type V collagen-like domain inserted between the catalytic and hemopexin domain. It degrades type IV, V, and XI collagen, denatured collagen, the N-telopeptides of type I collagen, aggrecan, the cartilage link protein and elastin (Lemaitre and D'Armiento 2006). The expression of MMP-9 has been found to be affected by many growth factors and cytokines. Majority of growth factors, such as TGF-β, leukemia inhibitor factor (LIF), IL1β, IL1α and lipopolysaccharide (LPS), and cytokines increase the expression of MMP-9 (Vu and Werb 1998). For example, the expression of MMP-9 activated by human T-cells may be mediated in an autocrine fashion by the release of IL-2 (Montogery, Sabzevari et al. 1993). A number of growth factors and cytokines reduce the expression of gelatinase B. The expression of MMP-9 induced by cocanavalin A in monocytes is downregulated by IL-10 (Mertz, Dewitt et al. 1994). On the other hand, MMP-9 activates cytokines such as IL1-β and growth factors TGF-β (Ito, Mukaiyama et al. 1996; Yu and Stamenkovic 2000). MMP-9 plays central roles in skeleton development. MMP-9 deficient mice have an abnormal pattern of skeletal growth plate vascularization and ossification (Vu, Shipley et al. 1998). In these mice, ossification is delayed due to the delay of vascular invasion into the cartilage ECM (Vu and Werb 1998). These delays as well as a delay in apoptosis result in

progressive lengthening of the growth plate (Vu, Shipley et al. 1998). Bone marrow cell induced MMP-9 releases soluble Kit-ligand, permitting the transfer of endothelial and hematopoietic stem cells from the quiescen to the proilferative niche, promoting hematopoietic reconstitution (Heissig, Hattori et al. 2002).

1.4.3 Stromelysins

Stromelysins consist of MMP-3 (stromelysin 1) and MMP-10 (stromelysin 2). Stromelysins have similar structures with collagenases. The biggest difference between them is that stromelysins do not digest the triple helical regions of interstitial collagens (Nagase 1998). Stromelysins degrade a wide range of substrates including fibronectin, proteoglycans, nidogen, lamin, casein and decorin (Nagase 1998). Although two enzymes have similar substrate specificities, the catalytic efficiency of MMP-10 is lower than that of MMP-3 (Nicholson, Murphy et al. 1989). Apart from degrading extracellular components, stromelysin 1 activates a number of proMMPs especially in proMMP-1 which is critical for the production of fully active MMP-1 (Suzuki, Enghild et al. 1990). Stromelysin 3 (MMP-11) is usually grouped into other MMPs due to the difference of the specificity of substrate and sequence from those of MMP-3 (Visse and Nagase 2003).

MMP-3 degrades Collagen types III, IV, and V, fibronectin, elastin, laminin, perlecan, and vitronectin (Nagase 1998) and is expressed by several types of cells including vascular smooth muscle and endothelia cells (Pintucci, Yu et al. 2003). It is secreted and synthesized as an inactive zymogen and can be activated by both nonproteolytic agents such as 4-aminophenylmercuric acetate (APMA) and proteinases such as matriptase (Nagase 1998; Jin, Yagi et al. 2006). Once activated, MMP-3 has the ability to degrade the ECM components and to activate other members of the MMP family (Lark, Bayne et al. 1999). Like most MMPs, the level of MMP-3 is usually regulated by several natural inhibitors TIMPs and α_2-macroglobulins (Nagase 1998). MMP-3 is also found in stromal cells during mammary gland development and is upregulated during mammary involution

postlactation (Lund, Romer et al. 1996). The expression of activated MMP-3 in epithelium cells during development of mammary glands of transgenic mice led to the increase in expression of stromelysin 1, neovascularization, and tenascin-C (Thomasset, Lochter et al. 1998). MMP-3 also promotes the development of spontaneous premalignant and malignant lesions, and mammary cancers in these transgenic mice demonstrating the role of stromelysin 1 in promotion of natural cancer (Sternlicht, Lochtest et al. 1999). MMP-3 plays an important role in bone and cartilage diseases. The expression of MMP-3 in joint fluids of patients with rheumatoid arthritis is approximately 1000-folder higher than of people without the disease (Lohmander, Hoerrner et al. 1993). In an animal test model of arthritis, MMP-3 knockout mice were resistant to cartilage erosion (Van Meurs, Van Lent et al. 1999). In a model of herniated disc resorption, chondrocytic MMP-3 was required for disc resorption and generation of macrophage chemoattractant (Haro, Crawford et al. 2000). Interestingly, MMP-3 plays both positive and negative roles in atherosclerosis. On the one hand MMP-3 contributes to reduce plaque, possibly by degradation of matrix components, and on the other hand, contributes to aneurysm formation by degradation of the elastic lamina (Silence, Lupu et al. 2001).

MMP-10 has the same degradation capability as MMP-3 for components of ECM but with lower catalytic efficiency (Nagase 1998). It is expressed in keratinocytes, carcinomas, T lymphocytes, and would healing tissues(Nagase 1998). The expression of MMP-10 in keratinocytes of epithelial tongue of skin wounds illustrates its role in the migration of keratinocytes (Krampert, Bloch et al. 2004). Recently, it has also been reported that MMP-10 is involved in vascular development and atherogenesis (Rodriguez, Orbe et al. 2008).

1.4.4 Matrilysins

MMP-7 and MMP-26 are grouped into matrilysin and are called matrilysin 1 and matrilysin 2, respectively. The matrilysins are characterized by the lack of the hinge region and hemopexin-like domain of other MMPs.

MMP-7, the smallest known member of the MMP family, degrades a broad range of substrates such as fibronectin, gelatins of types I, III, IV, and V, type IV collagen, entactin/nidogen and laminin (Wilson and Matrisian 1998). Beside ECM components, MMP-7 processes cell surface molecules such as Fas-ligand, pro-tumor necrosis factor (TNF)-α, and E-cadherin (Visse and Nagasee 2003). MMP-7 is detected in mucosal and exocrine gland epithelia cells and postpartum uterus, and activates defensin, an antibacterial peptide (Rudolph-Owen, Hulboy et al. 1997; Wilson, Heppner et al. 1997). MMP-7 has been detected in human cancer tissues and early stage colorectal tumors and is associated with cancer progression. Overexpression of MMP-7 has been found in invasive cancers of digestive organs such as stomach, esophagus, liver, colon, and pancreas (Ii, Yamamoto et al. 2006). In addition, overexpression of matrilysin 1 is detected in cancers of other organs such as skin, breast, lung, postate and neck (Ii, Yamamoto et al. 2006). Decreased development of tumors throughout the intestinal tract is observed in MMP-7 deficient mice.

MMP-26 is detected in normal adult tissues such as the uterus, kidney, lung, and epithelia cancers such as breast, lung, endometrial and prostate carcinomas (Yamamoto, Vinitketkumnuen et al. 2004). It degrades a number of substrates such as type IV collagen, fibrinogen, vitronectin, and fibronectin and is an activator of proMMP-9 (Uria and Lopez-Otin 2000). Expression of MMP-26 in uterus during the estrous cycle and early pregnancy suggests its role in the cycling changes and in embryo implantation (Liu, Zhang et al. 2005). MMP-26 is upregulated in keratinocytes during wound repair and early skin carcinogenesis (Ahokas, Skoog et al. 2005). It has also been reported that MMP-26 is associated with depth of invasion and lymph node metastasis.

1.4.5 Membrane-type MMPs

There are six membrane-type MMPs (MT-MMPs) including four type I transmembrane proteins (MMP-14, MMP-15, MMP-16, and MMP-24) and two glycosylphosphatidylinositol (GPI) anchored proteases (MMP-17 and MMP-25). All

MT-MMPs are probably expressed in the active form because they have a furin cleavage motif between the propeptide and catalytic domain. Most MT-MMPs have the ability to activate pro-MMP-2 with the exception of MMP-17 (knauper and Murphy 1998).

MMP-14 (MT1-MMP) digests a number of ECM molecules and has collagenolytic activity on type I, II, and III collagens (Ohuchi, Imai et al. 1997). MMP-14 is involved in a variety of physiological processes such as cell migration, angiogenesis, wound repair (Knauper and Murphy 1998). It also participates in numerous diseases such as cancer, heart failure and asthma (Lemaitre and D'Armiento 2006). MT1-MMP deficient mice have severe defects in skeletal development, develop dwarfism, osteopenia and arthritis, and have alveolar abnormalities, emphasizing the role for MMP-14 in normal development (Holmbeck, Bianco et al. 1999; Zhou, Apte et al. 2000; Atkinson, Holmbeck et al. 2005).

Although MMP-16 (MT3-MMP) was first detected in tumor samples, expression of MMP-16 has been found in normal tissues such as lung, brain, placenta, and in vascular smooth muscle cells (Shofuda, Yasumitsu et al. 1997). MMP-17 (MT4-MMP) was identified in 1996, cloned from a human breast carcinoma cDNA library (Puente, Pendas et al. 1996). It is the first GPI-anchored proteinase and can be shed from the cell surface by the action of other metalloproteinases (Itoh, Kajita et al. 1999).

MMP-24 (MT5-MMP) is mainly expressed in the cerebellum in embryos (Sekine-Aizawa, Hama et al. 2001). MMP-24 is the most strongly expressed throughout the nervous system and is localized in the membranous structure of expressing neurons suggesting that MMP-25 may contribute to neuronal development (Sekine-Aizawa, Hama et al. 2001). MMP-25 (MT6-MMP) was identified in 2000 and normally expressed in peripheral blood leukocytes, lung and spleen (Velasco, Pendas et al. 1999). A high level of MMP-25 has been found in cancers of the colon and brain, but not in normal colon or brain, suggesting the

enzyme could be involved in tumor progression thought to be due to its ability to activate proMMP-2 at the membrane of cells (Sekine-Aizawa, Hama et al. 2001).

1.4.6 Other MMPs

The remaining eight MMPs are included in this group because of the divergenceing in sequence and substrate specificity compared to the above categories.

MMP-11, stromelysin-3, was identified in 1990 in human breast cancer tissues (Bassed, Bellocq et al. 1990). It is the first MMP that can be processed directly to its active from by an obligate intracellular proteolytic events (Pei and Weiss 1995). MMP-11 only degrades a very small number of known substrates, including insulin-like growth factor-binding protein-1 (Mañes, Mira et al. 1997). MMP-11 is involved in many physiological processes including ovulation, wound healing, and post-partum involution (Wolf, Chenard et al. 1992; Hägglund, Ny et al. 1999). In addition, MMP-11 is also detected in several pathological remodelling processes such as inflammation, tumor proliferation and tissue invasion (Matziari, Dive et al. 2007).

Macrophages are the main source of MMP-12 (metalloelastase) which is essential for macrophage migration (Shapiro, Kobayashi et al. 1993; Shipley, Wesselschmidt et al. 1996). Besides elastin, MMP-12 can degrade a number of other matrix proteins such as fibronectin, type IV collagen, entactin, and various proteoglycans (Shapiro and Senior 1998). Macrophages from MMP-12 deficient mice lose the capacity to degrade ECM and emphysema has not been developed in response to long-term exposure to smoke in MMP-12 knockout mice (Shipley, Wesselschmidt et al. 1996; Hautamaki, Kobayashi et al. 1997). It has been reported that MMP-12 may promote plaque instability and aneurysm formation (Luttun, Lutgens et al. 2004; Johnson, George et al. 2005).

MMP-19 was identified by cDNA cloning from liver and is expressed in the placenta, lung, pancreas and intestine (Shipley, Wesselschmidt et al. 1996; Pendas, Knauper et al. 1997). It has the ability to degrade type IV collagen, gelatine, laminin,

nidogen, tenascin, and aggrecan (Stracke, Fosang et al. 2000; Stracke, Hutton et al. 2000). MMP-19, constitutively expressed in the basal layer of the epidermins, can cleave the insulin-like growth factor binding protein-3 resulting in an increase in of proliferation of keratinocytes (Sadowski, Dietrich et al. 2003).

MMP-20 (enamelysin) is primarily located in the secretory and transitional stage of dental enamel formation (Bartlett, Simmer et al. 1996). Significant reductions of the enamel mineral and its hardness were observed in MMP-20 deficient mice, demonstrating that MMP-20 can facilitate the removal of enamel proteins during the maturation stage of enamel development (Bartlett, Beniash et al. 2004).

MMP-21 is expressed in cancer and in mouse neuronal tissues and is able to activate its secretory pathway by furin-like proteases (Ahokas, Lohi et al. 2002; Marchenko, Marchenko et al. 2003). MMP-22 was first cloned and characterized from chicken embryonic fibroblasts and has activity on gelatin and casein *in vitro* (Yang and Kurkinen 1998). MMP-23, called cysteine array MMP, has a cysteine-rich sequence followed by an immunoglobulin-like domain (Pei 1999) which is primarily expressed in reproductive tissues such as ovary, testis and prostate (Velasco, Pendas et al. 1999). MMP-28, or epilysin, is mainly expressed in keratinocytes at the wound edge, suggesting it might function in wound repair (Lohi, Wilson et al. 2001).

1.5 Pathological roles of Gelatinases

Gelatinases play an important role in a wide range of pathological conditions, among which, the role in cancer and metastasis has been extensively studied. Elevation of gelatinase activity has been detected in a wide variety of pathological conditions, including, cancer, cardiovascular diseases, and inflammatory bowel diseases.

1.5.1 Cancer and metastasis

The ability of cancer cells to invade normal cells and tissues is an often-fatal characteristic of malignant tumors. MMPs, especially gelatinases, have been recognised as major critical proteinases facilitating invasion of tumor cells due to

their ability to degrade ECM. In many cancers, increased plasma levels of gelatinases were found to be associated with poor overall survival of metastases in different types of cancers (Bjorklund and Koivunen 2005; Nikkola, Vihinen et al. 2005). A series of studies show the expression of MMPs can be induced by interacting tumor cells and stromal cells, and those proteinases, in turn, could promote tumor progression (Crawford and Matrisian 1994). For example, co-cultures of prostate cancer cells with fibroblasts can induce pro-MMP-9 expression in prostate cancer cells, although pro-MMP-9 was expressed by both cell types at a very low level when cultured alone (Dong, Nemeth et al. 2001).

Gelatinase A and B have been highly expressed in cancer tissues and their roles in facilitating tumor progression have been widely studied. MMP-2 and MMP-9 are expressed by stromal cells in the tumor. Significant increases in levels of gelatinase expression have been observed from tumor cells in culture to primary tumors and to metastasis in animal models. Elevated gelatinase expressions in cancers correlate with increased invasiveness, metastasis, and decreased overall survival (Deryugina and Quigley 2006). The level of MMP-2 and MMP-9 were significantly increased in metastatic tumors in an orthotopic murine model of head and neck cancer (Dasgupta, Bhattachaya-Chatterjee et al. 2006). Overexpression of MMP-9 has also been found in the high metastatic potential of rat osteosarcoma cell lines (Kido, Tsutsumi et al. 1999). Expression of MMP-2 and MT1-MMP is correlated with tumor progression both in the xenograft model and in human melanocytic lesions. In the rat model of spontaneous metastasis, MMP-9 was involved in the development and extent of metastases in the lung and lymph nodes (Nakajima, Welch et al. 1993). In breast cancer, although the role of MMP-9 in clinical progression of breast carcinoma is still unclear, MMP-2 has been extensively studied (Turpeenniemi-Hujanen 2005). MMP-2 has been detected in breast carcinoma and high expression of MMP-2 is associated with shortened survival (Jezierska and Motyl 2009). MMP-2, together with some proteins, for example bone sialoprotein, can promote the metastasis process (Jezierska and Motyl 2009). Gelatinases are also related to uterine cervical

carcinoma. The expression and activities of gelatinases are highly up-regulated in pre-cancer and cancer lesions of the uterine cervix (Libra, Scalisi et al. 2009). In addition, MMP-2 and MMP-9 are expressed in stromal cells and inflammatory cells around tumors, which play vital roles in further production of various growth factors, proteinase, cytokines, and angiogenic factors, resulting in the progression of cancer (Libra, Scalisi et al. 2009).

A great number of studies have indicated that MMPs, particularly MMP-9, are involved in tumor-induced angiogenesis, which is necessary for growth of solid tumors to the size when they become invasive and capable of generating metastasis (Stetler-Stevenson 1999; Bergers and Benjamin 2003). MMP-9 has also been identified as a functional component of the angiogenic switch in RIP1-Tag2 transgenic mice mode and is the vital enzyme for development of angiogenic vasculature (Bergers, Brekken et al. 2000).

1.5.2 Cardiovascular diseases

It is well accepted that gelatinases are associated with most cardiovascular diseases, including atherosclerosis, coronary syndrome, and coronary restenosis (Jones, Sane et al. 2003; Raffetto and Khalil 2008). For example, MMP-2 is expressed in atherosclerosis, aneurysm, and myocardial infraction (Goodall, Crowther et al. 2001; Spinale 2002). The roles of gelatinases in cardiovascular diseases are very complicated because they are involved in many events of cardiovascular diseases in both positive and negative ways, including intimal thickening, limiting plaque growth and promoting a stable plaque, platelet aggregation, and plaque rupture (Fernandez-Catalan, Martinz-Cuesta et al. 1999; Jones, Sane et al. 2003; Reel, Oktay et al. 2009).

In murine models, inhibition of MMP-2 prevents cardiac rupture, protects the ECM degradation, and delays the phagocytic removal of infarcted myocardium by macrophages (Matsumura, Iwanaga et al. 2005). MMP-9 has a similar role in cardiac rupture after myocardial infarction (Romanic, Harrison et al. 2002). The fragments

of fibronectin and laminin cleaved by MMP-2 are considered as the key factors to promote macrophage accumulation in the infarcted myocardium (Matsumura, Iwanaga et al. 2005). In addition, significantly higher levels of MMP-2 and MMP-9 were observed in smooth muscle cells isolated from abdominal aortic aneurysms than cells obtained from normal arterial tissues and the increased MMP-9 expression may contribute to the expansion of abdominal aortic aneurysms (Patel, Melrose et al. 1996; McMillan, Tamarina et al. 1997). The increase of MMP-9 expression observed in the coronary atherectomy specimens from patients with unstable angina and the correlation of severity of coronary atherosclerosis with a MMP-9 promoter polymorphism associated with increase of MMP-9 expression demonstrates MMP-9 has the ability to modulate the expansion and severity of plaque (Brown, Hibbs et al. 1995; Zhang, Ye et al. 1999). ApoE knockout mice deficient in MMP-9 had impaired macrophage infiltration, reduced atherosclerosis, decreased collagen deposit, and plaque disruption has been induced by retroviral overexpression of active MMP-9 in macrophages of atherosclerotic lesions of mice, illustrating the key roles of MMP-9 in these diseases (Luttun, Lutgens et al. 2004; Gough, Gomez et al. 2006). MMP-2 and MMP-9 are also involved in the stenosis after balloon injury of the vascular wall. For example, increased MMP-2 expression was determined in the neointima after balloon injury to the rat carotid artery, and increased expression of MMP-2 and MMP-9 were found in carotid pig arteries (Southgate, Fisher et al. 1996; Jenkins, Grow et al. 1998). In heart diseases, deletion of MMP-9 decreases collagen accumulation and improves the left ventricular function by altering remodelling (Ducharme, Frantz et al. 2000). These studies provide evidence that gelatinase could be 'bad' for cardiovascular diseases.

On the other hand, many studies have demonstrated that gelatinases could play protective roles in cardiovascular diseases. ApoE/MMP-9 double knockout mice showed a significant increase of brachiocephalic cartery plaques and the number of buried fibrous layers and exhibited cellular compositional changes, demonstrating

the protective roles of MMP-9 in limiting plaque growth and promoting plaque stability (Johnson, George et al. 2005).

Due to the ability of gelatinase in degrading components of blood vessel ECM, their activities are required to be tightly regulated in normal arteries. Numerous studies have been carried out to investigate impacts of inhibition of MMP activities on cardiovascular diseases using natural inhibitors and non-specific inhibitors. However mixed results were obtained from these experiments. Inhibition of MMP by Batimastat in pigs significantly reduced late luminal loss following balloon angioplasty, demonstrating MMP inhibition reduce constrictive arterial remodelling, whereas neointima formation was not inhibited (De Smet, De Kleijn et al. 2000). Yet another study with RO113-2908, a broad-spectrum MMP inhibitor, to iliac artery angioplasty and stenting in atherosclerotic cynomolgus monkeys showed no reduction in intimal hyperplasia or constrictive remodelling (Cherr, Motew et al. 2002). The reason for the differences in results is that these inhibitors are non-selective and provide little insight into the role of individual MMPs in cardiovascular diseases. However, the results affirm the contribution of MMPs on cardiovascular diseases progression.

1.5.3 Inflammatory bowel disease

Inflammatory bowel disease (IBD), including ulcerative colitis (UC) and Crohn's diseases (CD), is a chronic, relapsing condition with inflammation and tissue remodelling of the gastrointestinal tract. Many people believe that the dysregulated response of the intestinal immune system results in the activation and release of several factors, including cytokines, nitric oxide, and proteolytic enzymes, which lead a cascade of events resulting in intestinal injury (Podolsky 2002). Interestingly, MMPs are expressed in different connective tissue cells in response to proinflammatory cytokines, such as TNF-α (Sternlicht and Werb 2001). Moreover, increased levels of MMPs have been detected in homogenates of inflamed tissues of IBD patients (Naito and Yoshikawa 2005).

The role of MMP-2 in IBD is complicated. In IBD, MMP-2 is up-regulated in patients suffering from pouchitis, inflammation of ileoanal pouch anastomsis after proctocoletomy in ulcerative colitis patients (Stallmach, Chan et al. 2000). After treatment with metronidazole for six weeks, MMP-2 expression was significantly decreased in the patients, with the corresponding improvement of clinical symptoms (Stallmach, Chan et al. 2000). However, MMP-2 has been found to play a protective role in the development of acute colitis possibly by contributing to barrier function (Garg, Rojas et al. 2006).

In fact, MMP-9 is the most abundantly expressed protease in inflamed tissues and is highly up-regulated in human IBD (Baugh, Perry et al. 1999). A significantly increased MMP-9 expression was clearly observed in patients with ulcerative colitis and Crohn's disease, demonstrating the correlation between gelatinase B and disease activities (Bailey, Hembry et al. 1999; Baugh, Perry et al. 1999). In Crohn's disease, abundant MMP-9 has also been detected in platelets, which is a major contributor for thrombosis and might facilitate platelet release, indicating MMP-9 is related to Crohn's disease-associated platelet hyperactivation and thrombosis (Menchen, Marin-Jimenez et al. 2009). In addition, MMP-9 may be involved in pathophysiological processes such as inflammation, fibrosis and development of fistulae in Crohn's disease (Kirkegaard, Hansen et al. 2004; Meijer, Mieremet-Ooms et al. 2007). MMP-9 has also been found to be responsible for tissue damage in IBD. MMP-9 null mice have shown a significantly reduced extent and severity of colitis (Castaneda, Walia et al. 2005). The Caco-2 cell line, an intestinal epithelia cell line which may produce several immunolodulatory substances, has shown increased expression and activity of MMP-9 when treated with TNF-α, resulting in loss of intestinal epithelium integrity and intestinal inflammation, suggesting overexpression of MMP-9 is a response to diverse inflammatory stimuli (Medina and Radomski 2006). In addition, MMP-9 has been found to impair wound healing and epithelia cell adhesion to appropriate matrices which is considered to be an

important component of would healing (Castaneda, Walia et al. 2005). All these studies together demonstrate that MMP-9 could be a target for treatment of IBD.

Besides, MMP-9 is also involved in other inflammatory diseases, such as rheumatoid arthritis, atherosclerosis, and asthma. For example, in MMP-9 knockout mouse model of asthma, there were significant decreases of lymphocytic inflammation and peribronchial mononuclear cell infiltration, suggesting the importance of MMP-9 in the development of airway inflammation after allergen exposure (Cataldo, Tournoy et al. 2002).

Apart from these three aspects, gelatinases are reported to be involved in many other diseases. The expression of MMP-9 has also been detected in neurological diseases. MMP-9 deficient mice were significantly less susceptible to the development of experimental autoimmune encephalomyelitis and showed a decrease in neutrophil infiltration (Dubois, Masure et al. 1999). MMP-2 and MMP-9 have been proved to be associated with arthritis. These two enzymes, along with MMP-13, can degrade the non-collagen matrix components of the joints and play a role in osteoclastic resorption in pathological conditions (Murphy and Nagase 2008).

1.6 Differences between MMP-2 and MMP-9

MMP-2 and MMP-9 are both gelatinases which share structure and substrate similarity and both have epithelial origins, but there are significant and emerging differences between the two proteins.

The major difference in the structure of gelatinases is MMP-9 has additional type V collagen-like domain that is highly glycosylated and MMP-2 has a short loop separating the hemopexin domain from the catalytic domain. This glycosylated domain changes MMP-9 substrate specificity and protects MMP-9 from being degraded by TIMPs (Ravi, Garg et al. 2007). Besides, there are some differences in catalytic domain that affect the substrate binding and are useful for designing gelatinase inhibitors (Tochowicz, Maskos et al. 2007).

A great number of studies have been performed and focused on the biological functions of gelatinases in physiological and pathological conditions. It has been shown that MMP-2 and MMP-9 have totally different functionalities. Studies showed that MMP-2 and MMP-9 have some overlapping roles in cancer progression. However, it has been reported that the roles of MMP-9 distinguish it from MMP-2 in many disease, even in the same processes. MMP-9, but not MMP-2 may be involved in the pathogenesis of IBD. The proteins have distinct effects on the development of acute colitis. In the rat model of colitis induced by trinitrobenzene sulfonic acid (TNBS), MMP-9 is the main MMP involved in TNBS-induced colitis, but the level of MMP-2 was unaltered (Medina and Radomski 2006). In addition, in both a chemical- and bacteria-induced acute colitis model of mice, MMP-$2^{-/-}$ mice are highly susceptible to the development of colitis, while MMP-$9^{-/-}$ mice are protected from the development of acute colitis (Garg, Rojas et al. 2006). MMP-2 may promote vasoconstrictor effects of some vasoactive peptides, an effect not shared by MMP-9 (Fernandez-Catalan, Stewart et al. 2000). MMP-2 and MMP-9 also play different roles in platelet aggregation. It has been found that MMP-2, released from platelets, can mediate platelet aggregation (Sawicki, Salas et al. 1997). The clear mechanism of stimulating platelet aggregation by MMP-2 is still unknown, but it is believed that the ability of MMP-2 to increase GPIb abundance in platelets amplifies the pro-aggregatory effects of different agonists facilitating platelet aggregation (Santos-Martínez, Medina et al. 2007). However, human platelet released MMP-9 exerts inhibitory effects on platelet aggregation stimulated by collagen (Sheu, Fong et al. 2004). In addition, MMP-2 and MMP-9 have different activation pathways and storage mechanisms and they promote tumour angiogenesis by distinct mechanisms (Deryugina and Quigley 2006; Martin and Matrisian 2007).

1.7 MMP inhibitors

Since MMPs play important roles in both physiological and pathological conditions, including tumor invasion, inflammatory reactions, and metastasis, therapeutic inhibition of MMP activities is a promising approach for treatment of various diseases.

Modulation of MMP regulation is possible at several different biochemical sites on the enzyme, but the direct inhibition of enzyme action provides a very attractive target for therapeutic intervention. Inhibition of the various MMPs has proven to be an active area of research for the past 30 years. With the elucidation of a large number of MMP crystal structures and NMR studies since 1994, subtle differences in the active site of MMPs have been revealed and exploited in the design of specific inhibitors (Rao 2005). A large number of potent inhibitors have been discovered and tested in clinical trials for cancer therapy or arthritis.

Different classes of MMP inhibitors, including hydroxamic acids, carboxylates and thiols have all been documented. Most of these entities mimic the peptides that normally bind to the Zn catalytic site of the MMPs in a similar way to that of the corresponding peptide substrates. An essential component of any MMP inhibitor may be a zinc binding group.

1.7.1 Hydroxamic acids

Hydroxamic acids are one of the first generation of MMP inhibitors designed to attach zinc-binding group (ZBG). Hydroxamates are the most popular MMP inhibitors developed by pharmaceutical companies due to their extreme potency. Many hydroxamates have entered clinical trials including batimastat, marimastat, Solimstat, Ro32-3555, and MMI-270. In the hydroxamate inhibitors, the hydroxylation group provides two oxygen atoms to bind to zinc at the catalytic site while the nitrogen atom binds to the alanine residue on the enzyme and the substitutions on the hydroxamate can fit into the different pockets to improve the binding affinity and selectivity (Fig. 1.7). Based on the substitutions on the hydroxamic acid, this category of inhibitors can be divided into a number of subgroups.

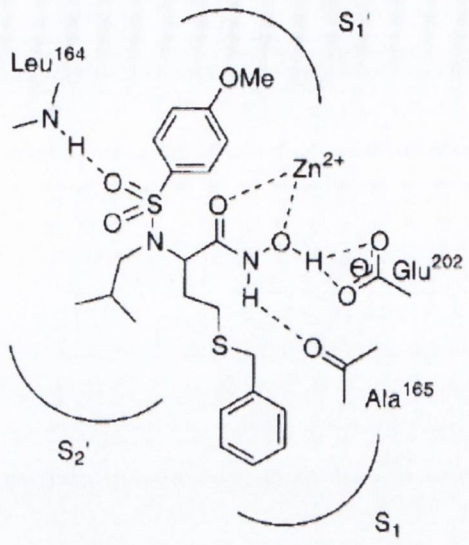


Figure 1.7. *Proposed model of 4-benzylsulfanyl-N-hydroxy-2-[isobutyl-(4-methoxy-benzenesulfonyl)-amino]-butyramide binding with the active site of MMP-3 from docking stimulation (adapted from (Hanessian, Moitessier et al. 2001)). The two oxygen atoms and hydrogen atom in the hydroxylation group bind with the active zinc and glu residues, respectively. In addition the N-H atom binds with Ala165 residue. The side chains of S-benzyl, isobutyl, and methoxyphenyl fit into three different pockets.*

The first subgroups are phosphonamide-based hydroxamic acid inhibitors. The potency of these inhibitors is mainly based on the electronic environments of the phosphorus atom. The substitutions on the phosphonamide group fit in to the right side pockets of the active zinc i.e. S1', S2' and S3' (Fig. 1.8). Therefore, changing the positive charge on phosphorus atom would result in a change of potency. A great number of phosphonamide-based hydroxamate inhibitors have been synthesized and the inhibitory effects were evaluated against various matrix metalloproteinase to improve the potency and selectivity. A number of studies have shown that substitutions on the phosphorus atom, fit into different pockets of MMPs, significantly affect the inhibition potency and selectivity of MMP-1, -3, and -9 (Table 1). The results show the change of substitutions on S1/S2, S1', and S2'/S3' can dramatically enhance biding affinity on enzymes.

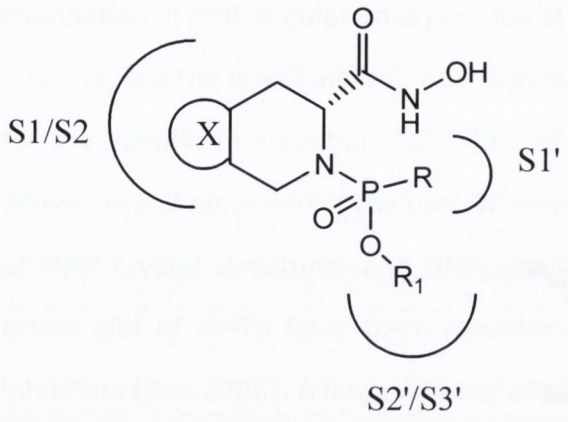


Figure 1.8. *Binding of phosphonamide-based hydroxamate inhibitors to MMPs (Sawa, Kiyoi et al. 2002).*

Table 1.1. *List of phosphonamide-based hydroxamic acid inhibitors.*

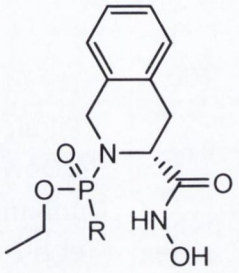
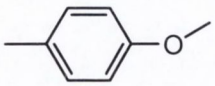
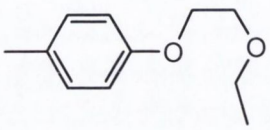
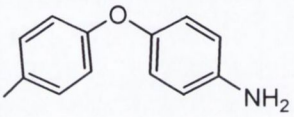
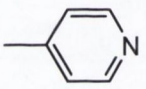
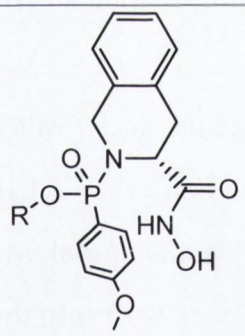
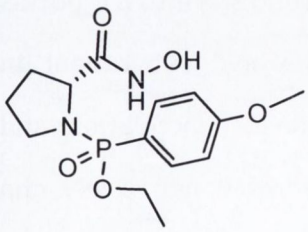
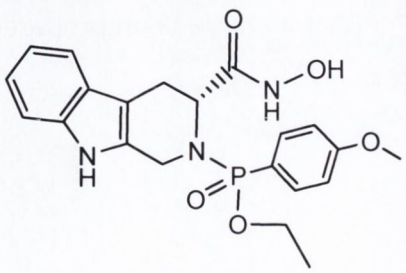
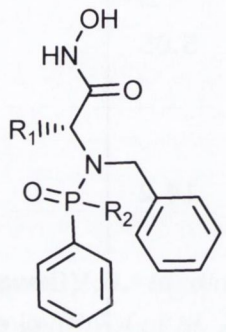
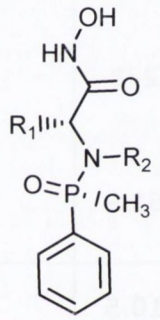
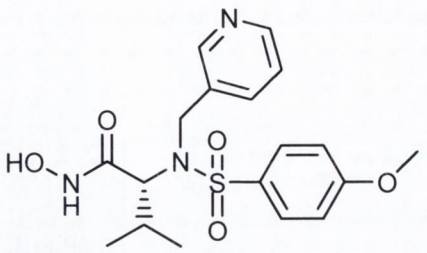
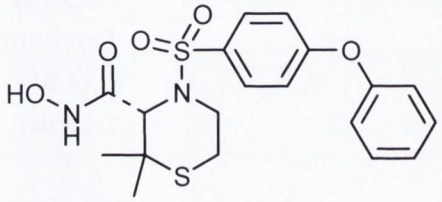
Structure	R	K_i (nM)			Ref.
		MMP-1	MMP-3	MMP-9	
		4.58	5.20	5.05	(Sawa, Kiyoi et al. 2002)
		>850	29.6	14.2	
		6.50	0.50	0.10	
		17.4	190	278	
		0.97	64.4	51.9	
	CH_2CH_2F	10.5	9.07	10.5	(Sawa, Tsukamoto et al. 2002)
	CH_2CHF_2	6.00	6.67	4.97	
	CH_2CF_3	6.57	6.57	3.68	
	$CH_2CH_2CF_3$	2.21	3.33	4.46	
		>850	527	316	(Sawa, Kiyoi et al. 2002)
		2.02	1.04	1.13	

Table 1.1 *contd.*

Structure	R_1	R_2	IC_{50} (nM)		Ref
			MMP-1	MMP-3	
	Me	Ph	6790	10300	(Pikul, McDow Dunham et al. 1999)
	Me	Et (S)	33300	49300	
	Me	Et (R)	608	700	
	CH_2i-Pr	Me (S)	7120	917	
	CH_2i-Pr	Me (R)	20.5	24.4	
	H	$(CH_2)_2C_6H_5$	525	700	
	CH_3	$CH_2C_6H_5$	120	67.9	
	CH_3	n-C_6H_{13}	1290	1600	
	CH_2i-Pr	H	2510	2550	

Another important subgroup is the sulphonamide-based hydroxamic acids, which among the most extensively developed MMP inhibitor group. The first orally active inhibitor from this subgroup of compounds was CGS 27023A. This inhibitor shows strong inhibitory ability on MMP-1, -9, and -13. The binding of CGS 27023A with the MMP is shown in Fig. 1.9, in which the methoxyphenyl group sits into S1′ pocket and the pyridine ring points to the S2′ pocket. The isopropyl substituent in the compound protects the hydroxamic acid from metabolic deactivation and the 3-pyridyl side chain may aid partitioning into the hydrated negatively charged environment of cartilage (Macpherson, Bayburt et al. 1997; Whittaker, Floyd et al. 1999). A great number of sulphonamide-based MMP inhibitors have been prepared and many of them exhibit great inhibitory effects on MMPs (Table 1.2).

Table 1.2 *Sulphonamide-based inhibitors of MMPs.*

Structure	K_i (nM)	Ref.
	MMP-1 = 33; MMP-2 = 20; MMP-3 = 43; MMP-9 = 8	(Macpherson, Bayburt et al. 1997)
	IC_{50} (nM): MMP-1 = 8.3 MMP-2 =0.08 MMP-3 = 0.27; MMP-7 = 54; MMP-9 = 0.26; MMP-13 = 0.4	(Skiles, Gonnella et al. 2004)

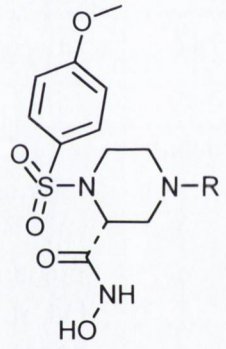
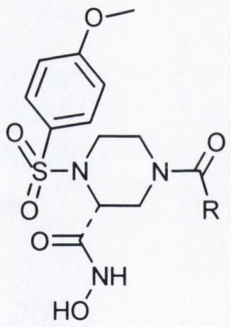
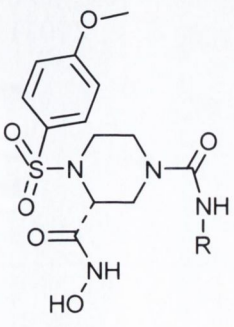
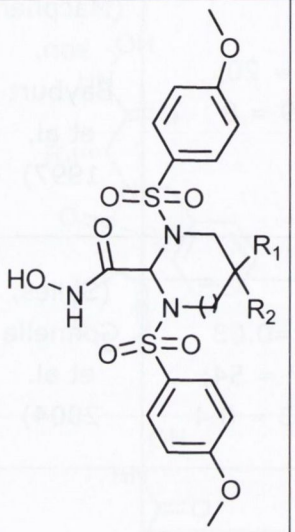
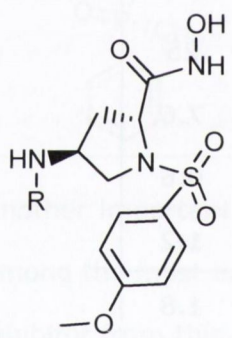
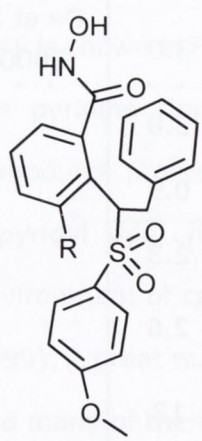
	R	IC_{50} (nM)				Ref.
		MMP-1	MMP-3	MMP-7	MMP-9	
	Me	1260	269	>10000	25	(Cheng, De et al. 2000)
	Bn	324	75	14000	7.6	
	$MeSO_2$-	8.0	3.5	483	0.6	
	BOC	81	60	1460	1.2	
	Me	73	18	821	1.8	
	n-C_5H_{11}	115	39	787	1.7	
	CH_2Ph	92	9.5	908	3.0	
	Ph	81	66	1522	3.0	
	Ph-Ph	43	23	931	0.9	
	H	115	20	537	2.3	
	n-C_6H_{13}	30	28	497	2.6	
	CH_2Ph	99	17	1200	13	
	CH_2CH_2Ph	70	27	824	3.6	
	m-MeOPh	80	13	1100	4.1	

Table 1.2 *contd.*

Structure	n	R_1,R_2	IC_{50} (nM)			
			MMP-1	MMP-3	MMP-7	
	0	H,H	4650	1060	n.d.	(Pikul, McDow Dunham et al. 1998)
	1	H,H	79	33	460	
	2	H,H	827	1290	n.d.	
	1	H,OH	51	41	366	
	1	Me,Me	24	18.4	30	
	1	-S(CH_2)$_3$S-	79	19.5	123	

Structure	R	IC_{50} (nM)				
		MMP-1	MMP-3	MMP-7	MMP-13	
	H	250	23	4300	5	(Natchus, Booklan d et al. 2000)
	-(CH_2)$_2$$CH_3$	150	87	2200	5	
	-(CH_2)$_2$Ph	560	57	1400	1	
	-SO_2CH_3	260	42	2700	2	
	-CONHMe	3100	300	n.d.	27	

Structure	R	IC_{50} (nM)			
		MMP-1	MMP-9	MMP-13	
	H	639	650	555	(Levin, Du et al. 2001)
	CH_3	115	23	50	
	OCH_3	520	23	138	
	Cl	38	31	n.d.	
	NO_2	202	13	42	
	$OCCH_2CONHOH$	24	2	1	
	OC(CH_3)2CONHOH	597	4	6	

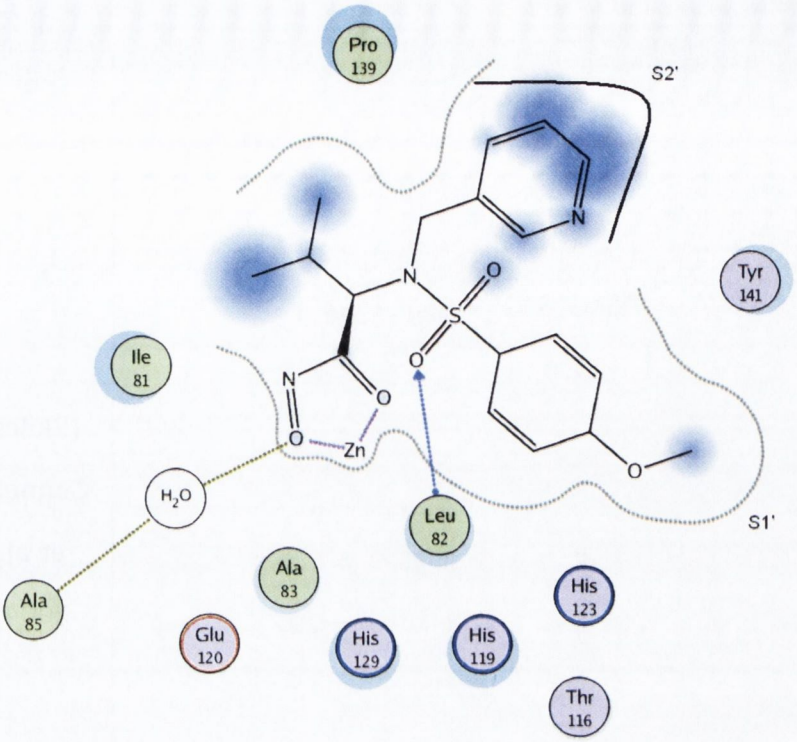
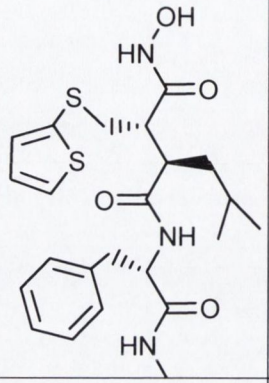
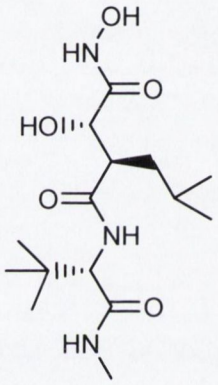


Figure 1.9. *The interaction of MMP-12 with CGS 27023A. The picture was generated by the programme MOE based on the crystal structure of MMP-12 (pdb code: 1jiz).*

Succinate-based hydroxamic acids are important MMP inhibitors. Like most hydroxamic acids, they exhibit potent MMP inhibition (Table 1.3). Batimastat and marimastat are first generation MMP inhibitors exhibited broad-spectrum MMP inhibition. Although they show low nanomolar potency against MMPs, the inhibition on cellular TNF-α release is modest. Thus a new succinate-based inhibitor series based on the structure of marimastat were synthesized to increase inhibitory activities for cellular TNF-α release (Kottirsch, Koch et al. 2002). After the modification, the IC_{50} values of cellular TNF-α release were significantly decreased (Fig. 1.10) (Kottirsch, Koch et al. 2002).

Table 1.3 *Succinate-based MMP inhibitors.*

<table>
<tr><th>Structure</th><th colspan="5">IC_{50} (nM)</th><th>Ref.</th></tr>
<tr><td>  </td><td colspan="5">MMP-1 = 10; MMP-2 = 4;
MMP-3= 20; MMP-8 = 10;
MMP-9 = 1; MMP-13 = 3

BB-94</td><td rowspan="2">(Skiles, Gonnella et al. 2004)</td></tr>
<tr><td>  </td><td colspan="5">MMP-1 = 5; MMP-2 = 6;
MMP-3= 200; MMP-7 = 20;
MMP-8 = 2; MMP-9 = 3;
MMP-13 = 12

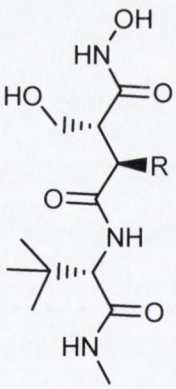
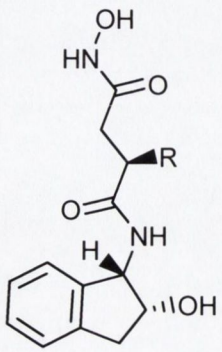
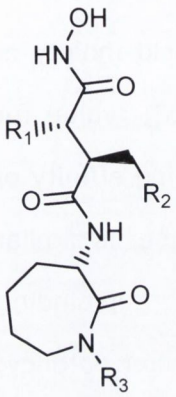
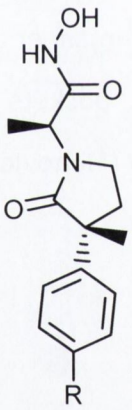
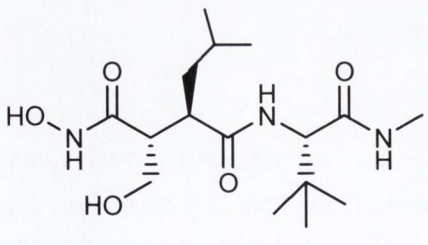
BB-2516</td></tr>
<tr><td rowspan="5">  </td><td rowspan="2">R</td><td colspan="4">K_i (nM)</td><td rowspan="5">(Kottirsh, Koch et al. 2001)</td></tr>
<tr><td>MMP-1</td><td>MMP-2</td><td>MMP-3</td><td></td></tr>
<tr><td>iso-butyl</td><td>0.6</td><td>0.3</td><td>9.8</td><td></td></tr>
<tr><td>phenyl</td><td>3.5</td><td>4.8</td><td>13.2</td><td></td></tr>
<tr><td>4-methyl-phenyl</td><td>2.0</td><td>0.3</td><td>15.2</td><td></td></tr>
<tr><td>4-methoxy-phenyl</td><td>1.1</td><td>0.5</td><td>0.9</td><td></td></tr>
<tr><td rowspan="5">  </td><td rowspan="2">R</td><td colspan="4">K_i (nM)</td><td rowspan="5">(Yao, Wasserman et al. 2001)</td></tr>
<tr><td>MMP-1</td><td>MMP-2</td><td>MMP-8</td><td>MMP-9</td></tr>
<tr><td>4-OH-Bn</td><td>946</td><td>408</td><td>70</td><td>166</td></tr>
<tr><td>i-butyl</td><td>82</td><td>73</td><td>37</td><td>162</td></tr>
<tr><td>4-OMe-Bn</td><td>1163</td><td>52</td><td>9.2</td><td>203</td></tr>
<tr><td>3-OH-Bn</td><td>30953</td><td>1507</td><td>8600</td><td>3324</td></tr>
</table>

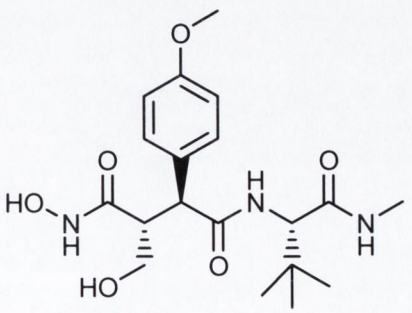
Table 1.3 *cond.*

Structure	R_1	R_2	R_3	IC_{50} (nM)		Ref.
				MMP-1	MMP-3	
	H	*i*-Pr	CH_2CO_2Me	225	11,900	(De, Natchus et al. 1999)
	H	*n*-pentyl	CH_2CO_2Me	129	2900	
	H	*n*-heptyl	CH_2CO_2Me	10	1040	
	Me	*n*-heptyl	$(CH_2)_2OMe$	112	30	
	n-propyl	*i*-Pr	$(CH_2)_2OMe$	83	94	
	3-hydroxy propyl	*i*-Pr	$(CH_2)_2OMe$	72	102	
	3-dimethyl amino	*i*-Pr	$(CH_2)_2OMe$	237	1410	

	R	K_i (nM)			(Duan, Chen et al. 2002)
		MMP-1	MMP-2	MMP-9	
	methoxy	92	4.8	9	
	allyloxy	335	14	11	
	benzyloxy	>5000	19	29	
	phenoxy	143	<2.8	<2.1	
	2-nitrobenzyloxy	>5000	35	66	
	4-nitrobenzyloxy	>5000	11	40	



TNFα IC_{50} = 1606 nM



TNFα IC_{50} = 48 nM

Figure 1.10. *The inhibition of cellular TNF-α release by modified marimastat.*

1.7.2 Carboxylates

Apart from hydroxamates, many carboxylate compounds exhibit MMP inhibition and some of them have entered clinical trials including BAY 12-9566 and S-3304. Generally, the potency of carboxylate-based MMP inhibitors is weaker than of hydroxamic acids, for example, directly changing the hydroxamic acid moiety of CGS 27023 to carboxylic acid leads to a 50-fold increase of the IC_{50} value for MMP-13 (Monovich, Tommasi et al. 2009). It indicates that the binding affinity of carboxylates to the active zinc is relative weaker. Their binding manner is similar with that of hydroxamates, with two oxygen atoms in the carboxylate group binding with the active zinc and glu residue. Although carboxylates have weaker potency, some of them show great selectivity, exemplified by piperidine-based carboxylic acids, which exhibit nanomolar potency against MMP-13 and greater than 20,000-fold *in vitro* selectivity for MMP-13 over MMP-1 (Monovich, Tommasi et al. 2009). The two side chains of those compounds fit well into S1 and S1' pockets of MMP-13, which may result in their selectivity for the enzyme (Fig. 1.11) (Monovich, Tommasi et al. 2009).

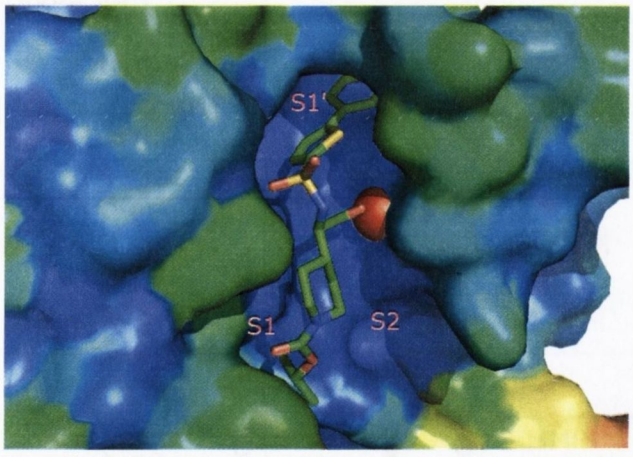
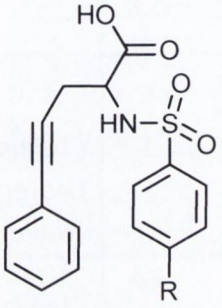
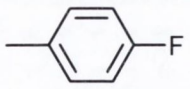
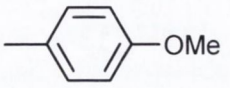
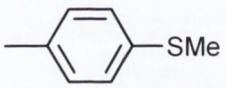
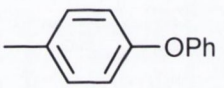
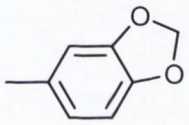
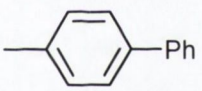
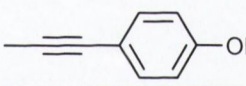


Figure 1.11. Picture of a caboxylate compound binding with MMP-13 (Monovich, Tommasi et al. 2009). It was generated by the programme PyMOL® based on the crystal structures of MMP-13 (PDB code 3ELM). The oxygen atoms on the carboxylate group bind into the active zinc (shown as red).

Table 1.4 *Carboxlate inhibitors of MMPs.*

Structure	R	IC_{50} (nM)			Ref.
		MMP-1	MMP-2	MMP-13	
		5600	175	2150	(Natchus, Booklan d et al. 2001)
		2000	12	21	
		631	6	16	
		>10000	1475	2146	
		10300	29	104	
		>10000	29	59	
		>10000	9	35	

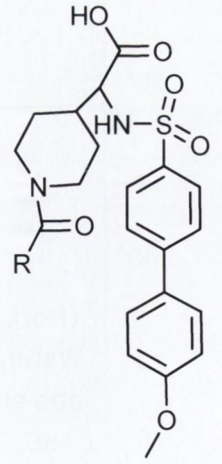
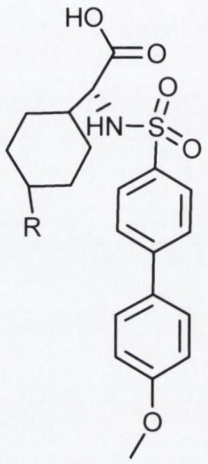
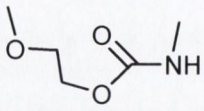
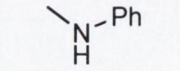
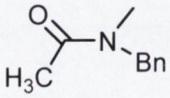
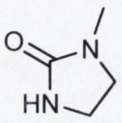
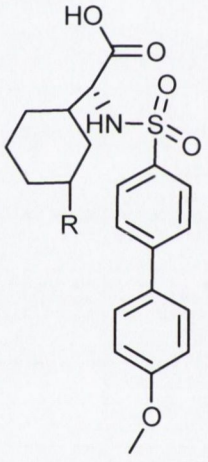
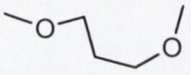
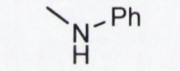
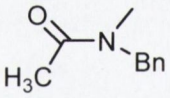
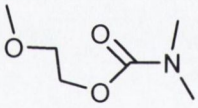
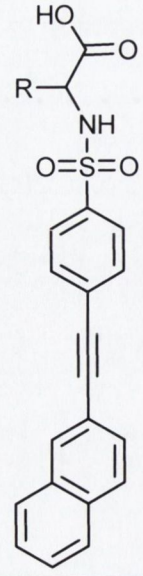
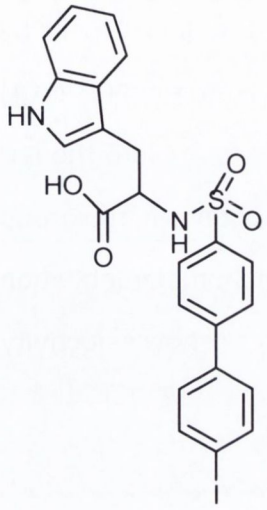
	R	MMP IC_{50} (nM)					(Pikul, Ohler et al. 2001)
		1	2	3	8	9	
	OMe	5210	2.8	657	6.7	176	
	OEt	2760	1.0	162	2.7	94.9	
	O*i*-Pr	1400	<0.4	41.8	1.5	11.7	
	(***R***)O*t*-Bu	1370	<0.4	33.7	1.5	6.6	
	(***S***)O*t*-Bu	3490	7.2	345	3.0	71.5	
	CH_2*i*-Pr	4900	3.2	739	5.3	137	
	OCH_2CH_2OMe	8.1	<0.4	13.8	0.5	<0.4	

Table 1.4 *contd.*

Structure	R	MMP IC_{50} (nM)					Ref.
		1	2	3	7	13	
		4183	5	520	9128	17	(Tuillis, Laufersweiler et al. 2001)
		8270	12	1340	20498	26	
		284	0.6	26	845	0.8	
		4785	1	98	3307	1	
		3780	9	630	>10000	13	
		2190	5	250	5470	8	
		5350	6	210	6340	16	
		4730	8	230	>10000	11	
	R	MMP IC_{50} (nM)					
		2	8	9	12	13	
		400	570	770	7.6	300	(Hori, Watanabe et al. 2000)
	(***R***)*i*-Pr	110	1060	330	14	14	
	(***s***)*i*-Pr	400	570	770	760	76	
	(***s***)Me	570	2440	3280	16	16	
	CH_2CH_2MeS	110	1320	620	10	10	

Another example is a α-position substituted by an iodo-bisphenyl-sulphonylamino and a methylindolyl group, which has been prepared as an iodine-123-labeled, gelatinase specific inhibitor (Fig. 1.12) (Oltenfreiter, Staelens et al. 2004).



IC_{50} (nM)

MMP-2 = 9.3

MMP-9 = 201

MMP-14 = 859

MMP-15 = 679

Figure 1.12. *IC_{50} values of 3(1H-indol-3-yl)-2-(4'-iodo-biphenyl-4-sulphonylamino)-propionic acid.*

1.7.3 Thiols

Thiol-based MMP inhibitors contain a sulfur group which is able to bind to the active zinc (Fig. 1.13) (Gram, Reinemer et al. 1995). Most thiol inhibitors have a carbonyl group close to the sulfur atom, which can improve the binding affinity between the inhibitors and protein due to the extra interaction of the zinc with the carbonyl group. BMS-275291, or D-2163, is potent broad-spectrum MMP inhibitor which showed good inhibitions on several MMPs including MMP-1, -2, -3, -7, -8, -9, -13, and -14 (Table 1.5) (Naglich, Jure-Kunkel et al. 2001). The compound has entered in to Phase III clinical studies. In the preclinical studies, the compound has not shown musculoskeletal side effects, despite the compound does not have significant inhibition on TNF-α converting enzyme (TACE), which is believed to result in the failure of the first generation MMP inhibitors in clinical trials (Skiles, Gonnella et al. 2004). For this reason, more attentions has been paid to inhibition of TACE in recent developed MMP inhibitors including thiols. Thus, *Bandarage et al.* developed a new

group of thiol-based inhibitors, which posses inhibitions on both MMPs and TACE (Bandarage, Wang et al. 2008).

To improve the binding affinity with zinc, *Hurst et al.* have developed a new type of zinc binding thiol-based MMP inhibitors, mercaptosulphide, which chelat with zinc by two sulfur atoms unlike others interacted with sulpur and oxygen atoms (Fig. 1.14) (Hurst, Schwartz et al. 2005). The side chain of these compounds fits into the S1' and S2' pockets to gain better potency and selectivity. Most compounds in the group exhibit great potency on MMP-1, -2, -3, -7, 9, and -14 with low nanomolar inhibition constant values (Table 2.6). The compound MAG-42 and -292 also show selectivity on MMP-2 and MMP-9 against other MMPs, particularly MMP-3.

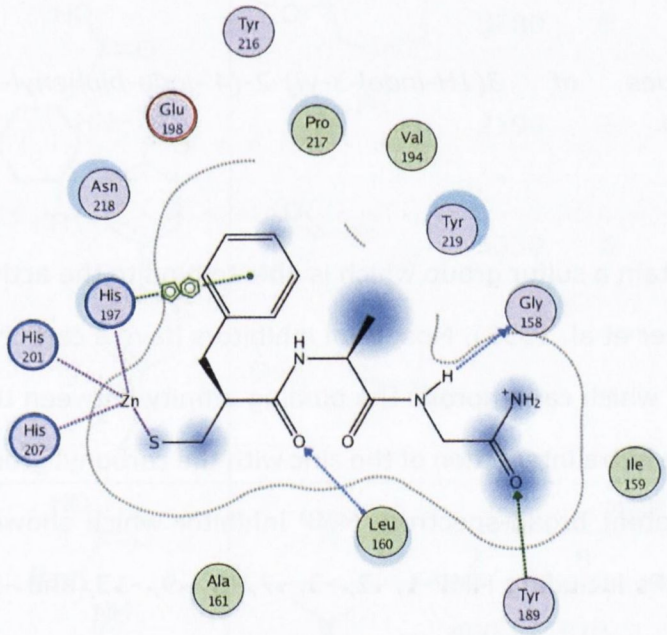
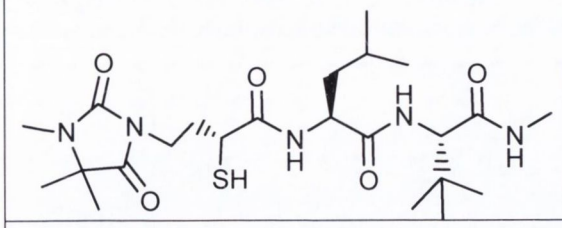
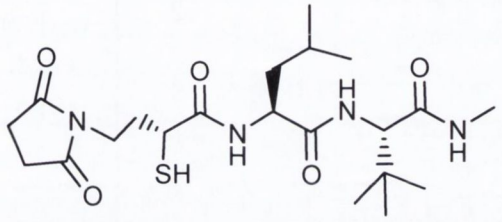


Figure 1.13 *The binding of a thiol compound with MMP-8 generated in MOE based on their crystal structure (pdb code 1jao).*

Table 1.5 *Thiol-based MMP inhibitors.*

<table>
<tr><th>Structure</th><th>IC₅₀ (nM)</th><th>Ref.</th></tr>
<tr><td>  </td><td>MMP-1 = 9; MMP-2 = 40;
MMP-3 = 160; MMP-7 = 25
MMP-9 = 30; MMP=14 = 40

D2163</td><td>(Naglich, Jure-Kunkel et al. 2001)</td></tr>
<tr><td>  </td><td>MMP-1 = 12; MMP-2 = 130;
MMP-3 = 381; MMP-7 = 36
MMP-9 = 53; MMP=14 = 58

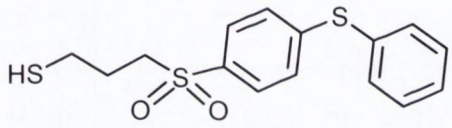
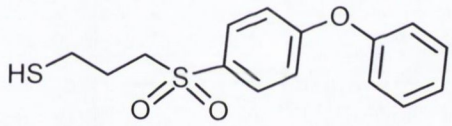
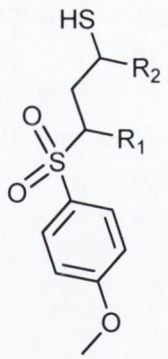
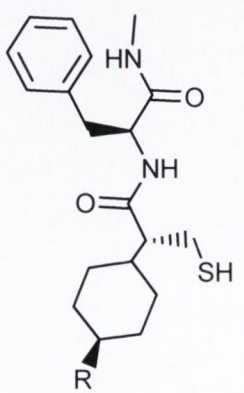
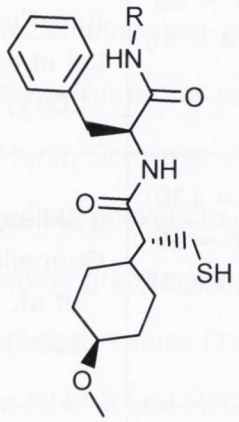
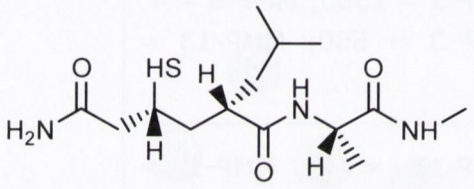
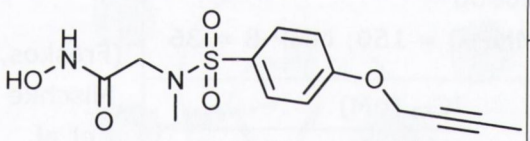
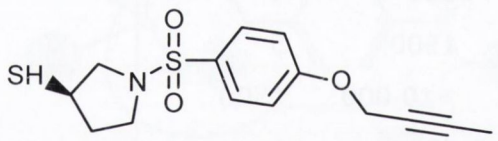
D1927</td><td>(Skiles, Gonnella et al. 2004)</td></tr>
<tr><td>  </td><td>MMP-1 = 1500; MMP-8 = 4
MMP-3 = 500; MMP-13 = 0.5</td><td rowspan="4">(Freskos, Mischke et al. 1999)</td></tr>
<tr><td>  </td><td>MMP-13 = 2; MMP-1 > 10000
MMP-3 = 150; MMP-8 = 36</td></tr>
<tr><td>  </td><td colspan="2"><table>
<tr><th>R1</th><th>R2</th><th>IC₅₀ (nM)
MMP-1</th><th>IC₅₀ (nM)
MMP-13</th></tr>
<tr><td>Et</td><td>H</td><td>600</td><td>4</td></tr>
<tr><td>Pr</td><td>H</td><td>1500</td><td>5</td></tr>
<tr><td>Ph</td><td>H</td><td>>10,000</td><td>1500</td></tr>
<tr><td>Bn</td><td>H</td><td>60</td><td>1</td></tr>
<tr><td>H</td><td>Me</td><td>8000</td><td>32</td></tr>
<tr><td>H</td><td>Bu</td><td>>10,000</td><td>45</td></tr>
</table></td></tr>
<tr><td>  </td><td colspan="2"><table>
<tr><th>R</th><th>IC₅₀ (nM)
MMP-1</th><th>IC₅₀ (nM)
MMP-3</th><th>IC₅₀ (nM)
MMP-9</th></tr>
<tr><td>OMe</td><td>110</td><td>926</td><td>35</td></tr>
<tr><td>OEt</td><td>700</td><td>640</td><td>18</td></tr>
<tr><td>OPr</td><td>6032</td><td>187</td><td>630</td></tr>
<tr><td>CF₃</td><td>669</td><td>4474</td><td>108</td></tr>
</table></td><td>(Fink, Carlson et al. 1995)</td></tr>
</table>

Table 1.5 *contd.*

Structure	R	IC_{50} (nM)			Ref.
		MMP-1	MMP-3	MMP-9	
	isopropyl	680	568	40	(Fink, Carlson et al. 1995)
	Cyclohexyl	2933	617	79	
	p-(F)-phenyl	2153	87	52	
	p-(Cl)-pheny	5909	113	79	
	p-(OCF_3)-pheny	>10000	175	81	
	3-pyridyl	135	73	17	
		MMP-1 = 480; MMP-2 = 3.0; MMP-3 = 280; MMP-7 = 14; MMP-8 = 1.1; MMP-9 = 2.3			(Sang, Jia et al. 2002)
		K_i (nM)			(Bandarage, Wang et al. 2008)
		MMP-2 = 27; MMP-7 = 3400 MMP-8 = 43; MMP-9 = 800 MMP-13 = 17; TACE = 10			
		MMP-2 = 5000; MMP-7 > 6000 MMP-8 = 1900; MMP-9 = 200 MMP-13 = 1200; TACE = 28			

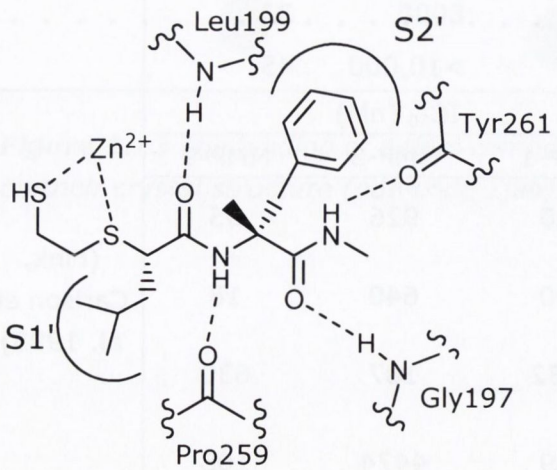
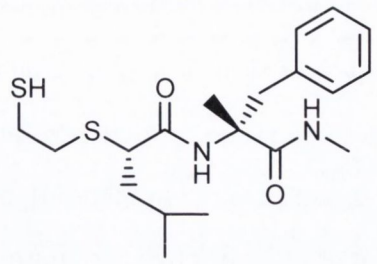
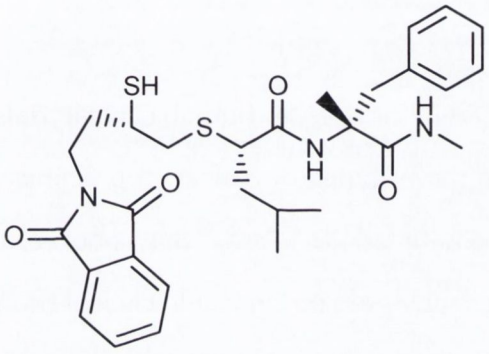
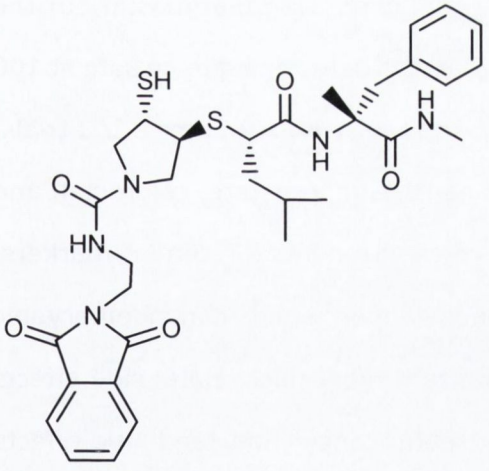


Figure 1.14. *The binding of MAG-182 with MMP-14 in schematic model.*

Table 1.6 *Ki values of mercaptosulphide inhibitors (Hurst, Schwartz et al. 2005).*

Structure	Identity	K_i (nM)
	MAG-42	MMP-1 = 52; MMP-2 = 0.28; MMP-3 = 250; MMP-7= 56; MMP-9 = 0.43;MMP-14 = 27
	MAG-292	MMP-1 = 0.95; MMP-2 = 0.77; MMP-3 = 22; MMP-7= 15; MMP-9 = 0.09;MMP-14 = 4.5
	YHJ-133	MMP-1 = 8.8; MMP-2 = 0.7; MMP-3 = 6; MMP-7= 6.5; MMP-9 = 1.1;MMP-14 = 1.2

Although hydroxamic acid based MMP inhibitors are extremely potent, their side effects and poor pharmacokinetic profiles, such as poor absorption and rapid metabolism, are the key factors for the failures in clinical trials. Because of these liabilities, non-hydroxamates MMP inhibitors have been brought into sight for researchers.

1.7.4 Clinical trials of MMP inhibitors

The design of MMP inhibitor has evolved over the last 20-25 years and mostly relies on structure-based design approaches rather than knowledge of the matrix protein sequences that are hydrolyzed by MMPs. Some MMP inhibitors have the ability to inhibit TNF-α release in all cells, tissues, and species examined both *in vitro* and *in vivo* (Gearing, Beckett et al. 1994). Therefore, many zinc binding MMP inhibitors have been tested in clinical trials for cancer and most of them are hydroxymate- and carboxylate-based compounds

Batimasat (BB-94) was the first synthetic MMP inhibitor to enter human clinical trials. It has been shown to inhibit MMP activities in many types of cancer in preclinical studies (Goss, Brown et al. 1998; Zervos, Shafii et al. 1999). But, poor oral bioavailability and unexpected side effects has supplanted batimasat in clinical trials. Thereof, a series of orally bioactive synthetic MMP inhibitors have been used in clinical trials. The first orally bioavailable MMP inhibitor was marimastat. In the phase I studies on healthy volunteers, marimastat was determined to be safe at 100 mg twice daily with few side effects (Milar, Brown et al. 1998). In phase I/II trials, marimastat was administered to patients with pancreatic, prostate, colorectal, and ovarian cancers to evaluate the change in measurements of tumor markers, including CA-19-9, CA-125, prostate-specific antigen, and carcinoembryonic antigen (Bloomston, Zervos et al. 2002). Significant musuculoskeletal side effects appeared after 28 days of treatment for pancreatic cancer and tendinitic effects were noted after 5 months of treatment in human cancer patients (Drummond, Beckett et al. 1999; Rosemurgy, Harris et al. 1999). These side effects have impacted on the development of marimastat.

A number of MMP inhibitors have been tested in the treatment of cardiovascular diseases. In a clinical trial for prevention of ventricular remodelling after myocardial infarction, PG-116800, a selective inhibitor of MMP-2, -3, -8, -9, -13, and -14 failed, although it had impressive outcomes in reduction of left ventricular volume along

with infarct zone collagen content in post-myocardial infraction in preclinical animal studies (Hudson, Armstrong et al. 2006). The failure of the test may be due to insufficient knowledge of determinants of left ventricular remodelling. Furthermore, PG-116800 may not be specific enough, although it has some extent selectivity.

Beside these compounds, many other broad-spectrum MMP inhibitors were evaluated in clinical trials for cancer therapy, but the results were disappointed (BAY 12-9566, AG3340, MMI-270) (Rao 2005). It is generally believed that the cause of these failures is that they are non-selective MMP inhibitors. Thus, numerous researches are focused on the synthesis of selective MMP inhibitors.

Although most of MMP inhibitors have been failed in the clinical trials of cancers, doxycycline hyclate, the only Food and Drug Administration approved collagenase inhibitors, has been successfully used in the treatment of periodontitis. The side effects, especially musculoskeletal syndrome side effects, does not appeared in the low dose doxycycline treated patients (Sorsa, Tjaderhane et al. 2006).

As different biological functions of MMP-2 and MMP-9 emerge, there is a growing demand for inhibitors capable of discriminating between MMP-2 and MMP-9 to investigate the actually roles of MMP-2/MMP-9 in the biological processes or diseases. Although the structures of MMP-2 and MMP-9 are very similar, there are some differences between the two proteins (Fig. 1.14). The first difference is in the S1′ pocket, where MMP-2 and MMP-9 have Thr227 and Arg424 respectively (Dhanaraj, William et al. 1999; Tochowicz, Maskos et al. 2007). The second one exists in the S2′ pocket, where MMP-2 has Ile222 and MMP-9 has Met 222. Attempts to design selective inhibitors between MMP-2 and MMP-9 has been long pursued, but with limited success due to their high sequence similarity.

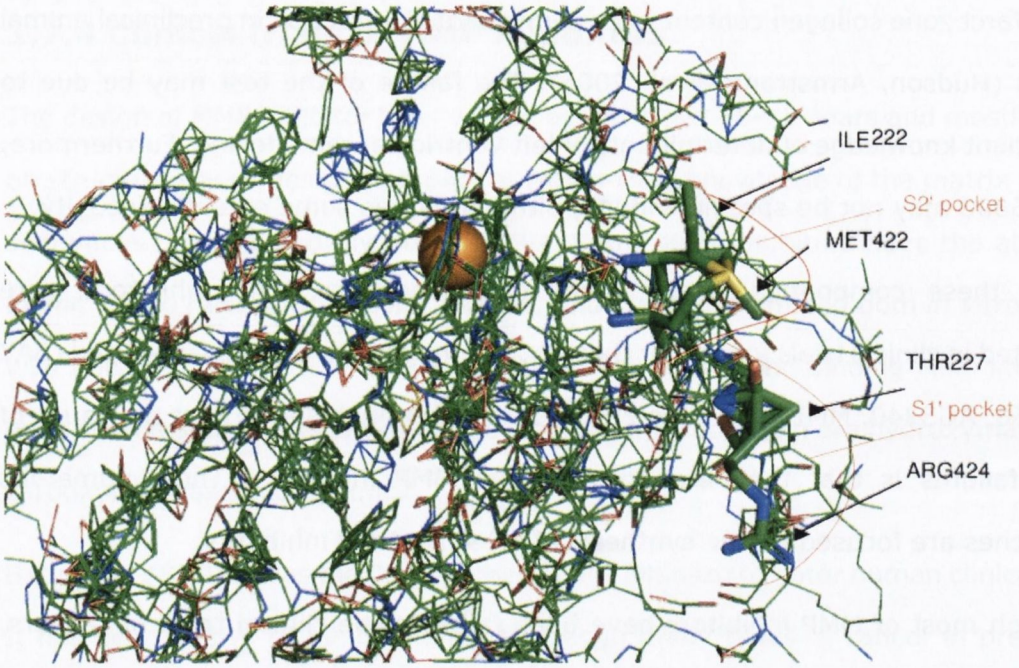


Figure 1.15. *The structure overlay of MMP-2 and MMP-9 with key residues. The picture was generated by the programme PyMOL® based on the crystal structures of MMP-2 (PDB code 1qib) and MMP-9 (PDB code 2ovx). The sequence differences in S1′ and S2′ pockets are highlighted.*

1.8 Aims and objectives

1.8.1 Aims

The aim of this project was to explore barbiturate-based inhibitors of gelatinases, using synthesis, enzyme assays and modelling.

1.8.2 Objectives

1. Design of inhibitors of gelatinases capable of discriminating between MMP-2 (gelatinase A) and MMP-9 (gelatinase B). We were especially interested in exploring differences at P2' for selectivity (Fig. 1.16), as this is where ILE and MET exchange occurs.

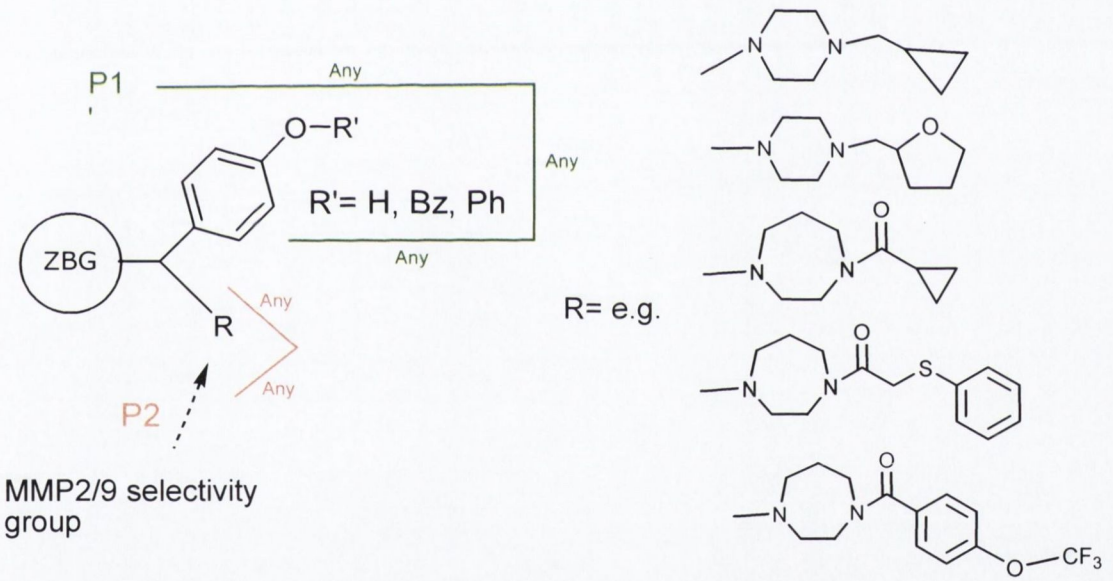


Figure 1.16. *The design of gelatinase selective inhibitors by exploring at P2 position.*

2. The design of inhibitors of MMPs that would be unable to undergo absorption and therefore be combined to the intestinal tract. Two approaches for that would be used— barbiturate dimers that would be too large for passive diffusion or by attachment of a large hydrophilic molecule.

3. Using the designed template to incorporate nitric oxide releasing group or other complementary pharmacological modalities into MMP selective inhibitors. We

proposed to introduce ONO_2 groups at the P2′ extension (Fig. 1.17) and investigate the effects of nitric oxide on cell invasiveness.

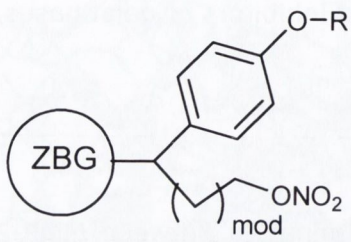


Figure 1.17. *The design of nitrate MMP inhibitors.*

The three approaches will be elaborated on at the start of each chapter.

Chapter 2

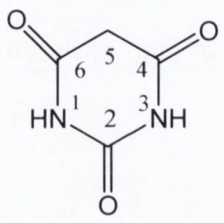
Synthesis of novel piperazine- and homopiperazine-based barbiturates

2.1 Introduction

2.1.1 Barbiturates as sedatives and hypnotics

2.1.1.1 History of sedative and hypnotic barbiturates

Barbiturates are a class of drugs that exert effects on the central nervous system. They are derived from barbituric acid, an organic compound which has a pyrimidine heterocyclic skeleton with three carbonyl groups at positions 2, 4 and 6. They are useful as sedatives when both hydrogens in the 5-position are substituted, which decreases acidity and increases lipophilicity and blood brain barrier penetrability.



Barbituric acid

The first unsubstituted barbituric acid was made in 1864 by German researcher Adolf von Baeyer. This was prepared by condensing diethyl malonate with urea, but it did not have significant biological properties (Brown 1994). The first barbiturate with sedative or hypnotic effects, barbital, was synthesized in 1903 by the Bayer company. Bayer introduced a new barbiturate, phenobarbital in 1912. Since then, a huge number of barbiturates have been synthesized and tested, and many have been used as sedatives and hynotics, including aphenal, hexobarbital, quinalbarbitone and amobarbital (Fig. 2.1). However, many barbiturates developed during that time have side effects and safety issues. For example, Vesparax, containing 150 mg secobarbital, 50 mg brallobarbital, 50 mg hydroxyzine, was used in treatment of sleep disorders but was withdrawn from the market in most countries due to its side effects including tiredness and drowsiness, loss of effect with frequent use, and lethal overdose (Fischbach 1983). The introduction of benzodiazepines in 1961 resulted in decreased use of

barbiturates. This is because benzodiazepines exhibit high anxiolytic efficacy in relation to their depression of central nervous system (CNS) function and have less potential for lethal overdose. Although benzodiazepines have replaced barbiturates in most areas, there are still some barbiturates using in clinical treatment. Quinalbarbitone, also known as secobarbital, was synthesized in 1928 and possesses sedative, hypnotic, anaesthetic, and anticonvulsant properties. It is still being used in the treatment of epilepsy and anaesthesia for surgery. In addition, some newly designed barbiturates have overcome certain side effects and have been used to replace those barbiturates with dangerous side effects. For example, hexobarbital was used for inducing anesthesia for surgery in the 1940s-1950s, but it was replaced by thiopental due to its difficulty in controlling of depth of anesthesia.

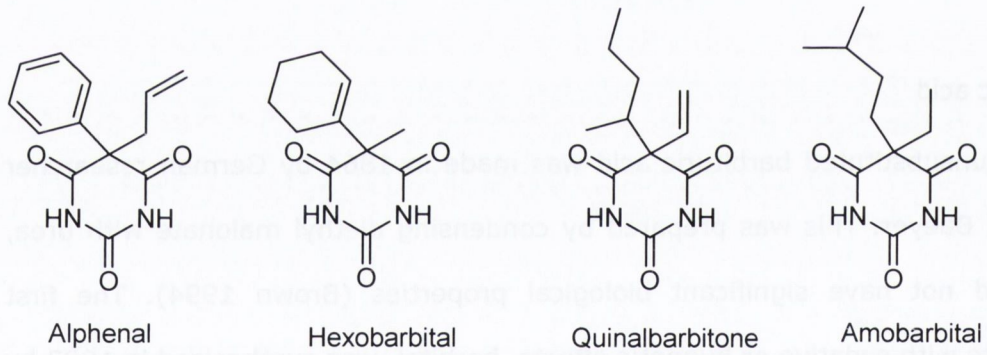


***Figure 2.1**. Examples of sedatives and hypnotic substituted barbiturates.*

2.1.1.2 Pharmacological effects of sedative and hypnotic barbiturates

Barbiturates exert a depressant effect on the cerebrospinal axis and decrease neuronal activity, as well as skeletal muscle, smooth muscle and cardiac muscle activity. By acting on GABAa receptors, they cause a wide spectrum of effects ranging from mild sedation to anesthesia. Activation of a GABAa receptor by an agonist increases the inhibitory synaptic response of central neurons to GABA, which leads to CNS depression.

More than 50 barbiturates have been used in therapeutics. Based on their duration of clinical effects, barbiturates are classified as long acting, intermediate

acting, short acting, and ultra-short acting. The barbiturates that produce effects after 1 h and last for 6—10 h are classified as long acting, including barbital and phenobarbital. These barbiturates are often used as hypnotic or anticonvulsant drugs. Intermediate acting barbiturates act after 30 mins and the duration of action is 2 to 6 h. These include allobarbital and butobarbitone, which can be used as sedative and hypnotic drugs. Short acting barbiturates, such as hexobarbital and phentobarbital sodium, take effect within 15 min and their hypnotic action lasts for 1—2 h. They are usually used in the treatment of insomnia. The onset of action of ultra-short acting barbiturates is visible within one minute after administration, such as thiopental sodium and methohexital sodium. These barbiturates are used to produce general anaesthesia for surgery. Although the use of barbiturates for anxiolytics and hypnotics has been replaced by benzodiazepines, some are still widely used in surgical anesthesia, including sodium thiopental, thiamylal, and methohexital. Except for methohexital, very large of doses of both thiopental and thiamylal can cause unconsciousness lasting several days This is because clearance of methohexital is much faster acting than thiopental and thiamylal, resulting in its less accumulation during prolonged infusions (Schwilden and Stoeckel 1990).

Besides producing a general anesthesia, barbiturates are also used in the treatment of insomnia and seizure. For example, phenobarbital can help treat tension and anxiety when taken during the daytime, and can decrease sleep latency and the number of awakenings when taken during the night (Goodman, Gilman et al. 2006). However, the use of barbiturates for these treatments has been limited due to risk of lethal overdose. Barbiturates can also induce other side effects, including reducing cerebral metabolism, decreasing blood pressure, and decreasing respiratory rate (Goodman, Gilman et al. 2006).

2.1.1.3 Chemistry of sedative and hypnotic barbiturates

The barbiturate ring can exist as an enolic tautomer (Fig. 2.2). The position of the equilibrium between the two forms is pH dependent. Substituted barbituric acid is a weak acid and can be ionized in base conditions. It has been reported that the pK_a values for the first ionization of substituted barbituric acids range between 6.85 to 8.35 and the constant for the second ionization ranges from 11.77 to 12.67 (Fig. 2.3) (Krahl 1940; Butler, Ruth et al. 1954).

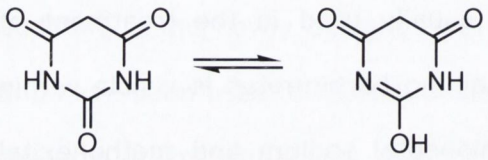


Figure 2.2. *Tautomerisation of barbituric acid.*

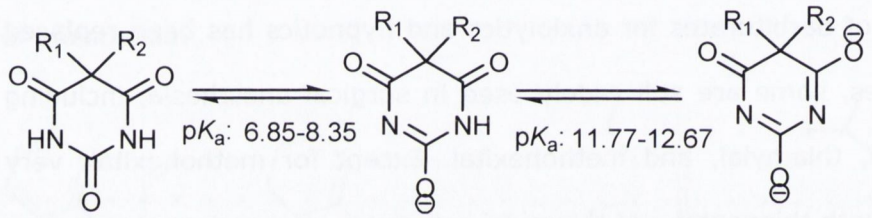
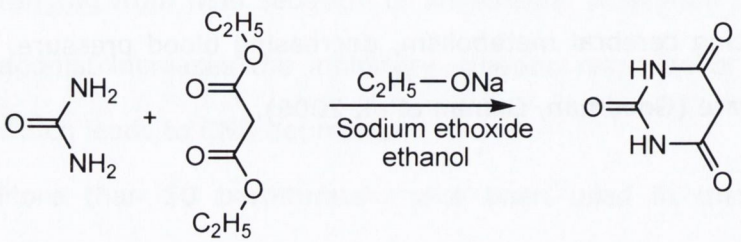
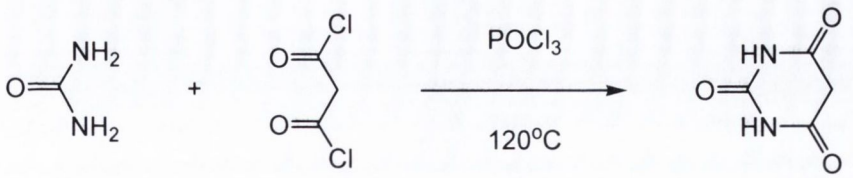


Figure 2.3. *Ionization of substituted barbituric acids.*

Although barbiturates have been used over one hundred years, synthetic methods for their preparation have not much changed. The formation of the barbituric acid ring is usually done by reaction of either malonic acid or appropriate ester and urea. For example, 5,5-diethyl barbituric acid was made from diethyl malonic ester and urea (Scheme 2.1). Reacting malonyl dichloride with urea is another method to form barbiturate rings (Scheme 2.2). For synthesis of barbiturates with thiol on the C-2 position, thiourea is used instead of urea.

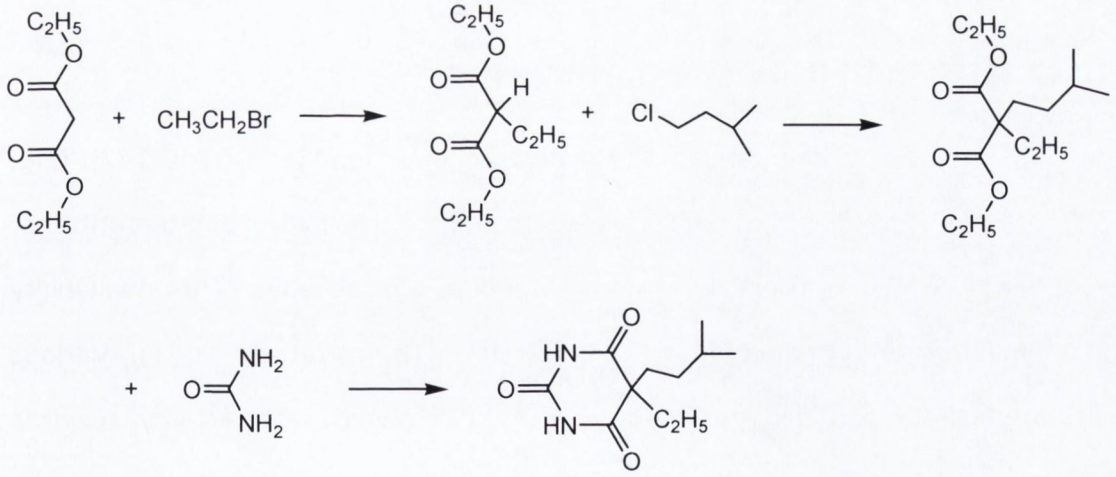


Scheme 2.1. *Preparation of barbituric acid by malonic ester* (Kar 2006)

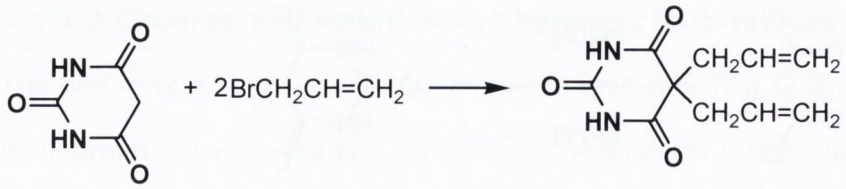


Scheme 2.2. *Forming barbituric acid by malonyl dichloride* (Kar 2006).

As for the preparation of barbiturates with substitutions on the C-5 position, substituents usually can be introduced before or after formation of the barbiturate ring. In the first case, the first substituent is normally added on in the process of preparation of the malonate. The second substituent is added to the malonate by reacting with the appropriate bromides or chlorides. Then doubly subsituted malonates react with urea to from the barbiturate. Most marketed barbiturates including barbitone, amobarbital and phenobarbital were synthesized by this route (Scheme 2.3). In the case of the two substituents added after forming the barbiturate ring, unsubstituted barbituric acids normally react with bromides (Scheme 2.4).



Scheme 2.3. *Preparation of amobarbital (Kar 2006). The two substitutions were attached before forming the barbiturate ring.*



***Scheme 2.4**. Preparation of allobarbital barbiturate (Kar 2006). The two substitutions were added on after forming of barbiturate ring.*

Generally, only barbiturates with two active hydrogen atoms at C-5 position replaced with appropriate substituents show hypnotic activity. Hypnotic activity is highly dependent on the nature of these substituents. Some important points on the relationship between the structure of two substituents on the C-5 position and activity have been drawn from published barbiturates (Kar 2006): 1) The total number of carbons of two substituents should be more than 4 and less than 10; 2) Only one substituent can be a closed chain; 3) Aromatic and alicyclic substituents have greater potency than the same number of aliphatic moieties; 4) Polar substituents (e.g. OH, NH_2, CO, COOH, etc.) reduce potency; 5) Introduction of halogen atoms on the C-5 increases potency.

2.1.2 MMP inhibition and barbiturates

In 2001 workers at the Hoffman La-Roche company identified RO200-1770 (Fig. 2.4) in a high throughput screen while searching for non-hydroxamate antitumor compounds. MMP-8 was used for as a screening tool because of its availability and similarity to the gelatinases (Brandstetter, Grams et al. 2001). Various barbiturates compounds were subsequently discovered with activity towards MMP-1, 2, -3, -8, -9, and MMP-14. Barbiturate inhibitors of the MMPs generally possess selectivity towards gelatinases (Table 2.1). They do not exhibit any sedative character in animal models and depart significantly from the sedative SAR pattern. In the past decade, a great number of barbiturates have been synthesized and tested to build up relationships between structure and activity with the aim of producing active compounds with MMP subtype selectivity.

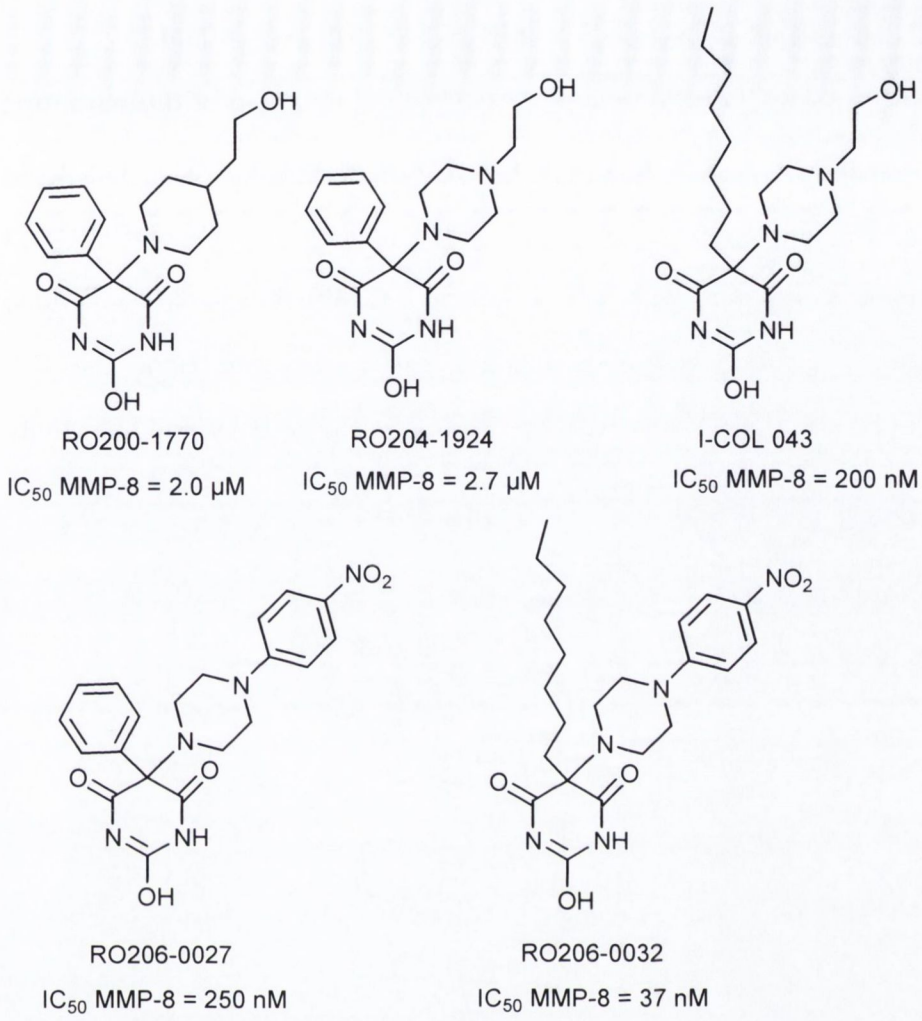


Figure 2.4. *The first reported barbiturate-based MMP inhibitors (Grams, Brandstetter et al. 2001).*

Table 2.1. *IC_{50} values of the first synthesized barbiturate-based MMP inhibitors (nM).*

Inhibitor	MMP-1	MMP-2	MMP-3	MMP-8	MMP-9	MMP-14
RO200-1770	5130	2870	30,000	1700	2000	670
RO204-1924	25,000	3940	30,000	3190	3160	2050
RO206-0027	2700	210	3400	250	410	830
I-COL 043	22,000	344	3500	260	81	1350
RO206-0032	14,000	202	3700	48	16	210

2.1.2.1 Structure and activity relationship of barbiturate on MMPs

The inhibition of MMPs by barbiturates is primarily due to binding of the barbituric acid moiety with the active zinc in the MMPs. The binding interaction has been extensively investigated in structural studies using NMR and X-ray. Barbiturates bind in a tridentate manner with the zinc in the catalytic domain (Grams, Brandstetter et al. 2001) (Fig. 2.5). Besides the barbiturate ring, the C-5 substituents can fit into the S1′ and S2′ pockets imparting potency and selectivity for gelatinases (Breyholz, Schafers et al. 2005) (Fig. 2.6).

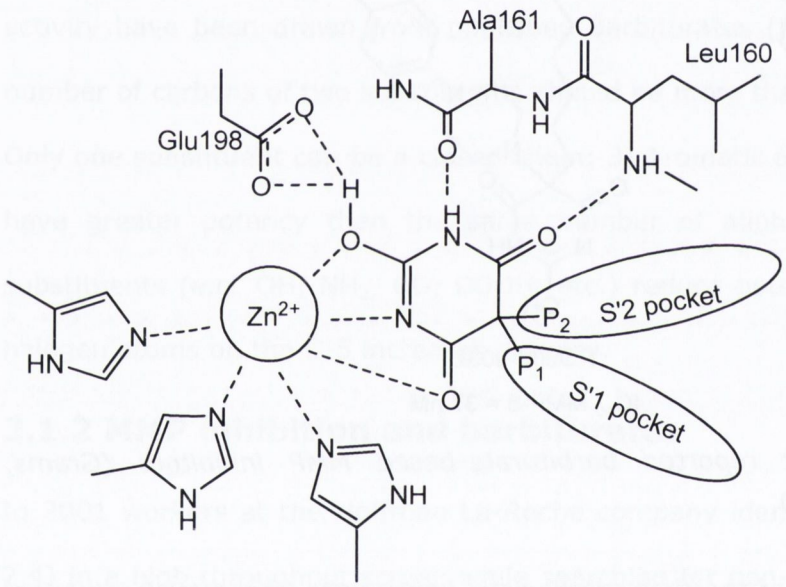


Figure 2.5. *The binding of barbiturates with MMP-8.*

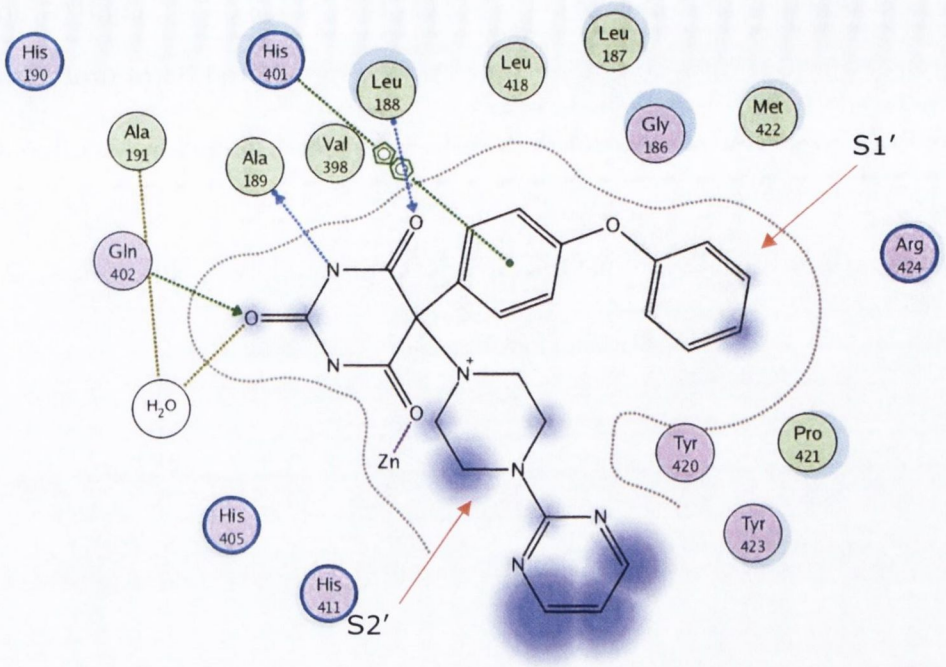
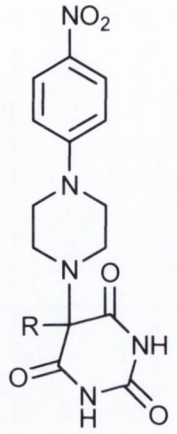
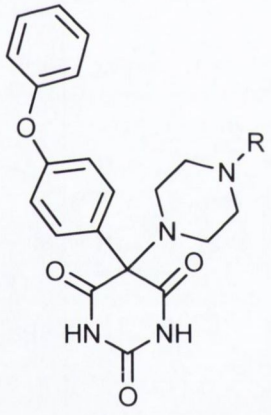
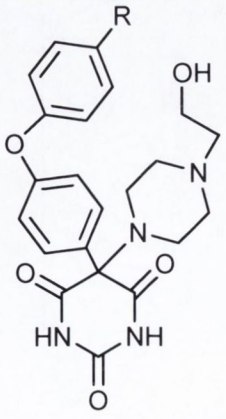


Figure 2.6. *A picture of interaction of a substituted barbiturate with MMP-9. The phenoxyphenyl and the piperazine fit into the S1′ and S1′ pocket of MMP-9. The picture was generated by MOE (pdb code: 2ovx).*

Most inhibitors (barbiturate or not) have better binding affinity in the S1′, S2′ and S3′ side of the active zinc since the primed side has more defined pockets than the unprimed side where ligands compete with water for the exposed protein surface. The two substitutions on the C-5 position of barbiturate ring (P1′ and P2′) insert into the S1′ and S2′ pockets. Numerous computational studies have found the S1′ pocket is crucial for substrate specificity, for inhibitor potency and selectivity (Skiles, Gonnella et al. 2004; Rao 2005). The medicinal chemistry of MMPs inhibitor design has frequently targeted the S1′ pocket through extensive P1′ substitution. The binding affinity of inhibitors to the S2′ pocket seems to be weaker than S1′ pocket, but potency can also be enhanced by modification of P2′ substitution (Ryuichi, Tamura et al. 1999; Breyholz, Schäfers et al. 2005). Barbiturate inhibitors unsubstituted with P2′ groups bind in the 1 μM range when P1′ substitution is optimal. This is about three orders of magnitude weaker

indicating the overall contribution of P2′ to the binding is high (Grams, Brandstetter et al. 2001). On the other hand, singly substituted barbiturates may not have the correct conformation to bind into either pocket making it hard to tell the contribution of the second binding group or indeed the first. Lists of recent synthesized barbiturate-based MMP inhibitors are shown in Table 2.2.

Table 2.2 *MMP inhibition of published barbiturate derivatives.*

No.	Structure	IC_{50} (nM)					Ref.
E1		No.	R	MMP -8	MMP -2	MMP -9	(Grams, Brandstetter et al. 2001)
		E1a	phenyl	250	160	160	
		E1b	octyl	37.4	37.4	17	
		E1c	4-phenoxy -phenyl	17	17	n.d.[a]	
		E1d	4-biphenyl	15	10	12	
E2		No.	R	MMP -8	MMP -2	MMP -9	
		E2a	2-hydroxy-ethyl	47	11	11	
		E2b	3-hydroxy-propyl	11	4.4	3.5	
		E2c	4-hydroxy-butyl	16	7	7	
		E2d	5-hydroxy-pentyl	13	6	4	
E3		No.	R	MMP -8	MMP -2	MMP -9	
		E3a	Br	6.6	2	1.2	
		E3b	Cl	11	5	1.7	
		E3c	CH_3	11	9	2.3	
		E3d	MeO	n.d.	8	1.3	

a) n.d. = not determined

Table 2.2 *contd.*

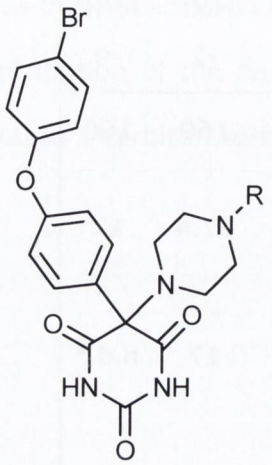
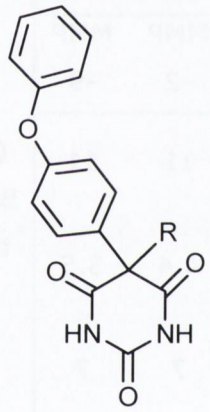
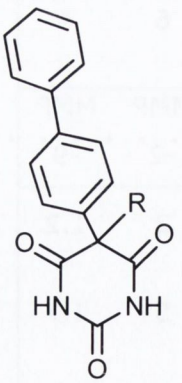
No.	Structure	IC_{50} (nM)				Ref.
E4		No.	R	MMP-2	MMP-9	(Breyholz, Schäfers et al. 2005)
		E4a	2-bomo-ethyl	30	26	
		E4b	H	5	2	
		E4c	isopropyl	26	1	
		E4d	2-amino-ethyl	10	14	
		E4e	4-nitro-phenyl	16	57	
E6		No.	R	MMP-3	MMP-2	MMP-9	(Foley, Palermo et al. 2001)
		E5a	methyl	2000	81	52	
		E5b	2-hydroxy ethyl	n.d	59	118	
		E5c	hexyl	2000	21	18	
		E5d	(benzyloxy)methyl	930	19	17	
E6		No.	R	MMP-3	MMP-2	MMP-9	
		E6a	hexyl	n.d.	868	863	
		E6b	ethyl	9	898	696	

Table 2.2 *contd.*

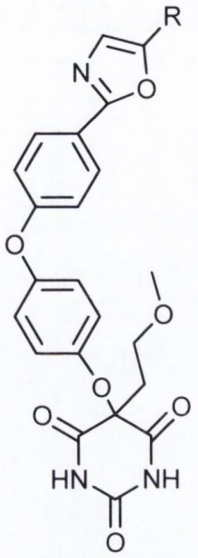
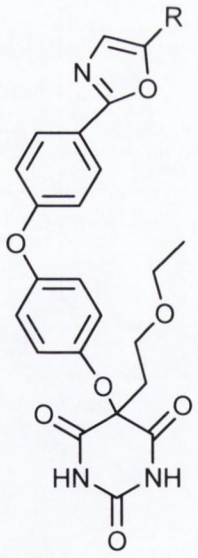
No.	Structure	IC_{50} (nM)					Ref.
E7		No.	R	MMP -13	MMP -8	MMP -2	MMP -12	(Reiter, Freeman-Cook et al. 2006)
		E7a	2-F-ph	1.4	209	403	847	
		E7b	3-F-ph	0.46	70	110	604	
		E7c	4-F-ph	0.57	193	203	547	
		E7d	2-CN-ph	0.73	377	126	250	
		E7e	3-CN-ph	0.63	88	18.3	114	
		E7f	4-CN-ph	0.36	142	143	223	
E8		No.	R	MMP -13	MMP -8	MMP -2	MMP -12	
		E8a	2-F-ph	0.93	251	523	807	
		E8b	3-F-ph	0.36	47.9	105	326	
		E8c	4-F-ph	0.68	165	309	390	
		E8d	2-CN-ph	0.88	501	125	157	
		E8e	3-CN-ph	0.53	82.2	16.4	71.0	
		E8f	4-CN-ph	0.45	105	193	168	
		E8g	2-pyridyl	1.0	57	74	158	
		E8h	3-pyridyl	0.34	90.1	12.9	42.2	
		E8i	4-pyridyl	0.40	100	28	212	

Table 2.2 *contd.*

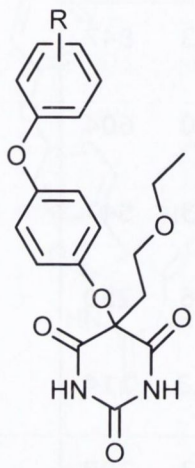
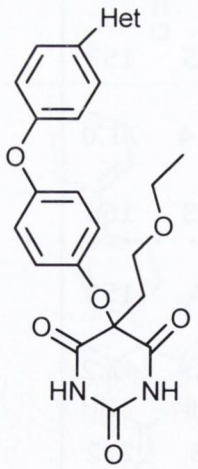
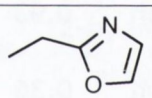
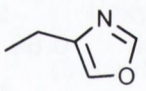
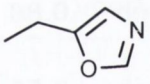
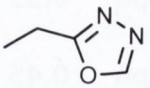
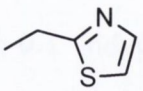
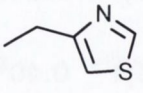
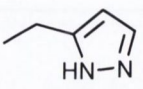
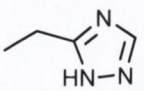
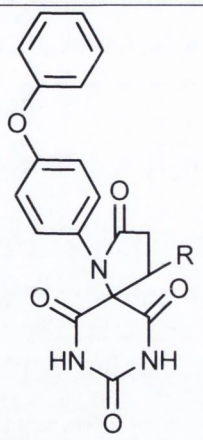
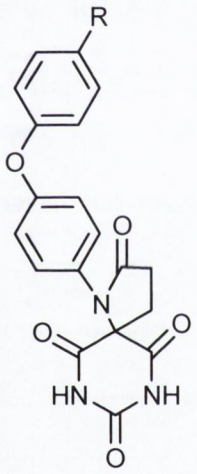
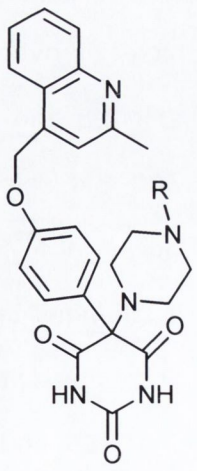
No.	Structure	IC_{50} (nM)				Ref.
E9		No.	R	MMP-13	MMP-14	(Blagg, Noe et al. 2005)
		E9a	4-fluoro	0.87	23	
		E9b	2-fluoro	3.1	16	
		E9c	4-chloro	1.4	18	
		E9d	3-chloro	53	120	
		E9e	4-*tert*-butyl	190	6700	
		E9f	4-ph	1.7	36	
		E9g	4-cyano	2.9	200	
		E9h	4-MeNHCO-	6.0	650	
		E9i	4-Me_2NCO-	56	9300	
E10		No.	Het	MMP-13	MMP-14	
		E10a		1.4	238	
		E10b		18	340	
		E10c		0.54	3.0	
		E10d		1.0	220	
		E10e		3.1	75	
		E10f		3.6	150	
		E10g		4.1	27	
		E10h		15	1400	

Table 2.2 *contd.*

No.	Structure	K_i (nM)					Ref.
E11		No.	R	MMP-2	MMP-3	MMP-9	MMP-13	(Kim, Pudzianowski et al. 2005)
		E11a	H	1.6	4500	4.7	4.7	
		E11b		0.40	92	0.87	0.54	
		E11c		1.7	1200	7.2	0.95	
E12		No.	R	MMP-2	MMP-3	MMP-9	MMP-13	
		E12a	Cl	0.43	430	0.73	0.95	
		E12b	CO_2Me	4.7	1300	1.2	4.2	
		E12c	CO_2H	0.23	3200	0.72	2.7	
		E12d	OPh	1.8	110	1.9	0.33	
E13		No.	R	MMP-2	MMP-9	MMP-13		(Duan, Lu et al. 2005)
		E13a	methyl	>3300	>2130	>5020		
		E13b	$Ph(CH_2)_2$	83	85	95		
		E13c	$Ph(CH_2)_3$	3100	2040	>5020		
		E13d	4-NO_2-Ph	116	138	356		

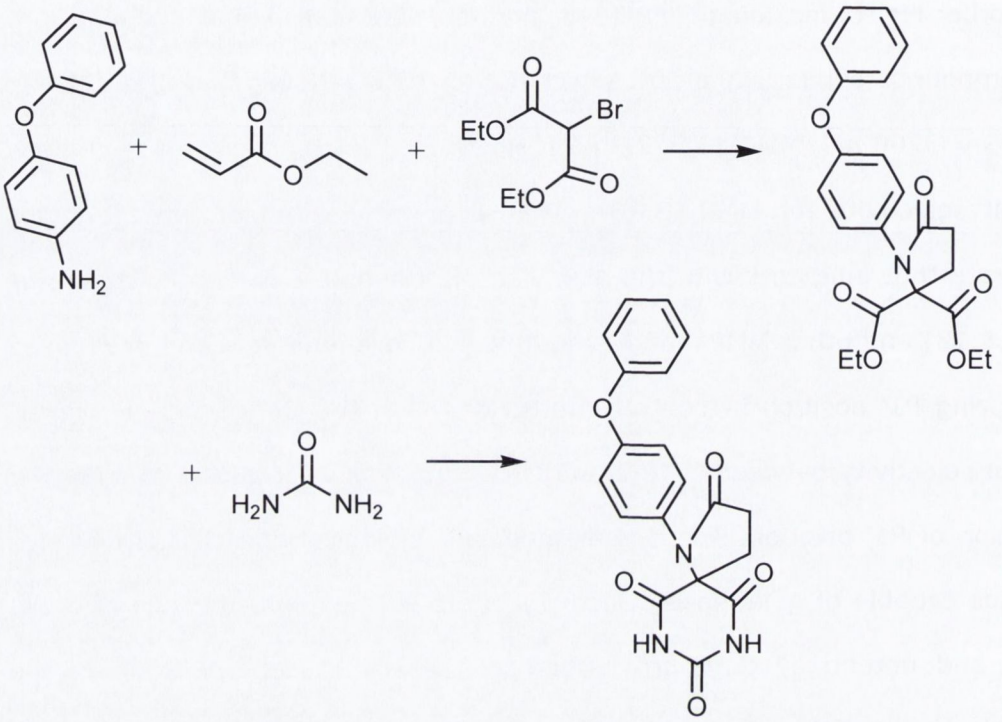
The data in Table 2.2 indicates that S1′ pocket interactions can play an important role in binding affinity between the MMP proteins and inhibitors that can influence potency and selectivity. Compounds **E1a-d** have the same side chain on the P2′ position and different groups on P1′, but their IC_{50} values for MMP-8 range from 250 nM to 15 nM (Grams, Brandstetter et al. 2001). The difference between the compounds **E5c** and **E6a** is the P1′ substitution, which have phenoxyphenyl and biphenyl groups respectively, but the replacement of biphenyl with a phenoxyphenyl group results in over 800 nM decrease in IC_{50} for MMP-2 and MMP-9 (**E5c** IC_{50}: (MMP-2) = 21 nM, (MMP-9) = 18 nM; **E6a** IC_{50}: (MMP-2) = 868 nM, (MMP-9) = 863 nM) (Foley, Palermo et al. 2001). The loss of potency in biphenyl substituted inhibitors is probably due to the rigidity of the group. It has been shown that flexible groups fit better in the S1′ pocket (Tamura, Watanabe et al. 1998; Ryuichi, Tamura et al. 1999). The *Reiter* group in Pfizer has successfully synthesized a series of highly selective MMP-13 inhibitors (**E7** and **E8**) by optimizing the P1′ position on the barbiturate ring (Reiter, Freeman-Cook et al. 2006). These inhibitors have methoxyethyl or ethoxyethyl on the P2′ substitution and phenoxyphenoxy with different subgroups on P1′. These compounds have shown more than 100-fold selectivity for MMP-13 over MMP-2, -8 and -12. The most MMP-13 selective in the group over MMP-12 is **E7b**, which has over 1300-fold selectivity. The most MMP-13 selective compounds over MMP-8 and MMP-2 are the compounds **E8d** and **E8a**, which both have over 500-fold selectivity. Binding of the long phenoxyphenoxy moieties in the deep S1′ pocket of MMP-13 is the key reason for the great potency and selectivity. However, changes between methoxyethyl and ethoxyethyl only slightly affect potency and selectivity. The *Blagg* group in Pfizer has also prepared a number of compounds (**E9** and **E10**), which showed good selectivity on MMP-13 against MMP-14 (Blagg, Noe et al. 2005). The most MMP-13 selective **E10d** has 200-fold selectivity for MMP-13 over MMP-14 (IC_{50}: MMP-13 = 1.0 nM. MMP-14 = 220 nM). These compounds have

similar scaffolds to the compounds prepared by the *Reiter* group. The only departure is on the end of P1′ positions where different subgroups were attached. Another research group, *Kim et al.,* has also focused on the selectivity for MMP-13 over other MMPs, including MMP-2, -3, and -9 (Kim, Pudzianowski et al. 2005). These compounds exhibit significant selectivity for MMP-13 over MMP-3 e.g. **E12c** (K_i: MMP3 = 3200 nM, MMP-13 = 2.7 nM). However, the compounds do not show significant selectivity for MMP-13 over MMP-2 or MMP-9. All of these findings demonstrate that inhibitors with the ability to discriminate between collagenases (MMPs 1,8,13) and other MMPs, and even between collagenases, can be achieved by optimizing P1′ position to control interactions with the S1′ pocket. However, significant selectivity between MMP-2 and MMP-9 has not been achieved so far by modification of P1′ position. There is a significant biological and clinical need for compounds capable of gelatinase selectivity in order to explore the role of these enzymes and potentially to improve medical therapy in cancer. None of the compounds in the Table 2.1 exhibited selectivity between MMP-2 and MMP-9, apart from isopropyl substituted piperazine-based barbiturate (**E4c**), which reportedly has 26-fold selectivity for MMP-9 over MMP-2 (IC_{50}: MMP2 = 26 nM, MMP9 = 1 nM). It seemed to us that this interesting result and potential for selectivity has been under explored in the barbiturate class. Since the models indicated that the isopropyl group in **E4c** is directed towards S2′ and out to solvent we hypothesized that gelatinase subtype selectivity might be achieved by focusing on S2′ occupying 5-substituents (P2′) of the barbiturates.

2.1.2.2 Synthetic methods for barbiturate-based MMP inhibitors

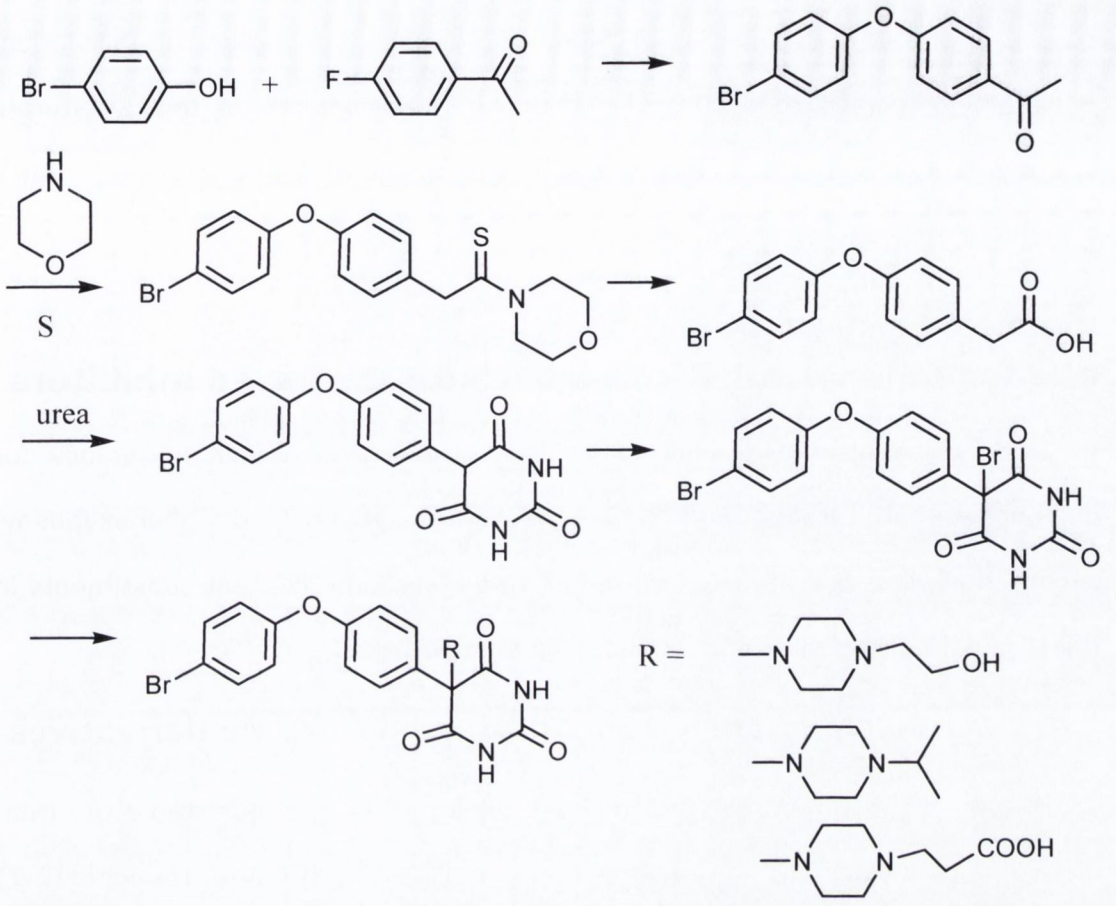
The synthetic approaches to barbiturates with MMP inhibitory properties are broadly similar to those used to produce sedative and hypnotic barbiturates. Formation of the barbituric acid ring is accomplished by refluxing malonate ester and urea in the presence of sodium ethoxide in ethanol. However, addition of the substitutions on P1′ and P2′ position is approached differently. Some MMP

inhibitory barbiturates are synthesized like most sedative barbiturates, which form the barbiturate ring after two 5-substitutions have been made. An example is shown in Scheme 2.5 (Kim, Pudzianowski et al. 2005).



Scheme 2.5. *Preparation of a spiro barbiturate-based inhibitor with two substitutions introduced before formation of the barbiturate ring.*

Most barbiturate-based MMP inhibitors are prepared by adding the first substitution before reacting with urea. The second substitution is connected afterwards by bromination and reaction with desired subgroups (Scheme 2.6).



Scheme 2.6. *Preparation of piperazine substituted barbiturate-based MMP inhibitors, in which the second substituents were added on after the formation of the barbiturate ring (Breyholz, Schäfers et al. 2005).*

As already described, pyrimidine-2,4,6,-triones have been used in humans for a long time as antiepileptic agents, hypnotic and sedatives. Barbiturates on the market have a good bioavailability and good pharmacokinetic profile as well as very few side effects, and may not have the problems that the hydroxamates and carboxylates have shown in clinical trials (Mutschler 1991; Drummond, Beckett et al. 1999). Therefore, the barbiturate zinc-binding group was selected as a template for exploration of new gelatinase inhibitors in the present work.

In order to investigate the influence of the S1′ pocket interaction on potency, we began by exploring different substitutions applied to the P1′ position of barbiturates. We were primarily interested in probing for interactions at the mouth of the S2′ pocket that might impart gelatinase type or sub-type selectivity. We were in this regard attracted to the piperazine model as these provide the

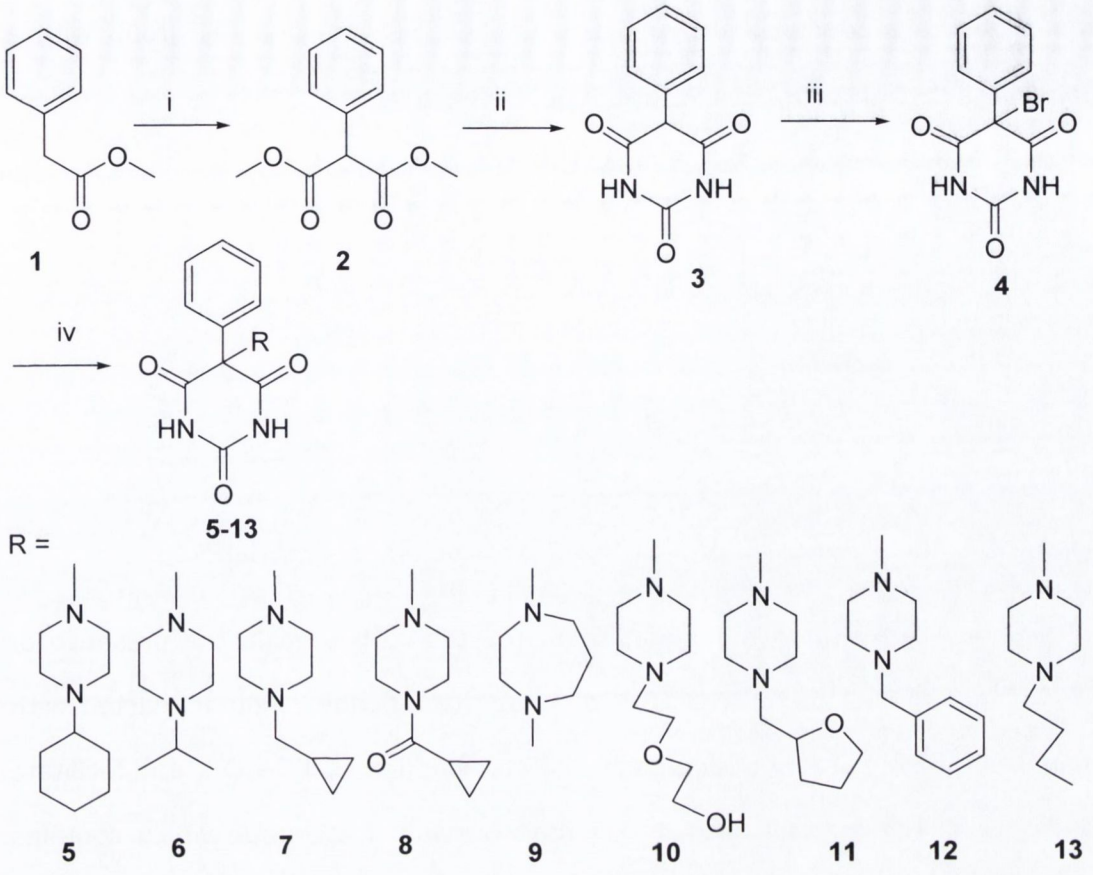
possibility for distal substitution through simple N-acylation or alkylation. However, it seemed to us from inspection of X-ray models of the barbiturate docking into collagenases that the S2′ pocket might be better occluded with a seven membered homo-piperazine rather than the standard piperazine.

2.2 Synthesis of phenyl, benzyloxyphenyl, and phenoxyphenyl substituted barbiturate-based inhibitors

In order to investigate impact of P1′ substitutions on inhibition potency for gelatinases barbiturates with 5-phenyl, benzyloxyphenyl, or phenoxyphenyl substitution were prepared. These barbiturates had nine different substituents in the P2′, eight piperazine- and one homopiperazine-based.

2.2.1 Synthesis of phenyl substituted barbiturate derivatives

The 5-phenyl substituent compounds were prepared using a four-step route from methyl 2-phenylacetate in analogy to a published procedure (Scheme 2.7) (Breyholz, Schafers et al. 2005).



Scheme 2.7. *Preparation of phenyl substituted barbiturate derivatives. i) $(CH_3O)_2CO$, NaH, dry THF, 105°C, 5 h. ii) Na, urea, EtOH, 100°C, 7 h. iii) Br_2, HBr, H_2O, 0°C, 5 h. iv) substituted piperazines or homopiperazines, MeOH, RT, 24 h.*

The first step was to synthesize dimethyl 2-phenylmalonate (**2**) by introducing a methyl ester group into methyl 2-phenylacetate (**1**), under strong base conditions (Fig 2.7). The solvent THF and reagent dimethyl carbonate used for the reaction were fully dried because NaH is highly sensitive to water. Any water present in the reaction would react with NaH and produce NaOH and H_2, resulting in ester hydrolysis. During the reaction, addition of methyl 2-phenylacetate to the mixture of NaH, dimethyl carbonate and THF was done slowly, normally over one hour. The mixture turned to a pink colour after approximately 30 min. When the reaction finished, the mixture was poured onto ice water and extracted with DCM. The crude products were purified by flash column chromatography using hexane and ethyl acetate as mobile phase. The ^1H NMR spectrum showed two ester

groups on the products, which had two CH_3 groups and one CH group with a chemical shift (δ in ppm) of 3.78 and 4.68, respectively.

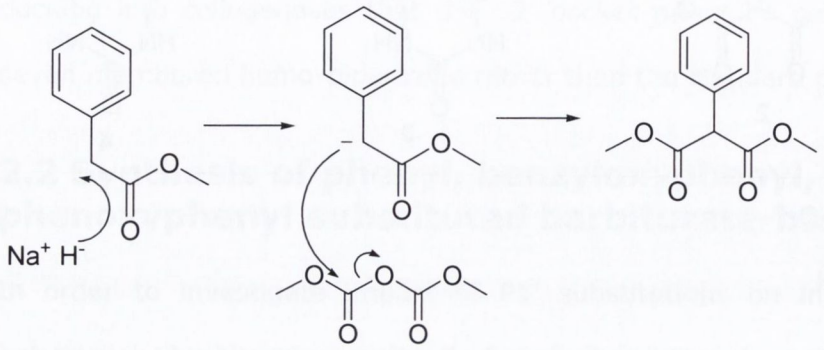


Figure 2.7. *The mechanism of dimethyl 2-phenylmalonate formation.*

The 5-phenyl substituted malonate, then, reacted with urea in the presence of sodium and ethanol to form **3** (Fig 2.8). In the reaction, sodium reacted with ethanol to produce a very strong base, the ethoxide ion ($CH_3CH_2O^-$), and facilitate the reaction. The ethanol used in the reaction was HPLC grade which contains small amounts of water and did not affect significantly affect the yield. The impact of water in this reaction is similar to the previous reaction. The precipitates were started to form after 1 h of refluxing. When the reaction was finished, the mixture was poured onto ice water and adjusted to pH 2, using 2 M HCl. Formation of the barbiturate ring was confirmed by ^1H and ^{13}C NMR spectra, which both showed loss of ester group comparing to the malonate (**2**). In addition, two protons at chemical shift (δ in ppm) 10.78 and 11.41 in the ^1H NMR spectrum demonstrated the existence of a barbiturate ring (Fig. 2.9). The reason for two different protons on the barbiturate ring is because 5-phenyl barbituric acids is subject to keto-enol tautomerisim giving rise to different chemical shifts in ^1H NMR. The Fig. 2.9 shows there were a half proton at 10.78 ppm and 1.5 at 11.41 ppm, indicating the two forms exist in the proportion of 3:1 in the synthesized compounds.

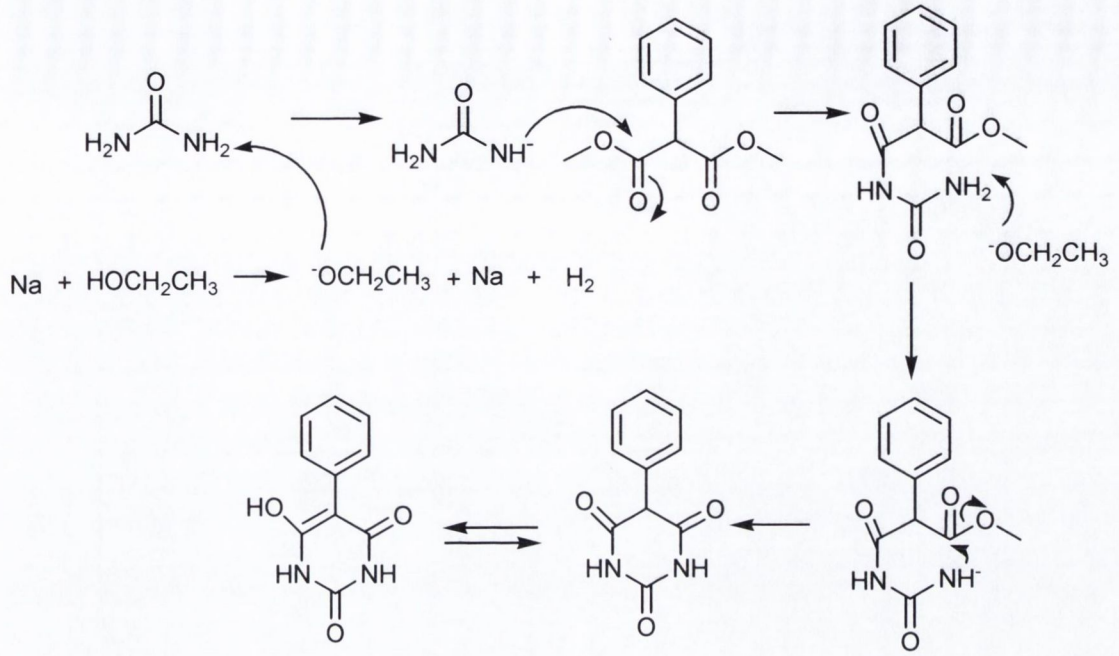


Figure 2.8. *The mechanism of forming the barbiturate ring* in 5-phenylbarbituric acid.

Keto-enol tautomerisim may explain the low potency of 5-monosubstituted compounds since the planar form directs the remaining substituent away from both S1′ and S2′ pockets.

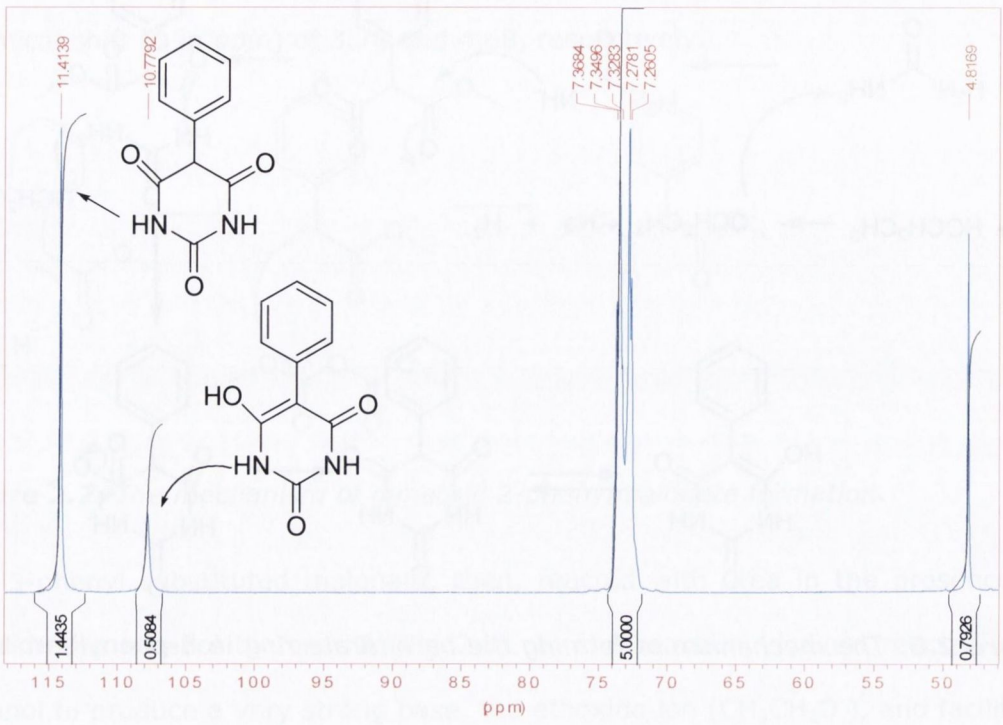


Figure 2.9. *The ^{1}H NMR spectrum of 5-phenylpyrimidine-2,4,6(1H,3H,5H)-trione.*

The barbiturate product was brominated using bromine in the presence of hydrobromic acid in water. A possible reaction mechanism for this is shown in Fig. 2.10. The proton in the C5 position of the barbiturate ring should have weak acidity due to the two neighbouring carbonyl groups and easily react with Br_2. The loss of proton in ^{1}H NMR and the change of chemical shift from 55.1 ppm to 76.1 ppm in ^{13}C NMR caused by substitution of CH on C-5 position demonstrated the successful bromination.

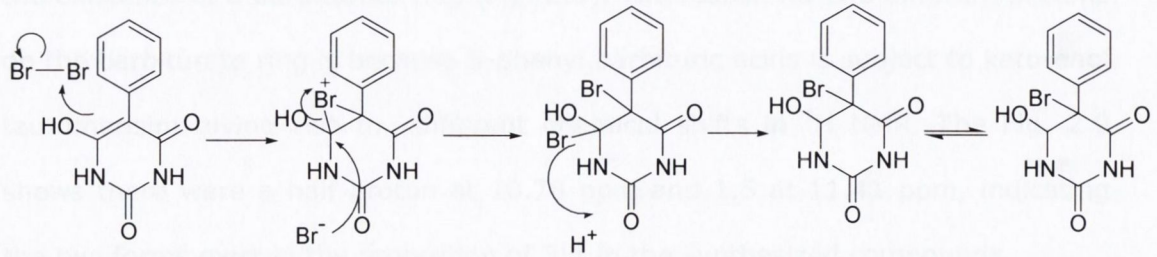


Figure 2.10. *The mechanism of bromination of phenyl barbiturate.*

To obtain the final compounds, the substituted piperazines and methylhomopiperazine were attached to the C5 position of the barbiturate through replacement of Br (Fig. 2.11). The reaction was carried out at RT for 24 h. In the reaction for making the compounds **5**, **10**, **11**, **12**, and **13**, precipitates started to form after 30–60 min. The precipitates were collected by suction filtration and washed with methanol to yield pure products. In the case where precipitates did not appear in the reaction for preparation of compound **6**, **7**, **8**, and **9**, the final compounds were obtained by purification of reaction mixture using flash column chromatography with ethyl acetate and methanol. All reactions had reasonable yields ranging from 50.2% to 70%.

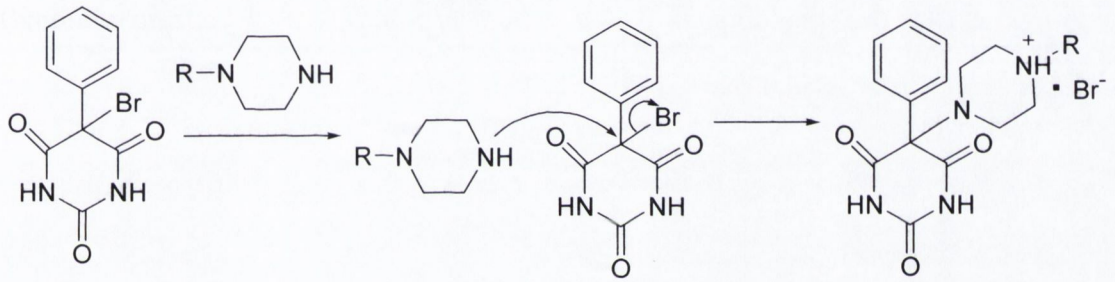


Figure 2.11. *The mechanism of reactions of barbiturates and piperazines.*

2.2.2 Synthesis of benzyloxyphenyl substituted barbiturate derivatives

The procedures adopted for preparation of benzyloxyphenyl substituted compounds are very similar to those for phenyl substituted compounds. The only difference was that the former compounds require one more step and use methyl 4-hydroxyphenylacetate **14** as starting material (Scheme 2.8). The preparation of methyl 2-(4-benzyloxyphenyl)acetate **15** used compound **14**, benzyl bromide, and dry acetone in the presence of K_2CO_3 (Fig. 2.12). After refluxing for 5 h, the reaction mixture was poured onto ice water and extracted with DCM. All the remaining steps for making piperazine- or homopiperazine-based barbiturate inhibitors were similar to the preparation of phenyl substituted inhibitors. Compounds **19**, **20**, **21**, **23**, and **26** precipitated from methanol solution when

18 was reacted with the substituted piperazines or methyl homopiperiazine. The precipitates were washed and dried *in vacuo*. In the case of **22**, **24**, **25**, and **27**, no precipitates formed. The reaction mixtures in these instances were purified by flash column chromatography.

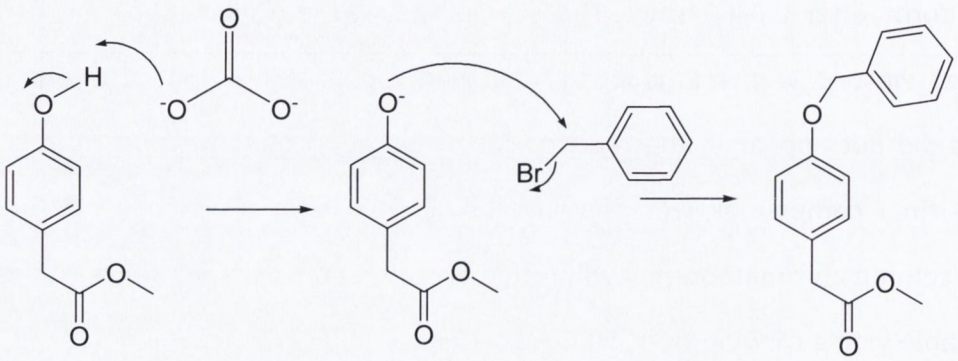
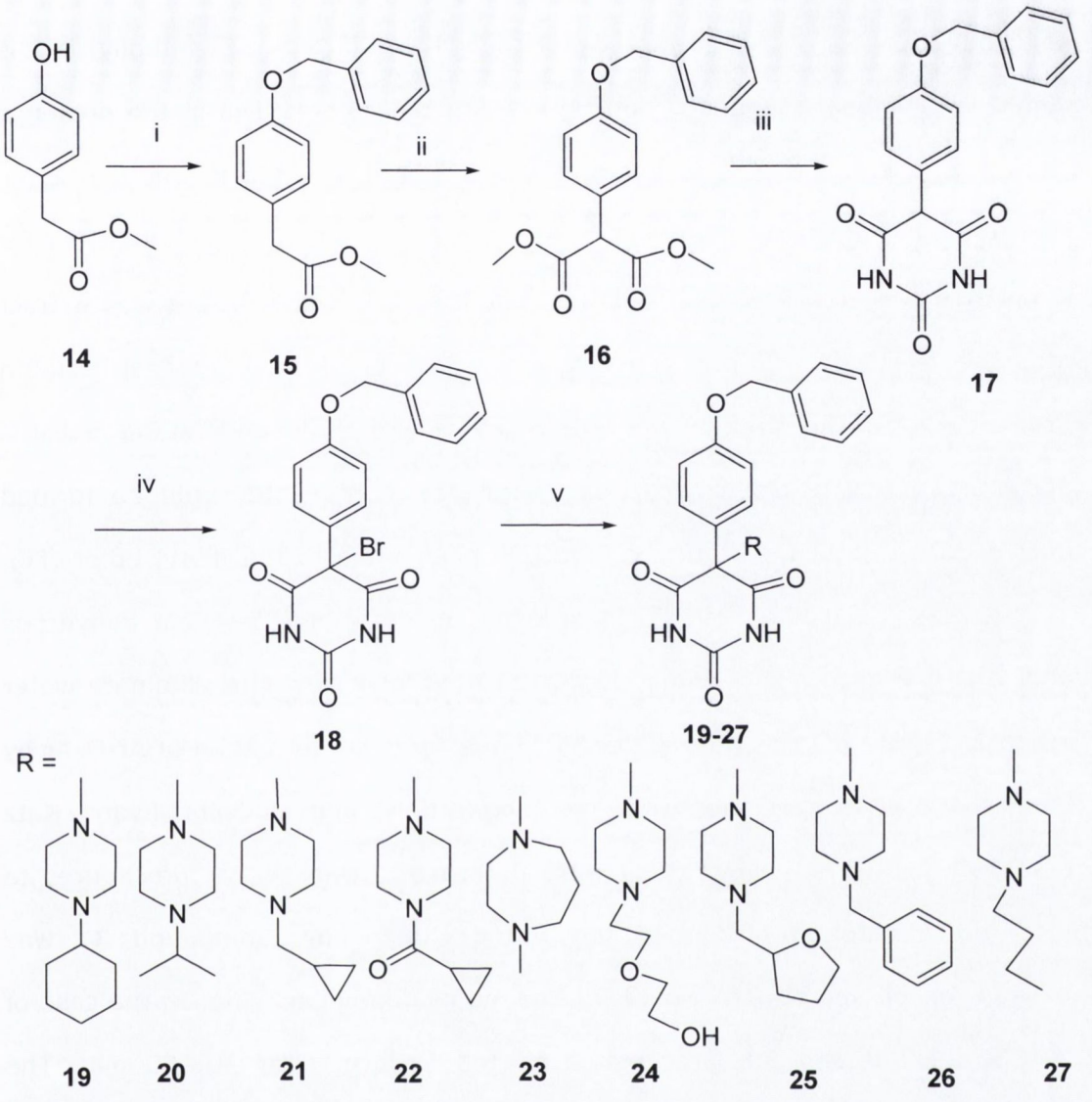


Figure 2.12. *The mechanism of formation of methyl 2-(4-benzyloxyphenyl) acetate.*

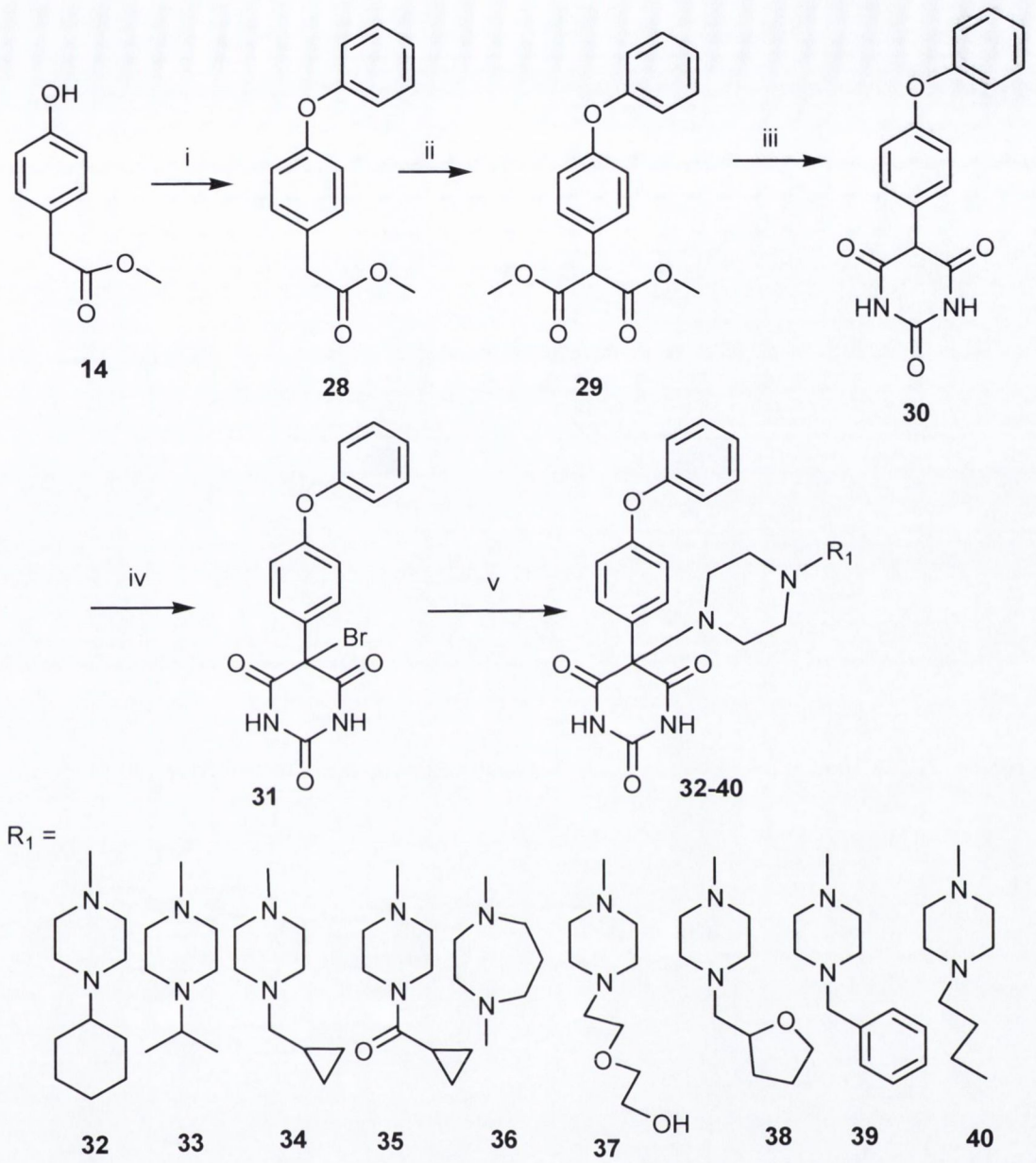


Scheme 2.8. *Preparation of benzyloxyphenyl substituted barbiturate derivatives. i) $C_6H_5CH_2Br$, K_2CO_3, dry acetone, 60°C, 5 h. ii) $(CH_3O)_2CO$, NaH, dry THF, 105°C, 5 h. iii) Na, urea, EtOH, 100°C, 7 h. iv) Br_2, HBr, H_2O, 0°C, 5 h. v) substituted piperazines or homopiperazines, MeOH, RT, 24 h.*

2.2.3 Synthesis of phenoxyphenyl substituted barbiturate derivatives

The strategy for producing 5-phenyloxyphenyl compounds (Scheme 2.9) was overall similar to that adopted in the previous two series apart from the first step which required coupling of the phenyl group. This is still a problematic transformation in organic chemistry. A number of different methods were tried such as microwave assisted reactions or the Ullmann coupling (Fig. 2.13) (Li, Wang et al. 2003; Chen, Xu et al. 2004; Paul and Gupta 2004). These approaches

either gave low yield or presented problems with purification. Eventually, it was found that a copper-mediated coupling with phenyl boronic acid in the presence of copper acetate and dry pyridine worked well, producing methyl 2-(4-phenoxyphenyl) acetate (**28**) in good yield. The reaction was carried out at RT for 24 h. Then the green reaction mixture was filtered and the filtrate was extract with diethyl ether, and the brownish oily products purified by flash column chromatography. The mechanism of the reactions is not fully understand, but it is speculated the plausible acrylcopper phenoxide intermediate could be formed which then undergoes subsequent reductive elimination to the diaryl ether (Fig. 2.14) (Evans, Katz et al. 1998). In order to generate and maintain anhydrous conditions, we used dry pyridine along with molecular sieves to eliminate water generated during the reaction. Water could interfere with formation of Ar-O-Ar by reacting with arylcopper phenoxide, resulting in unwanted products (Evans, Katz et al. 1998). The remaining steps were performed using similar procedures to those for preparation of phenyl substituted compounds. Compound **31** was treated with the appropriate piperazines or methylhomopiperazine. In the case of **32**, **33**, **34**, **38** and **39**, precipitates started to form after 30—60 min. The precipitates were collected by filtration and washed with methanol to yield the pure compounds. As for compounds **35**, **36**, **37**, and **40**, the solvent was removed and the residues purified by a chromatography.



Scheme 2.9. *Preparation of phenoxyphenyl substituted barbiturate derivatives. Conditions: i) $C_6H_5B(OH)_2$, copper (II) acetate, pyridine, DCM, RT, 24 h. ii) $(CH_3O)_2CO$, NaH, dry THF, 105°C, 5 h. iii) Na, urea, EtOH, 100°C, 7 h. iv) Br_2, HBr, H_2O, 0°C, 5 h. v) substituted piperazines or homopiperazines, MeOH, RT, 24 h.*

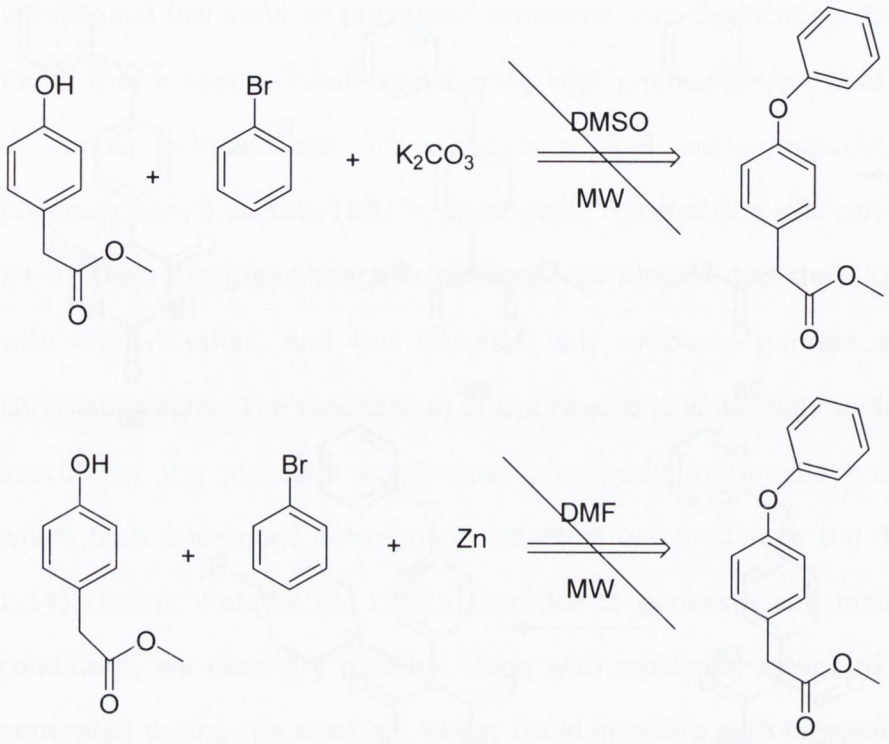


Figure 2.13. *Unsuccessful reactions for synthesizing the diaryl ether.*

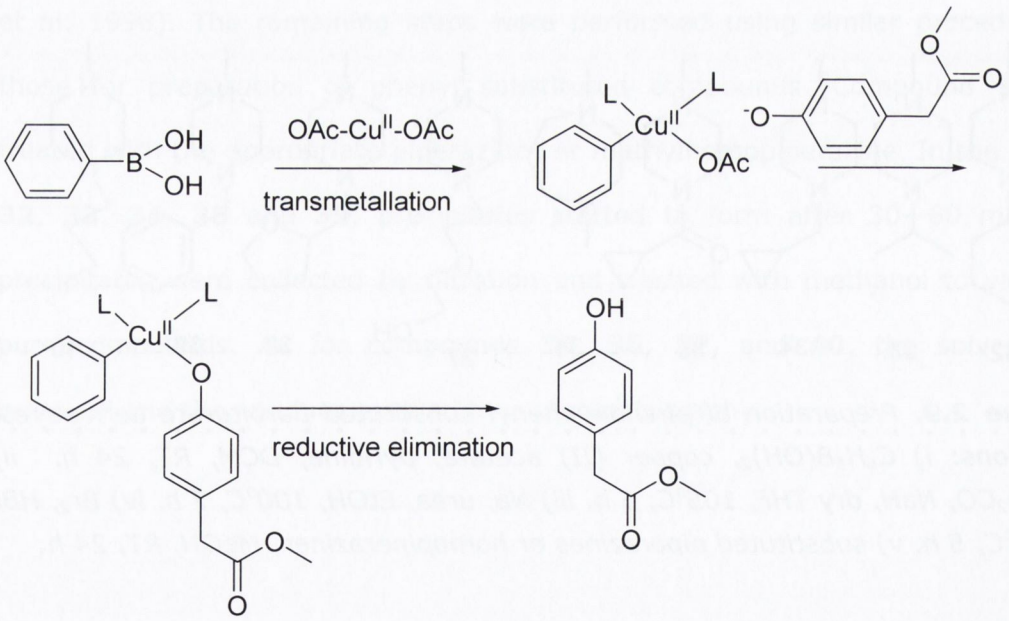


Figure 2.14. *The possible mechanism of synthesis of methyl 2-(4-phenoxyphenyl) acetate.*

2.3 Evaluation of gelatinases inhibition of phenyl, benzyloxyphenyl, and phenoxyphenyl substituted barbiturate-based compounds

Zymography was used to evaluate the inhibitory effects of the synthesized compounds with different P1′ substituents. Zymography is a simple, quantifiable, sensitive and functional electrophoretic method for measuring proteolytic activity. The method is based on sodium dodecyl sulfate gels impregnated with gelatin. MMP-2 and MMP-9 are loaded onto the gel and separated according to their molecular weight by electrophoresis. MMP-2 and MMP-9 are capable of degrading the gelatins in gels and give white bands on blue gels after staining with coomassie blue. A reader (Bio-RAD, Universal hood II) can be used to quantify the bands by UV light and giving pictures of white bands and black background (Fig. 2.15). The values given by the machine are calculated by density × area.

The MMP-2 and MMP-9 separated using zymography were supernatants from HT1080 cell suspensions treated with 2-*O*-tetradecanoylphorbol-13-acetate (PMA) based on published methods (Lohi and Keski-Oja 1995). Different concentrations of PMA were added to the cell lines and incubated at 5% CO_2, 37°C for 6, 12 and 24 h. Then media supernatants were taken out to measure activities of MMP-2 and MMP-9 by zymography (Fig. 2.15). Before running zymography, a Bradford protein assay was carried out to make sure that the same amount of protein was added onto each line of the zymography gels. The results showed HT1080 cell lines could secrete adequate amounts of MMP-2 and MMP-9 for zymography when incubated with final concentration of 10 μM PMA for 24 h.

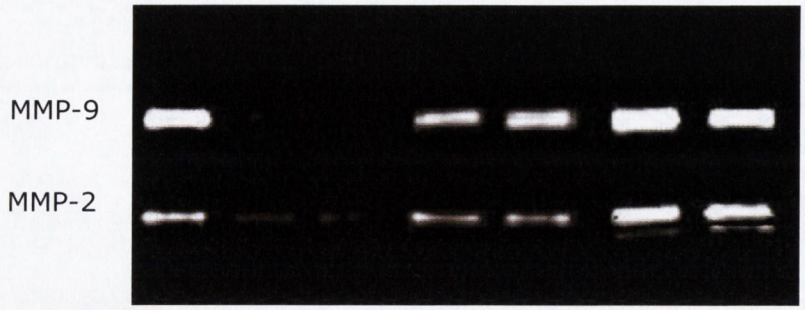


Figure 2.15. *Representative zymography following incubation of 5 ng recombinant gelatinases (1st line from left) or suspensions of HT1080 cells treated with 12-O-tetradecanoylphorbol-13-acetate (PMA) at 10 μM for 6 h (2nd and 3rd lines), 12 h (4th and 5th lines), and 24 h (6th and 7th lines) for 48 h in zymography buffer.*

We did not expect inhibitor compounds to survive bound to the proteins over the separation phase before allowing digestion to proceed. Instead, for evaluation of inhibition by synthesized compounds, PMA induced MMP-2 and MMP-9 was loaded onto gels and separated by electrophoresis. Then the gels were cut into strips which were incubated in solutions of the inhibitors at varying concentrations. The inhibition of gelatinases by compounds was estimated by comparing the intensity of control bands to those incubated in the presence of test compounds. Generally, the more potent inhibitors, the smaller on the bands (Fig. 2.16). Residual enzyme activity following incubation with test compounds was quantified by the gel reader. The inhibition of gelatinases by test compounds could be calculated using the following formula.

$$\text{Inhibition } \% = \left(1 - \frac{\text{compounds}(\text{density} \times \text{areas})}{\text{control}\,(\text{density} \times \text{areas})}\right) * 100\% \qquad 2\text{-}1$$

Where; compounds (density × areas) means values given by the bands incubated with synthesized compounds.

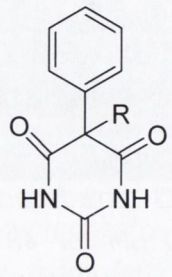
Control (density × areas) means values given by the bands incubated without any inhibitors.



Figure 2.16. *Representative zymography following incubation of suspension of HT1080 cell lines treated with 12-O-tetradecanoylphorbol-13-acetate (PMA) with compounds* ***22***, ***23*** *and* ***24*** *at 10 μM for 48 h. The first three columns were control bands which were incubated without inhibitors. The second and the third set of columns bands were incubated with 22 and 23, respectively. The last three columns bands were treated with* ***24***.

All the synthesized phenyl, benzyloxyphenyl, phenoxyphenyl substituted inhibitors were tested using zymography. All compounds were tested in triplicate and repeated three times. The approach gave surprisingly good reproducibility. The results of inhibition of MMP-2 and MMP-9 mediated are shown in Tables 2.3 — 2.5.

Table 2.3. *The inhibition by phenyl substituted compounds at 10 μM estimated using zymography (n=3).*



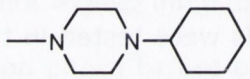
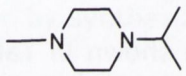
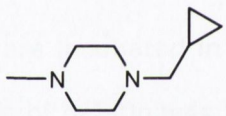
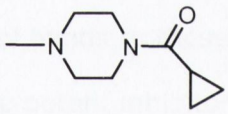
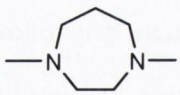
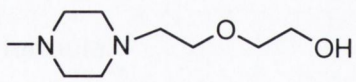
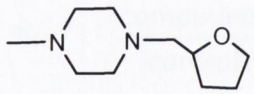
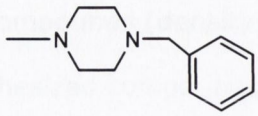
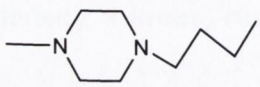
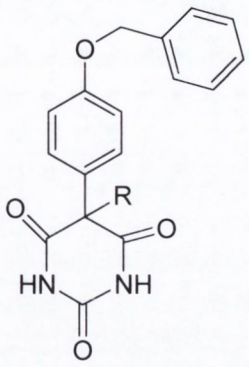
Compounds	MMP-2 inhibition	MMP-9 inhibition
R=		
5 	0%	0%
6 	0%	0%
7 	2.3%± 2.3%	5.4%±4.3%
8 	0%	4.4%±3.1%
9 	0%	0%
10 	1.6%±5.5%	2.1%±5.2%
11 	0%	0%
12 	20.2%±9.3%	27.3%±8.7%
13 	17.5%±6.3%	14.3%±6.7%

***Table 2.4**. The inhibition by benzyloxyphenyl substituted compounds determined by zymography at 10 μM (n=3).*



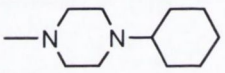
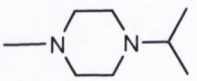
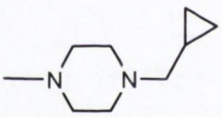
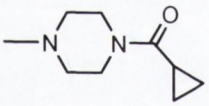
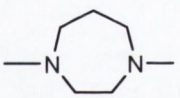
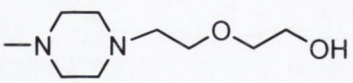
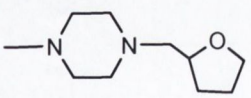
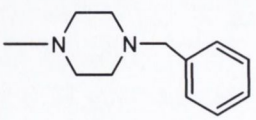
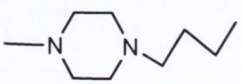
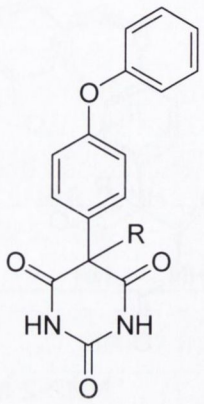
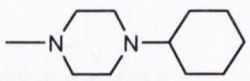
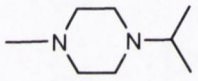
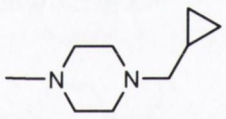
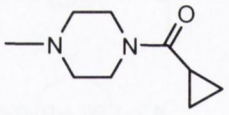
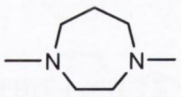
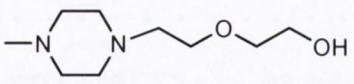
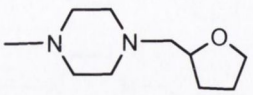
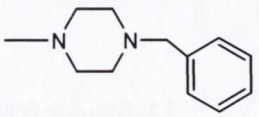
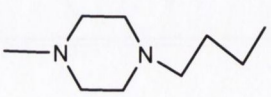
Compounds	MMP-2 inhibition	MMP-9 inhibition
R=		
19 	34.2%±3.5%	14.0%±2.4%
20 	39.8%±3.9%	16.5%±4.8%
21 	20.9%±5.6%	4.1%±3.6%
22 	68.3%±7.3%	37.7%±9.8%
23 	70.8%±6.4%	42.5%±8.8%
24 	38.2%±10.9%	21.6%±7.8%
25 	25.3%±6.8%	3.1%±2.9%
26 	35.6%±5.7%	16.2%±3.6%
27 	34.8%±4.4%	11.6%±4.6%

Table 2.5. *The inhibition by phenoxyphenyl substituted compounds determined by zymography at 0.5 μM (n=3).*



Compounds	MMP-2 inhibition	MMP-9 inhibition
R=		
32 	74.3%±5.1%	64.2%±5.2%
33 	70.5%±5.0%	62.3%±4.8%
34 	54.6%±9.6%	37.4%±8.3%
35 	76.4%±11.8%	68.7%±12.6%
36 	76.5%±7.1%	28.4%±6.9%
37 	30.4%±11.3%	25.3%±6.6%
38 	64%±6.9%	55.1%±10.6%
39 	51.5%±11.2%	53.0%±12.3%
40 	62.8%±7.3%	42.1%±6.4%

The phenyl substituted compounds had the least inhibitory potency for the gelatinases while the phenoxyphenyl group compounds were the most potent. In the phenyl class, four compounds (**5**, **6**, **9**, and **11**) showed no inhibition on either MMP-2 or MMP-9 at 10 μM while compounds (**6**, **7**, and **9**) caused very little inhibition (1.6–5.4 %). Two compounds (**12** and **13**) exhibited modest MMP-2 and MMP-9 inhibition. When the phenyl group was replaced by benzyloxyphenyl, a significant increase of inhibition on both MMP-2 and MMP-9 was observed with most compounds at 10 μM, especially for carbonyl and homopiperazine substituted compounds (**22** and **23**). For example, **22** inhibited over 70% of MMP-2 activity compared to zero inhibition by **9** at 10 μM. The least potent compound, **25**, caused only 3.1% inhibition of MMP-9 and 25.3% of MMP-2, but it was still more potent than phenyl substituted analogue **11**. Compounds **26** and **27** showed increased potency compared to corresponding phenyl substituted compounds (**12** and **13**). We supposed this might have resulted from the orientation of the compounds in gelatinases. Therefore, those two compounds were docked into MMP-2 and MMP-9 using AutoDock. The pictures in Fig. 2.17 illustrates that the phenyl moiety of compounds (**12** and **13**) occupied the S2′ pocket in the model and the piperazine fitted into the S1′ pocket, which may be the reason why **26** and **27** have similar potency with **12** and **13**. It also demonstrates that contact with the S1′ pocket is important for improving potency.

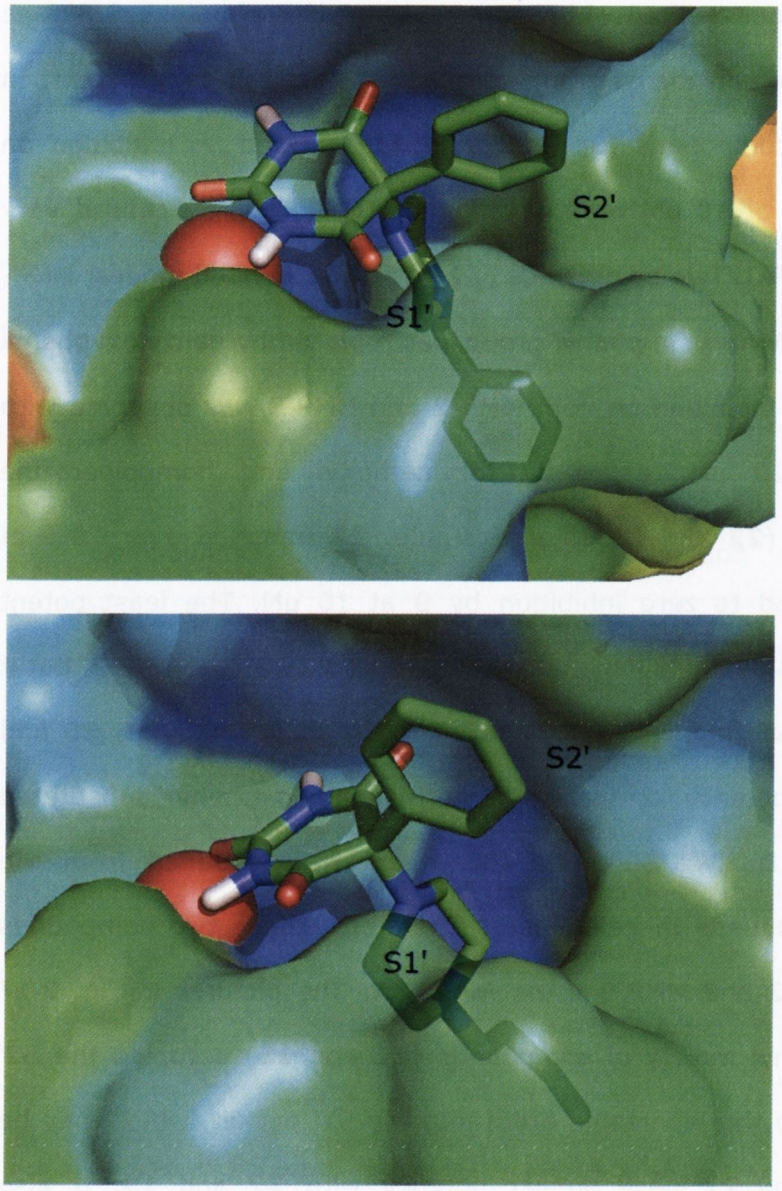


Figure 2.17. *Pictures of* ***12*** *(upper) and* ***13*** *(lower) docking with a 'Connolly' surfaces on MMP-2. The surfaces were generated by the programme PyMOL® based on the crystal structures of MMP-2 (pdb code 1qib) Ligand orientations were used which had the lowest binding energy of the conformations of 50 runs with 25000000 energy evaluations in Autodock4 and displayed by PyMOL®. The active site zincs are shown as the red spheres.*

The phenoxyphenyl substituted compounds showed the best potency in the library for MMP-2 and MMP-9. As all the compounds exhibited nearly complete inhibition at 10 μM, the experiment was repeated at successively lower concentration. More than half of compounds in this group exhibited more than 50% inhibition of MMP-2 and/or MMP-9 at 500 nM. Compound **35** exerted a very

strong inhibitory effect on both MMP-2 (76.4%) and MMP-9 (68.7%). Although **36**, which has methyl homopiperazine moiety, showed weakest inhibition on MMP-9 in this class, it was the most potent compound for inhibition of MMP-2 and thus has the best MMP-2 selectivity. These results are consistent with the known fact that the hydrophobic S1′ pocket in both MMP-2 and MMP-9 is a very deep cleft that is a critical subsite for binding (Foley, Palermo et al. 2001; Nicolotti, Miscioscia et al. 2007). While the benzyloxyphenyl and phenoxyphenyl groups are both long, the inhibitory potency of these two compound groups was different. The compounds with longer benzyloxyphenyl substituent showed weaker inhibition than the phenoxyphenyl compounds. We believe that this is because of the shape of S1′ pocket of the gelatinases. In the middle of S1′ pocket of MMP-2, Thr 227, Leu 218 and Leu 197 form a narrow hydrophobic neck. When the phenoxyphenyl moiety goes into S1′ pocket, the benzene ring at the end of the moiety sits just into the hydrophobic neck. But when benzyloxyphenyl moiety goes into S1′ pocket, the benzene ring at the end of P1′ substitution just passes the neck and sits into a wider area due to extra CH_2, resulting in a significant loss of binding affinity with S1′ pocket (Fig. 2.18). The S1′ pocket is sometimes considered as potential site for achieving gelatinase sub-type selectivity (Pirard 2007). This is because the residues of S1′ site in MMP-2 and MMP-9 are different, where MMP-2 has Thr227 and MMP-9 has Arg424 at the end (Dhanaraj, William et al. 1999; Tochowicz, Maskos et al. 2007). In addition, it has been found that the hydrophobic properties of S1′ pocket in MMP-2 is slightly weaker than that of MMP-9 (Xi, Du et al. 2009).

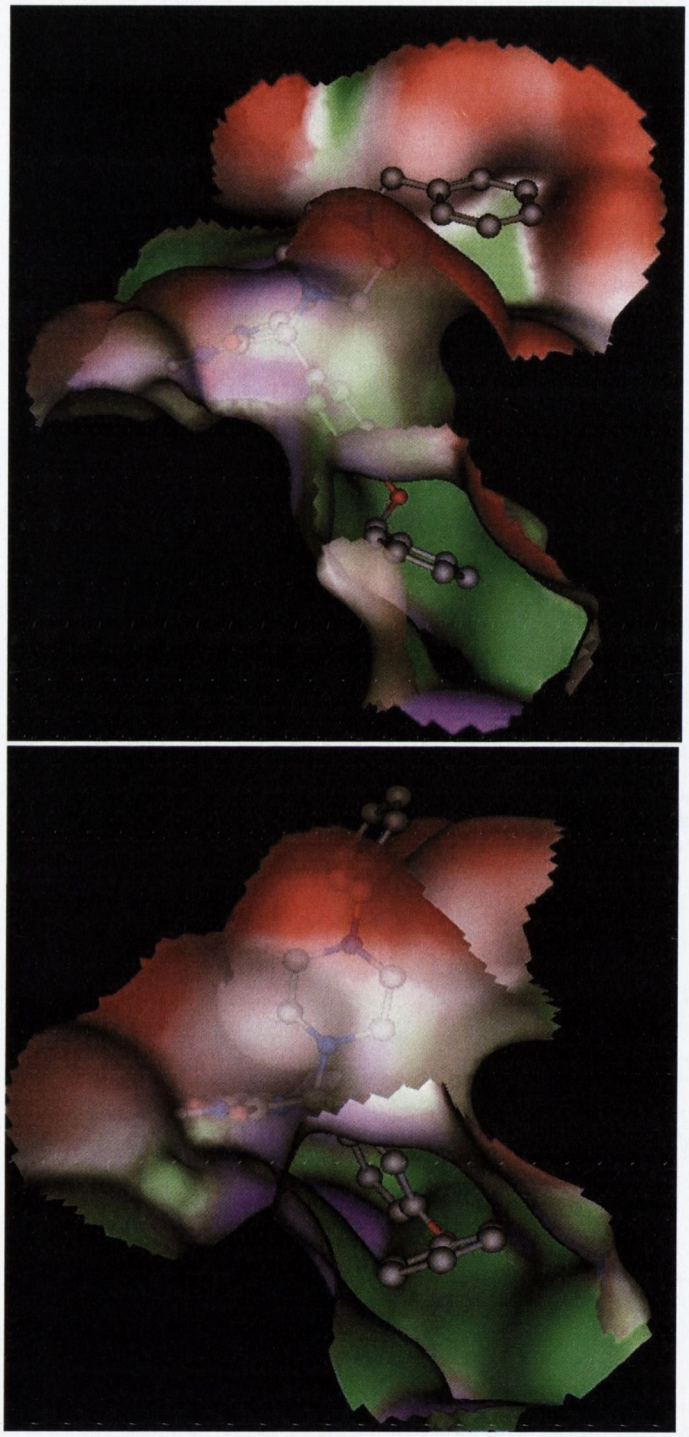


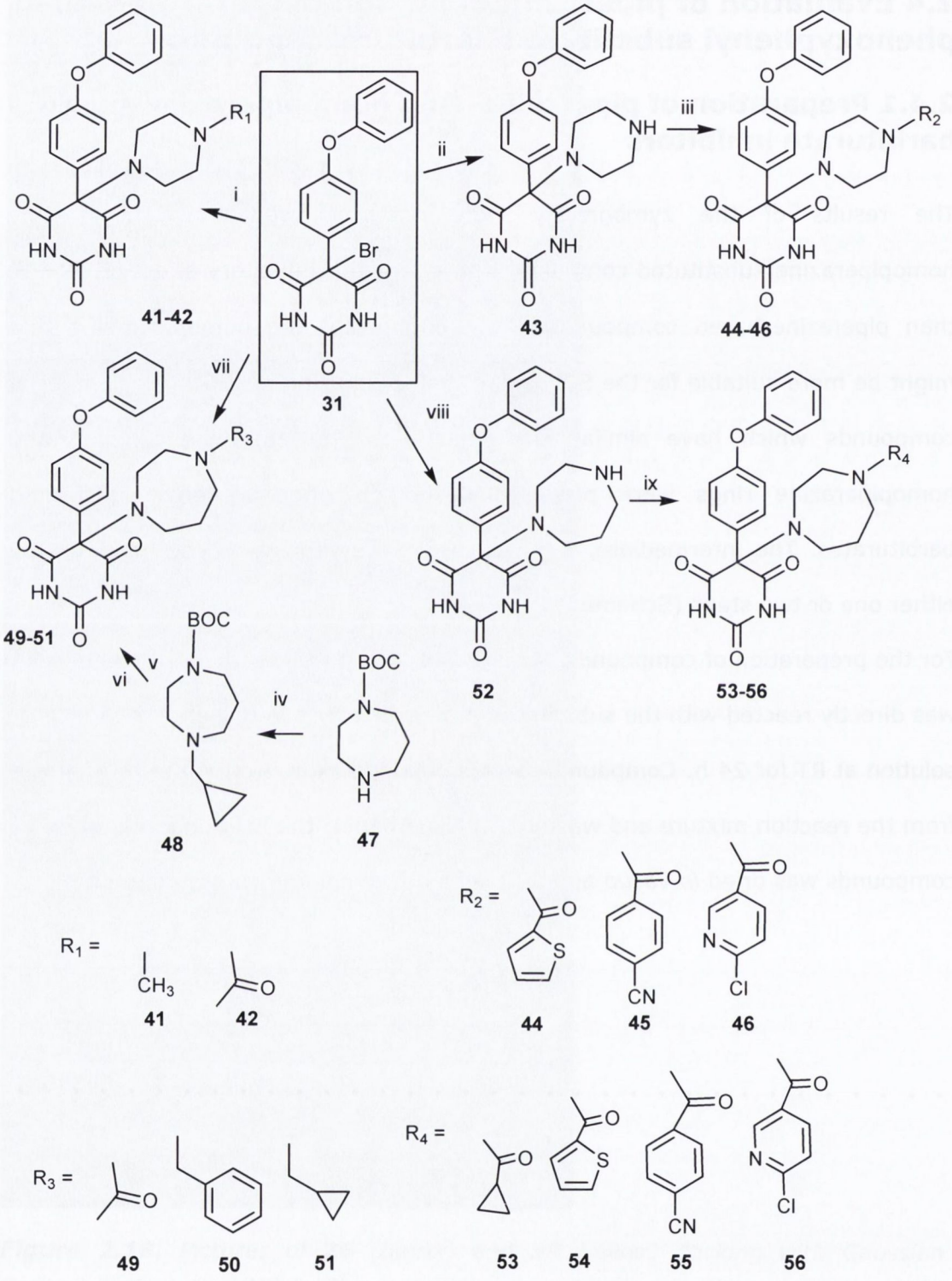
Figure 2.18. *Pictures of* ***26*** *(upper) and* ***39*** *(lower) docking with Gaussian Contact surface on MMP-2. The surfaces were generated by the programme MOE based on the crystal structures of MMP-2 (pdb code 1qib). Ligand orientations were used which had the lowest binding energy of the conformations of 50 runs with 25000000 energy evaluations in Autodock4 and displayed in MOE. The polar surface is shown as red and hydrophobic surface is shown as green. The purple represents H-bonding.*

2.4 Evaluation of piperazine- and homopiperazine-based phenoxyphenyl substituted barbiturate inhibitors

2.4.1 Preparation of piperazine- and homopiperazine-based barbiturate inhibitors

The results of the zymography experiments showed that the methyl homopiperazine substituted compound had a stronger inhibitory effect on MMP-2 than piperazine-based compounds. We thought that the homopiperazine ring might be more suitable for the S2' pocket than piperazine ring. Thus a number of compounds which have similar side chains on the end of piperazine and homopiperazine rings were prepared based on phenoxyphenyl substituted barbiturates. The intermediate, **31**, was used to synthesize these inhibitors by either one or two steps (Scheme 2.10).

For the preparation of compounds (**41**, **42**, **49**, **50**, and **51**), the intermediate **31** was directly reacted with the substituted piperazines or homopiperazines in MeOH solution at RT for 24 h. Compound **41** was obtained by collecting the precipitates from the reaction mixture and washing with methanol; the resulting mixture of all compounds was dried *in vacuo* and purified by flash column chromatography.



Scheme 2.10. *Preparation of piperazine- and homopiperazine-based phenoxyphenyl substituted barbiturate derivatives. Conditions: i) substituted piperazines, MeOH, RT, 24 h. ii) piperazine, MeOH, RT, 24 h. iii) acid chlorides, THF, -70°C, 5 h. iv) $C_3H_5CH_2Br$, MeOH, RT, 12 h. v) CF_3COOH, DCM, 0°C, overnight. vi) MeOH, compound 31, RT, 24 h. vii) substituted homopiperazines MeOH, RT, 24 h. viii) homopiperazine, MeOH, RT, 24 h. ix) acid chlorides, THF, -70°C, 5 h.*

For the synthesis of compounds (**44**, **45**, **46**, **53**, **54**, **55** and **56**), compound **31** was either reacted with piperazine or homopiperazine to form **43** and **52**. These two compounds were precipitated out as white solids from methanol solution, which is a key reason that products **43** and **52** didn't further react with compound **31**. To obtain the desired substituted barbiturate inhibitors, two compounds were coupled with the corresponding acid chlorides in the presence of triethylamine in THF at -70°C. THF was used as a solvent because it could dissolve a little bit of **43** and **5** as well as their carbonyl products. Another reason is that the melting point of THF is below the reaction temperature, -70°C. We performed the reaction at very low temperature because initial attempts at 0°C suggested there was competition between the piperazinyl nitrogen and barbiturate nitrogen with the formation of several byproducts (Fig. 2.19). At -70°C the more reactive piperazinyl nitrogen was selectively acylated. Thus, -70°C was used as the reaction temperature to reduce impurities, although it resulted in longer reaction times. The pure compounds were obtained by flash column chromatography. The synthesis of **51** took two more steps comparing to **50**. A cyclopropylmethyl substituted BOC-homopiperazine (**48**) was synthesized by coupling of BOC-homopiperazine with (bromomethyl)cyclopropane. Then **48** was deprotected by TFA to remove the BOC group followed by reaction with **31** to form **51**.

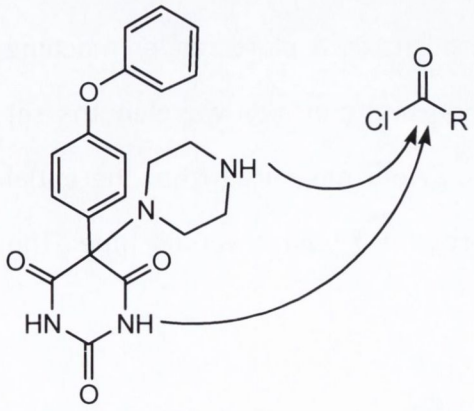


Figure 2.19. *The competitions between NH group on piperazine ring and NH group on barbiturate ring when reacting with acid chlorides.*

2.4.2 Structure-Activity Relationships

Although zymography is a good method to examine inhibition potency, results obtained by zymography did not have ideal precision. The main reason is because the gelatinases used in zymography were supernatants obtained from PMA treated HT1080 cell lines, which may also contain other proteinases with ability to degrade the gelatins in the gel. Therefore, zymography was only used for general screen. For measurement of the IC_{50} values of new compounds, a fluorogenic assay was applied.

The fluorogenic assay provides an accurate and precise method for testing the potency of the inhibitors. This has been widely used for obtaining IC_{50} values of newly synthesized MMP inhibitors (Breyholz, Schäfers et al. 2005; Whitlock, Dack et al. 2007). The potency was obtained by measuring remaining proteinase activity after the incubation of APMA (*p*-aminophenylmercuric acetate) activated MMP-2 or MMP-9 and inhibitors at 37°C for 30–40 min. When a suitable substrate is added to the mixture of MMPs and inhibitors, the remaining activity of proteinase is capable of cleaving an amide bond between the fluorescent group and quencher group, which causes an increase in fluorescence. The substrate used here was Mac-Pro-Leu-Gly-Leu-Dap-Ala-Arg-NH_2 (R&D system, UK), which is cleaved at bond of Gly-Leu and gives a highly fluorescent Mac-Pro-Leu-Gly part and an efficient quench Leu-Dap-Ala-Arg-NH_2 part (Knight, Willenbrock et al. 1992). The fluorescence changes were monitored using a plate reader machine (Fluostar OPTIMA, BMG LABTECH) with excitation and emission wavelengths set to 330 and 405 nm, respectively. Reaction rates were measured from the initial 10 min. A slope was obtained by plotting fluorescence values versus time. The inhibition was calculated using the formula 2-2

$$\text{Inhibition } \% = \left(1 - \frac{\text{Slope (compounds)}}{\text{Slope (control)}}\right) * 100\% \qquad 2\text{-}2$$

Where Slope (compounds) means slope values given by solutions incubated with tested compounds and Slope (control) means slope values given by solution incubated without any inhibitors.

The IC_{50} values were calculated by plotting the logarithm of the concentration versus the %inhibition in the Sigmoidal dose-response formula. GraphPad Prism® 4 was used to get the IC_{50} values and 95% confidence intervals, an example shown in the Figure 2.20.

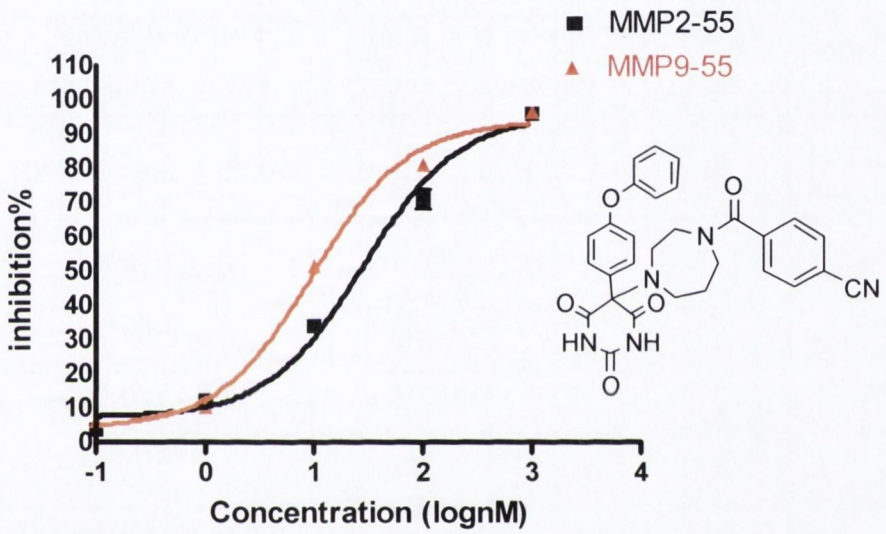
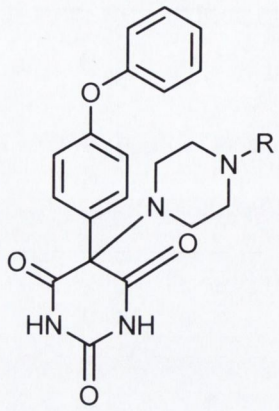


Figure 2.20. *Curves for compounds* ***55*** *in GraphPad Prism® 4 for calculation of* IC_{50} *values of MMP-2 (black) and MMP-9 (red).*

Eight piperazine and homopiperazine compounds, which had the similar moieties attached, were assayed to obtain their IC_{50} values (Table 2.6 and Table 2.7).

Table 2.6. *IC_{50} values of piperazine substituted compounds.*



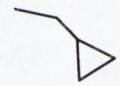
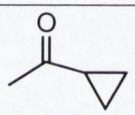
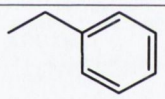
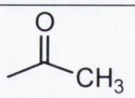
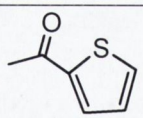
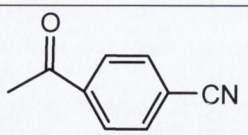
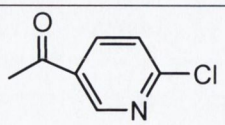
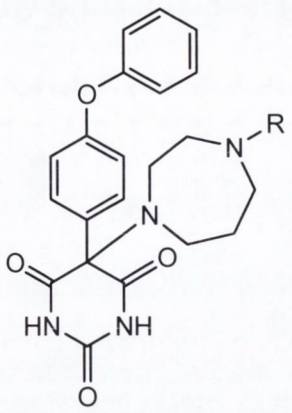
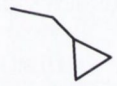
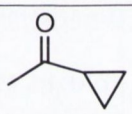
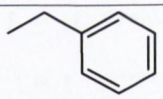
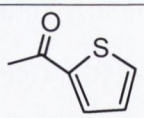
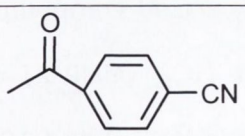
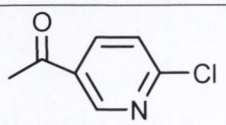
Structure R=	Cpd No.	MMP-2 IC_{50} (nM) (95% confidence)	MMP-9 IC_{50} (nM) (95% confidence)
	**34**	5.20 (3.52 – 7.68)	10.25 (7.96 – 13.20)
	**35**	26.80 (21.26 – 33.78)	15.44 (12.11 – 19.69)
	**39**	131.12 (113.75 – 151.14)	85.94 (70.99 – 104.12)
	**41**	15.95 (10.94 – 23.25)	9.42 (7.84 – 11.33)
	**42**	13.66 (13.66 –15.72)	15.72 (12.58 – 19.66)
	**44**	43.63 (30.84 – 61.71)	72.72 (58.37 – 90.60)
	**45**	43.25 (33.70 – 55.51)	45.30 (36.46 – 56.28)
	**46**	45.17 (33.71 – 60.53)	54.01 (44.81 – 65.11)

Table 2.7. *The IC_{50} values of homopiperazine substituted compounds.*



Structure R=	Cpd No.	MMP-2 IC_{50} (nM)	MMP-9 IC_{50} (nM)
	51	1.08 (0.74 – 1.55)	1.12 (0.84 – 1.48)
	**53**	13.01(10.60 – 15.97)	12.65 (8.62 – 18.58)
	**50**	26.04 (19.49 – 34.79)	22.35 (16.49 – 30.29)
	**36**	1.93 (1.61 – 2.31)	7.54 (6.25 – 9.09)
	**49**	1.50 (1.09 – 2.08)	2.90 (2.14 –3.93)
	**54**	18.83 (13.30 – 26.66)	15.54 (12.10 – 19.95)
	**55**	28.49 (19.66 –41.29)	9.81 (7.66 – 12.56)
	**56**	110.50 (97.32 – 125.45)	104.28 (88.57 – 122.78)

The barbiturate derivatives with a homopiperazine ring had superior potencies to the piperazine substituted compounds apart from **56** (IC_{50} (MMP-2) = 110.50 nM,

(MMP-9) = 104.28 nM) with homopiperazine ring and **46** (IC_{50} (MMP-2) = 45.17 nM, (MMP-9) = 54.01 nM) with piperazine ring. The MMP-2 and MMP-9 inhibition by cyclopropylcarbonyl substituted barbiturate derivatives slightly increased when the piperazine ring (**35**) (IC_{50} (MMP-2) = 26.80 nM, (MMP-9) = 15.44 nM) was replaced by the homopiperazine ring (**53**) (IC_{50} (MMP-2) = 13.01 nM, (MMP-9) = 12.65 nM). A larger increase in potency was found with **54**; the IC_{50} values reduced from 43.63 nM on MMP-2 and 72.72 nM on MMP-9 to 18.83 nM and 15.54 nM respectively when the piperazine ring was substituted. The largest impact on of IC_{50} values was with benzyl substituted compounds (**39** and **50**). The IC_{50} value of homopiperazine **50** decreased over 100 nM on MMP-2 and 60 nM on MMP-9 comparing to the corresponding piperazine compound. Substitution of acetyl group of homopiperazine inhibitor **49** (IC_{50} (MMP-2) = 1.50 nM, (MMP-9) = 2.90 nM) increased potency more than 9-fold in MMP-2 and 5-fold in MMP-9 comparing with piperazine-based **42** (IC_{50} (MMP-2) = 13.66 nM, (MMP-9) = 15.72 nM). The methyl homopiperazine compound **36** (IC_{50} (MMP-2) = 1.93 nM) showed 8-fold higher potency in MMP-2 than piperazine **41**. Although there was not a significant increase in inhibitory effect on MMP-9, the replacement of piperazine with homopiperazine in methyl substituted compound produced the most MMP-2 selective inhibitors in the library, **42**, which showed nearly four fold selectivity on MMP-2 over MMP-9. Replacement of piperazine in **34** (IC_{50} (MMP-2) = 5.20 nM, (MMP-9) = 10.25 nM), the most potent piperazine-based compound for MMP-2 in the library, with homopiperazine generating **51** (IC_{50} (MMP-2) = 1.08) nM, (MMP-9) = 1.12 nM) improved potency 5-fold towards MMP-2 and 10-fold for MMP-9.

The homopiperazine compounds were prepared because of an intuition that the S2′ pocket, which is large and solvent exposed, is not fully filled by piperazine substituents. The homopiperazine compounds did turn out to be generally more potent. In order to investigate the reasons for this, piperazine and

homopiperazine substituted (**42** and **36**) compounds were docked into both MMP-2 and MMP-9 to look at the way the ligands bound to the two proteins at the mouth of S2′ pocket using the programme Autodock 4. After 50 runs, with 25000000 energy evaluations in each run, conformations with lowest binding energy were used for evaluation. The pictures of docking results of **42** and **36** illustrate the orientation of the ligands in MMP-2 (Figure 2.21). The barbiturate bound in the model as expected from relevant X-ray crystal structures. The piperazine ring of **42** was seated into the S2′ pocket and left quite a wide gap with the surface of the mouth of the S2′ pocket. The gap between the surface of mouth of the S2′ pocket and the P2′ substituent significantly reduced when **36** was docked, suggesting that a homopiperazine ring could be more suitable for filling the mouth of the S2′ pocket, forming more contact and improving potency.

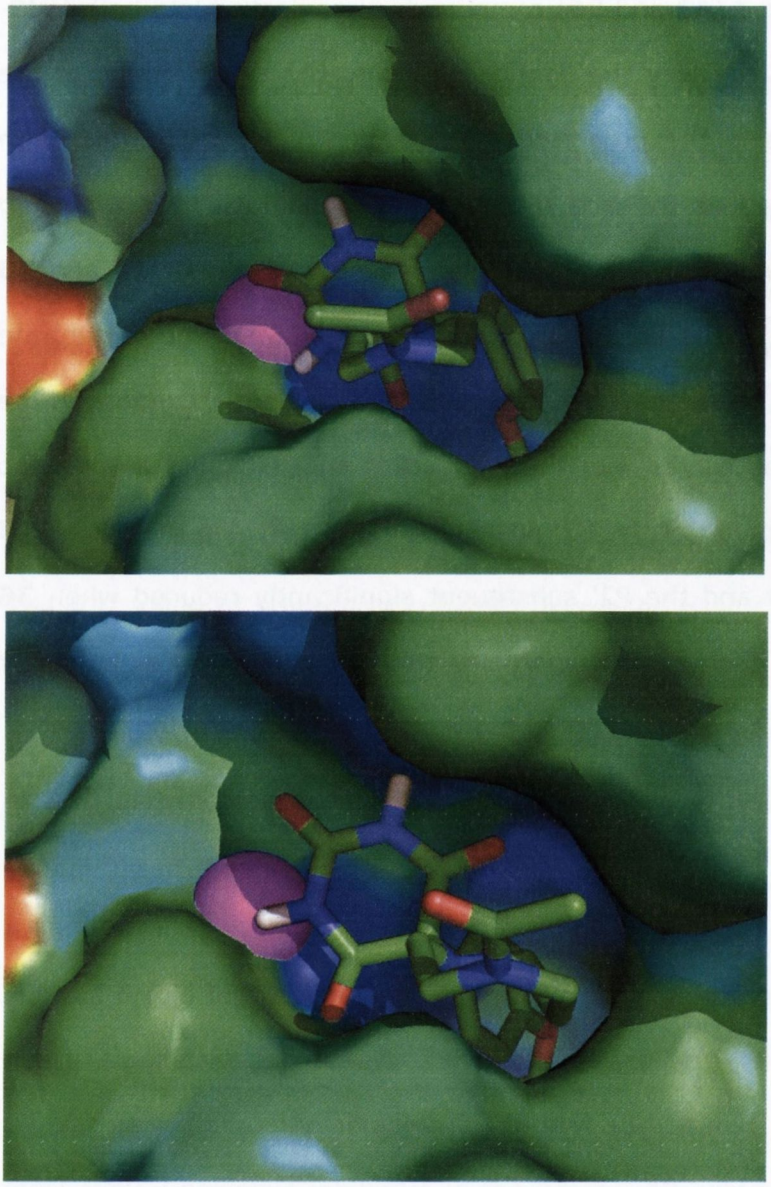


Figure 2.21. *Pictures of model* ***42*** *(upper) and* ***36*** *(lower) docking with a 'Connolly' surface on MMP-2. The surfaces were generated by the programme PyMOL® based on the crystal structures of MMP-2(pdb code 1q1b). Ligand orientations were used which had the lowest binding energy of the conformations fitted into the designated pockets in the Autodock4 and displayed by PyMOL®. The active site zinc atoms are shown as magenta spheres.*

2.5 Conclusion

Gelatinases are implicated in many diseases including cancers, arthritis, cardiovascular diseases, and inflammatory bowel diseases. They play an important role in tumor cell invasion and metastasis by digestion of matrix membranes and collagenolysis (Deryugina and Quigley 2006). Therefore, gelatinases have been considered as promising targets for many diseases.

Certain 5-substituted barbiturates, a drug type that exerts effects on the CNS, have been found to have inhibitory effects on MMPs due to their ability to bind zinc and occupy adjacent substrate binding pockets (Foley, Palermo et al. 2001; Grams, Brandstetter et al. 2001). A series of compounds with three different substitutions at P1′ position were prepared to investigate interactions at S1′ pocket where P1′ substituents bind. Phenyl group compounds were the weakest MMP inhibitors because phenyl is too short to fill the long and deep S1′ pocket. Two compounds in this group exhibited some inhibition on both MMP-2 and MMP-9 at 10 μM. However, when these were modelled into the active site(s), the phenyl group went to S2′ pocket and the P2′ substituents which were supposed to fit into S2′ pocket, went to the S1′ pocket. The longer benzyloxyphenyl and phenoxyphenyl substituents showed good gelatinase inhibition on, especially the phenoxyphenyl group compounds, which were able to inhibit gelatinase activity in the nanomolar range. Although the benzyloxyphenyl substituent is longer than phenoxyphenyl group, compounds with phenoxyphenyl group exhibited better inhibition. This is because the shape of S1′ pocket, which has a narrow neck in the middle of pocket that is optimally occupied with phenyloxyphenyl rather than benzyloxyphenyl.

Apart from the S1′ pocket, the S2′ pocket is also important for potency and selectivity. A number of piperazine- and homopiperazine-based barbiturates were synthesized to investigate binding in the mouth of S2′ pocket where the two groups fit. Most of the homopiperazine-based compounds gave lower IC_{50} values

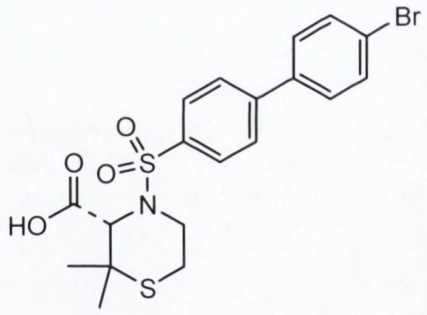
for both MMP-2 and MMP-9 than the corresponding piperazine-based compounds. The results of docking support our hypothesis that the larger ring could better fill the S2′ pocket. However none of the compounds exhibited pharmacologically promising selectivity. We next planned to elaborate the potent homopiperazine compounds towards this goal.

Chapter 3

Optimizing homopiperazine-based MMP inhibitors for gelatinase selectivity

3.1 Introduction

It has been widely accepted that lack of MMP subtype selectivity is the major reason for the clinical failure of MMP inhibitors. Therefore, extensive research has been carried out with a view to improving selectivity. Some progress has been made in understanding possible vectors for selectivity leading to the development of semi-selective hydroxamates, carboxylates, thiols, barbiturates, and sulfonamides, which can show broad selectivity towards MMP-1, -2, -3, -8, -9, and -13 over other MMPs. For example, a sulphonamide inhibitor of MMPs exhibits selectivity for MMP-2, -3, -13, and -14 over MMP-7 (Fig. 3.1). We are still some way off being able to generate inhibitors with sufficient selectivity for MMP types that could be clinically harnessed especially in the area of the gelatinases.



IC_{50} (nM)

MMP-1 = 3100; MMP-2 = 6;

MMP-3 = 3; MMP-7 = 10,000;

MMP-9 = 260; MMP-13 = 16

MMP-14 = 48

Figure 3.1 . *IC_{50} values of a sulphonamide-based MMP inhibitors with selectivity for MMP-2, -3, -16, and -14 over MMP-1 and MMP-7 (Barvian, Ann Arbor et al. 2002).*

Selectivity can in theory be achieved by modification of substituents off the Zn-binding scaffold which can interact with slight differences in amino acid sequence in the pockets around the active site. Generally, substitutions on hydroxamic acids fill the S1, S1′ and S2′ pockets. Fig. 3.2 shows an example of a substituted hydroxamic acid MMP inhibitor bound in MMP-3. This compound has selectivity for MMP-2, -3, and -13 over MMP-7 (Cheng, De et al. 1999). Substitutions on carboxylate-based inhibitors go into different pockets. Side chains on most carboxylates fit into the S1′ and S2′ pockets. Fig. 3.3 shows a carboxylate-based

MMP inhibitor which has great potency and selectivity for MMP-13 and -2 over MMP-1 and -3 (Natchus, Bookland et al. 2001).

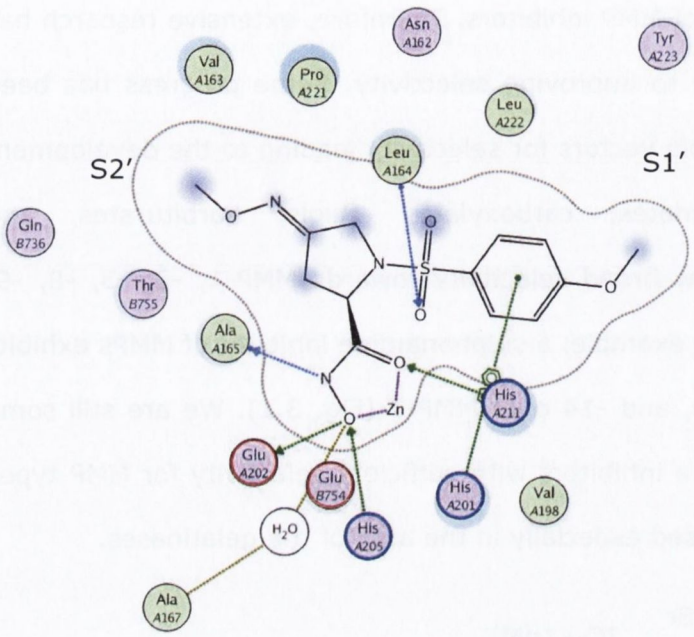
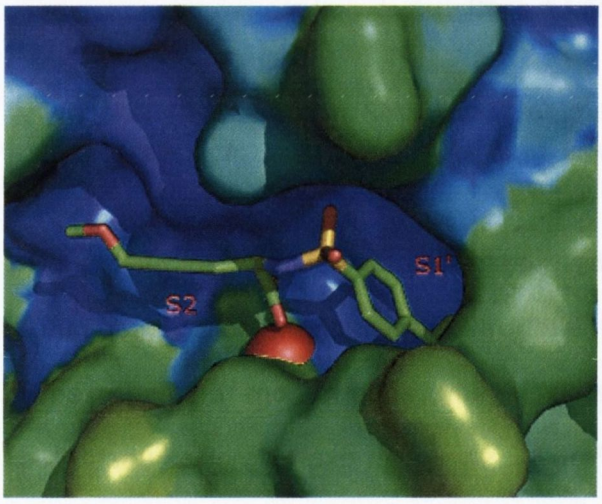
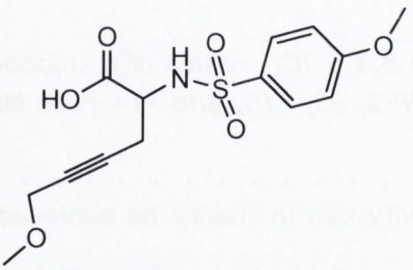


Figure 3.2. *The interaction of a hydroxamic acid with MMP-3. The picture was generated by the programme MOE based on the crystal structure of MMP-3 (pdb code: 1d7x). The methoxyphenyl moiety and the methoxyiminopyrrolindine group are fitted into S1' and S2' pocket, respectively.*





IC_{50} (nM)
MMP-1 = 6150; MMP-2 = 20;
MMP-3 =4090; MMP-13 = 76.

Figure 3.3. *A picture of a substituted carboxylic acid in MMP-3. The surfaces were generated by the programme PyMOL® based on the crystal structures of MMP-3 (pdb code: 1hy7). The methoxyphenyl and alkyne substituents are inserted into the S1' and S2 pockets.*

Binding into the S1′ and S2′ pockets, which are relatively well defined (especially in the former case), is associated with improved affinity and potency relative to the unprimed S1 and S2 pockets (left-side) which are flat and solvent exposed (Rao 2005). Barbiturate inhibitors already described in this work had greater potency with the classical P1 phenoxyphenyl group which binds deeply into the S1 pocket in the barbiturate and non-barbiturate classes. Therefore, we decided to retain the phenyoxyphenyl group for affinity while examining options for increasing selectivity. We focussed in this regard on potentially important differences between the gelatinases at the mouth of the S2′ pocket where Ile222 and Met422 are found in MMP-2 and MMP-9, respectively. As well as the phenoxyphenyl group, we proposed to retain the homopiperazine group because we had shown that it imparts good affinity relative to piperazine, while retaining the synthetic merit of presenting a distal N-atom for potential incorporation of a wide variety of chemical types rapidly by acylation. Therefore we decided to make and screen a large number of 5-phenoxyphenyl-*N*-acylhomopiperazines in order to probe for differential interactions at the mouth of the S2′ pocket that might impart selectivity (Fig. 3.4). As we shall see, the approach was only partially successful probably because of the similar physicochemical characteristics of Met424 and Ile222 side chains.

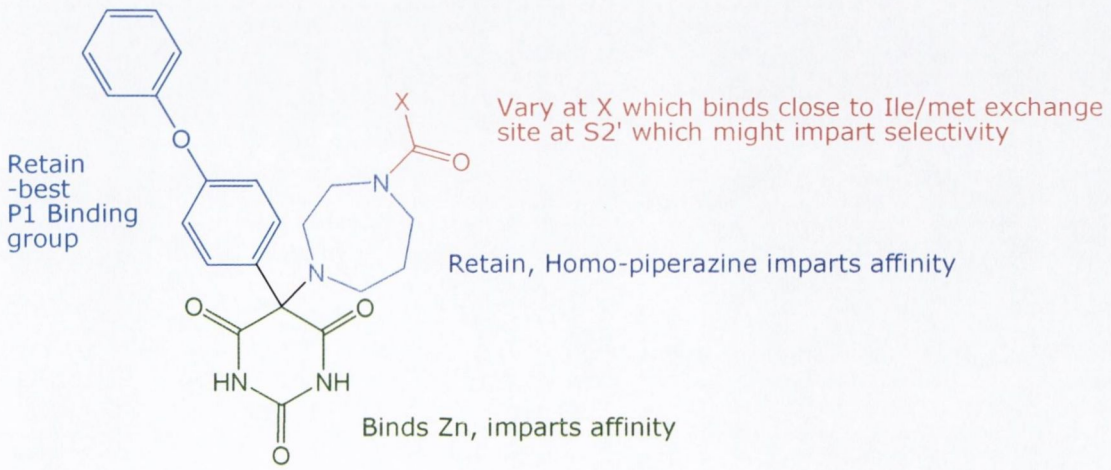
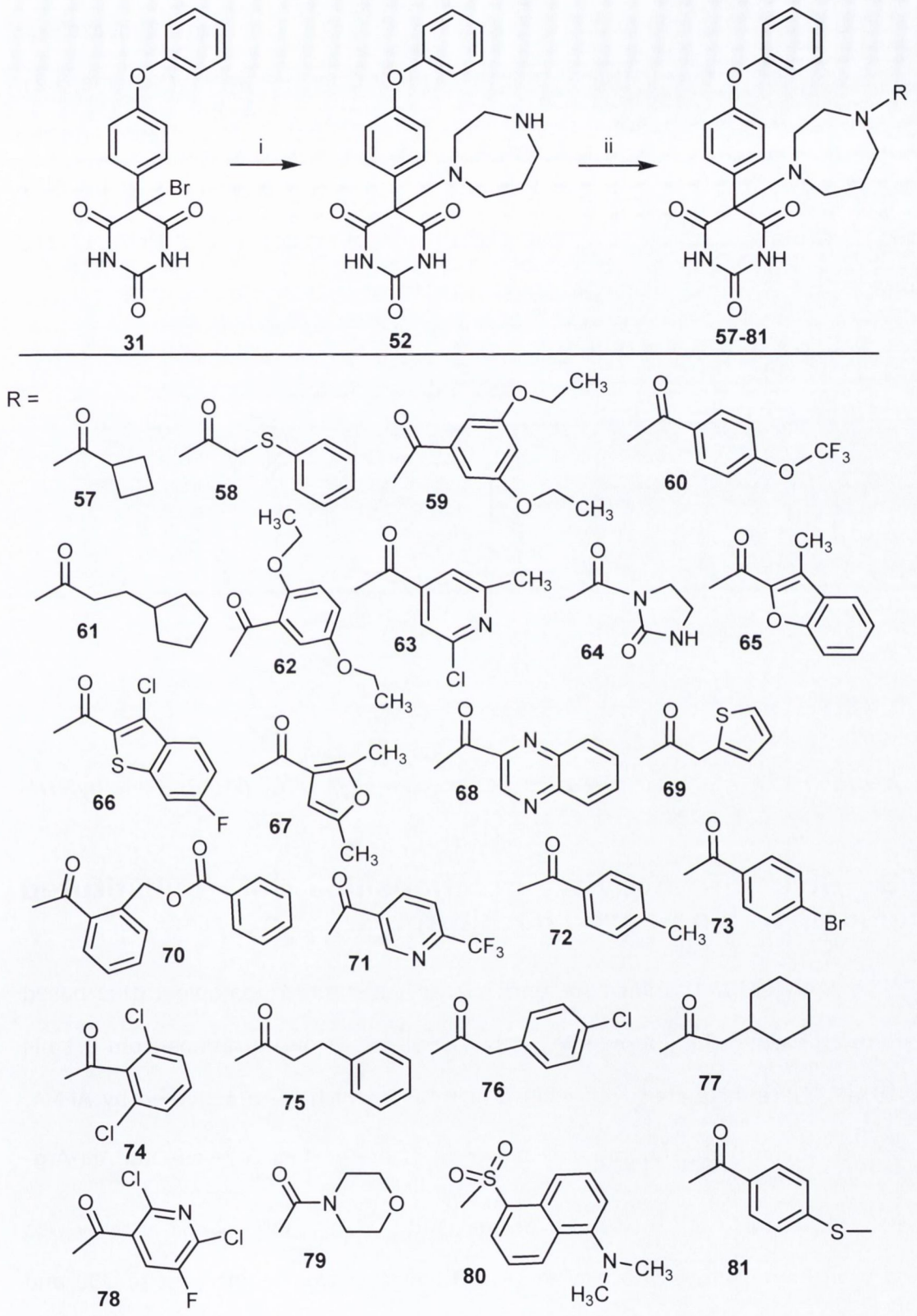


Figure 3.4. *Strategy for improving gelatinase selectivity by acyl substitution on the distal N of the homopiperazine substituted barbiturate scaffold.*

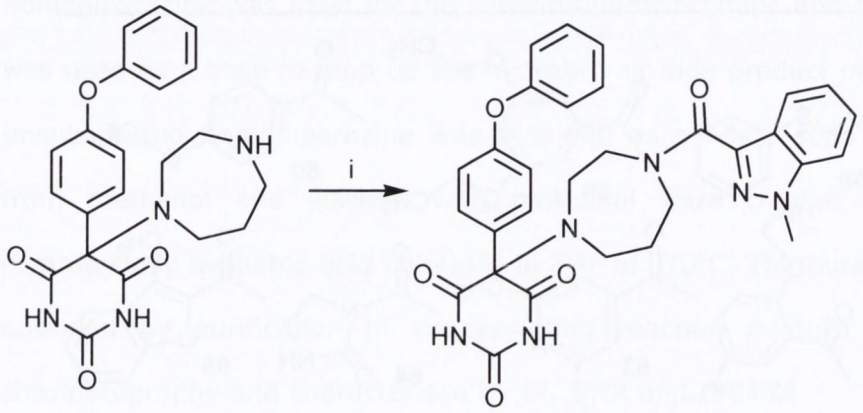
3.2 Preparation of substituted homopiperazine-based MMP inhibitors

The synthesis of most of the target homopiperazine-based barbiturates involved use of the procedure described for the preparation of **52** in the Chapter 2, which used **31** (Scheme 3.1). Compound **31** was allowed to react with 2 equivalents of homopiperazine in methanol at room temperature for 24 h. One equivalent of homopiperazine was used for the substitution of bromine and another equivalent was used as a base to mop up the hydrobromic side product of the reaction. The unsubstituted homopiperazine was obtained as a white solid (**52**) precipitated from methanol and washed with methanol were treated with a range of commercially available acid chlorides in THF at -70°C. The pure compounds were obtained by purification of the resulting reaction mixture by flash column chromatography and characterised by IR, NMR and HRMS.



Scheme 3.1 *Preparation of substituted homopiperazine-based barbiturates. i) piperazine, MeOH, RT, 24 h. ii) acid chlorides, THF, -70°C, 5 h.*

Compound **82** was synthesized by treating **51** with 1-methyl-1H-indazole-3-carboxylic acid in the presence of DMAP and DCC in THF at RT (Scheme 3.2). After 12 h, the reaction mixture was filtered. The filtrate was collected and the solvent was removed *in vacuo*. The resulting residues were purified by flash column chromatography. The final product was characterised by NMR, IR and HRMS.



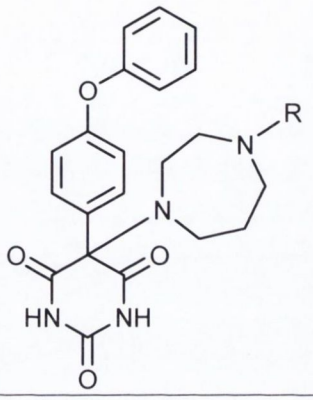
***Scheme 3.2**. Preparation of **82** by DCC coupling. i) DCC, DMAP, 1-methyl-1H-indazole-3-carboxylic acid, THF, RT, 12 h.*

3.3 Structure-Activity relationships of substituted homopiperazine-based barbiturates.

IC_{50} values were determined for each of the substituted homopiperazine-based barbiturates using the fluorogenic assay. Usually 5–6 concentrations from 0.1 nM to 10 μM, were incubated with MMP-2 or MMP-9 which were activated by APMA. After 30–45 min, the fluorogenic substrate (Mac-Pro-Leu-Gly-Leu-Dap-Ala-Arg-NH_2) was added to the mixture of protein and inhibitor. Fluorogenic activity was measured immediately with excitation and emission wavelengths set to 330 and 405 nm, respectively. The reading interval was set to 1 min. The first 10 min readings were recorded and a slope was obtained by plotting fluorescence values versus time. Inhibition by the tested compounds was calculated using formula 2-2. The IC_{50} values were obtained by plotting the logarithm of concentration versus

the inhibition% in the Sigmoidal dose-response formula in GraphPad Prism® 4. Each compound was assessed three times in duplicate. The IC_{50} values of the compounds were shown in Table 3.1, along with 95% confidence intervals.

Table 3.1 *IC_{50} values of substituted homopiperazine-based barbiturates.*



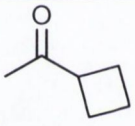
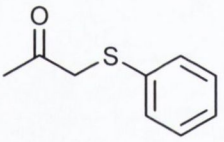
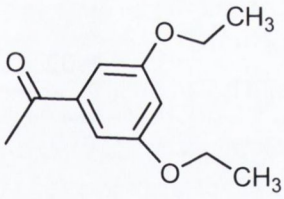
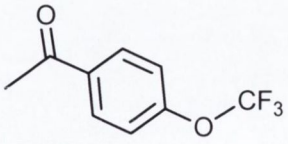
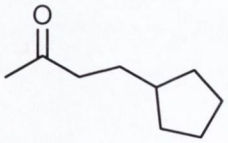
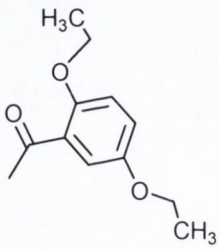
R	compd	MMP-2 (nM)	MMP-9 (nM)	MMP-9 selectivity
	**57**	14.20 (12.08 - 16.70)	13.24 (10.99 - 15.95)	1.06
	**58**	36.37 (28.10 - 47.08)	28.96 (23.83 - 35.21)	1.26
	**59**	1190.11 (974.67 - 1453.18)	269.33 (219.56 - 330.37)	4.41
	**60**	70.33 (60.95 - 81.15)	59.96 (50.92 - 70.60)	1.17
	**61**	154.96 (121.08 - 198.33)	49.55 (41.97 - 58.48)	3.13
	**62**	375.59 (294.09 - 479.69)	328.85 (286.46 - 377.51)	1.14

Table 3.1 *contd.*

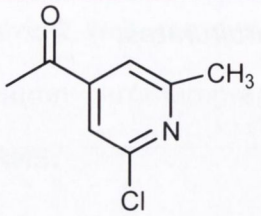
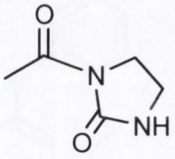
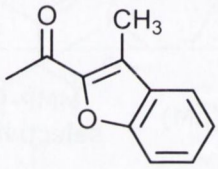
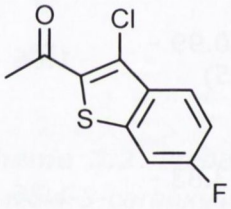
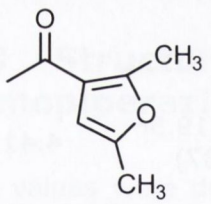
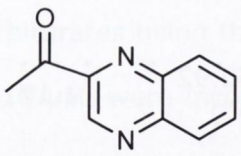
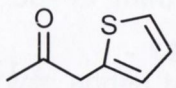
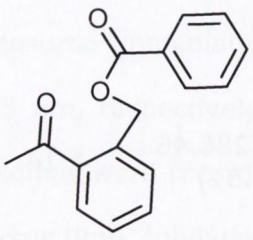
R	compd	MMP-2 (nM)	MMP-9 (nM)	MMP-9 selectivity
	**63**	28.22 (21.99 - 36.21)	85.68 (63.68 - 115.3)	0.33
	**64**	190.89 (156.18 - 233.32)	263.89 (217.78 to 319.77)	0.72
	**65**	2.88 (2.35 - 3.52)	2.55 (1.955 - 3.32)	1.13
	**66**	214.87 (180.87 - 255.26)	307.63 (250.99 – 377.06)	0.70
	**67**	24.66 (20.44 - 29.75)	24.08 (20.18 - 28.73)	1.02
	**68**	34.45 (27.70 – 42.86)	29.95 (24.58 – 36.51)	1.15
	**69**	51.09 (43.94 – 59.40)	47.10 (39.11 – 56.72)	1.15
	**70**	119.77 (96.17 – 149.16)	106.21 (83.35 – 135.34)	1.13

Table 3.1 *contd.*

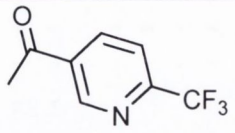
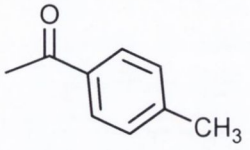
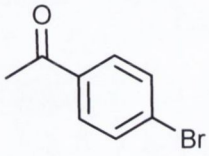
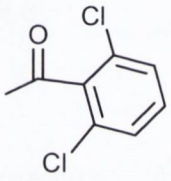
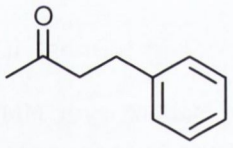
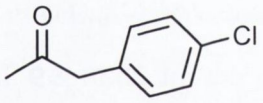
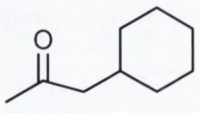
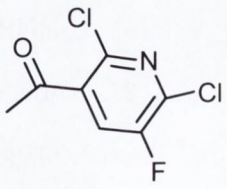
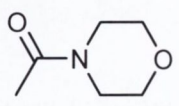
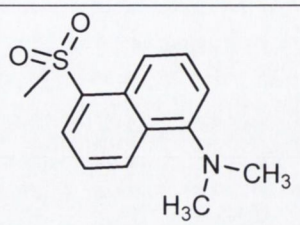
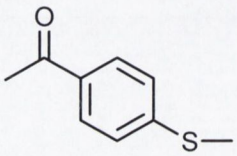
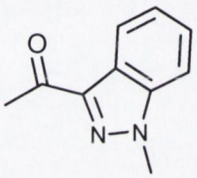
R	compd	MMP-2 (nM)	MMP-9 (nM)	MMP-9 selectivity
	**71**	198.18 (172.50 – 227.68)	264.02 (212.88 – 327.44)	0.75
	**72**	43.58 (37.01 – 51.32)	80.37 (69.16 – 93.40)	0.54
	**73**	282.07 (232.03 – 342.91)	268.21 (219.76 – 327.33)	1.05
	**74**	86.50 (76.90 – 97.29)	22.71 (19.57 – 26.37)	3.81
	**75**	61.74 (50.26 – 75.84)	30.93 (22.40 – 42.70)	2.00
	**76**	173.19 (127.08 – 236.04)	94.89 (72.29 – 124.55)	1.77
	**77**	76.94 (68.69 – 86.17)	100.47 (81.60 – 123.72)	0.76
	**78**	81.23 (67.80 – 97.32)	25.34 (21.36 – 30.05)	3.20
	**79**	23.81 (18.67 – 30.37)	24.80 (19.41 – 31.69)	0.96

Table 3.1 *contd.*

R	compd	MMP-2 (nM)	MMP-9 (nM)	MMP-9 selectivity
	**80**	74.46 (65.62 – 84.49)	310.88 (232.06 – 416.49)	0.24
	**81**	92.88 (76.11 – 113.35)	411.45 (266.66 – 634.85)	0.22
	**82**	213.79 (168.71 – 270.93)	23.90 (20.69 – 27.60)	8.94

The test compounds showed good inhibitory effects on both MMP-2 and MMP-9, most of them showed nanomolar potencies. Compound **59** had the highest IC_{50} value on MMP-2, but it showed more than 4-fold selectivity for MMP-9 over MMP-2 (IC_{50}: MMP-2 = 1190.11 nM, MMP-9 = 269.33 nM). Compound **74** (IC_{50}: MMP-2 = 86.50 nM, MMP-9 = 22.71 nM) was over 11-fold more potent than **59** in inhibition of gelatinases and had nearly 4-fold selectivity for MMP-9 over MMP-2. In addition, compounds **61** (IC_{50}: (MMP-2) = 154.96 nM, MMP-9 = 49.54 nM) and **78** (IC_{50}: MMP-2 = 81.23 nM, MMP-9 = 25.34 nM) also exhibited MMP-9 selectivity. The most MMP-9 selective compound in the library was **82**, showing nearly 9-fold selectivity for MMP-9 over MMP-2 (IC_{50}: MMP-2 = 213.79 nM, MMP-9 = 23.90 nM).

Compound **81** (IC_{50}: MMP-2 = 92.88 nM, MMP-9 = 411.45 nM) was the weakest MMP-9 inhibitor, but was the most MMP-2 selective inhibitor. Other compounds such as **63** (IC_{50}: MMP-2 = 28.22 nM, MMP-9 = 85.68 nM) and **80** (IC_{50}: MMP-2 = 74.46 nM, MMP-9 = 310.88 nM) also showed reasonable selectivity for MMP-2 over MMP-9.

The most potent inhibitor in the library was **65** (IC_{50}: MMP-2 = 2.88 nM, MMP-9 = 2.55 nM), which had very low IC_{50} values on both MMP-2 and MMP-9, but it had no selectivity between the two proteins. Other inhibitors such as **57** (IC_{50}: MMP-2 = 14.20 nM, MMP-9 = 13.42 nM), **67** (IC_{50}: MMP-2 = 24.66 nM, MMP-9 = 24.08 nM), and **79** (IC_{50}: MMP-2 = 23.81 nM, MMP-9 = 23.90 nM) were potent MMP-2 and MMP-9 inhibitors, but showed poor selectivity. Furthermore, several synthesized inhibitors exhibited neither great potency nor selectivity, with IC_{50} values were near or over 200 nM on both MMP-2 and MMP-9, including **62** (IC_{50}: MMP-2 = 375.59 nM, MMP-9 = 328.85 nM), **64** (IC_{50}: MMP-2 = 190.89 nM, MMP-9 = 263.89 nM), **66** (IC_{50}: MMP-2 = 214.87 nM, MMP-9 = 307.63 nM), **71** (IC_{50}: MMP-2 = 198.18 nM, MMP-9 = 264.02 nM), and **73** (IC_{50}: MMP-2 = 282.17 nM, MMP-9 = 268.21 nM).

Compound **65** is structurally similar to **66** but the inhibitory potencies of the two compounds were very different, with **65** (IC_{50}: MMP-2 = 2.88 nM, MMP-9 = 2.55 nM) showing nearly 100-fold greater inhibition of MMP-2 and MMP-9 than **66** (IC_{50}: MMP-2 = 214.87 nM, MMP-9 = 307.63 nM). The lower potency of **66** could be due to the size of sulfur and chlorine substitutions on the indene ring, which are bigger than oxygen and methyl in **65**. Compound **66** with its bulky, rigid substituent attached to homopiperazine might be sterically excluded from the mouth of the S2′ pocket resulting in loss of binding affinity between the compound and proteins. Therefore, the size and rigidity of the subgroup attached to homopiperazine might be important for potency. This would be an explanation for the observation that compounds **59** and **62** showed weak inhibition towards MMP-2 and MMP-9. Compound **60** has a smaller side chain ($-OCF_3$) on the 4 position of the benzene ring compared to **59** bearing ethoxyl groups on positions 3 and 5. The two ethoxyl groups in **59** appear to affect the homopiperazine substitution going to the mouth of S2′ pocket. The pictures (Fig. 3.5) showed that the homopiperazine ring on **59** was laid outside of the mouth of S2′ pocket, but the homopiperazine ring on **60** was still in the mouth of the S2′ pocket. The

change of the homopiperazine ring in MMP-2 would significantly affect the interaction between the homopiperazine substituted group and the enzymes.

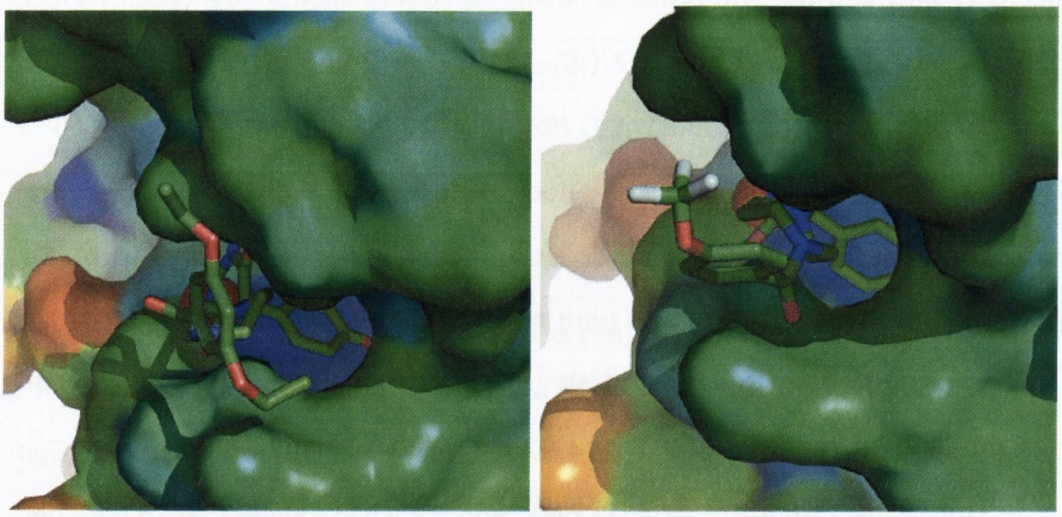


Figure 3.5. *Pictures of* ***59*** *(left) and* ***60*** *docking with a 'Connolly' surfaces on MMP-2 (pdb code: 1qib) generated by the programme PyMOL. The ligand orientations were used which had the lowest inhibition constants of the conformations fitted into the designed pockets in Autodock4 and displayed by PyMOL. The active site zinc atoms are shown as the red spheres.*

The most MMP-9 selective compound was **82**. This may be because of the orientation the compound can adopt in the gelatinases (Fig. 3.6). When the compound was docked with MMP-9, the nitrogen of indazole ring and the methyl group connected with the nitrogen were pointing towards the sulfur on Met422 resulting in enhancement of binding affinity and inhibitory effects. Although **82** could be docked with a similar orientation in MMP-2, the interaction between the nitrogen and Ile222 was not as strong as the interaction with the corresponding Met422 in MMP-9.

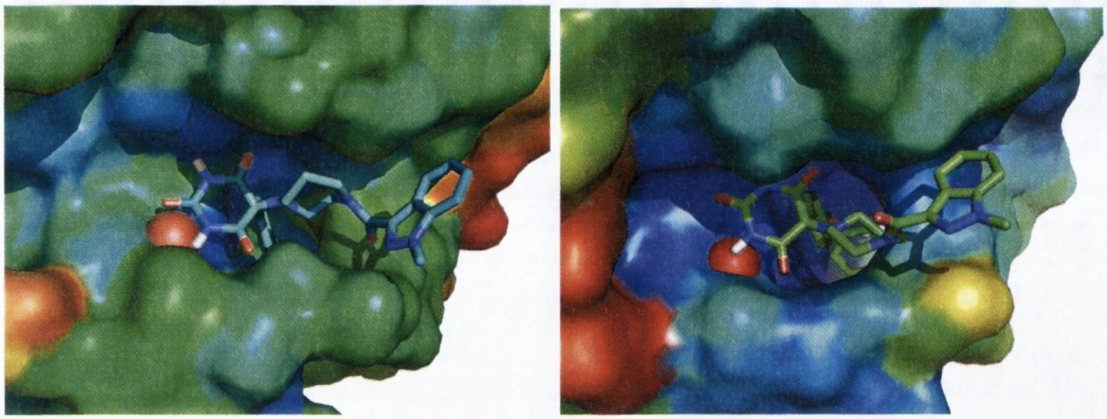


Figure 3.6. *Pictures of* ***82*** *docked with 'Connolly' surfaces on MMP-2 (left) and MMP-9 (right). The surfaces were generated by the programme PyMOL based on the crystal structures of MMP-2 (pdb code: 1q1b) and MMP-9 (pdb code: 2ovx). The ligand orientations were used which had the lowest inhibition constants of the conformations fitted into the designed pockets in Autodock4 and displayed by PyMOL. The nitrogen atom and methyl group on the indazole were close to the differences which exists between MMP-2 and MMP-9, where Ile222 and Met422 were on the two proteins respectively. The active site zincs are shown as the red spheres.*

Another reason for selectivity of **82** on MMP-9 might be the size and rigidity of subgroup attached to the homopiperazine ring, i.e. methyl indazole. When the nitrogen atom and methyl group in the indazole ring pointed toward the Met422 residue, it had the best binding affinity because the methyl indazole just fitted into the mouth of the S2′ pocket (Fig 3.7). If the methyl group turned to other directions, the walls of the S2′ pocket would push the indazole group away from the mouth of the pocket, resulting in loss of potency.

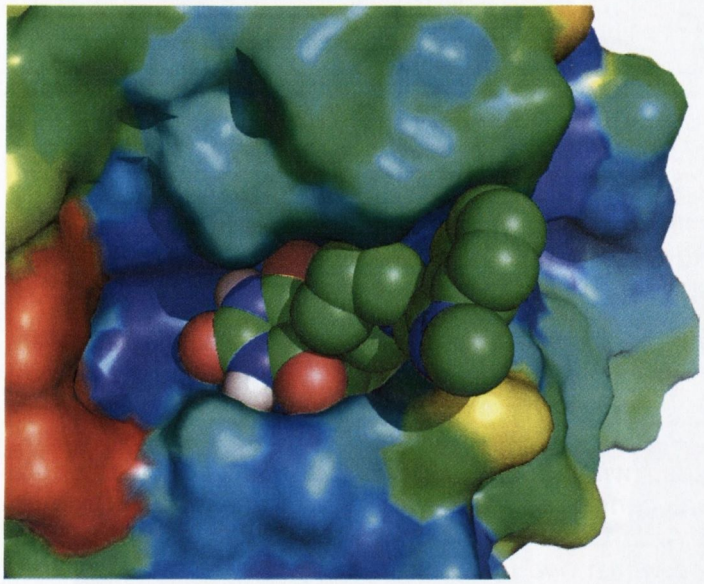


Figure 3.7. *A picture of* ***82*** *docking into MMP-9. Compound* ***82*** *is shown in CPK. The indazole group just fits into the mouth of the S2′ pocket.*

In addition, we found that the mouth of S2′ pocket of MMP-2 was smaller than of MMP-9. Substituents of appropriate size attached to the homopiperazine ring could go deeper into the S2′ pocket of MMP-9 than MMP-2, which might produce selectivity for MMP-9. This might be the reason why **59**, **74** and **78** exhibited selectivity on MMP-9. All three compounds have substitutions on the benzene ring, which should go to the mouth of the S2′ pocket. But due to the size of the mouth in the S2′ pocket, these substitutions fitted better into mouth of the S2′ pocket in MMP-9 than in MMP-2, resulting some selectivity. Fig. 3.8 shows pictures of **78** docking into MMP-2 and MMP-9. Analysis of the X-ray models indicates that the mouth of the S2′ pocket in MMP-2 is smaller than inMMP-9.

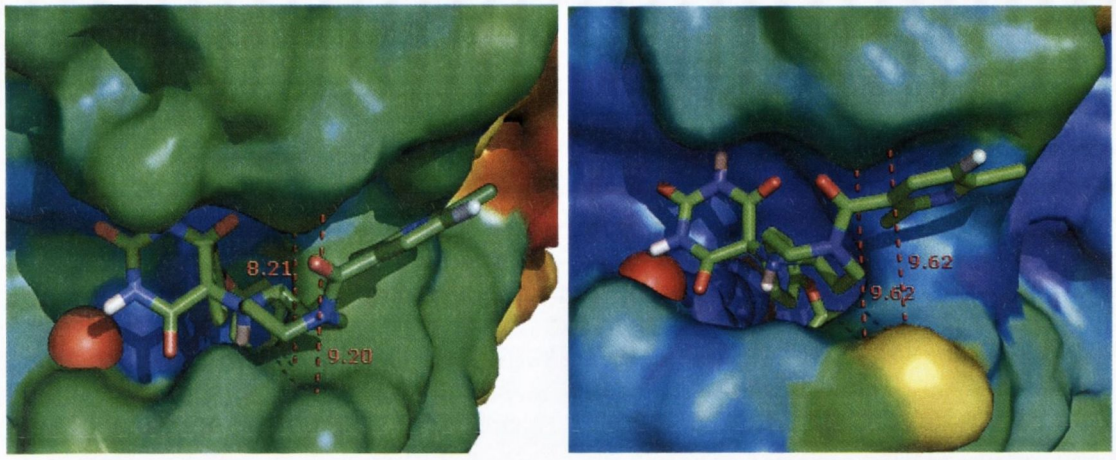


Figure 3.8. *Pictures of compound **78** docking with 'Connolly' surfaces on MMP-2 (left) and MMP-9 (right). The surfaces were generated by the programme PyMOL based on the crystal structures of MMP-2 (pdb code: 1q1b) and MMP-9 (pdb code: 2ovx). The ligand orientations were used which had the lowest inhibition constants of the conformations fitted into the designed pockets in Autodock4 and displayed by PyMOL. The active zincs are shown as red spheres.*

3.4 Docking of 5-homopiperazine substituted barbiturates

Molecular modeling has become an important tool for drug discovery. It has been used in many aspects of drug design, including identification of proteins, lead optimization, screening potential inhibitors for proteins, and evaluation of interactions between proteins and designed compounds. Different computer methods are generally applied for different purposes. For example, molecular mechanics is used to calculate the potential energy of proteins or ligands and minimize their energy using force fields. Docking is one of the most common tools in molecular modeling. Docking means 'docking' small molecules (ligands) into the structure of macromolecular binding sites and 'scoring' the potential abilities of binding, which is used to calculate interactions between proteins and ligands and to predict activity of ligands in proteins (Ketchen, Decornez et al. 2004). Since the first docking of small molecules to protein binding sites, the method has been widely used for drug discovery (Kuntz, Blaney et al. 1982). Successful prediction of binding models of HIV-1 reverse transcriptase with Sustiva is a good example of implication of docking (Rizzo, D.P. et al. 2000).

The programme Autodock4 was used to dock the ligands (synthesized substituted homopiperazine-based inhibitors) into the proteins (MMP-2 and MMP-9) to explain and predict potency and selectivity by exploring their conformations and orientations within the two proteins. Before docking, conformations of the ligands were energy minimized by the programme Molecular Operating Environment (MOE). The crystal structures of MMP-2 (1qib) and MMP-9 (2vox) in which the original bound ligands and water were removed were applied to the study. The zinc parameters were changed to zinc radius: 0.87 Å; well depth: 0.35 kcal/mol; and zinc charges: +0.95 e (Hu and Shelver 2003). The 3D affinity grid box was designed to include the full active site and possible residues. The setting of the center of grid boxes was based on the value of active zinc atom. Docking calculations were carried out using AutoDock version 4.0, with the Lamarckian genetic algorithm (LGA) (Morris, Goodsell et al. 1998). Docking calculations were set to 100 runs. 25000000 energy evaluations were allowed as a maximum in each run. At the end of the calculation, AutoDock performed cluster analysis. Docking solutions with ligand all-atom root mean square deviation (RMSD) within 2.0 Å of each other were clustered together and ranked by the lowest energy representative. Compounds (**57**–**82**) were docked into both MMP-2 and MMP-9 to compare the results obtained from computer calculation and experiment and to examine the orientations when binding with the proteins. Each docking took 24-28 h on a single processor (Intel Pentium 4 670 microprocessor) on Linux Fedora Core 6. The experimental results were transformed from IC_{50} values to ΔG (binding) using formula 3-1 (Table 3.2).

$$\Delta G = -RT(\ln 1/IC_{50}) \qquad 3\text{-}1$$

Where: R is gas constant, which is 1.986 $cal \cdot K^{-1}$; T is thermodynamic temperature (K).

Table 3.2 *Docking and experimental results of homopiperazine-based barbiturates.*

Compounds	Binding energy (kcal·mol^{-1}) based on docking		Binding energy (kcal·mol^{-1}) based on experiment	
	MMP-2	MMP-9	MMP-2	MMP-9
57	-11.56	-12.08	-6.88	-6.92
58	-12.98	-13.44	-6.30	-6.44
59	-9.14	-11.13	-4.15	-5.06
60	-11.49	-12.44	-5.89	-5.99
61	-12.65	-13.35	-5.40	-6.11
62	-10.29	-10.12	-4.86	-4.94
63	-11.77	-12.28	-6.45	-5.77
64	-11.10	-12.68	-5.27	-5.08
65	-12.31	-12.98	-7.86	-7.93
66	-11.67	-13.21	-5.20	-4.98
67	-12.45	-12.23	-6.54	-6.55
68	-11.16	-13.23	-6.33	-6.42
69	-12.77	-12.90	-6.09	-6.14
70	-11.77	-13.48	-5.56	-5.64
71	-10.85	-11.80	-5.25	-5.08
72	-11.82	-12.90	-6.18	-5.81
73	-10.05	-12.33	-5.03	-5.07
74	-12.23	-13.57	-5.76	-6.59
75	-12.2	-12.90	-5.97	-6.40
76	-12.41	-12.88	-5.33	-5.71
77	-11.06	-12.91	-5.83	-5.67
78	-11.62	-12.68	-5.80	-6.52
79	-11.03	-12.43	-6.56	-6.53
80	-10.93	-11.88	-5.85	-4.97
81	-11.13	-10.80	-5.72	-4.80
82	-10.77	-12.46	-5.21	-6.55

The docking results gave scores in binding energy (kcal•mol^{-1}). The lower binding energy represents better binding affinity and potency. We plotted the experimental binding energies of MMP-2 and MMP-9 of synthesized compounds against their binding energies calculated from docking (Fig. 3.9). A weak correlation emerges between the experimental and computer calculated binding energies. Generic docking approaches still have poor predictive power and the results here are not at all untypical.

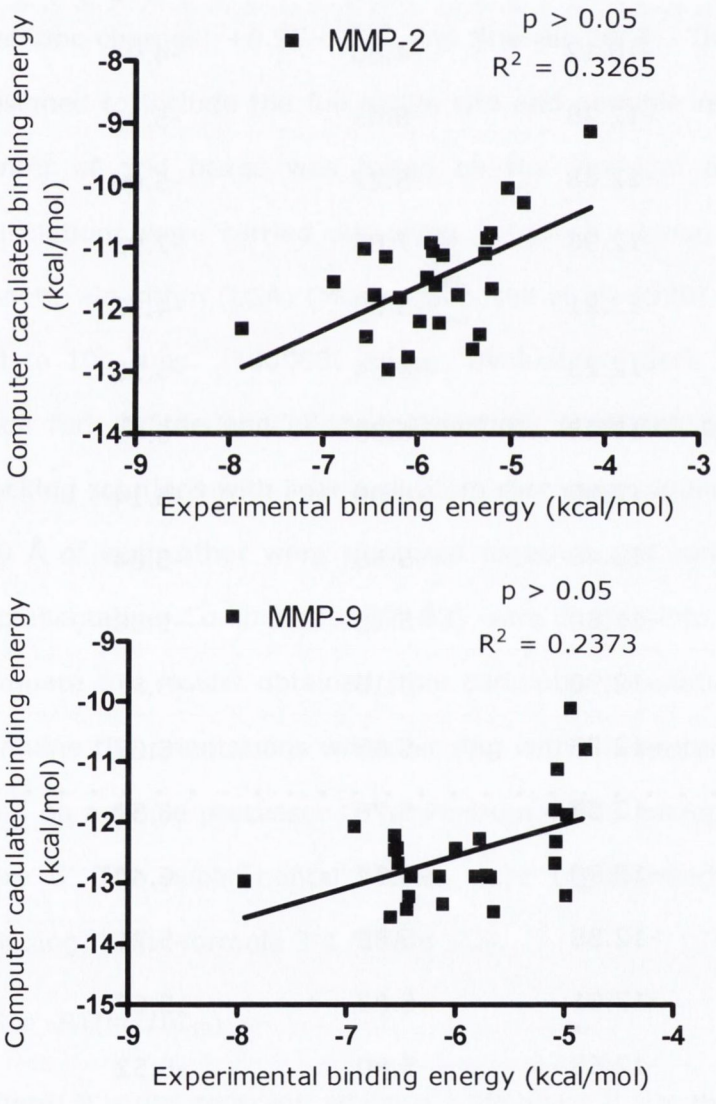
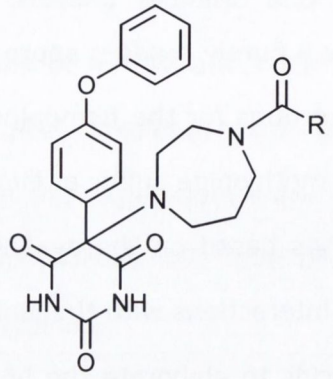


Figure 3.9. *Linear regression of experimental binding energies of synthesized homopiperazine-based barbiturates on MMP-2 and MMP-9 with computer calculated binding energies.*

Although the docking results poorly correlated with experimentally determined measures of affinity, we were tempted to try to use it in prediction of selectivity and design of new ligands since a purely random approach had been only partially successful. We chose pendant groups for the homopiperazine that might be able to offer a H-bond donor to the methionine sulfur at Met 422 on MMP-9. Therefore we built several potential ligands based on the availability of the corresponding acids and potential for H-bond interactions with the Met residue. We also selected a number of sterically bulky acids to elaborate the homopiperazine which might impart selectivity because of the differing sizes of the S2′ pockets in the two proteins. The new hypothetical compounds were docked into MMP-2 and MMP-9 using the previous described parameters and procedures expected for docking calculations which were set to 30 runs (Table 3.3). Each docking took 8-9 h. We proposed to synthesise and assay the most selective compounds emerging from this process.

Table 3.3 *Prediction of binding affinity of potential homopiperazine-based barbiturates with MMP-2 and MMP-9.*



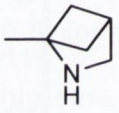
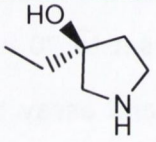
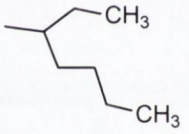
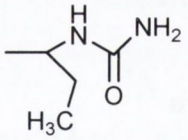
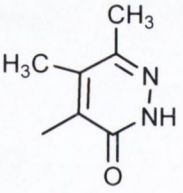
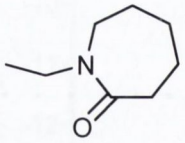
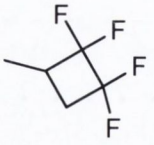
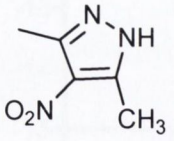
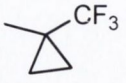
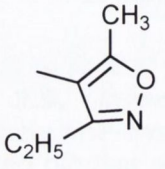
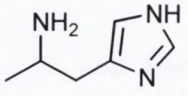
No.	R	Binding energy (kcal/mol)		No.	R	Binding energy (kcal/mol)	
		MMP-2	MMP-9			MMP-2	MMP-9
S1		-9.9	-11.39	**S2**		-12.51	-13.63
S3		-10.03	-11.11	**S4**		-11.52	-11.67
S5		-9.79	-11.29	**S6**		-10.55	-11.01
S7		-11.55	-11.88	**S8**		-10.43	-10.80
S9		-10.91	-12.06	**S10**		-10.35	-12.33
S11		-11.46	-12.45	**S12**		-11.42	-12.50

Table 3.3 *contd.*

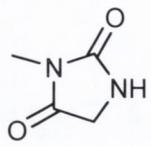
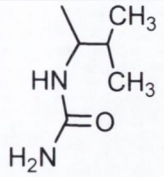
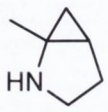
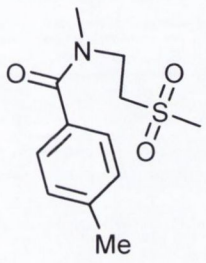
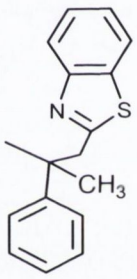
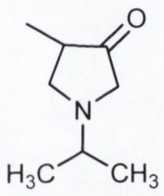
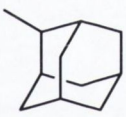
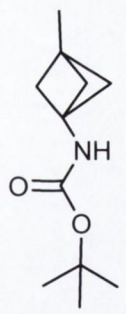
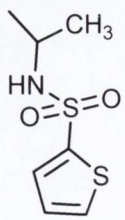
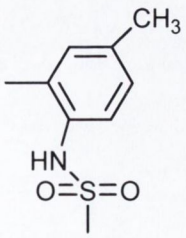
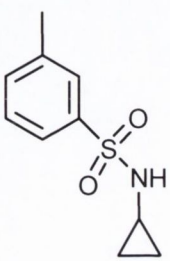
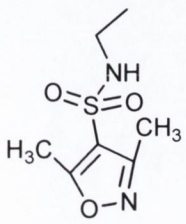
No.	R	Binding energy (kcal/mol)		No.	R	Binding energy (kcal/mol)	
		MMP-2	MMP-9			MMP-2	MMP-9
S13		-10.54	11.58	**S14**		-11.78	-12.1
S15		-10.61	-10.70	**S16**		-10.12	-12.03
S17		-9.85	-11.95	**S18**		-9.47	-10.38
S19		-8.89	-10.00	**S20**		-8.95	-11.79
S21		-11.83	-12.76	**S22**		-10.75	-12.69
S23		-12.16	-12.59	**S24**		-10.68	-11.73

Table 3.3 *contd.*

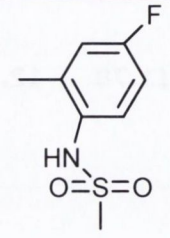
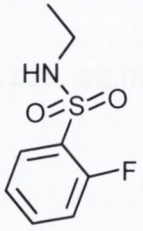
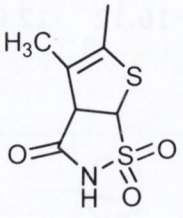
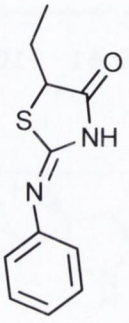
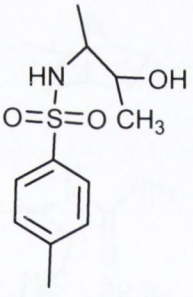
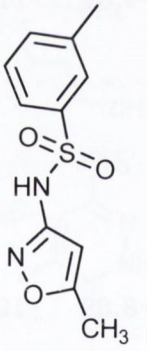
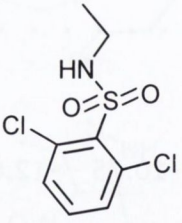
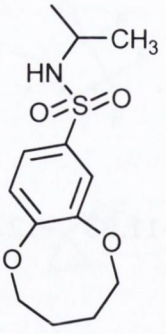
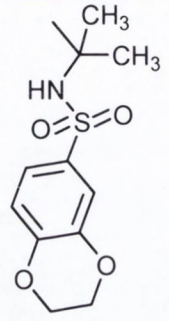
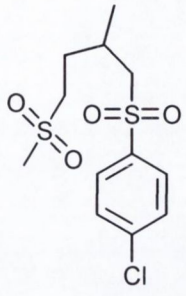
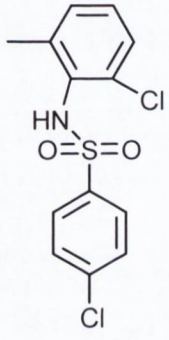
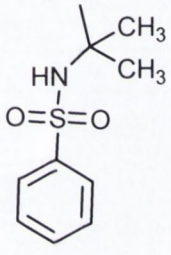
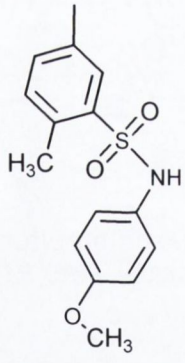
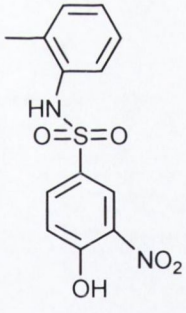
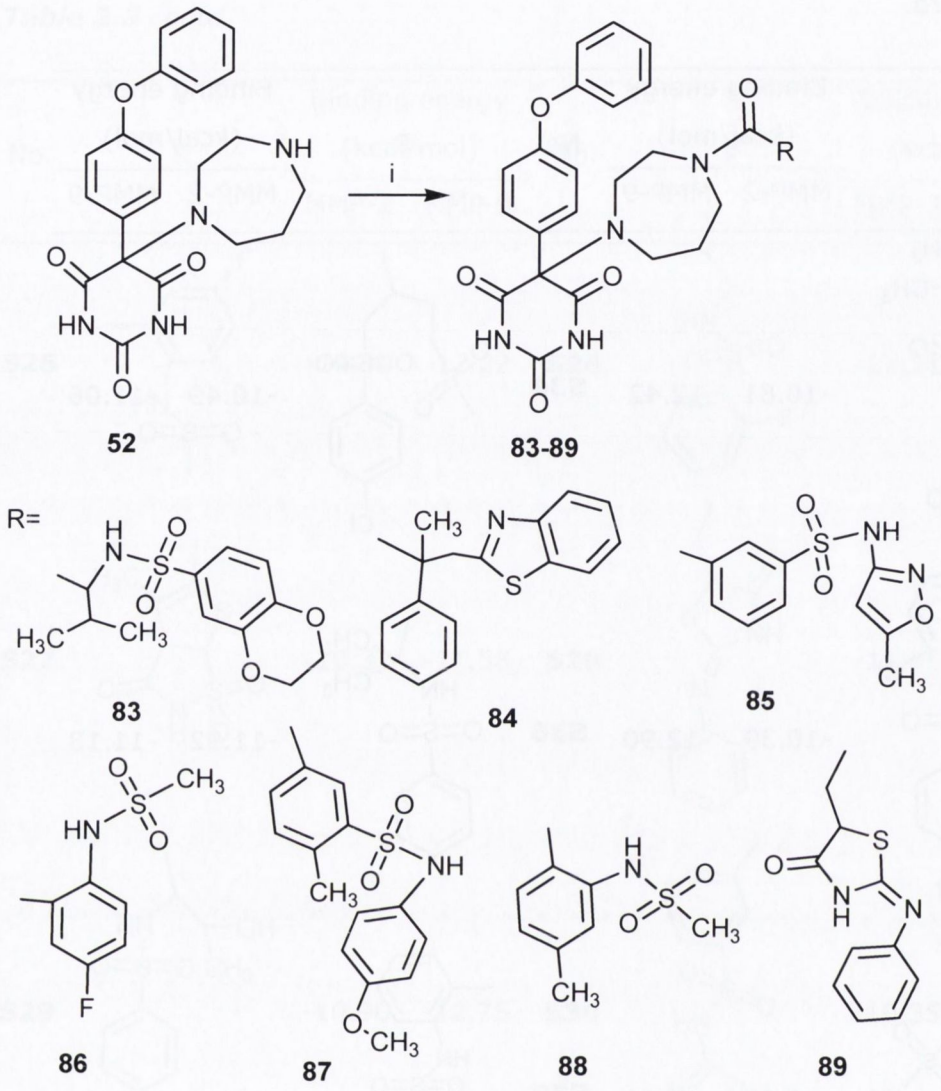
No.	R	Binding energy (kcal/mol)		No.	R	Binding energy (kcal/mol)	
		MMP-2	MMP-9			MMP-2	MMP-9
S25		-10.80	-12.22	**S26**		-12.31	-11.88
S27		-10.37	-11.58	**S28**		-11.75	-13.14
S29		-10.90	-12.75	**S30**		-10.35	-12.22
S31		-12.09	-11.24	**S32**		-11.77	-11.11

Table 3.3 *contd.*

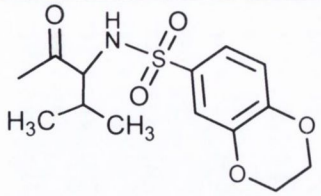
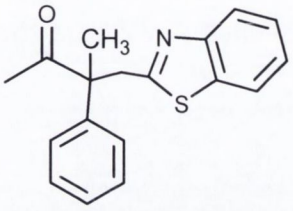
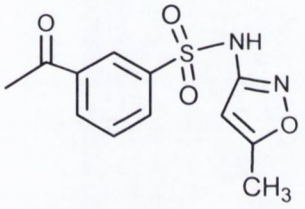
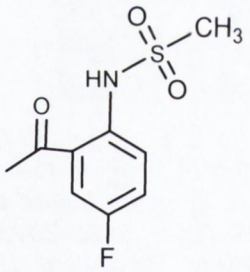
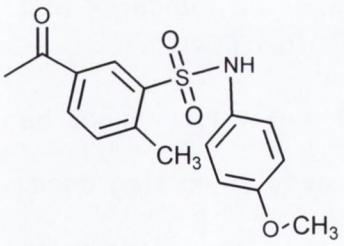
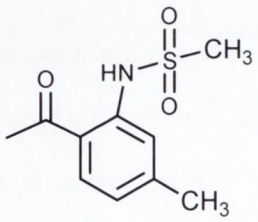
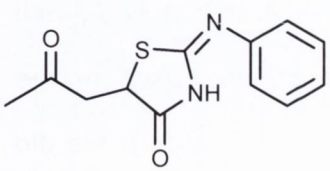
No.	R	Binding energy (kcal/mol)		No.	R	Binding energy (kcal/mol)	
		MMP-2	MMP-9			MMP-2	MMP-9
S33		-10.81	12.42	**S34**		-10.49	-11.06
S35		-10.39	-12.90	**S36**		-11.92	-11.13
S37		-10.65	-12.86	**S38**		-10.12	-10.40

On the basis of the modeling results, seven acids were selected to attach with homopiperazine ring producing **S17**, **S22**, **S25**, **S28**, **S30**, **S33**, and **S37**, due to their selectivity exhibited in the docking experiments. The compounds were produced by DCC-mediated coupling as already described and purified by a rapid filter through flash column chromatography. These compounds were evaluated using the fluorogenic assay (Table 3.4).



Scheme 3.3 *The preparation of the screened homopiperazine-based barbiturates by coupling with the carboxylic acids. i) DCC, DMAP, carboxylic acids, THF, RT, 12 h.*

Table 3.4 *IC_{50} values of the screened homopiperazine-based barbiturates.*

R	Compd	MMP-2 (nM)	MMP-9 (nM)	MMP-9 selectivity
	**83**	697.61 (595.14 – 817.72)	706.44 (523.58 – 953.16)	0.99
	**84**	977.98 (799.82 – 1195.82)	681.04 (524.54 – 901.40)	1.436
	**85**	15.29 (12.81 – 18.24)	20.27 (14.73 – 24.89)	0.75
	**86**	57.18 (48.26 – 67.74)	83.03 (68.84 – 100.79)	0.69
	**87**	27.77 (21.73 – 35.49)	53.54 (38.32 – 74.82)	0.52
	**88**	79.52 (63.61 – 99.41)	141.55 (117.64 – 170.31)	0.56
	**89**	76.36 (64.90 – 89.85)	183.63 (152.79 – 220.69)	0.42

None of the seven new compounds exhibited significant selectivity between MMP-2 and MMP-9 and the data was not consistent with expectations raised by the docking results. The poor potency of **84** on inhibition of MMP-2 and MMP-9 might be due to the methyl and phenyl group attached to α position of carbonyl group. These two side fragments appeared too large to be accommodated by the S2′ pocket which could cause the whole homopiperazine group pushed away from the S2′ pocket and result in the loss of binding affinity (Fig. 3.10).

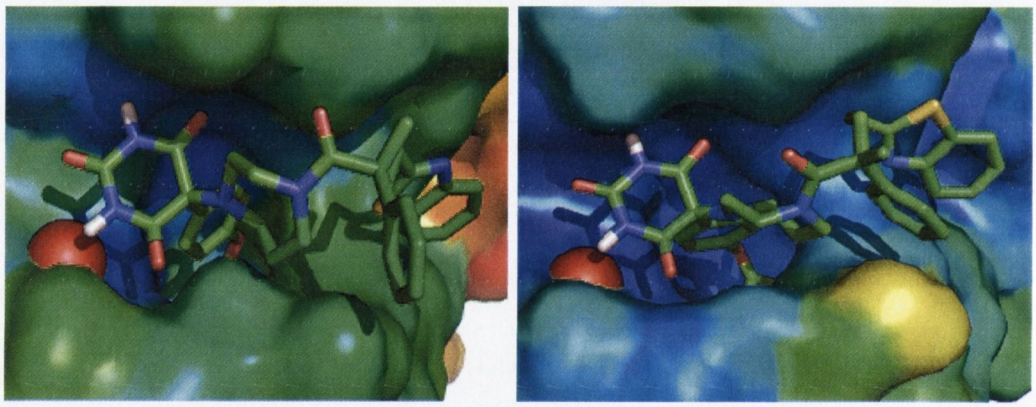


Figure 3.10. *Pictures of* ***84*** *docked with a 'Connolly' surface on MMP-2 (left) and MMP-9 (right). The surfaces were generated by the programme PyMOL® based on the crystal structures of MMP-2 (Pdb code 1qib) and MMP-9 (pdb code 2ovx). Ligand orientations were used which had the lowest binding energy of the conformations of 30 runs with 25000000 energy evaluations in Autodock4 and displayed by PyMOL®. The active site zincs are shown as the red spheres.*

The poor correlation of docking results with the experiment values might be caused by inappropriate parameters used and the complexity of docking itself. Because docking is a multistep process and each step contains one or more degree of complexity (Brooijmans and Kuntz 2003), any incorrect parameters would result in variable results. We only modified some parameters including changing the charges of the active zinc to + 0.95e in the proteins, removal of water molecules in the proteins, and modified the zinc atom (radii: 0.87 Å, well depth: 0.35 kcal/mol) in the AD4_paramters.dat file which was used in the docking for generating grid maps of the receptor (Hu and Shelver 2003). We did not set up any parameters on the S1′ and S2′ pockets of proteins, which might be

the reason why the compounds with selectivity in the docking did not exhibit any selectivity on the experimental values. In addition, the docking method we carried out was rigid docking, in which conformational attributes that can affect bond lengths, bond angles, and torsion angles cannot be changed during the docking process. Because conformations of proteins are always changing when ligands bind with protein, results are generally improved if flexible docking is used. The science of protein ligand binding prediction is complicated because binding results from numerous very small contacts between ligand and protein which are hard to estimate. This phenomenon termed cooperativity sometimes is difficult to model and any error in one contribution can have a major effect on the predicted affinity.

Overall at this point we felt that we had exhausted what could reasonably be achieved in an academic lab in pursuit of selectivity between the two highly homologous enzymes. We had prepared a large number of compounds with different P2' groups with modest success in terms of potency and selectivity. We decided to adopt two different medicinal chemistry strategies to harness what we had learnt and to overcome the selectivity obstacle in pursuit of interesting compounds. These investigations are described in Chapters 4 and 5. In the meantime having gone to such trouble to make the compounds it was rational to try to use them to look at some of the biochemical/pharmacological issues for which they were ultimately being designed. We therefore decided to examine some of the more interesting compounds in a model of metastasis in order to see if the moderate level of potency and selectivity that we had achieved could be potentially useful therapeutically or in determining the relative roles of the two enzymes in metastatic processes.

3.5 Inhibition of cancer cells invasiveness

3.5.1 Backgroud

To inhibit the ability of cancer cells to undergo migration and invasion is one of the most crucial issues in the cancer research field. Cancer and tumor cells can spread to normal cells by means of physiological process including wound healing and embryonic morphogensis (Friedl and Brocker 2000). It has been reported that ECM providing a physical support or barrier for cells plays important role in maintenance of tissue structure and cell migration (Stamenkovic 2003). During invasion, neoplastic cells detached from the primary tumors enter the lymphatic and blood vessels by crossing the epithelial basement membrane, and undergo metastatic growth at distant sites (Nagase and Woessner Jr 1999). MMPs are involved in most parts of the process (Nagase and Woessner Jr 1999). The degradation of ECM component is necessary for cell migration (Friedl and wolf 2003). MMPs have been considered to be a major regulator of ECM composition and to be promoters for cell migration due to their ability to degrade the ECM components and remove the barriers. For example, MMP-2 and MMP-9 can cleave a major protein component of basement membrane-type IV collagen (Vu, Shipley et al. 1998; Yu, Murphy et al. 1998).

Some biologically active modular breakdown products released from the proteolytic remodeling of ECM can promote cell migration. For example, laminin-5 cleaved by MMP-2 produces a gamm2 subunit, which has been shown to induce migration of breast epithelial cells (Gianneli, Flak-Marziller et al. 1997). Recently it has been clearly demonstrated that MMPs are involved in regulation of cytokines, chemokines, growth factors, and a variety of enzymes (Stamenkovic 2003). Degradation of ECM molecules results in release of various growth factors and cytokines stored in the ECM molecules. For example, decroin, a small proteoglycan, functions as a reservoir for TGF-β, and cleavage of decroin by

various of MMPs results in release of TGF-β and its biological functions (Imai, Hiramatsu et al. 1997).

In addition, MMPs are able to cleave cell-cell adhesion proteins, to release bioactive cell surface molecules, and to degrade signal-transducing molecules (Sternlicht and Werb 2001). For example, the cleavage of signal-transducing molecule E-cadherin and the soluble E-cadherin fragment by MMP-3 and MMP-7 inhibits cell aggregation and promotes cell invasion (Noe, Fingleton et al. 2001).

Therefore, inhibition of MMP activity can counteract cancer cell invasion by inhibiting degradation of ECM and release of cytokines and growth factors. Homopiperazine-base barbiturates with potent inhibition on MMP-2 and MMP-9 were tested in an invasion assay to investigate the potential of inhibition of gelatinase activity on cancer cell invasion. Many types of cells have been used in invasion assays such as HT1080, MCF-7, and Caco-2 cells. Migration of Caco-2 cells was monitored in our assay using a Matrigel membrane.

3.5.2 Assessment of invasion inhibition by selected homopiperazine-based barbiturates

A number of selected substituted homopiperazine-based barbiturates were tested in the invasion assays with two concentrations (10 μM and 100 nM) or one concentration (100 nM). Matrigel membranes with 8.0 μm pore were used in the assay. In addition, hepatocyte growth factor (HGF) was used to stimulate growth and invasiveness of Caco-2 cells (Kermorgant, Aparicio et al. 2001). When Caco-2 cells were in confluence, cells were collected and resuspended in serum-free medium. Cells were then counted in a cell-counting machine. After counting, 25,000 Caco-2 cells, 75 ng HGF, and the tested inhibitors (with final concentrations at 10 μM and/or 100 nM) were added to each invasion assay insert. 2% fetal calf serum (FCS) medium was added to inserts to make the total volume of 1 ml each flask. The negative control inserts contained only Caco-2 cells and 2% FCS medium and positive control inserts contained Caco-2 cells, HGF and 2%

FCS. The inserts were then transferred to the assay chambers containing FCS medium and left in cell culture incubator for 48 h. After incubation, supernatants were taken out and the non-migratory cells on the upper surface of the membranes were removed with serum-free medium using cotton swabs. The cells that had invaded through the Matrigel membranes and attached in the bottom of the inserts were fixed and stained by the Diff-Quik kit. The inserts were left to dry when the migrated cells were counted under the microscope. The experiments were carried out in duplicate and repeated three times for each concentration inhibitor. Inhibition was estimated using the formula: 3-1

$$\text{Inhibition\%} = \left(1 - \frac{\text{No. of cells in inhibitor's insert)}}{\text{No. of cells in control insert}}\right) * 100\% \qquad 3\text{-}1$$

The negative control in this assay consisted of cells untreated with HGF, and positive control consisted of HGF treated wells. The treated cells were shown to undergo more migration. Fig. 3.11 showed pictures of a validated invasion assay of negative control and positive control inserts.

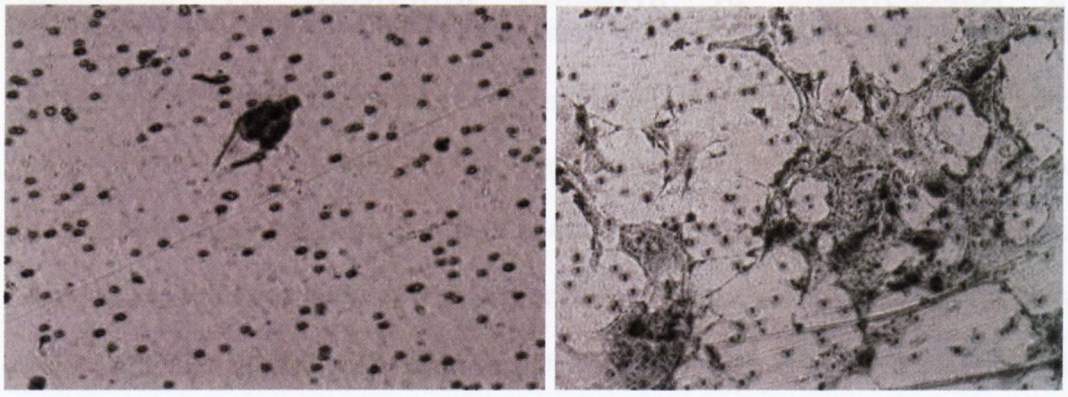


Figure 3.11. *Representative microscope images of a negative control insert (left) and a positive control insert (right). Representative images are shown.*

This assay is time consuming and expensive and it therefore was not practicable to perform the measurement on many compounds. Five substituted homopiperazine-based barbiturate inhibitors were tested with either one or two concentrations. Compounds **36**, **74**, and **82** were assayed at 10 μM and 100 nM;

compounds **65**, **80** were tested only at 100 nM. The results are shown in Fig. 3.12.

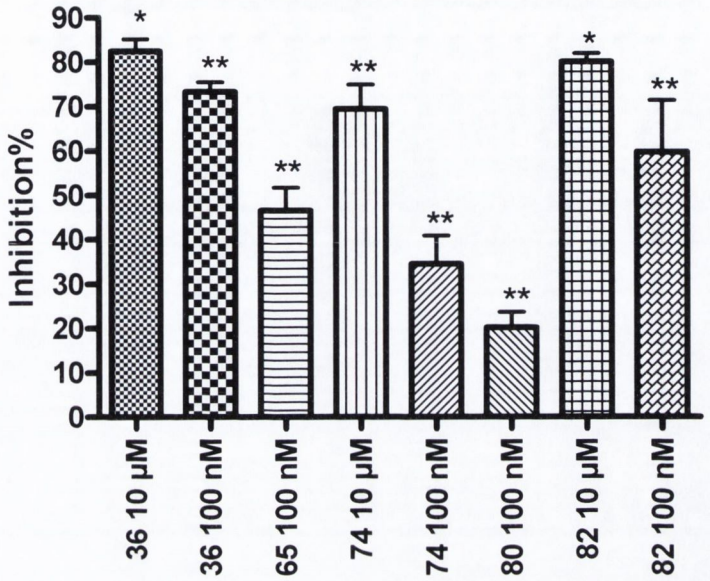


***Figure 3.12**. Invasion assays results for selected compounds (** significantly different from control P < 0.05; * not significantly different from control P > 0.05).*

All tested compounds caused significant inhibition of invasiveness at 10 µM and 100 nM. Compound **36** which had low IC_{50} values on both MMP-2 and MMP-9 (IC_{50}: MMP-2 = 1.93 nM, MMP-9 = 7.54 nM) showed the strongest inhibition (82.49% and 73.32% at 10 µM and 100 nM respectively) (Fig. 3.13).

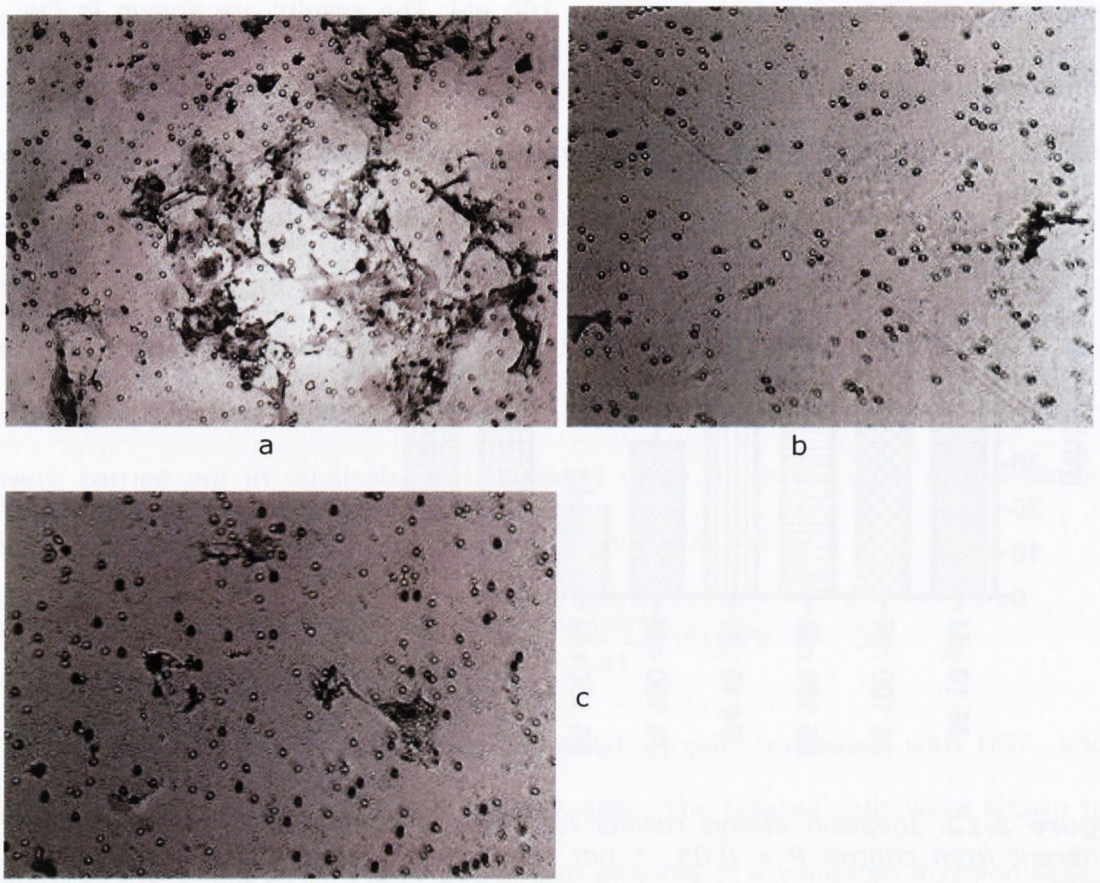


Figure 3.13. *Representative microscope images from invasion assays* ***36****. a) A positive control insert, incubated with Caco-2 cells and HGF. b) Insert incubated with Caco-2 cells, HGF, and 10 μM* ***36****. c) Insert incubated with Caco-2 cells, HGF, and 100 nM* ***36****.*

The inhibition of Caco-2 cells invasiveness by these compounds was dependent on their ability to inhibit activities of MMP-2 and MMP-9. The least potent compound (**80**) in the recombinant enzyme assay exerted weakest inhibition (20.15%) at 100 nM (Fig. 3.14). Compound **82** showed better inhibition of invasion of the cells than **74** at 10 μM and 100 nM, even though **82** (IC_{50}: MMP-2 = 213.79 nM, MMP-9 = 23.90 nM) had higher IC_{50} values on both MMP-2 and MMP-9 than **74** (IC_{50}: MMP-2 = 86.50 nM, MMP-9 = 22.71 nM). In addition, **82** had better ability to inhibit the invasiveness than **65** (IC_{50}: MMP-2 = 2.88 nM, MMP-9 = 2.55 nM) which possessed over 70-fold potency on MMP-2 and 9-fold on MMP-9 than **82**. It is possible that the out of trend inhibitory ability of **82** is due to its MMP-9 selectivity. MMP-9 may play a more important functional role in facilitating cancer cell migration than MMP-2. For example, MMP-2 and MMP-9 can both activate

latent TGF-β, but only MMP-9 coordinated with TGF-β could promote cancer cell growth and invasion (Yu and Stamenkovic 2000). It has also been demonstrated that tumor cell invasion is correlated and regulated by MMP-2 (Deryugina, Luo et al. 1997). Compound **36** which exerted 4-fold selectivity for MMP-2 over MMP-9 had lower potency on MMP-9 than **65**, but showed better inhibition of invasion. It seems that inhibition of only one protein's activity, either MMP-2 or MMP-9, may result in better inhibition of invasion. Because only five compounds were examined in the invasion assay, to obtain the correlation between IC_{50} values and inhibition of invasion, and to prove the relationships between selectivity and inhibition of invasion, more tests are required. But our results illustrated that inhibition of activity of MMP-2 and MMP-9 could decrease cancer cell invasive ability, affirming that MMP-2 and MMP-9 are important for cancer cell invasion and important targets for cancer therapy.

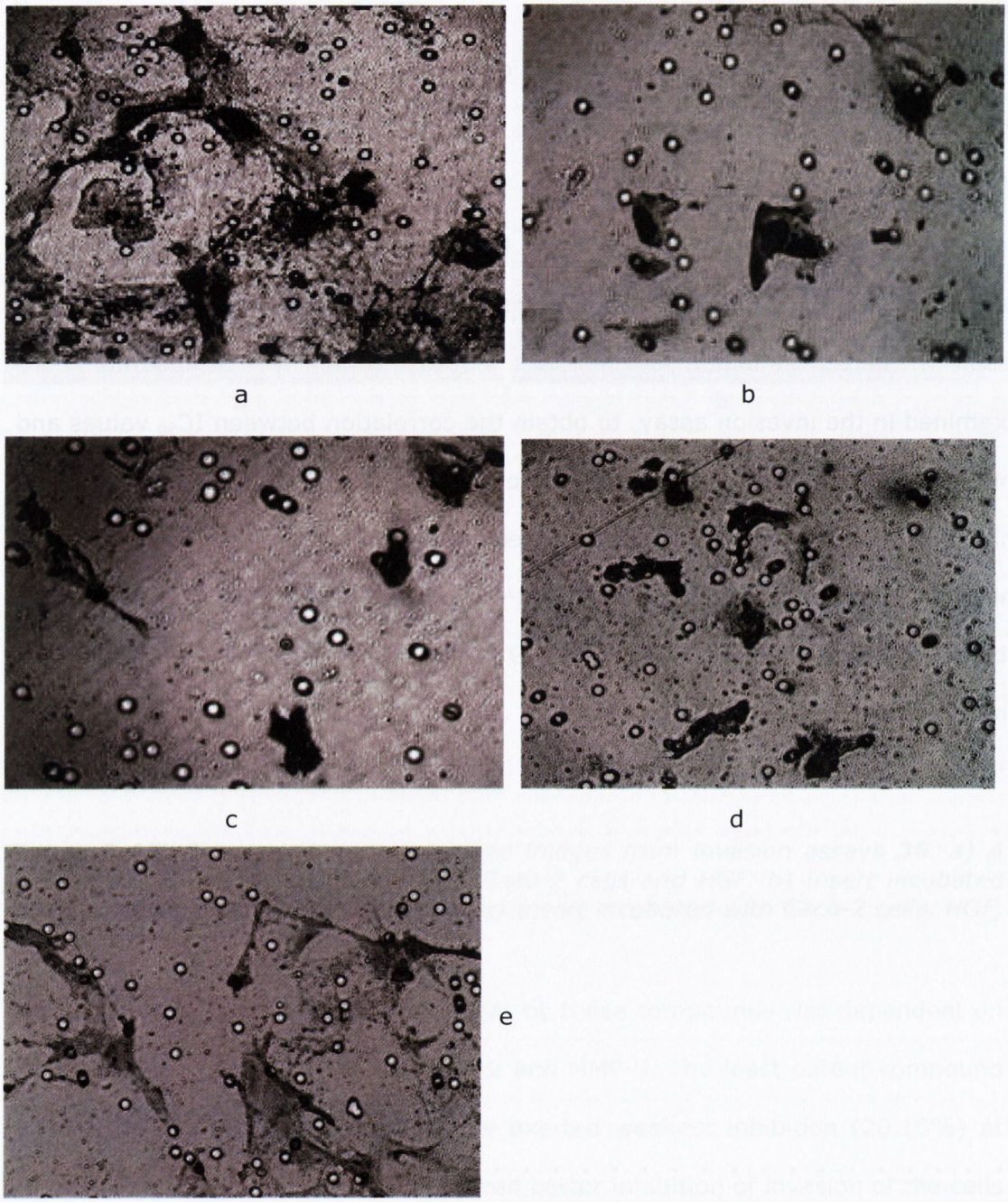
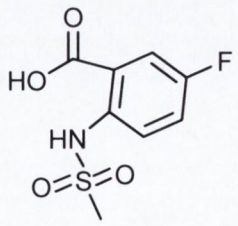


Figure 3.14. *Microscope images from invasion assays with* ***65***, ***74***, ***80***, *and* ***82***. *a) A positive control insert, incubated with Caco-2 cells and HGF. b) Insert incubated with Caco-2 cells, HGF, and 100 nM* ***65***. *c) Insert incubated with Caco-2 cells, HGF, and 100 nM* ***82***. *d) Insert incubated with Caco-2 cells, HGF, and 100 nM* ***74***. *e) Insert incubated with Caco-2 cells, HGF, and 100 nM* ***80***. *The number of Caco-2 cells invaded through the matrigel membrane significantly decreased when 100 nM of* ***65***, ***74***, *and* ***82*** *were added to the insert for incubation. Only small portion of the cells were inhibited from passing through the membranes when incubated with 100 nM* ***80***.

3.6 Gelatinase inhibition by carboxylic acids

As stated in Chapter 1, carboxylic acids, which can bind bivalent Zn can be used in the construction of MMP-inhibitors. During the course of the work described in the preceding Chapters of this thesis, we had assembled an interesting library of acids with which to acylate homopiperazine substituted barbiturates. Some of these were substituted close to the acid with an H-bond donor since we had hopes that H-bond donation to the MMP-9 methionine at S2′ might act as a selectivity vector for that enzyme. Since our barbiturate strategy in its simplest barbiturate formulation had achieved only modest success in terms of selectivity and since the assay was running in the lab it seemed a good idea to screen the acids themselves. The acids were screened using the recombinant gelatinases using the fluorogenic assay at 10 μM (Table 3.5).

Three carboxylic acids (**A14**, **A15**, and **A22**) showed >50% inhibition of MMP-2 and MMP-9 at 10 μM. Notably, there were two phenoxyphenyl acids in the library with **A15** a substituted acetic acid showing significant inhibition. The phenoxyphenyl group has of course already been identified as conferring strong inhibitory characteristics to barbiturates and other MMP-inhibitor types but it was interesting to see it turn up in a small random screen. **A22** is in this context perhaps the most interesting compound since it has a strong H-bond donor group alpha to the benzoate and wide scope for further substitution to improve potency and selectivity.



A22

Table 3.5 *The inhibition of MMP-2 and MMP-9 activities by small carboxylic acids at 10 μM (n=3).*

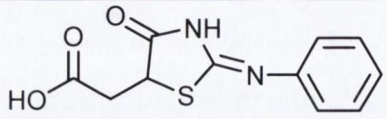
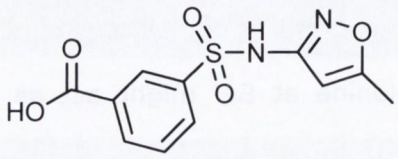
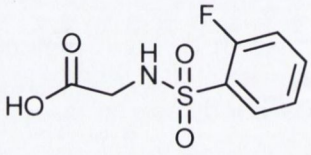
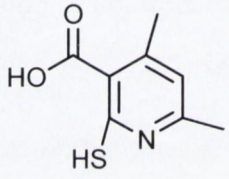
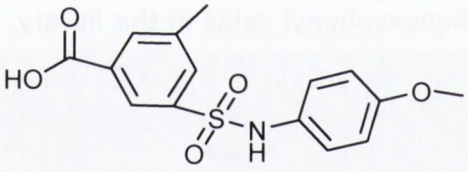
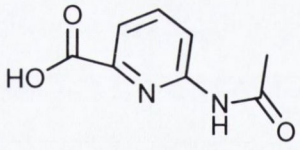
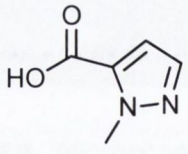
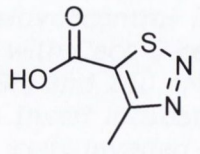
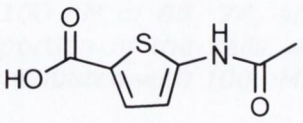
Structure	Carboxylic Acids	Inhibition%	
		MMP-2	MMP-9
	**A1**	8.94	2.42
	**A2**	24.38	16.62
	**A3**	25.53	11.75
	**A4**	20.76	15.79
	**A5**	16.37	12.93
	**A6**	1.20	2.62
	**A7**	19.30	9.92
	**A8**	13.96	8.87
	**A9**	22.50	12.16

Table 3.5 *contd.*

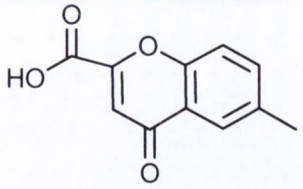
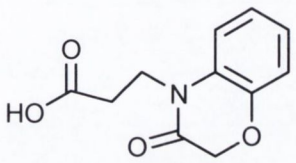
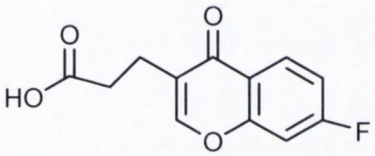
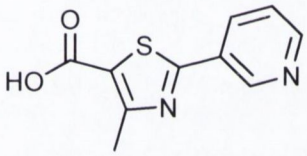
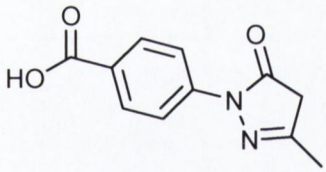
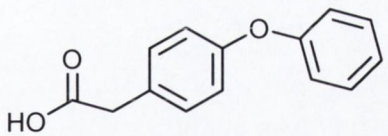
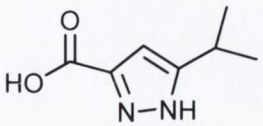
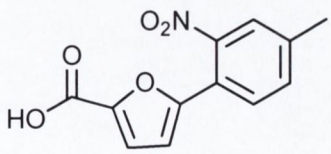
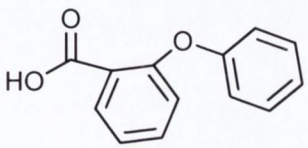
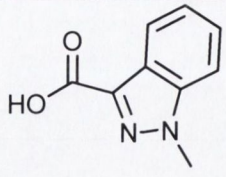
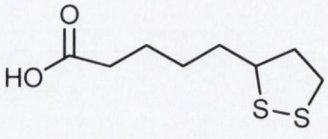
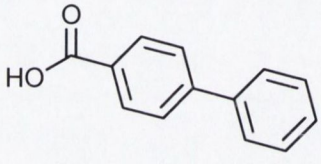
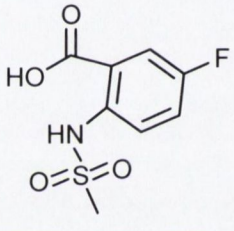
Structure	Carboxylic Acids	Inhibition%	
		MMP-2	MMP-9
	**A10**	9.48	25.69
	**A11**	9.05	1.77
	**A12**	40.94	20.72
	**A13**	33.30	5.94
	**A14**	62.04	52.59
	**A15**	61.21	60.50
	**A16**	48.03	32.00
	**A17**	32.79	10.37
	**A18**	24.01	12.04

Table 3.5 *contd.*

Structure	Carboxylic Acids	Inhibition%	
		MMP-2	MMP-9
	**A19**	25.01	6.22
	**A20**	11.33	6.09
	**A21**	34.01	14.49
	**A22**	66.33	52.58

3.7 Conclusion

Although many types of MMP inhibitors have been developed there are still only a few generally useful compound capable of discriminating between MMP-2 and MMP-9 (Breyholz, Schafers et al. 2005). Studies have shown that the deep S1′ pocket can be targeted to good effect in imparting collagenase selectivity because it is somewhat different in the collagenases. Few if any studies have systematically explored the possibilities for imparting selectivity by targeting the S2′ site partly because of the belief that it is too close to the protein surface and solvent accessible for good binding effects (Rao 2005). As described in previous Chapters, barbiturates are an important new class of MMP inhibitors (Brandstetter, Grams et al. 2001). Chapter 2 described our finding that homopiperazine-substitued compounds are more potent than their 6-membered counterparts. Therefore, in this Chapter a series of acyl homopiperazine-substituted compounds were prepared in order to target small differences between MMP-2 and MMP-9 pocket in the S2′ that might result in selectivity.

The synthesized homopiperazine-based barbiturates exhibited a wide range of IC_{50} values on both MMP-2 and MMP-9, especially for MMP-2 (**59** and **36**). The most MMP-9 selective compound in the library was **82**, which showed 9-fold selectivity for MMP-9 over MMP-2. Compound **81**, the most MMP-2 selective compound, had nearly 5-fold selectivity for MMP-2 over MMP-9. Overall the selectivity differences were disappointing. Docking studies were used in a failed attempt to try to predict selectivity in a second subclass of acyl homopiperazines.

Our studies showed the abilities of homopiperazine-based barbiturates of MMP inhibitors to counteract Caco-2 cell invasion through matrigel membranes by inhibition of MMP-2 and MMP-9 activities. The ability of the compounds to inhibit cell was apparently dependent on their inhibition of MMP-2 and/or MMP-9. Generally, more potent gelatinase inhibitors exhibited better inhibition of cancer cell invasion. There is a suggestion in the small number of data points of a

relationship between selectivity for MMP-9 and inhibitory potency. This requires further characterization.

Chapter 4

Synthesis of large molecular MMP inhibitors for intestinal diseases

4.1 Introduction

The roles of MMPs in intestinal diseases have been extensively studied. Apart from inflammatory bowel diseases, MMPs are associated with other intestinal inflammatory disorders. MMPs are involved in the host immune response under physiological conditions. MMPs play an important role in facilitating inflammatory cell invasion into the intestinal wall and other organs (Medina and Radomski 2006). It has been reported MMP activity is necessary for migration of lymphocytes from the bloodstream into lymph nodes via high endothelial venules, a prerequisite for the initiation of immune responses (Faveeuw, Preece et al. 2001). In addition, MMP-2 and MMP-9 are required for the migration of langerhans cells and dermal dendritic cells from the skin to the draining lymph nodes (Ratzinger, Stoitzner et al. 2002). MMPs have also been found to play roles in necrotizing enterocolitis, collagenous colitis, and diverticular disease (Medina and Radomski 2006). Necrotizing enterocolitis is an acute inflammatory disease affecting predominantly premature infant, and is characterized by systemic sepsis and multi-system organ failure resulting from intestinal inflammation (Sodhi, Richardson et al. 2008). Numerous studies have reported that overexpression of several MMPs, such as MMP-3, MMP-7, MMP-12, and MMP-26, in necrotizing enterocolitis (Pender, Braegger et al. 2003; Bister, Salmela et al. 2005).

MMP activity is tightly controlled by their endogenous inhibitors under normal conditions. In pathological conditions of intestinal disease such as IBD, MMPs induced by inflammatory cells cannot be regulated by TIMPs leading to excessive ECM remodeling and intestinal tissue destruction (Medina and Radomski 2006). Moreover, overexpression of MMPs disturbs the intestinal immune response. MMP inhibitors have been studied in several animal models of colitis and reduced colitis was observed (Sykes, Bhogal et al. 1999; Di sebastiano, Di Mola et al. 2001; Medina, Videla et al. 2001). Therefore, inhibition of MMP activity could be useful in the treatment of the disease.

It is now apparent that in addition to inflammatory cells, the intestinal epithelium may produce severe immunodulatory substances, such as cytokines, complement factors, immune receptors and MMP-9 (Su, Wen et al. 1999; Santana, Medina et al. 2006). The release of MMP-9 may contribute to the loss of intestinal epithelium integrity facilitating interactions between the luminal antigenic stimuli and the mucosal immune system, resulting in chronic intestinal inflammation (Rath, Schultz et al. 2001). In addition, epithelial-derived MMP-9 may impair wound healing and facilitate the recruitment of leukocytes by cleaving IL-8 (Fig. 4.1) (Castaneda, Walia et al. 2005).

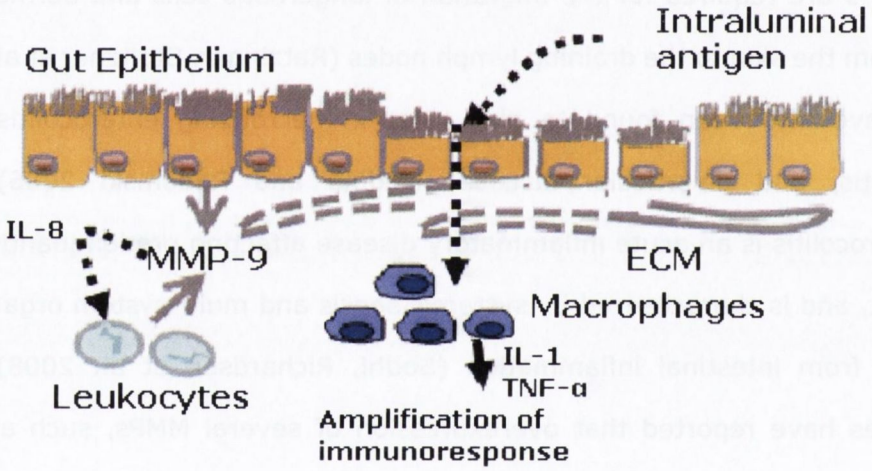


Figure 4.1. *The role of MMP-9 in intestinal inflammation.*

Gelatinases also play roles in colorectal cancer in animal models and patients (Mook, Frederiks et al. 2004). The protein levels of MMP-2 and MMP-9 are both increased in colorectal tumors comparing to normal mucosa (Emmert-Buck, Roth et al. 1994; Baker, Leaper, et al. 2002). It has been reported that proMMP-2, but little or no active MMP-2, has been found in health mucosa, but the active MMP-2 is significantly increased in colorectal cancer specimens, which is 20 fold higher than proMMP-2 (Parsons, Watson et al. 1998). MMP-9 is observed more frequently in advanced tumor and especially prevalent in invasive tumor, demonstrating the contribution of MMP-9 to invasion (Jeziorska, Haboubi et al. 1994). A study showed

that the survival time for the colorectal cancer patients with Duke's stage IV and elevated plasma levels of MMP-9 and/or the complex of MMP-9 with TIMP-1 was significantly shorter than patients with normal plasma levels (Zucker, Lysik et al. 1995).

In addition, gelatinases can facilitate the immigration of inflammatory cells by release of various growth factors and cytokines. MMPs can liberate inactive growth factors up matrix remodeling and can also activate released growths or degrade binding proteins, resulting in improvement of their bioactivity (Mook, Frederiks et al. 2004). For example, gelatinase can modulate insulin-like growth factor bioactivity by degradation of insulin-like growth factor binding proteins and MMP can activate TGF-β and proTNF-α (Bergers and Coussens 2000; Yu and Stamenkovic 2004; Fernandez-Patron, Zouki et al. 2001).

Typical therapies for intestinal diseases, such as IBD employ pharmacological strategies, anti-inflammatory, antibiotics, cytokine modulating, and immune-suppression (Fig. 4.2). Most drugs for the treatment of intestinal diseases are designed to be delivered to the sites of the diseases by different methods. Small molecular drugs usually are coated with polymers to slow down the dissolution and release of the drug, or are prepared as pro-drugs where the active compounds are released at the site of the disease. For example, aminosalicylates (5-ASA) can be delivered to the disease site either by prepared as azoprodrugs in which the azo bond can be broken by bacterial microflora in the colon releasing 5-ASA or by administrating 5-ASA in the form of foam, enemas, or suppositories (Klotz and Schwab 2005). Another approach for delivery of drugs to the disease site is to synthesize large molecular compounds that have poor absorption but with good pharmacological potency. Prednisolone sodium metasulfabenzoate is active topically with little systemic impact because of its poor absorption in the small and large intestine.

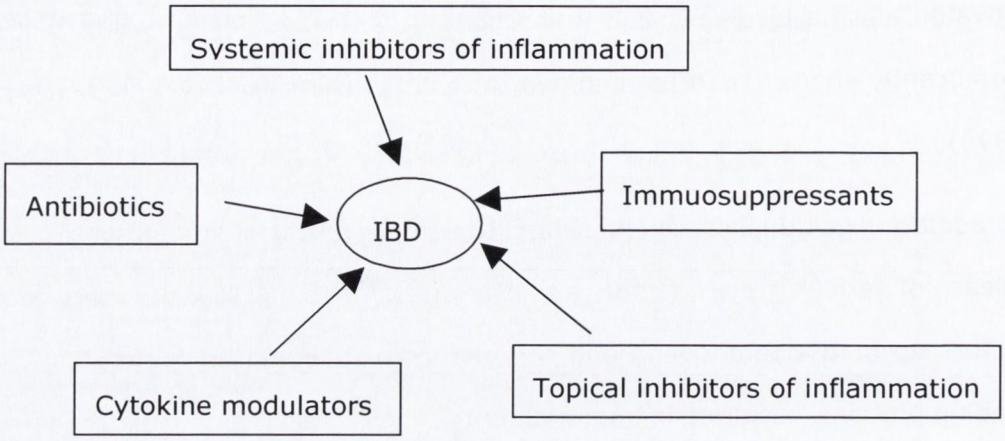


Figure 4.2. *Pharmacological approaches for treatment of IBD (Egan and Sandborn 2005).*

As already described, MMPs are involved in the immune system, inflammation and modulation of cytokines and therefore MMP inhibitors could be useful for the treatment of colon cancer. MMP inhibitors have had poor clinical development history because of their systemic toxicity and lack of selectivity. Since we ourselves had already found the selectivity obstacle between the gelatinases to be insurmountable we wondered if there might be an opportunity in cancer therapy design to mitigate the lack of selectivity of the compounds by specifically targeting them to the colon. One option might be to design prodrugs that release their payload site-specifically, reducing systemic exposure. Another less obvious approach emerged that could exploit an important architectural feature of the MMPs. Unlike esterases, for example, the MMP active zinc sits close to the protein surface and as we have seen, inhibitors with groups directed into the S2′ pocket protrude out to solvent. We therefore felt that attachment of a large group to the barbiturate P2′ position might suppress transepithelial transport resulting in the confinement of the inhibitor in the intestinal tract when administered orally. Correctly spaced with a linker to the barbiturate, a subsituent large enough or polar enough to suppress transport would not affect binding affinity and potency in the barbiturate class. Evidently, in order to exert any biological activity, the MMP target would need to be presented apically or extracellularlary at the disease site. Little is known about the

precise distribution of MMP-9 in colorectal cancer but it seemed rational to speculate that a significant amount would be accessible from the intestinal lumen especially at disease sites where barrier function is compromised. On the other hand, an effectively designed potent compound might find application in probing the distribution of MMP-9 in MMP progression in animal models of the disease. This Chapter describes some initial investigations into medicinal chemistry designs for gelatinase inhibitors with reduced absorption characteristics. In the first case we investigated barbiturate dimers in which two barbiturate groups were separated by an inert linker in order to produce compounds of increased mass but without decreasing potency. We also investigated the attachment of ursodeoxycholic acid at the distal site of the homopiperazine substituent in order to produce a compound with increased mass and polarity. The effect of these two approaches was investigated on gelatinase potency and selectivity, cancer cell invasiveness and we also examined intestinal stability. Since the dimer approach has other applications in medicinal chemistry and has been applied MMP inhibitors, it is appropriate here to review briefly some aspects of ligand dimer binding and selectivity.

4.2 Inhibition of Protein Dimers

Many proteins, cell surface and intracellular DNA binding receptors exist and function as dimers. Examples include protein-tyrosine kinase receptors, TNF-α, HIV-1 protease, G-protein-coupled receptors (e.g. opioids), nuclear receptors (e.g. the GR) and MMPs (Wlodawer, Miller et al. 1989; Heldin 1995; He, Smith et al. 2005; Ingvarsen, Madsen et al. 2008; Lohse 2010). Dimers can be formed between identical (homodimerization) proteins or different proteins (heterodimerization) by protein-protein interactions. Protein binding interactions with ligand dimers should theoretically exhibit higher affinity than with a single protein leading to increased potency because of the higher number of ligand-protein surface contacts.

The dimer strategy has been used in the design of inhibitors in many fields. In an example of a heterodimer, *He et al.* has reported that a compound with ability to bind to a TNF-α dimer showed increased potency (Fig. 4.3) (He, Smith et al. 2005).

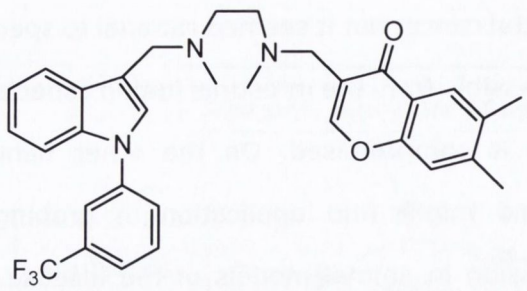


Figure 4.3. *chemical structure of the small molecule TNF-α inhibitor.*

There are many more examples of homodimers in the chemical literature than heterodimers. Many HIV-1 protease inhibitors are based on dimer approaches. Hwang et al. synthesized several dimers which exhibited nanomolar K_i values on HIV-1 protease (Fig. 4.4) (Hwang and Chemielewski 2005). Dimers can be used to probe the distance between neighboring proteins because binding affinity is found to be related to the spacer length becoming optimal when sufficiently long to allow dual occupancy. Morphine-based dimers (agonist and antagonist) were critical to the discovery and characterization of opioid (GPCR) homo- and hetero- dimers in the 1990s.

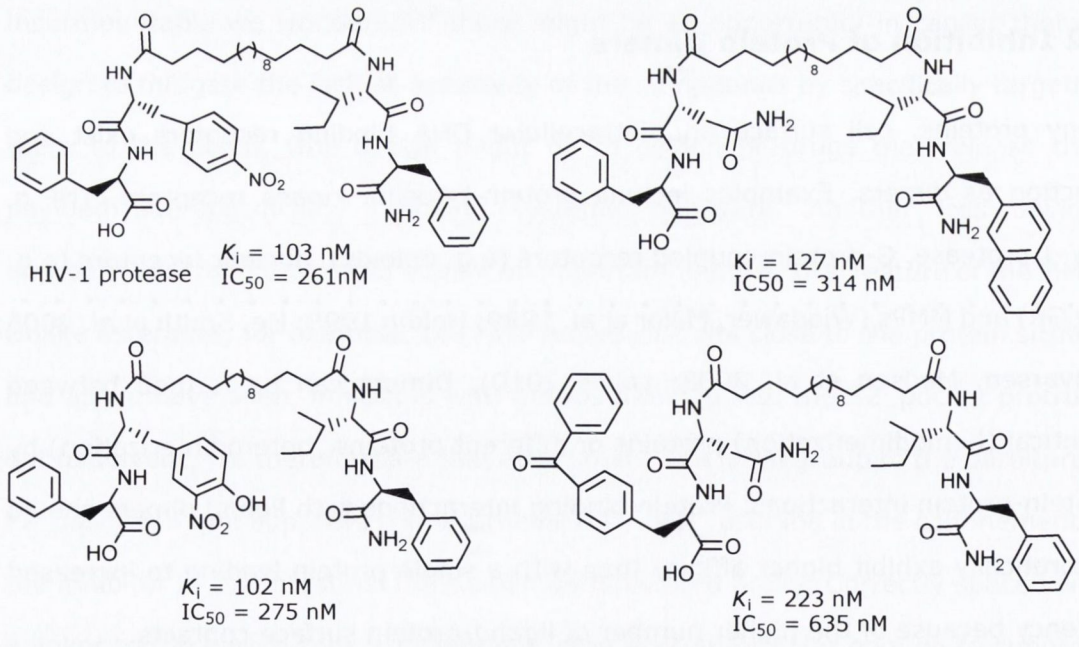


Figure 4.4. *Potent dimer inhibitors of HIV-1 protease (Hwang and Chemielewski 2005).*

A less immediately evident feature of the dimer approach is that it can impart protein sub-type selectivity if similar proteins are distributed differently with respect to dimer formation. This has been observed in several instances, for example, with bis-tetrahydromaineacrine inhibitors which showed 1000-fold selectivity for rat acetylcholinesterase over butyrylcholinesterase (Pang, Quiram et al. 1996).

In the present work the main reason for interest in dimers was to generate compounds with increased mass and reduced transepithelial transport but we were hopeful of potential benefits in selectivity. MMP-2 and MMP-9 are tightly regulated by TIMPs by forming complexes in normal conditions. ProMMP-2 forms complexes with TIMP-2, -3, and ,-4 by interaction of the C-terminal PEX domain in the enzyme with the C-terminal domain of the TIMP (Malla, Sjoli et al. 2008). ProMMP-9 binds to TIMP-1 and TIMP-3 through their C-terminal domains (Nagase, Visse et al. 2006). In pathological conditions, MMP-2 and MMP-9 are up-regulated and overexpressed in many tissues and organs. Activated MMP-2 and MMP-9 can form complexes with other MMPs or with itself. MMP-9 can form homodimers, whereas MMP-2 can only form heterodimers in which it is linked with proteins such as MMP-1 (Goldberg, Strongin et al. 1992; Cha, Kopetzki et al. 2002). Therefore, dimer selectivity for MMP-9 over MMP-2 can be anticipated if the dimer can occupy two adjacent MMP-9 sites increased binding affinity but not two MMP-2 sites since the latter does not dimerize. In order to exhibit increased selectivity/potency for MMP-9, the inhibitor would need to be spaced at the correct distance and therefore inhibitor potency/selectivity might emerge as a function of spacer length.

Recent studies have reported on the dimer approach to inhibition of MMP-1, -2, -9, and -14 (Fig. 4.5) (Rossello, Nuti et al. 2005). These dimers were prepared based on the structure of compound **D0** which has great potency on MMP-2, -9, and -14.

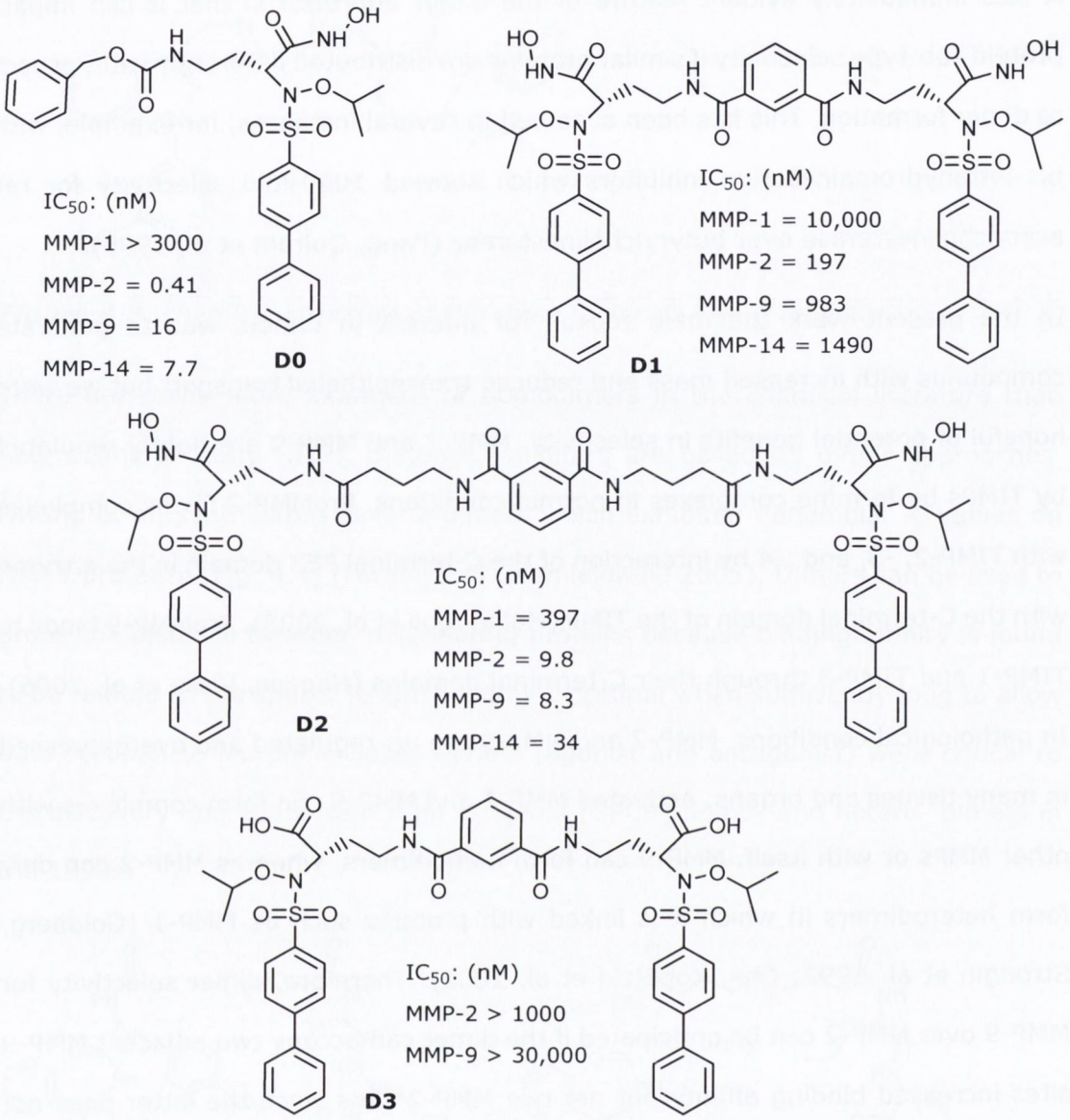


Figure 4.5. *IC_{50} values of hydroxamic acid dimers (Rossello, Nuti et al. 2005).*

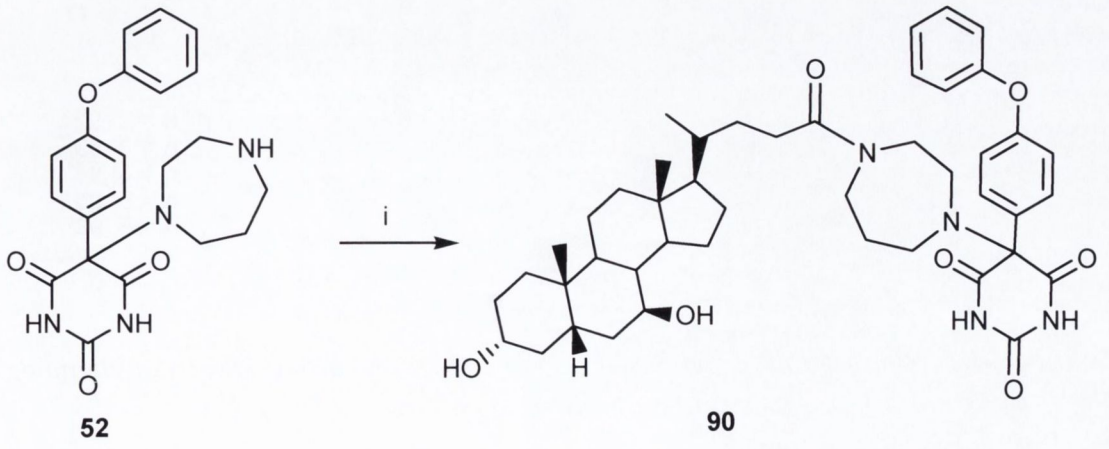
Apart from binding to active site of the MMP with one side of hydroxamic acid moiety, another hydroxamic acid of the dimer was designed to stretch out of the MMP and to bind with other MMPs, leading to enhancement of affinity. However, dimer potency in this class was disappointing. IC_{50} values of dimers (**D1**, **D3**) towards MMP-2 and MMP-9 were significantly increased compared to the monomolecular compound (**D0**) apart from **D2**, which showed 2-fold improvement in inhibition of MMP-9. In addition, these dimers exhibited worse selectivity between MMP-2 and MMP-9 than **D0**.

As described in the previous Chapter, we developed homopiperazine-based barbiturates that exhibited significant inhibition of both MMP-9 and MMP-2. Therefore, we decided to synthesize several dimers based on homopiperazine substituted barbiturates with different linker lengths potentially affording improvements in potency and selectivity. Moreover, because dimers are larger molecules, with poorer absorption characteristics they can potentially be delivered into the colon without loss of activity. When the MMP-9/MMP-9 complex binding dimers reach the disease site, they would significantly inhibit MMP-9 activity which is massively over-expressed in colon cancer.

4.3 Synthesis of a UDCA conjugate of homopiperazine-based barbiturate and formation of dimers

Seven homopiperazine-based MMP inhibitors were prepared for future investigation as colon targeting agents based on the dimer approach (n=6) or by attachment of the large hydrophilic ursodeoxycholic acid (UDCA). These compounds were synthesized by coupling of the intermediate **52** with UDCA or in the case of the dimers with the appropriate acid dichlorides.

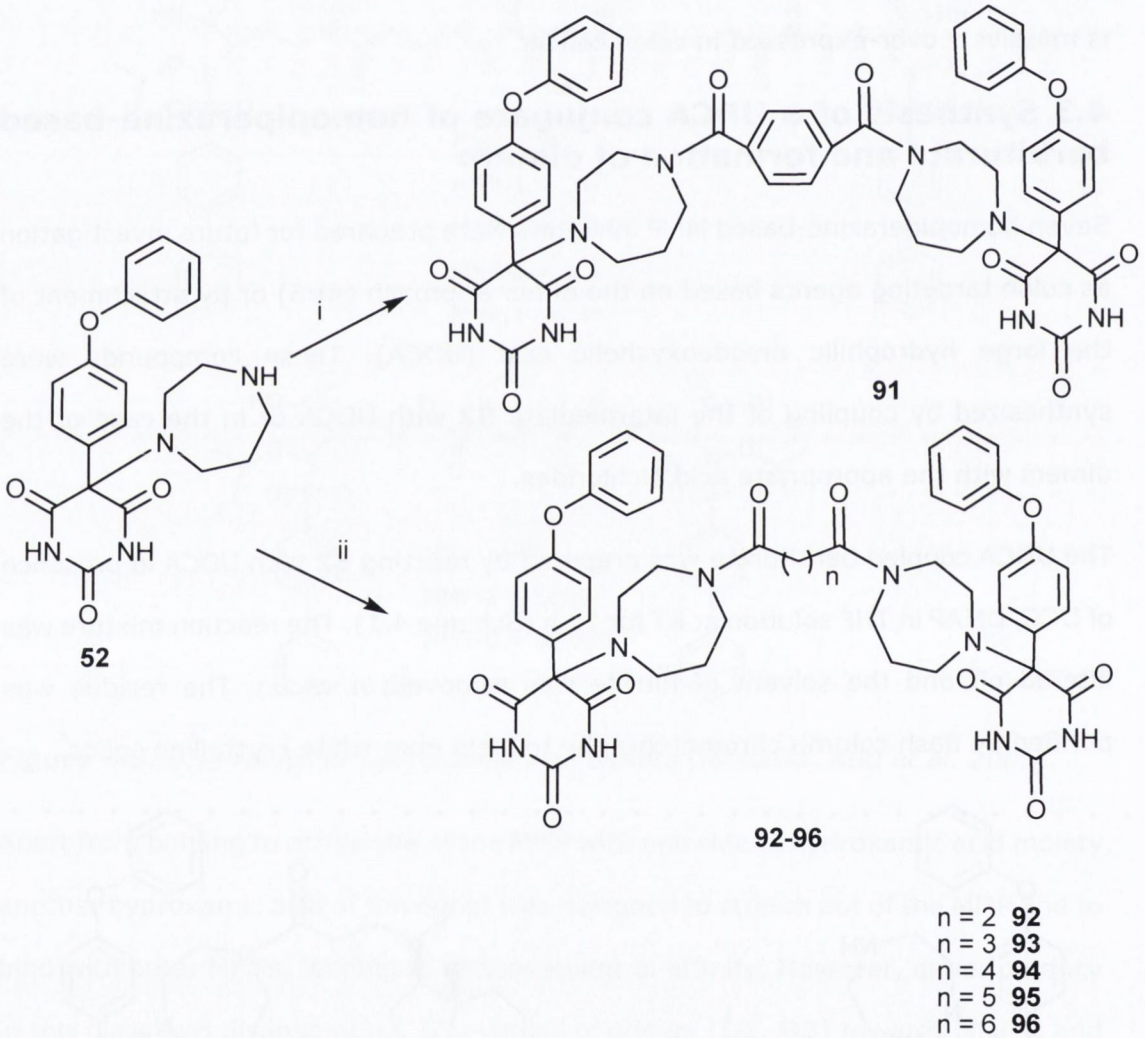
The UDCA coupled barbiturate was prepared by reacting **52** with UDCA in presence of DCC, DMAP in THF solution at RT for 12 h (Scheme 4.1). The reaction mixture was filtered off and the solvent of filtrate was removed *in vacuo*. The residue was purified by flash column chromatography to yield pure white crystalline solids.



52 **90**

Scheme 4.1. *Preparation of UDCA coupled homopiperazine-based barbiturate. i) UDCA, DCC, DMAP, THF, RT, 12 h.*

The six dimers were synthesized by coupling two equivalents of **52** with acid dichlorides in the presence of triethylamine in THF solution at -70°C for 8 h (Scheme 4.2). The reaction mixtures were dried *in vacuo* to remove the solvent. The residues were purified by flash column chromatography to yield pure products. Compound **91** has a phenyl group incorporated into the homopiperazine substituted barbiturate homodimer. The remaining five compounds possessed different alkyl groups in the middle of the homopiperazine substituted barbiturate.



Scheme 4.2. *Preparation of the dimers: i) terephthaloyl dichloride, triethylamine, THF, -70°C, 8 h. ii) acid dichlorides, triethylamine, THF, -70°C, 8 h.*

4.4 Biological activities of colon targeting compounds

4.4.1 Evaluation of gelatinase inhibition

The UDCA substituted homopiperazine-based barbiturates and six dimers were tested in the fluorogenic assay to obtain their IC_{50} values for MMP-2 and MMP-9. The compounds were tested at five different concentrations from 10 μM to 0.1 nM. The compounds were incubated with MMP-2 or MMP-9 for 45 min. Then the substrate Mac-Pro-Leu-Gly-Leu-Dap-Ala-Arg-NH_2 was added to the mixture of MMP and the compounds, and the changes of fluorescence were recorded. The IC_{50} values of the tested compounds were calculated by plotting the logarithm of the concentrations versus the percentage of inhibition using a Sigmoidal concentration-response function. GraphPad Prism® 4 was used to get the IC_{50} values and 95% confidence intervals (Fig. 4.6) (Table 4.1).

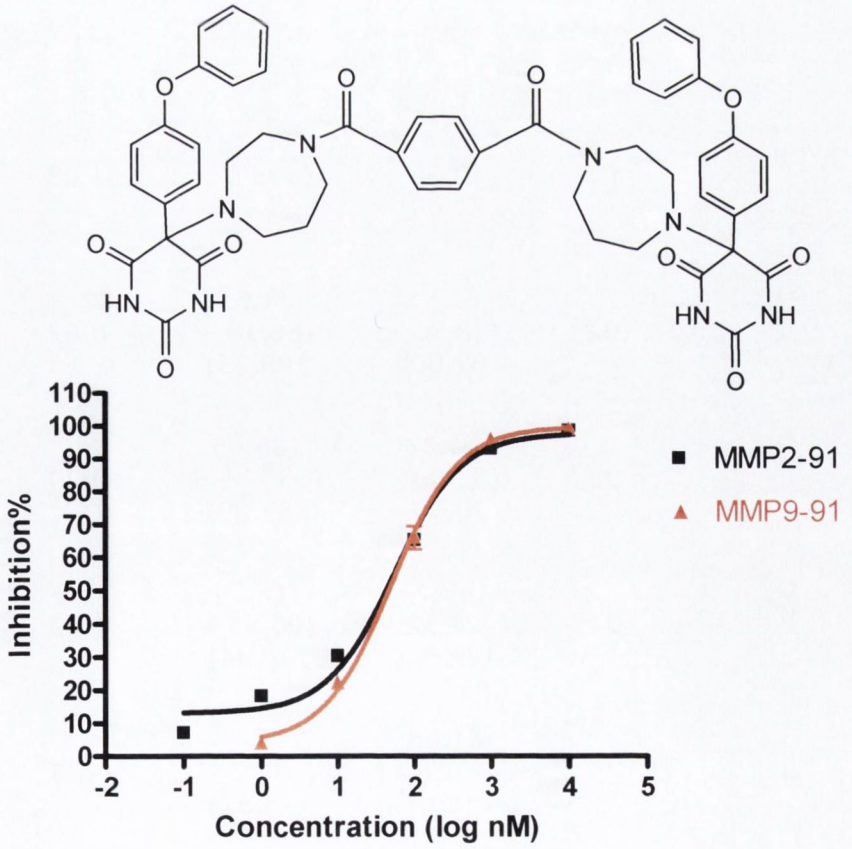
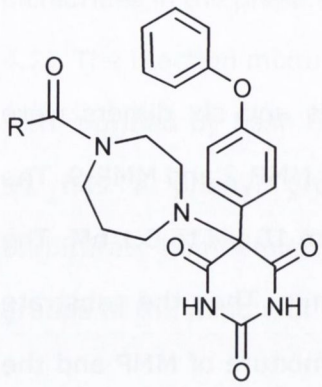
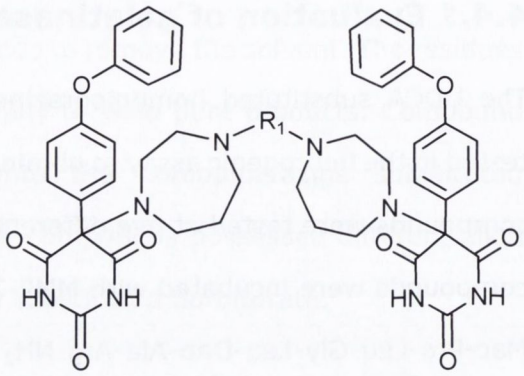
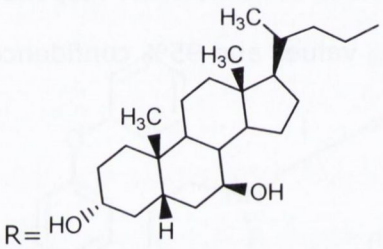
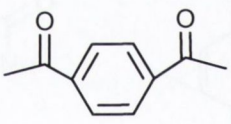
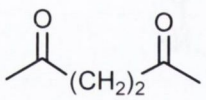
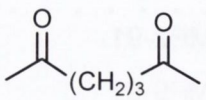
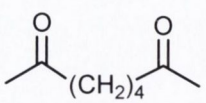
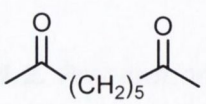
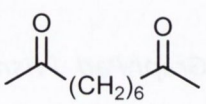


Figure 4.6. *Example curves for* ***91*** *generated using GraphPad Prism® 4 for estimating IC_{50} values of MMP-2 (black) and MMP-9 (red).*

Table 4.1. *IC_{50} values of the high molecular weight barbiturates.*





Structure	Compd No.	MMP-2 (nM)	MMP-9 (nM)	MMP9 selectivity
	**90**	299.82 (249.93 – 359.67)	409.96 (312.09 – 538.51	0.73
$R_1=$ 	**91**	54.42 (40.02 – 74.00)	50.38 (39.79 – 63.97)	1.08
$R_1=$ 	**92**	56.95 (48.36 – 67.06)	84.63 (66.18 – 108.23)	0.67
$R_1=$ 	**93**	54.37 (41.88 – 70.59)	188.65 (153.35 – 232.09)	0.29
$R_1=$ 	**94**	148.74 (121.52 – 182.06)	115.34 (90.84 – 146.44)	1.29
$R_1=$ 	**95**	81.88 (66.28 – 101.14)	120.78 (98.03 – 148.82)	0.68
$R_1=$ 	**96**	67.48 (57.82 – 78.74)	80.06 (69.92 – 91.67)	0.83

The UDCA substituted compound (**90**) (IC_{50}: MMP-2 = 299 nM, MMP-9 = 409 nM) exhibited least inhibitory potency towards MMP-2 and MMP-9. The dimers were more potent. The most potent inhibitors of MMP-2 and MMP-9 were **93** (IC_{50}: MMP-2 = 54 nM, MMP-9 = 188nM) and **91** (IC_{50}: MMP-2 = 54 nM, MMP-9 = 51 nM), respectively. In addition, **91** not only had the greatest potency on MMP-9 but also on MMP-2, which had nearly the same IC_{50} values on MMP-2 as **93**. Compound **93** was also the most MMP-2 selective inhibitor, which showed nearly 4-fold selectivity for MMP-2 compared with MMP-9. None of the compounds exhibited significant selectivity for MMP-2 or MMP-9. The strong inhibition shown by UDCA substituted barbiturate and the dimers was believed to result from P1′ substituents binding with the S1′ pocket and the active zinc binding of barbiturate ring. In addition the size of the substituent close to the carbonyl group were not too big to affect the binding of the homopiperazine with the mouth of S2′ pocket (Fig. 4.7). As illustrated, the alkyl group on UDCA fitted into the mouth of S2′ pocket and led to the large polycyclic steroid protruding from the narrow mouth, which made the homopiperazine ring sit into the mouth of the S2′ pocket well. Compound **93** presented a similar situation, with the linker group sitting just outside the pocket.

There are two reasons to believe that the dimers did not achieve dual occupancy. Firstly, bivalent occupancy of adjacent protein units would be expected to lead to an increase in binding affinity since a greater number of contacts are made. This is expected to endow the compound with some selectivity since it is unlikely to bind bivalently with both enzyme types. Secondly, the modeling suggests that the linkers we used were too short to permit the second barbiturate ring to bind at another enzyme site. Future work might therefore examine the use of longer linkers. Another unsatisfactory feature of the present investigation was the use of purified recombinant enzymes for determining potency and selectivity. In real tissue MMP-2 and MMP-9 have the opportunity to dimerize with other MMP and indeed non-MMP partners. MMP-2 as mentioned frequently dimerizes with MMP-1. In recombinant protein solutions this kind of heterogenous arrangement is not possible diminishing

the possibilities for enzyme sub-type selectivity. Indeed it is possible for a dimer compound with optimal spacer length for bivalent occupancy to catalyse homodimer formation. It would be interesting to assess the effects of the dimer compounds in real tissue with potential selectivity vectors such as distribution, access and protein heterogeneous dimer formation.

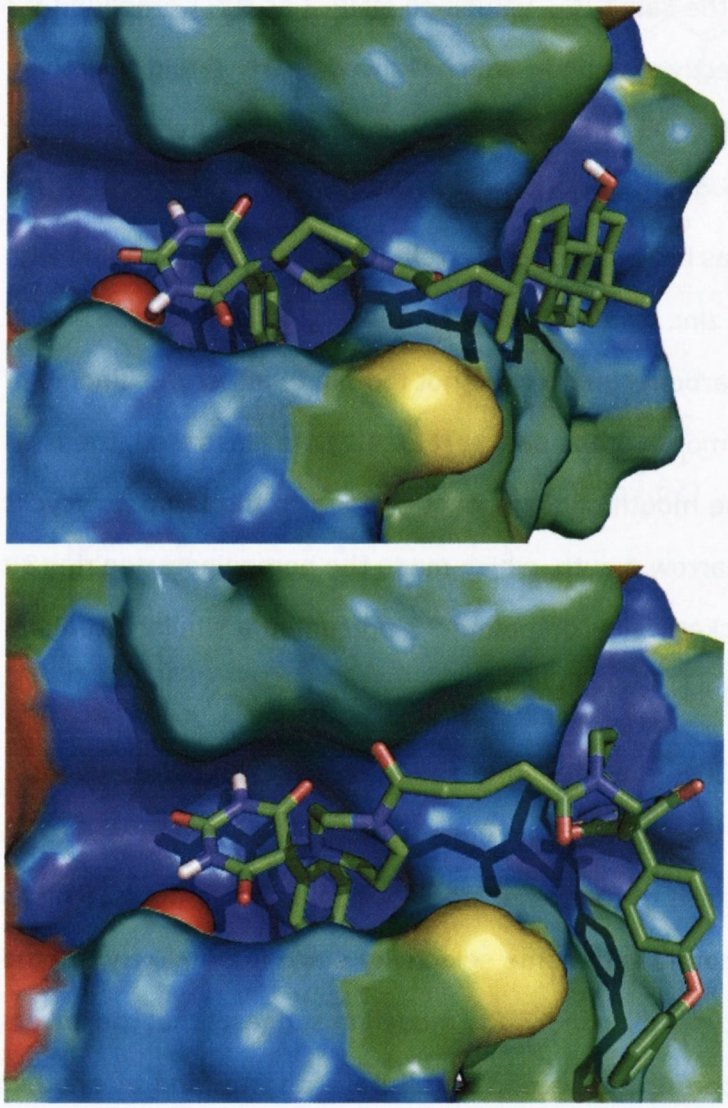


Figure 4.7 *Pictures of* ***90*** *(upper) and* ***93*** *(lower) docking with a 'Connolly' surfaces on MMP-9. The surfaces were generated by the programme PyMOL® based on the crystal structures of MMP-9 (pdb code 2ovx). Ligand orientations were used which had the lowest binding energy of the conformations of 50 runs with 25000000 energy evaluations in Autodock4 and displayed by PyMOL®. The active site zincs are shown as the red spheres. The polycyclic steroid nucleus of* ***90*** *and the second homopiperazine substituted barbiturate group in* ***93*** *sit outside of the mouth of S2' pocket.*

4.4.2 Inhibition of Caco-2 cell invasiveness

In intestinal diseases, inflammatory cells promoted by MMP activity can invade the intestinal walls and other organs. It was interesting to evaluate the abilities of the UDCA barbiturate and dimers to suppress invasiveness. We undertook a similar investigation to that described previously using the colonic CACO-2 cell line. Due to the higher IC_{50} values on MMP-2 and MMP-9, **90** was tested at 10 μM and 100 nM. Compound **93**, the most potent inhibitor of MMP-9 in the dimers, was also measured at these two concentration levels. Compounds **90** and **93** caused significant inhibition of cell invasion, with only a small number of cells migrating through the matrigel membrane (Fig. 4.8). Compounds **92** and **94** were tested at 100 nM in order to permit relative assessment of the dimers as inhibitors of cells invasiveness.

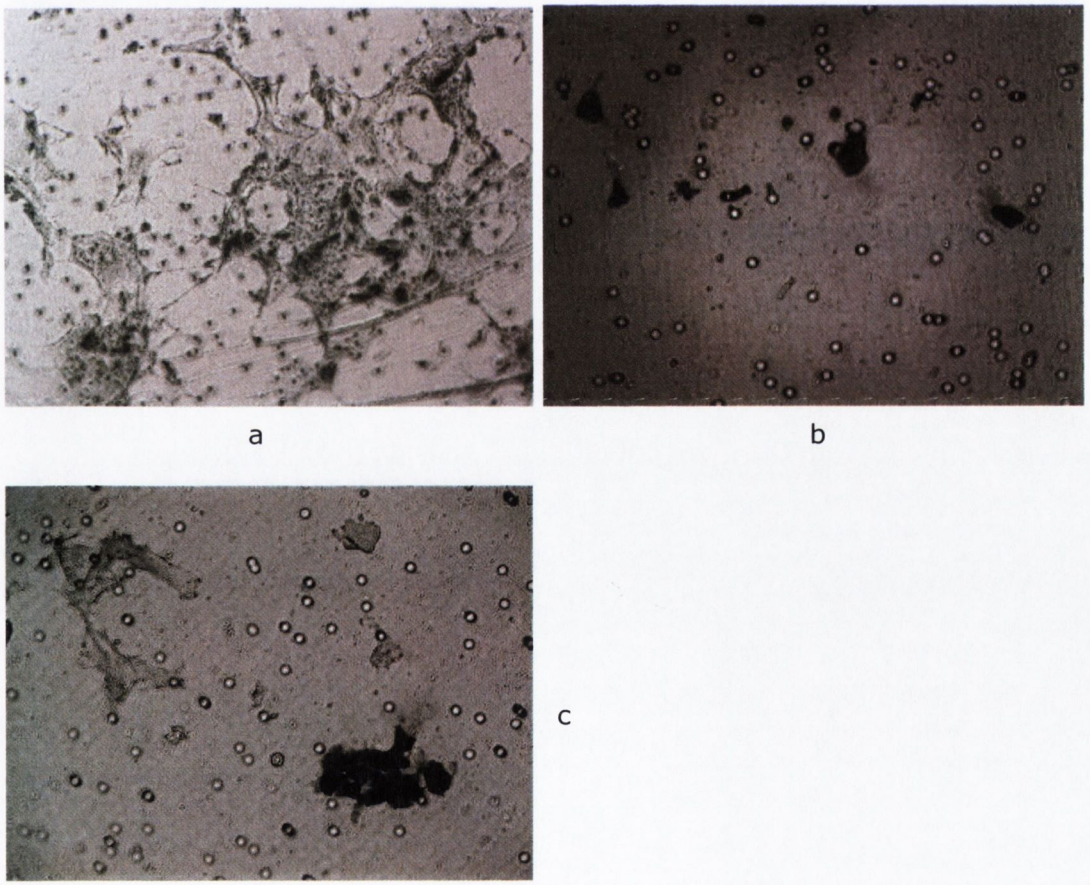


***Figure 4.8**. Microscope images of invasion assays with **90** and **93**: a) A positive control insert, incubated with Caco-2 cells and HGF. b) Insert incubated with Caco-2 cells, HGF, and 10 μM **93**. c) Insert incubated with Caco-2 cells, HGF, and 10 μM **93**. Compounds **90** and **93** significantly inhibited cell invasion at 10 μM.*

The percentage of inhibition for tested compound was calculated using the formula 3-1 and results are shown in Fig. 4.9.

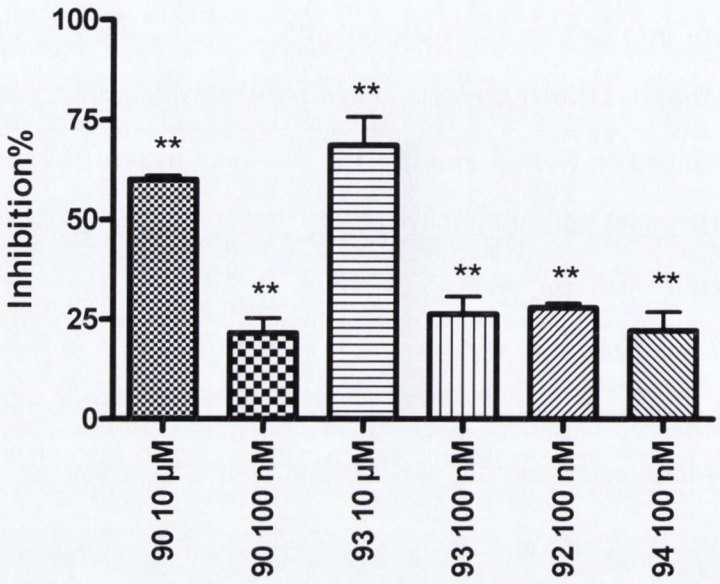
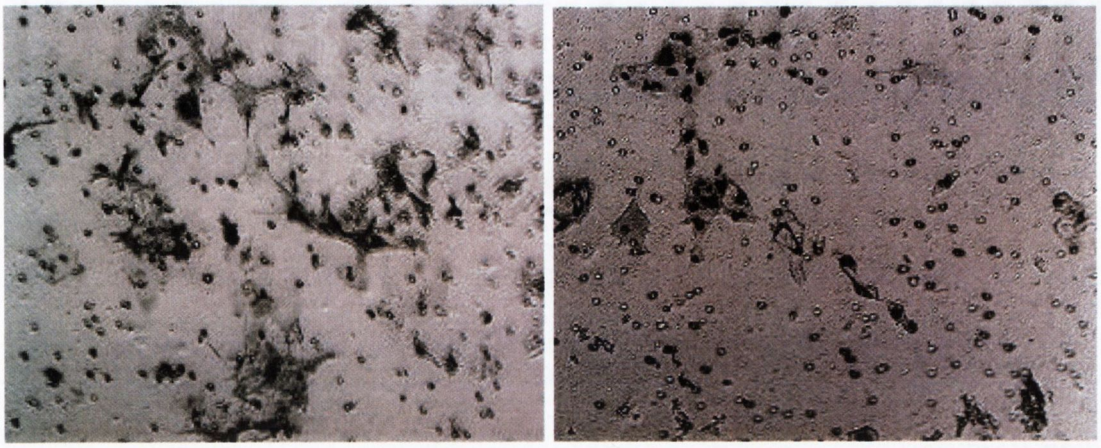
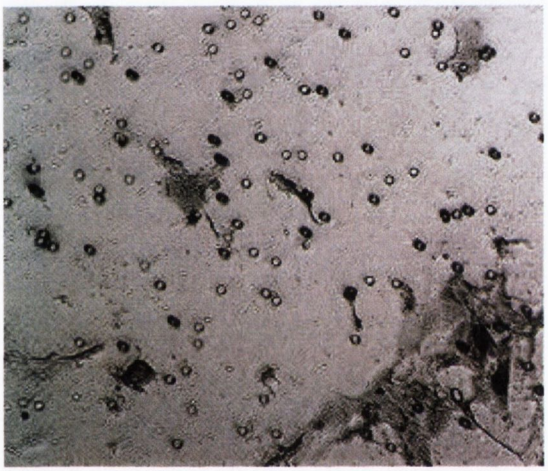


***Figure 4.9**. Inhibition of Caco-2 cell invasion by UDCA conjugate and dimer analogs (** significantly different from control $P < 0.05$).*

The results show that the UDCA substituted barbiturate and the dimers shared ability to significantly inhibit Caco-2 cells invasiveness at 100 nM. Interestingly **90** which was moderately potent inhibitor of the gelatinases was equally efficacious in the invasion model with the more potent dimer analogs (Fig. 4.10).



a b



c

***Figure 4.10**. Representative pictures of invasion assay results of compounds **93** and **94**. a) A positive control insert, which incubated with Caco-2 cells and HGF. b) Insert incubated with Caco-2 cells, HGF, and 100 nM **93**. c) Insert incubated with Caco-2 cells, HGF, and 100 nM **94**.The number cells in b and c were significantly less than the positive control inserts, demonstrating that compound **93** and **94** had the ability to inhibit Caco-2 invading through matrigel membranes at 100 nM.*

It has been reported that MMP-2 and MMP-9 play important roles in promoting cancer cell invasion (Deryugina and Quigley 2006), and therefore inhibiting MMP-2 and MMP-9 activity should block the cell invasion. The UDCA coupled homopiperazine-based barbiturates and dimers caused significant inhibitory effects on MMP-2 and MMP-9 activity and exhibited significant ability to block Caco-2 cell invasion, demonstrating the impact of inhibition of gelatinases activity on cell invasion. We were interested in seeing if there was a relationship between selectivity towards either gelatinase isoform and invasion or if selectivity was an

important parameter influencing this. Up till now we did not have sufficient compounds make to any analysis of these relationships but combing the results for the new compounds and those already reported in Chapter 3 allowed us to investigate this (Table 4.2, and Fig. 4.11)

***Table 4.2**. All the tested compounds' abilities of inhibition of invasion of Caco-2 cells at 100 nM and their IC_{50} values.*

Compounds No.	IC_{50} values (nM)		Invasive inhibition % on Caco-2 cells
	MMP-2	MMP-9	
36	1.93	7.54	73.32
65	2.88	2.55	46.54
74	86.50	22.71	38.16
80	74.46	310.88	20.15
82	213.79	23.90	59.69
90	299.82	409.96	21.56
92	56.95	84.63	27.88
93	54.37	188.65	26.26
94	148.74	115.34	22.10

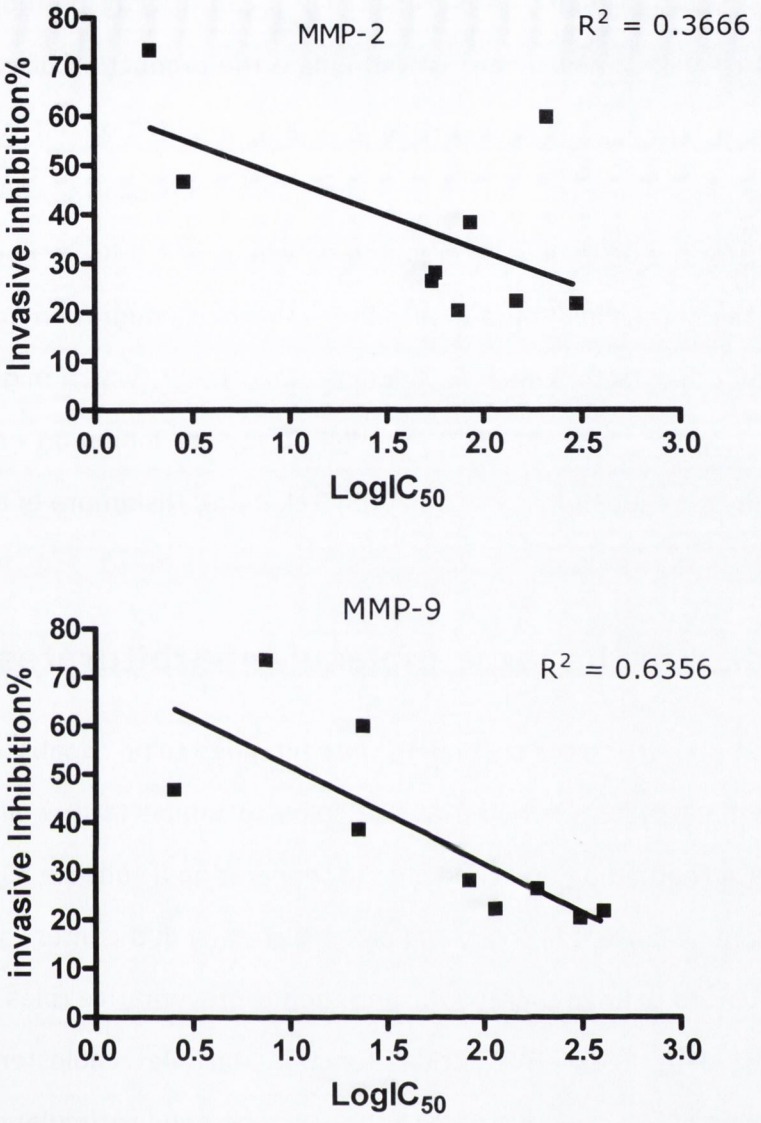


Figure 4.11. *The linearity of MMP-2 and MMP-9 IC_{50} values of the test compounds with the inhibition of invasion of Caco-2 cells. The upper picture indicates the correlation between the MMP-2 IC_{50} values with inhibition of the cell invasion. The lower picture shows the correlation of the MMP-2 IC C_{50} values with inhibition of the cell invasion.*

Table 4.2 and Fig. 4.10 illustrate the correlation between MMP-2 inhibition and invasive inhibition of Caco-2 cells was poor, but they reflected that the compounds with the stronger inhibition of MMP-2 activity blocked more Caco-2 cells invading through matrigel membrane, affirming the role of MMP-2 in promoting invasion of cells. Compared with MMP-2, MMP-9 IC_{50} values of the tested compounds had the better correlation with their inhibition of invasion of the cells. The better correlation

between MMP-9 with cell invasion might be because MMP-9 can directly promote cancer cell invasion, unlike MMP-2 which can only stimulate the production of cell invasion promoters such as TGF-β (Yu and Stamenkovic 2000). In addition, MMP-9 can also promote expression of some promoters for migration and invasion of cells, which might be the cause for the unsatisfied correlation between MMP-9 IC_{50} values and invasive inhibition (Takehara, Nishimura et al. 2009). However, migration and invasion involves in many other factors such as claduin-4, and IL-17, which might be also the poor correlations between MMP-2 and MMP-9 activity inhibition and inhibition of cell invasiveness (Zhu, Mulcahy et al. 2008; Takehara, Nishimura et al. 2009).

4.5 Stability Studies of the large molecular barbiturates

The UDCA substituted compound and the six dimers were intended to be capable of transit through the intestinal system arriving at the colon to inhibit MMP-2 and MMP-9. The bile acid UDCA seemed a good candidate for generating a suitable high molecular weight candidate because it is polar, and present anyway in the intestinal tract. Indeed UDCA is reported to have therapeutic and chemo-preventative roles in intestinal disorders including IBD. Bile acids function include cholesterol homeostasis and generation of bile flow that helps in the excretion and recirculation of drugs and vitamins, and aid in the absorption of dietary lipids (Roda, Hofmann et al. 1983; Jean-Louis, Akare et al. 2006). Compound **90** could play roles of MMP inhibitory barbiturate and the bile acid in the colon. A critical feature with regard to the intended actions of **90** was its intestinal stability since if it was cleaved by proteases in the intestinal tract, it would generate two monomers, each capable of undergoing passive diffusion into the portal vein. On the other hand, if dimer hydrolysis occurred in the colon, the hydrolysis products would cause gelatinase inhibition. Ideally both kinds of candidate- BA conjugate or dimer should be stable over the course of the oral-caecal transit time.

In this context we decided to study the stability of the UDCA conjugate **90** and a dimer **93** under conditions they would likely encounter in the intestinal tract if they were ever administered. The studies were performed using real duodenal juice that had been sampled from a 27 year old woman with IBD at St. James's hospital, Dublin. The compounds were dissolved in methanol to give the stock solutions at 20 mg/ml. The stock solutions were diluted to make up sample solutions at 40 µg/ml using the duodenal juice. The amount of compound remaining was measured using a reverse phase HPLC method, which involved elution on a Waters Xbridge C18 5 µm column (4.6 x 250 mm) with a binary mixture of methanol and water at 1 ml/min in gradient mode. A Waters photodiode array detector 996 was set up to 256 nm for the detection. A linear response was observed for each compound (r^2 > 0.999) in the range from 5 µg/ml to 100 µg/ml. During the studies, the sample solutions of the compound **90** and **93** were stored at 37°C oven and injected into HPLC for 6 times in 6 h at 0, 0.5, 1, 2, 3 and 6 h.

Initially, an isocratic method which was elution on a Waters Xbridge C18 5 µm column (4.6 x 250 mm) with mobile phase of 50% methanol and 50% water was applied but this gave very broad peaks and significant peak tailing. After trying for many times, a gradient HPLC method was successfully developed, which allowed separation of two isomer peaks in each case (Table 4.3)

Table 4.3. *The reverse phase HPLC gradient method for the stability study of compounds* ***90*** *and* ***93*** *(A was water and B was methanol).*

Time (mins)	Flow rate (ml/min)	% A	% B	Curve
0	1.00	50	50	
10	1.00	10	90	6
20	1.00	10	90	6
20.01	1.00	50	50	6
25	1.00	50	50	6

We were initially surprised to see more than one peak in each case. The two peaks arise in the case of the UDCA compound (**90**) because UDCA is itself chiral and so its conjugate with the enantiomeric barbiturate (C5) leads to a diastereomeric pair separable by HPLC. In the case of dimers, four isomers (RR, SS, SR, RS) are possible in two enantiomeric pairs because of the connection of two racemic compounds through the linkers. It would be interesting to separate these and determine if they are similar in potency in the biochemical assay.

The diastereomeric pair of compound **90** were stable in the duodenal juice at 37°C over 6 h (Fig. 4.12) suggesting its suitability for oral administration. A potential pitfall in the design of this compound, which might emerge in cell-based or *in vivo* work is that the bile acid might act as a substrate for transporters which are abundant in the GI tract especially the ileum where bile acids undergo uptake through an active transport mechanism. If the acid side chain is necessary for effective substrate recognition it is likely that the conjugate would not undergo active uptake. On the other hand the study shows that it is possible to conjugate quite large fragments to molecules in the homopiperazine class without paying a large potency penalty and that such compounds might show suitable intestinal stability.

Compound **93** did undergo hydrolysis in the duodenal juice at 37°C (Fig. 4.13) generating an earlier eluting compound. The peak areas of two isomer peaks versus the time were plotted and the points fitted to second order polynomial decay curves (r^2=0.99; Fig 4.14). There was a slight difference in the hydrolysis rates for the two peaks which is not surprising since the degradation was probably protease catalysed. The hydrolysis product was most likely the barbiturate monomer with linker attached but it was not identified. Half-lives in both cases were in excess of the oral-caecal transit time (3-6 h).

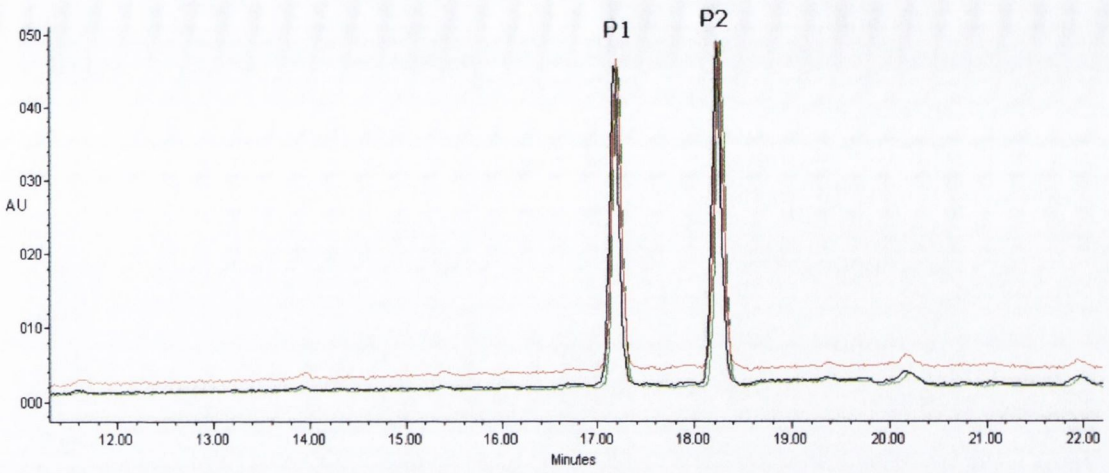


***Figure 4.12**. Overlaid chromatograms of the peaks for **90** in the duodenal juice at 37°C for 0 h (red), 3 h (cyan) and 6 h (green). P1 and P2 correspond to diastereomers of **90**.*

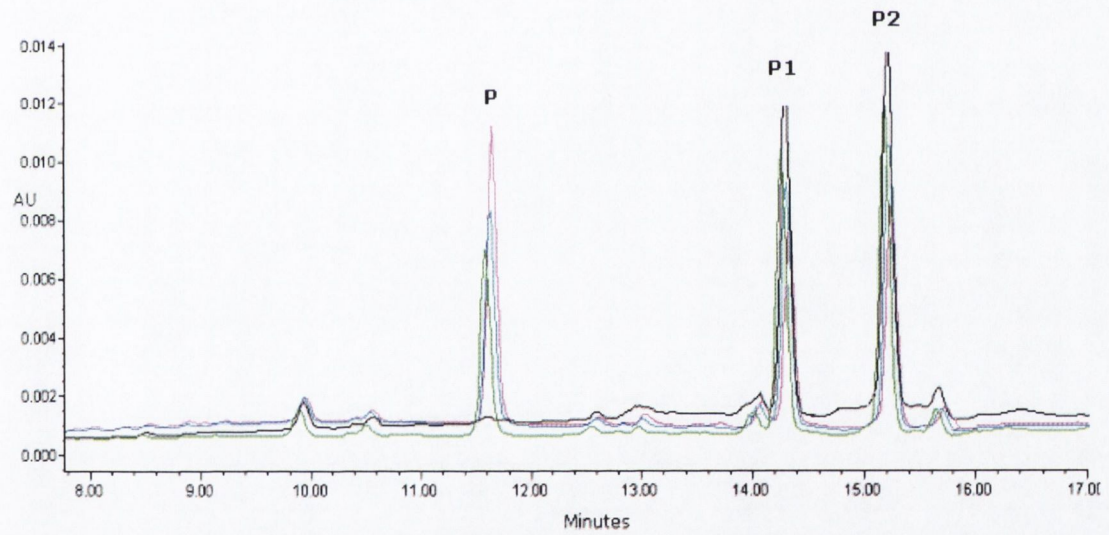


Figure 4.13**. Overlaid chromatogramsof the peaks for **93** in the duodenal juice at 37°C for 0 h (black), 2 h (green), 3 h (cyan) and 6 h (pink). P was the peak of the hydrolysis product. P1 and P2 correspond to diastereomers of **93.

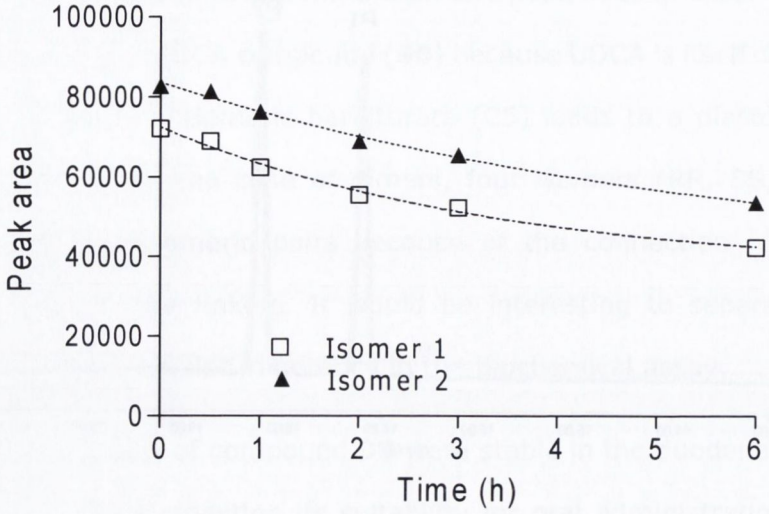


Figure 4.14. *Progress curves for P1 and P2 peaks of* ***93*** *in duodenal juice preparation at 37°C.*

4.6 Conclusion

MMP-2 and MMP-9 play important roles in intestinal diseases such as IBD, necrotizing enterocolitis, and colagenous colitis (Medina and Radomski 2006). Generally, treatment for IBD is involved in many pharmacological approaches including antibiotics, cytokine modulators, inhibitors inflammation and immosuppressants (Egan and Sandborn 2005). Because of their lack of selectivity, inhibitors of the gelatinases need to be targeted for the treatment of the intestinal diseases, especially IBD. In this Chapter we described some strategies for increasing the mass of established barbiturate-based inhibitors so that they may be confined to the intestinal tract following oral administration, without attenuating their inhibitory potency. Moreover one of the strategies the formation of barbiturate dimers could conceivably impart gelatinase sub-type selectivity in cases where dual occupancy of neighbouring MMP proteins could be achieved.

Accordingly, several high molecular weight gelatinase inhibitors were synthesized based on the structure of the homopiperazine-based barbiturate (**53**) and their IC_{50} values on MMP-2 and MMP-9 were measured in the fluorogenic assay. All of the dimers (**91-96)** showed good inhibitory potency but we were disappointed with their selectivity. It is possible that the linker choices were not suitable to permit dual occupancy of adjacent enzymes. Moreover the assay design was probably not adequate to explore the possibilities for selectivity that might present in real tissue. The UDCA conjugate was somewhat less potent and showed little selectivity.

The test results in the invasion assay showed that these seven compounds at 100 nM significantly inhibited Caco-2 cell migration. The inhibitory potency of the compounds was as good in this assay as the more potent inhibitors described in Chapter 3.

The stabilities of **90** and **93** were assessed in duodenal juice using a gradient reverse HPLC method in order to predict the potential of the compounds to under transit to the large bowel. Compound **90** was stable in the duodenal juice at 37°C for

at least 6 h. The dimer (**93**) underwent significant hydrolysis perhaps because it has two points of vulverability towards hydrolysis compared with one in the case of **90**. However it is possible that the hydrolysis products could possess gelatinase inhibition activity. Further studies investigating intestinal stability are warranted.

In conclusion, the results of the compounds in the fluorogenic assay, invasion assay, and stability studies demonstrate that the UDCA substituted homopiperazine-based barbiturate and the dimer compounds could be useful for inhibiting intestinal MMP-2 and MMP-9 activities and inflammatory cell invasion in the colon, and suggest these compounds could be potential drugs for the treatment for intestinal diseases.

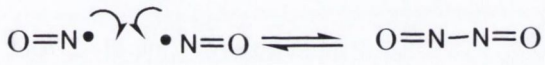
Chapter 5

Preparation and evaluation of barbiturate-based nitrates

5.1 Introduction

5.1.1 Chemistry of Nitric Oxide

Nitric oxide is a noxious, colourless, free radical gas, with chemical formula NO·. It can be liquefied at -151.8°C and solidified at -163.6°C; the liquid and solid are both blue in colour. Nitric oxide is stable and does not form the dimer in the gas phase at room temperature, but it's found as N_2O_2 in the liquid state (Thomas 2007).



Commercially, nitric oxide is prepared by the oxidation of ammonia at 850°C in the presence of platinum as catalyst (Fig. 5.1). In the laboratory, nitric oxide is prepared by reduction of nitric acid or nitrous acid in the form of sodium nitrate (Fig. 5.1). In addition, nitric oxide can be formed from the reaction of nitrogen with oxygen at high temperature or action of electric sparks.

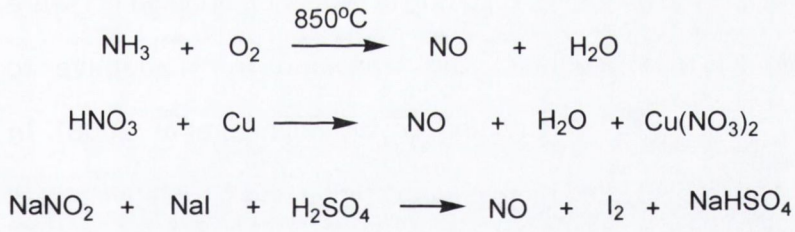


Figure 5.1. *The common methods for the preparation of nitric oxide.*

Nitric oxide has few applications in the chemical industry. It is an intermediate in the synthesis of nitric acid during the oxidation of ammonia. In addition, hydroxylamine, an intermediate in biological nitrification, can be prepared by hydrogenation of nitric oxide in the presence of a catalyst.

5.1.2 Biological functions of nitric oxide

Nitric oxide is involved in many biological processes as a major messenger molecule. The generation of nitric oxide is catalyzed from L-arginine by a family of enzymes

known as nitric oxide synthases (NOS). These have been classified as neuronal (nNOS), endothelial (eNOS) and inducible (iNOs) (Alonso and Radomski 2003). The nNOS and eNOS have similar properties and are expressed in host cells when activated by calcium, whereas cNOS is calcium-independent and is produced in response to inflammatory stimuli of host and bacterial origin (Thomas 2007). Nitric oxide plays important roles in both physiological and pathological conditions, including macrophage actions, vascular diseases, wound healing, platelet function, and cancers (Nathan and Hibbs 1991; Sneddon and Garaham 1992; Alonso and Radomski 2003; Coulter, McCarthy et al. 2008; lundberg, Weitzberg et al. 2008; Filippin, Moreira et al. 2009).

5.1.2.1 Nitric oxide and cardiovascular diseases

Nitric oxide is an important signaling molecule and modulator of cardiovascular diseases. It is responsible for the biological activity of endothelium-derived relaxing factor (EDRF) which has the ability to promote smooth muscle relaxation. It dilates the blood vessel and increases the flow rate, resulting in reduction of blood pressure. Endogenous myocardial NO may modulate the transition from adaptive to maladaptive hypertrophy and lead to heart failure (Loyer, Heymes et al. 2008). In addition, dysregulation of nitric oxide and increased oxidative and nitrosative stress is associated with the pathogenesis of heart failure (Pacher, Schutz et al. 2005). Peroxynitrite is a reactive oxidant generated from the reaction of nitric oxide with superoxide anion, which damages cardiovascular function through multiple mechanisms including activation of MMPs and poly (ADP-ribose) polymerase (Pacher, Schutz et al. 2005). In addition, nitric oxide is an important anti-atherosclerotic autocoid with inhibitory effects on platelet aggregation and anti-proliferative and dilatory effect on vasculature (Evgenov, Pacher et al. 2006). In the endothelial monolayer, L-arginine is converted by NOS to nitric oxide, which diffuses into both the vessel lumen and the vessel wall, activating soluble guanylate cyclase (sGC) for conversion of ganosine triphosphate (GTP) to cyclic guanosine

monophosphate (cGMP), and resulting in both vasorelaxation and inhibition of platelet aggregation (Fig. 5.2) (Evgenov, Pacher et al. 2006). Moreover, imbalance of production and decreased bioavailability of nitric oxide leads to formation, progression, and destabilization of atherosclerotic plaques which may result in adverse outcomes like death, myocardial infraction, and stroke (Pepine 2009).

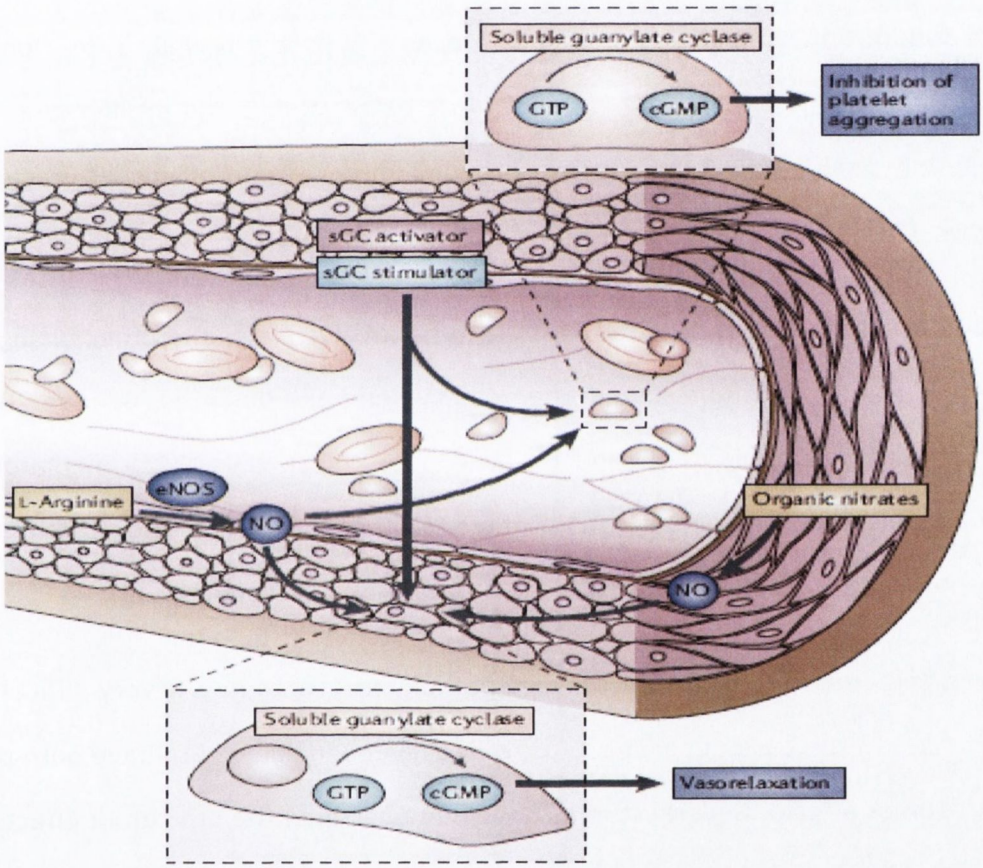


Figure 5.2. *NO-sGC-cGMP signaling in a blood vessel (adapted from (Evgenov, Pacher et al. 2006).*

5.1.2.2 Nitric oxide and cancer

Since a substance mediating tumoricidal activity which decreases mitochondrial respiration and interferes with iron metabolism resulting in the kill of tumors and pathogens was identified as nitric oxide, it has been brought into attention in cancer research (Wink, Ridnour et al. 2008). Nowadays, nitric oxide has been found to be associated with many cancer-related events including inflammation, apoptosis,

angiogenesis, invasion, and metastasis (Ying and Hofseth 2007). It impacts on several steps of metastasis such as regulation of vasodilatation and inhibition of platelet aggregation (Palmer, Ferrige et al. 1987; Radomski, Palmer et al. 19990). Vasodilatation, coupled with a decrease in platelet aggregation can decrease metastasis by reducing the arrest of tumor cell emboli in capillary beds (Tsuruo, Kawabata et al. 1986). Moreover, nitric oxide can inhibit angiogenesis in some organs and introduce apoptosis in the expressing and bystander cells (Xie, Dong et al. 1996). It has also been reported that nitric oxide inhibits the proliferation and invasion of pancreatic cancer cells through upregulation of insulin receptor substrate-1 protein degradation (Sugita, Kaneki et al. 2010).

In addition, nitric oxide has been reported to be involved in many other biological processes including immune system, nervous system, and diabetes (Bogdan 2001; Tyagi and Hayden 2003; Knott and Bossy-Wetzel 2009). It is a key mediator of neurodegeneration in many diseases of the nervous system including Alzheimer's, Parkinson's, and Huntington's diseases (Knott and Bossy-Wetzel 2009).

However, the precise role of nitric oxide in pathological conditions is very difficult to characterize. In the case of cancer, nitric oxide has been showed to have both pro- and anti-tumor effects. Several studies have demonstrated the pro-tumor effects of nitric oxide. For example, *Andrade et al.* have demonstrated that reduced tumor blood flow was observed after pharmacological inhibition of nitric oxide in murine adenocarcinoma and melanoma models by oral administration of N^G-nitro-L-arginine methyl ester (L-NAME), a non-specific NOS inhibitor (Andrade, Hart et al. 1992). Release of low concentrations of nitric oxide can stimulate angiogenesis, inhibit apoptosis, or stimulate proliferation and invasion (Ying and Hofseth 2007). On the other hand, nitric oxide can also play anti-tumor roles. *Jones et al.* have shown that over production of nitric oxide significantly generated anti-tumor effects by inhibition of angiogenesis (Jones, Tsugawa et al. 2004). In addition, it has been demonstrated that high levels of nitric oxide produced by the

inducible isoform of the NOS enzyme inhibited the metastatic murine melanoma cells (Dong, Starosesky et al. 1994). Collectivity, these studies indicated that the concentration of nitric oxide is important in determining its effects in cancer. High concentration nitric oxide can play a protective role by inhibiting cancer metastasis and tumor growth, whereas low levels of nitric oxide may promote cancer cell invasion.

5.1.3 Nitric oxide and MMP activity

The relationship between nitric oxide and MMP activity is complex. On the one hand, nitric oxide can inhibit expression of some MMPs. A decrease of MMP-2 and pro-MMP activity has been observed in eNOS gene expressed smooth muscle cells under basal and IL-β stimulated conditions and eNOS gene-transfected cell medium stimulated with IL-β respectively (Chakraborti, Mandal et al. 2003). It has been reported that eNOS induced nitric oxide can inhibit smooth muscle cell migration and reduce MMP-2 and MMP-9 activities (Gujar, Sharma et al. 1999). On the other hand, MMP expression can be stimulated by nitric oxide, exemplified by down-regulation of MMP-9 expression in uterine horn of L-NAME treated pregnant mice (Zhang, Wang et al. 2004). The downregulation of MMP-9 expression is believed to result from the decrease of activity of TIMP-3 because TIMP-3 is a very efficient inhibitor of MMP-9.

In addition, the impact of nitric oxide (NO) donors on expression of MMPs is dependent the donor half-life (Burrow, Koch et al. 2007). Increases of MMP-8 and MMP-9 expression were observed in the 1 day culture of diabetic fibroblasts with the long half-life NO donors, SNAP (half-life 5 h) and SNOG (half-life 80 h), but no change was found when treated with short half-life NO donor, NOR-3 (half-life 40 min). Furthermore, nitric oxide has been reported to be involved in the activation of proMMPs. For example, nitric oxide activates proMMP-9 by S-nitrosylation of the

cysteine residue and proMMP-8 through a non-proteolytic mechanism (Okamoto, Akaike et al. 1997; Gu, Kual et al. 2002).

Since nitric oxide plays similar roles in many biological processes to MMP inhibitors, including inhibition of platelet aggregation, blocking cancer cell invasion, and inhibition of MMP activities, we proposed to design MMP inhibitors bearing nitric oxide donor groups. Such hybrid compounds could potentially exhibit better protective effects in pathological conditions than MMP inhibitors alone. The design was inspired by the SAR of the barbiturate inhibitors already studied and the knowledge that the P2′ group has little interaction with the protein. Therefore we decided to generate nitrate-bearing compounds with the nitrate group attached through a linker at the barbiturate C5 which would direct the group towards the S2′ site, provided that the geminal phenoxyphenyl group entered the S1′ pocket. The choice of nitrate ($R\text{-}ONO_2$) as nitric oxide releasing group was based on experience with nitrate esters in the Gilmer Laboratory and their long history of clinical use as nitric oxide donors. Overall the strategy can be described as MMP-inhibitor NO-donor hybrids. There has been a very large body of work on NO-donor hybrids over the past decade with many drug types including acetylcholinesterase inhibitors, antihypertensives, anti-inflammatories, antihistamines, antioxidants, calcium channel antagonists, HMG-CoA reductase inhibitors, and β-adrenoreceptors antagonists (Fig. 5.3) (Lopez-Figueroa and Moller 1996; Paul-Clark, Roviezzo et al. 2003; Berndt, Grosser et al. 2005; Gilmer, Lally et al. 2005; Mallei, Aden et al. 2005; Burke, Wainwright et al. 2006; Sahara, Takahashi et al. 2006).

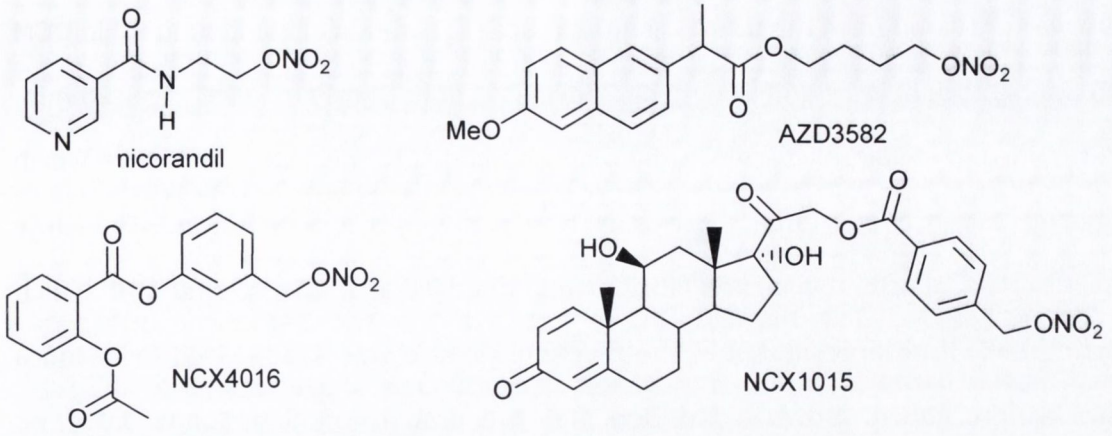
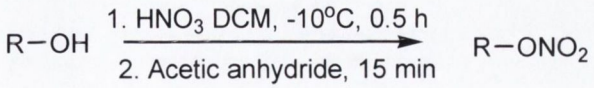


Figure 5.3. *Examples of drug-type nitrates that have been entered clinical trials.*

5.2 Synthesis and evaluation of nitric oxide released gelatinase inhibitors

5.2.1 Synthesis

Nitrate groups are usually synthesized from alcohols or bromides (Fig. 5.4) (Myers and Wright 1948; McCallum and Emmons 1956). The alcohols are modified by addition to a mixture of DCM and fuming nitric acid. In some cases, the resultant nitrate salts precipitate out of the reaction solutions after addition of acetic anhydride. The second general approach is to react the appropriate alkyl bromide with silver nitrate in dry acetonitrile at ambient temperature for 1-3 days. The reaction mixture generally requires purification in this case.



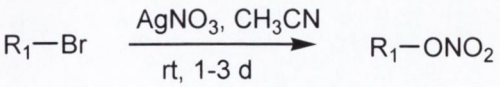
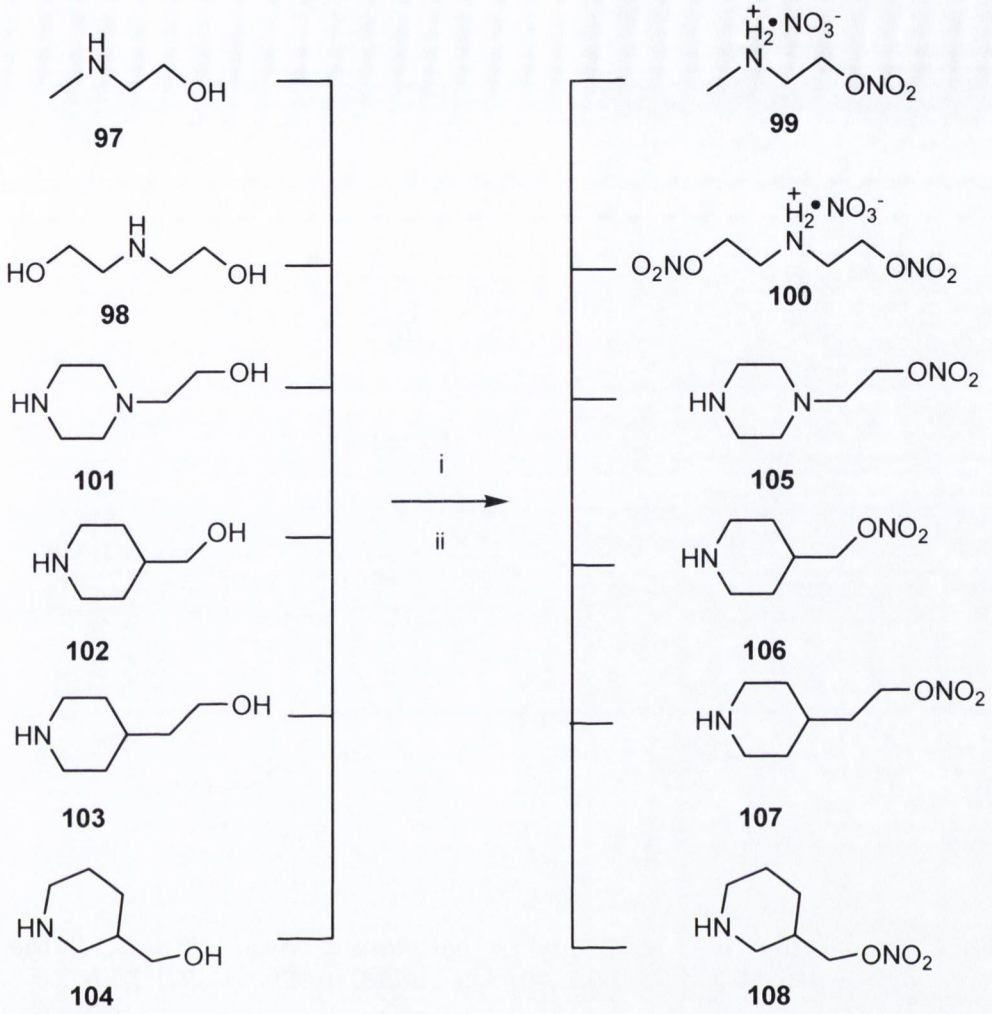


Figure 5.4. *Two common methods for preparation of nitrates.*

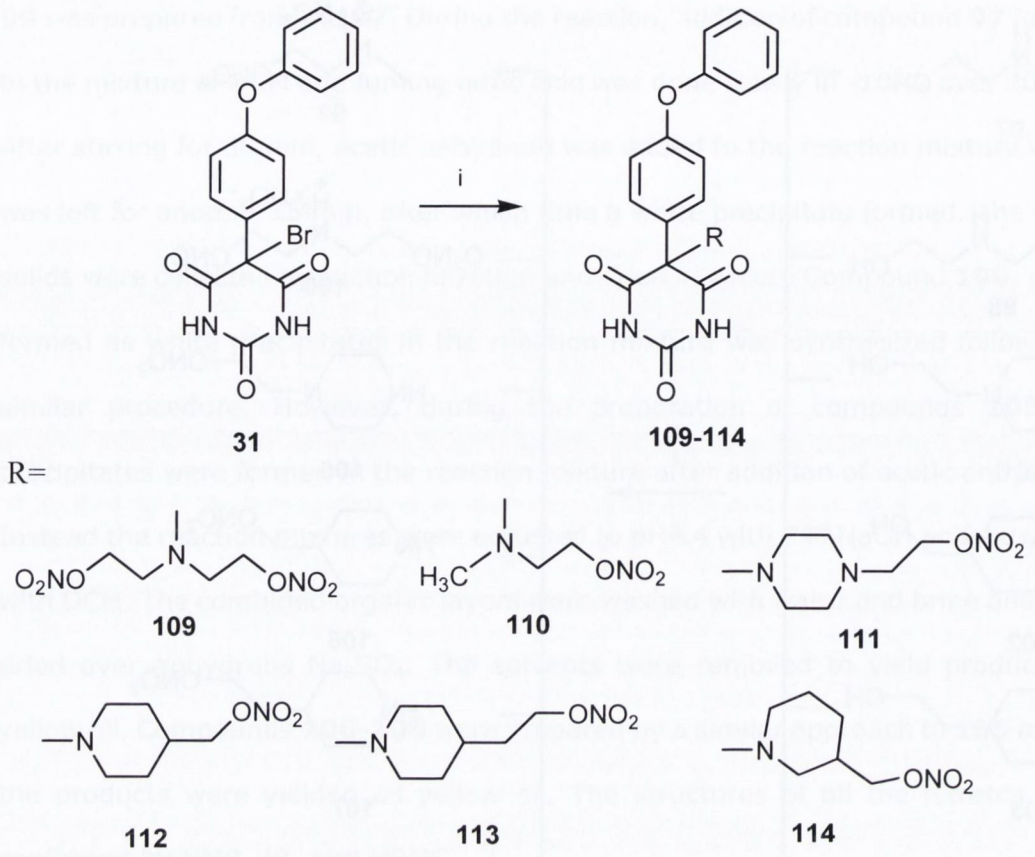
The preparation of the inhibitors in the present study was accomplished by reaction of the appropriate alcohols with fuming nitric acid (Scheme 5.1). Nitrate compound

99 was prepared from the **97**. During the reaction, addition of compound **97** in DCM to the mixture of DCM and fuming nitric acid was done slowly in -10°C, over 20 min. After stirring for 30 min, acetic anhydride was added to the reaction mixture which was left for another 15 min, after which time a white precipitate formed. The white solids were collected by suction filtration and dried *in vacuo*. Compound **100**, which formed as white precipitates in the reaction mixture was synthesized following a similar procedure. However, during the preparation of compounds **105**, no precipitates were formed in the reaction mixture after addition of acetic anhydride. Instead the reaction mixtures were adjusted to pH 14 with 7 M NaOH and extracted with DCM. The combined organic layers were washed with water and brine and then dried over anhydrous Na_2SO_4. The solvents were removed to yield products as yellow oil. Compounds **106-108** were prepared by a similar approach to **105** and all the products were yielded as yellow oil. The structures of all the nitrates were confirmed by NMR, IR, and HRMS.



Scheme 5.1. *Preparation of the nitrate using alcohols. i) DCM, fuming nitric acid, -10°C, 0.5 h. ii) acetic anhydride, 15 min.*

The phenoxyphenyl barbiturate-based nitrates were synthesized from brominated phenoxyphenyl barbiturate (**31**) which was reacted with the prepared nitrates in the presence of triethyl amine and methanol at RT for 24 h (Scheme 5.2). The solvents of the reaction mixture were removed *in vacuo* and residues were purified by flash column chromatography. The structures of the phenoxyphenyl barbiturate-based nitrates were confirmed by IR, NMR and HRMS.



Scheme 5.2. *Preparation of phenoxyphenyl barbiturate-based nitrates. i) the nitrates (compounds* ***99***, ***100***, ***105-108****), triethylamine, methanol, RT, 24 h.*

5.2.2 Gelatinase inhibition of phenoxyphenyl barbiturate-based nitrates

The inhibitory effects of the six phenoxyphenyl barbiturate-based nitrates **109-114** on MMP-2 and MMP-9 were measured using the fluorogenic assay as described in previous Chapters. The compounds were tested at five concentrations (10 μM, 1 μM, 100 nM, 10 nM, and 1 nM) following incubation for 45 min. IC_{50} values were estimated by plotting the logarithm of concentration versus the percentage of inhibition using a Sigmoidal dose-response formula as before. GraphPad Prism® 4 was used to calculate the IC_{50} values and 95% confidence intervals (Fig. 5.5) (Table 5.1).

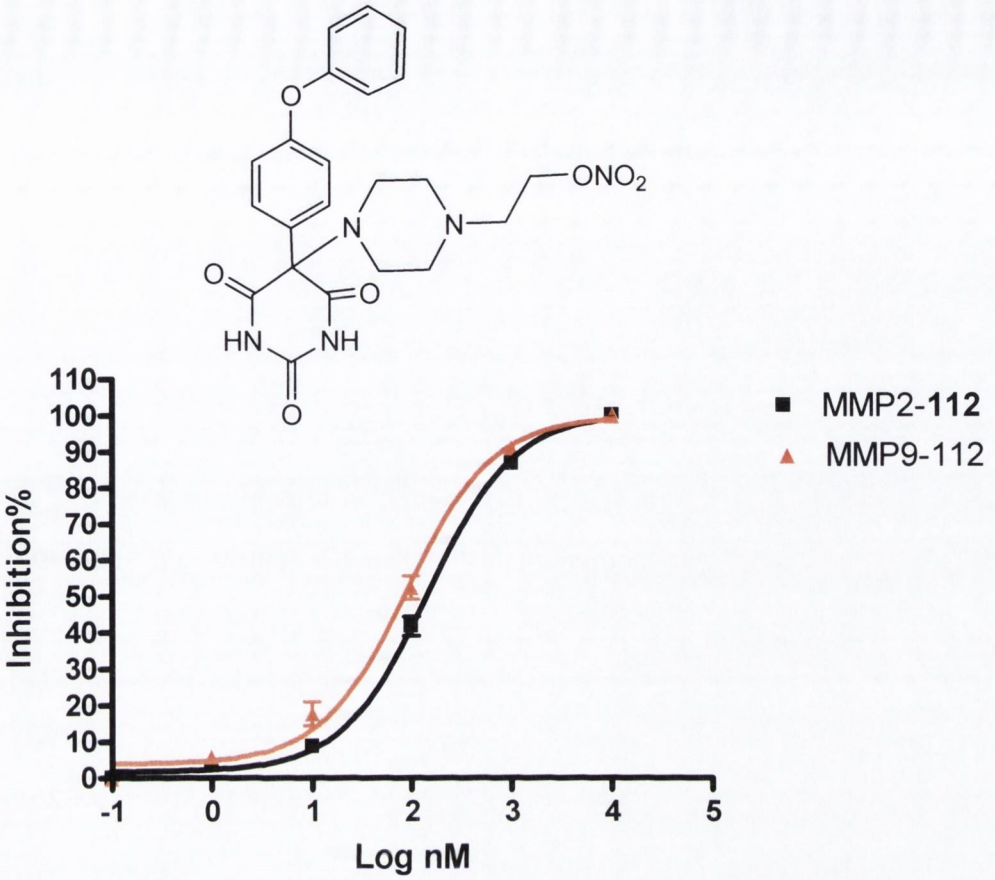
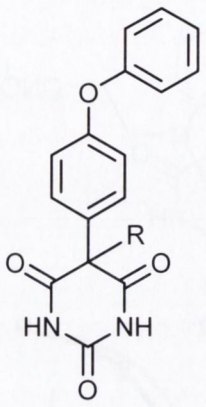
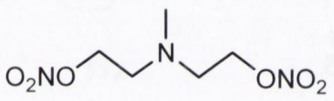
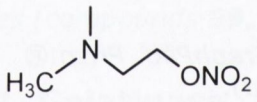
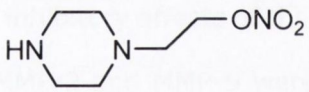
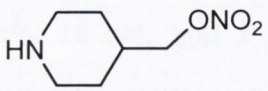
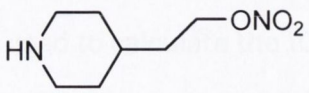
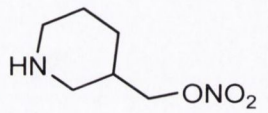


Figure 5.5. *Sigmoid curves for* ***112*** *generated in GraphPad Prism® 4 for calculation of* IC_{50} *values of MMP-2 (black) and MMP-9 (red).*

Table 5.1. *IC_{50} values of phenoxyphenyl barbiturate-based nitrates.*



Structure	Compd No.	MMP-2 (nM)	MMP-9 (nM)	MMP-9 selectivity
R=				
	**109**	328.25 (273.04 – 394.64)	90.72 (62.64 – 131.37)	3.62
	**110**	53.05 (42.98 – 65.49)	47.58 (37.76 to 59.95)	1.11
	**111**	148.67 (129.038 – 171.31)	91.53 (70.84 – 118.27)	1.62
	**112**	157.87 (125.16 – 199.15)	151.72 (119.52 – 192.60)	1.04
	**113**	218.48 (174.02 – 274.30)	212.31 (169.62 – 265.73)	1.80
	**114**	179.44 (154.81 – 207.98)	104.04 (77.39 – 139.86)	1.73

All six phenoxyphenyl barbiturate-based nitrates exhibited good potency for inhibition of MMP-2 and MMP-9. Compound **110** (IC_{50}: MMP-2 = 53.05 nM, MMP-9 = 47.58 nM) was the most potent inhibitor of both MMP-2 and MMP-9 among the six gelatinase nitrate hybrids. Compound **109** (IC_{50}: MMP-2 = 328.25 nM, MMP-9 = 90.72 nM) had the highest IC_{50} values on MMP-2 and compound **113** (IC_{50}: MMP-2 = 218.48 nM, MMP-9 = 212.31 nM) exhibited least potency on MMP-9 and MMP-2. None of the compounds exhibited significant selectivity between MMP-2 and MMP-9, apart from **109** which was over 3-fold selectivity on MMP-9 over MMP-2.

Overall the hybrid compound potencies were in the middle of the potency range of the homopiperazine-based barbiturates described in previous Chapters which had IC_{50} values ranged from low nanomole to micromole. Given the generally similar design and the integration of the phenyloxyphenyl group, it was expected that they would bind in a similar manner (Fig. 5.6). The figures show the results for docking experiments with the barbiturate ring of **109** and **111** bound to the active zinc and their phenoxyphenyl groups inserted into the S1′ pocket. The nitrate groups of the compounds were found directed into the S2′ pocket. Thus, the nitric oxide release function of the barbiturate-based nitrate appears not to affect the binding of phenoxyphenyl and barbiturate ring with MMPs, indeed there is evidence from the modeling that $-ONO_2$ group binds on the protein surface. These findings reinforce the idea that barbiturate-based nitrates could not only act as gelatinase inhibitors by binding to MMP-2 and MMP-9, but scaffolds for hybrid compounds possessing multiple pharmacological actions. Finally it is possible in vivo where nitrate metabolism is rapid that the compounds would act as prodrugs for the alcohol substituted compounds and the inhibitory activity of these should be considered.

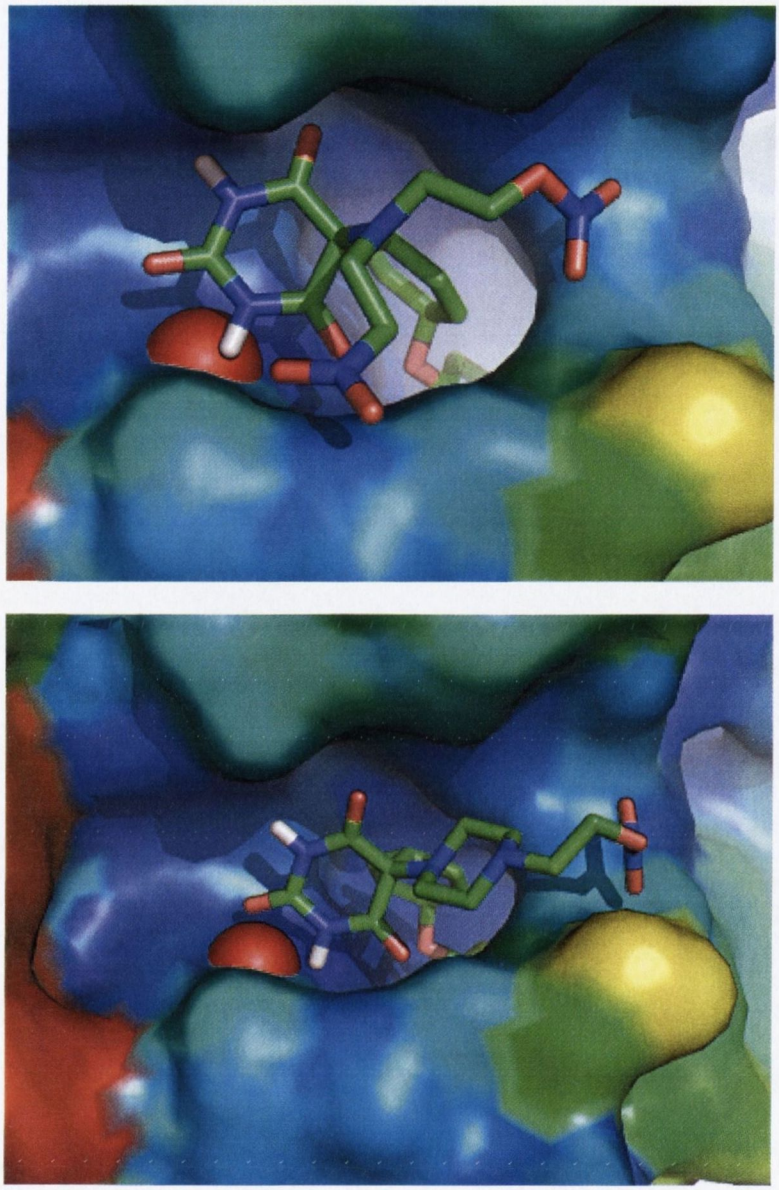


Figure 5.6. *Modelling pictures of* ***109*** *(upper) and* ***111*** *(lower) docking with a 'Connolly' surfaces on MMP-9. The surfaces were generated by the programme PyMOL® based on the crystal structures of MMP-2 (pdb code 1qib) Ligand orientations were used which had the lowest binding energy of the conformations of 50 runs with 25000000 energy evaluations in Autodock4 and displayed by PyMOL®. The active site zincs are shown as the red spheres.*

5.3 Inhibition of cell invasion of nitrates of gelatinase inhibitors

As already described in this thesis, MMPs can promote cancer cell invasion by degradation of various ECM components resulting in release of growth factor and cytokines (Stamenkovic 2003). Inhibition of MMP activity, especially MMP-2 and MMP-9, has the potential to inhibit tumor growth and metastases (Rudek, Venitz et al. 2002). In addition, nitric oxide donors have been report to inhibit cell proliferation and invasion, including pancreatic cancer cells, prostate cancer cells and bladder cancer cells (Wang, Zhang et al. 2007; Sugita, Kaneki et al. 2010). Moreover, as described in previous Chapters, homopiperazine-based barbiturates and related dimers significantly inhibited Caco-2 cell invasion through matrigel membranes. Therefore it was interesting to investigate the effect of the hybrid MMP-inhibitory nitrates on cancer cell invasiveness in vitro.

Because of the cost of the assay, only the most MMP-9 selective nitrate compound (**109**), the most potent nitrates (**110** and **111**) were selected for assessment. The invasion assay was similar to those applied in the assessment of homopiperazine-based barbiturates and dimers. Each insert was seeded with 25,000 Caco-2 cells and medium with 2% FCS. Besides, the positive control inserts contained 75 ng HGF and the sample inserts contained 75 ng HGF and the nitrate inhibitors at 100 nM. All the inserts were incubated in medium with 20% FCS for 48 h, after which time the non-migratory cells on the upper surface of the membranes were removed. The inserts were then treated with the Diff-Quik kit to fix and stain the migrated cells in the bottom of the inserts, which were then counted under a microscope (Fig. 5.7).

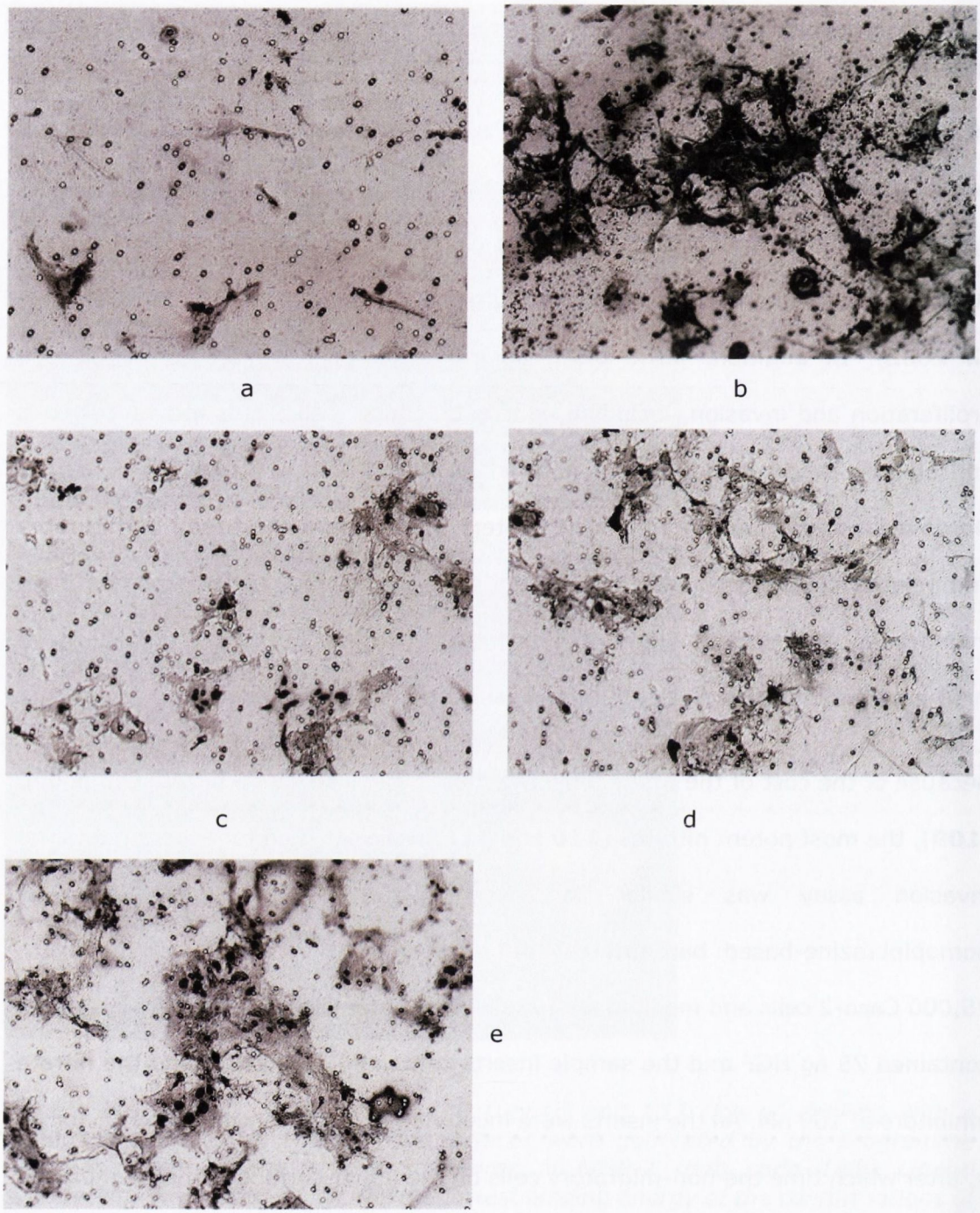


Figure 5.7. *Representative microscope images from invasion assay with selected nitrate hybrids. The pictures were taken from the parts which could mostly represent the whole insert. a) A picture of a negative control insert, incubated with Caco-2 cells only. b) A picture of a positive control insert, incubated with Caco-2 cells and HGF. c) A picture of an insert incubated with Caco-2 cells, HGF, and 100 nM* ***109****. d) A picture of an insert incubated with Caco-2 cells, HGF, and 100 nM* ***110****. e) A picture of an insert incubated with Caco-2 cells, HGF, and 100 nM* ***111****. Cells in the negative control insert were much less than those in the positive control insert, demonstrating the assay was valid. The inserts incubated with 100 nM of the barbiturate-based nitrates (c, d, e,) had significantly less cells than the positive control insert.*

The inserts incubated with **109** had fewer cells than **110** and **111** and significantly less cells than control (Fig. 5.7). The inserts incubated with **111** had the most cells among the three nitrates incubated, indicating the least inhibitory effects of **111** on cell invasion. Therefore, the orders of inhibition of cell invasion for these three barbiturate-based inhibitors from strong to weak were **109**, **110**, and **111**.

The invasion assays were performed in duplicate and repeated three times. The inhibition of cell invasion for each compound was as calculated by the formula 3-1 based on three independent assays. The results of inhibition were are presented in Fig. 5.8 and Table 5.2

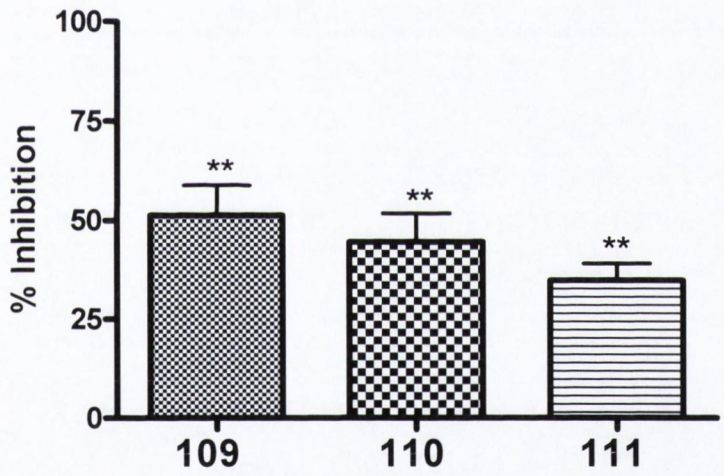
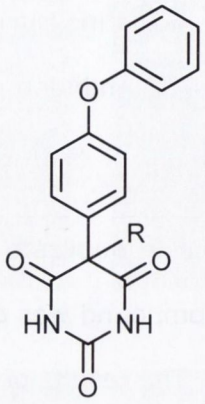
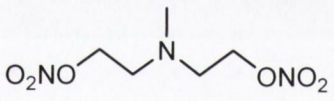
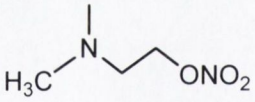
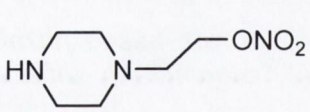


Figure 5.8. *Inhibition of Caco-2 cell invasion of the barbiturate-based nitrates hybrids based on three independent assays at 100 nM (** significantly different from control $P < 0.05$).*

Table 5.2 *The IC_{50} values of three barbiturate-based nitrates (**109**, **110**, and **111**) and their percentage of inhibition of cell invasion.*



Structure	Compd No.	IC_{50} (nM)		Inhibition (%)
		MMP-2	MMP-9	
R =				
	**109**	328.25 (273.04 – 394.64)	90.72 (62.64 – 131.37)	51.38
	**110**	53.05 (42.98 – 65.49)	47.58 (37.76 – 59.95)	44.57
	**111**	148.67 (129.038 – 171.31)	91.53 (70.84 – 118.27)	34.78

Compound **110** (IC_{50}: MMP-2 = 53.05 nM; MMP-9 = 47.58 nM) exhibited better inhibition of MMP-2 and MMP-9 activities than **111** (IC_{50}: MMP-2 = 146.67 nM; MMP-9 = 91.53 nM) consistent with the finding described in the Chapter 4 that percentage of inhibition of cell invasion increases with increased potency towards MMP-9 (Fig 5.9). It is difficult to say with so few compounds if nitric oxide release could have had any effect on the inhibition of cell invasion. Also, the concentrations used were probably too low to generate significant amounts of NO. However, the

extent of inhibition by the three nitrates was greater than that achieved with non nitrate compounds described in Chapters 3 and 4 that had similar IC_{50} values. The role of NO release from the hybrids in potentiating the effect of MMP inhibition on tumour cell invasion needs further work. However, it was overall pleasing to see that the hybrids at least retained the ability to inhibit cancer cell invasion. Since we had conducted a number of assays with the compounds assessing biochemical effects that might be attributable to NO release it was timely to make some evaluation of the compounds' ability to release NO in cellular environment.

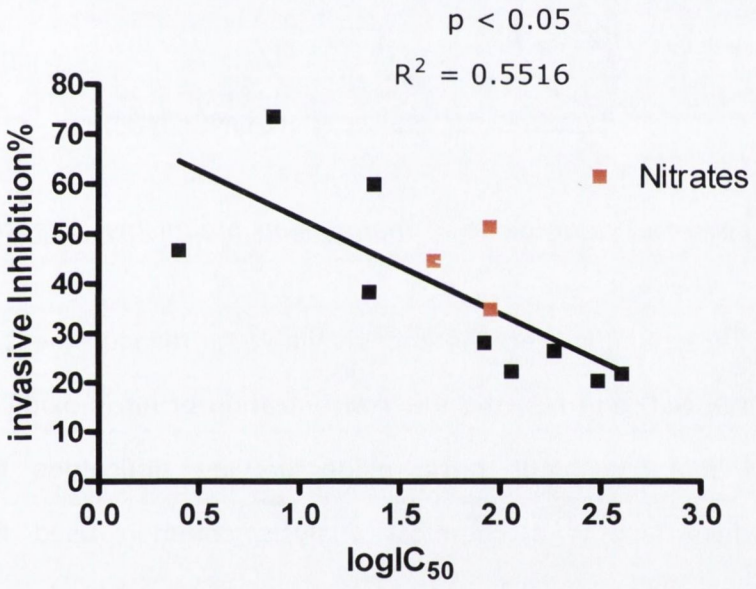


Figure 5.9. *The linearity of MMP-9 IC_{50} values with inhibition of invasion of Caco-2 cells. The nitrate compounds are shown as red squares.*

5.4 Nitric oxide release of the barbiturate-based nitrates

Studies have showed that nitric oxide can be bio-transformed to N-oxides via different metabolic routes in mammals (Fig 5.10) (Kelm 1999). A raised level of nitrite (NO_2^-) and nitrate (NO_3^-) in plasma and urinary indicate that the major metabolites of nitric oxide are nitrite and nitrate (Moncada and Higgs 1993). A high correlation between nitric oxide release and concentrations of nitrates and nitrite in biological samples has been established (Granger, Taintor et al. 1996). We decided

therefore to use nitrite and nitrate in cell suspensions as a marker for NO generation in vitro.

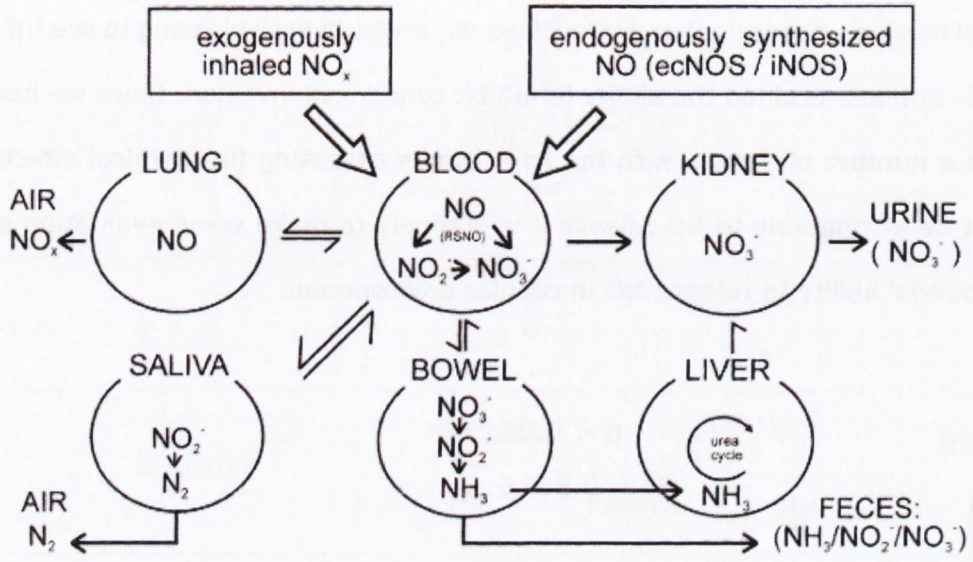


Figure 5.10. *The metabolism of nitric oxide in mammalian organisms (adapted from (Kelm 1999)).*

Although there are many direct and indirect methods available for measurement of nitric oxide including HPLC, GLC and MS, the low concentration of nitric oxide in biological samples and metabolism of nitric oxide provide difficulties for determinations. The Griess test is a chemical analysis common used for determination of nitrites. The Griess reaction is based on the formation of a coloured azo compound by reaction of sulfanilamide (SULF) with bicyclic amines such as *N*-1-(naphthyl)ethylenediamine (NED) under acid conditions (Fig. 5.11) (Miranda, Espey et al. 2001). The absorbance of the azo compound can be measured by UV at 540 nm. Besides nitrite, the level of nitrate can also be analyzed Griess test by treating samples with reducing metals such as cadmium and Cd/Cu complex (Gutman and Hollywood 1992; Marzinzig, Nussler et al. 1997; Miranda, Espey et al. 2001). A recent study reported the use of Vanadium (III) for reducing nitrates was better than the metals due to its short reaction time and less toxicity (Miranda, Espey et al. 2001). In addition, it has been reported that the sensitivity of Griess test would be increased 30% when determination is carried out at 4°C (Guevara,

Iwanejko et al. 1998). Therefore, the analysis of nitrite and nitrate concentration of barbiturate-based nitrate treated Caco-2 cells was performed by the modified Griess test using VCl_3 solution as reductant at 4°C.

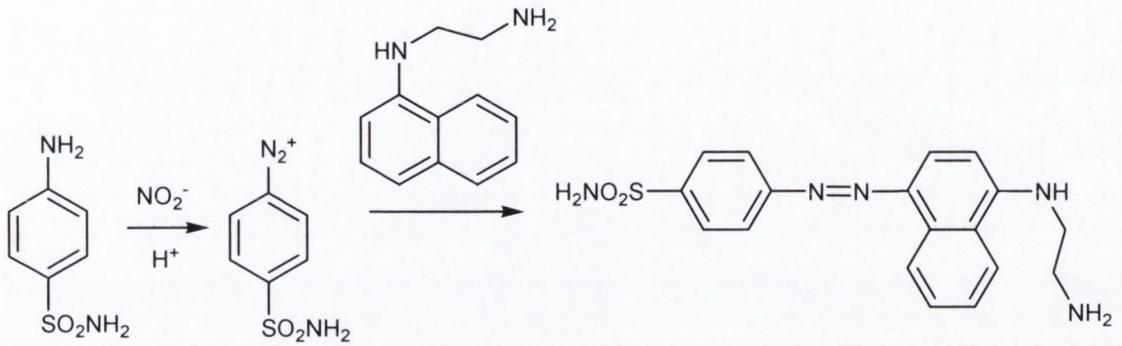


Figure 5.11. *Chemical reactions involved in Griess test for measurement nitrite.*

The nitrite and nitrate levels of these supernatants was measured by the modified Griess assay based on the procedures described by *Mirandan et al.* (Miranda, Espey et al. 2001). Before running samples, a series of nitrite and nitrate standard solutions were prepared by sodium nitrite and sodium nitrate from 3 µM to 200 µM. The standards were treated with VCl_3. The blank wells contained only 400 µl of water. All wells were treated with 100 µl of 4°C SULF and NED. The plate was shaken for 45 min and the absorbance was measured at 540 nm. The relationships between absorbance and the concentrations of nitrate and nitrite were established using the standard solutions (Fig. 5.12).

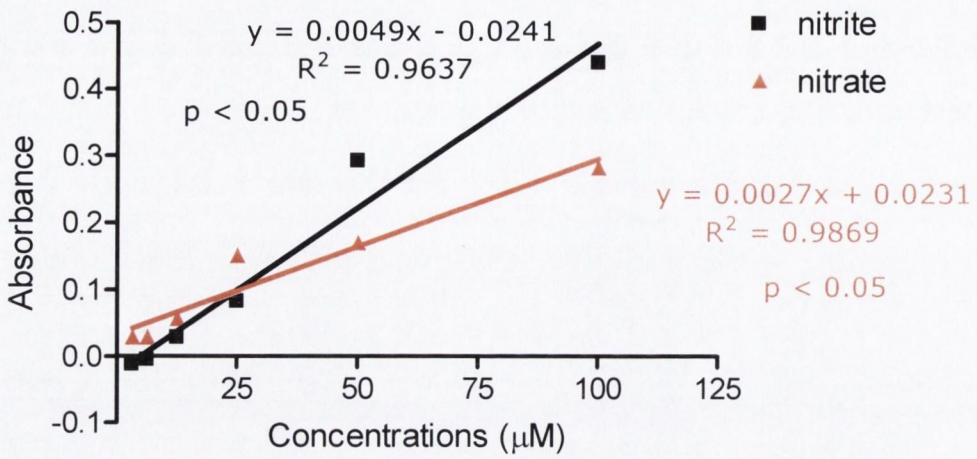


Figure 5.12. *The relationships between absorbance and the concentration of nitrite and nitrates.*

Three groups of samples were prepared. Two groups of samples were supernatants of Caco-2 cells incubated with 10 μM of PMA and 200 μM of the barbiturate-based nitrates for 3 h but with different numbers of cells. One group of samples (group 1) used 60% confluent Caco-2 cells and the second group (group 2) used 80% confluent Caco-2 cells. Another group (group 3) was the supernatants of Caco-2 cells incubated with 200 μM of the barbiturate-based nitrates for 3 h, where 80% confluent cells were used. Blanks consisted of the supernatants of Caco-2 cells treated without the nitrates. Nitrite was determined directly. Separately, VCl_3 was used to reduce nitrate to nitrite. The nitrate value was determined by substracting the initial nitrite value from the total nitrite following VCl_3 reduction. (Table 5.3).

Table 5.3. *Concentration of nitrite and nitrate in the homopiperazine-based nitrates treated Caco-2 cells.*

Comp No.	Group 1 (μM)			Group 2 (μM)			Group 3 (μM)		
	NO_2^-	NO_3^-	NO_x	NO_2^-	NO_3^-	NO_x	NO_2^-	NO_3^-	NO_x
109	18.57	82.55	101.12	24.28	109.42	133.70	15.10	113.78	128.89
110	1.43	30.06	31.49	5.51	63.38	68.89	2.86	44.18	47.04
111	23.47	10.98	34.45	18.98	1.39	20.37	13.68	13.73	27.41
112	2.45	7.93	10.38	5.92	5.19	11.11	1.84	8.53	10.37
113	2.45	2.00	4.45	3.67	-17.01	-13.33	2.45	7.92	10.37
114	3.67	0.78	4.45	1.22	-15.67	-14.44	1.23	4.33	5.56

The results of the Griess tests with the barbiturate-based nitrates showed the concentrations of NO_X of samples in group 2 and 3 were higher than those in group 1, which suggested that the concentrations of NO_2^- and NO_3^- might be influenced by the number of cells. In addition, samples in group 2 and group 3 had similar concentration of NO_x, indicating that concentrations of NO_2^- and NO_3 would not be affected by PMA present in the cells. A significantly high level of NO_3^- was detected in the supernatants of 200 μM **109** and **110** treated Caco-2 cells, suggesting high level of nitric oxide was released from these two compounds. A high concentration of NO_2^- in supernatants containing **111** was also observed. In addition, a reasonable NO_X level was found in **112** treated supernatants. The nitrite and nitrate levels were negligible in the supernatants incubated with compounds **113** and **114**, indicating that little if any nitric oxide was released from these.

In addition, the moiety attached to nitrate group could be another reason. Compounds **113** and **114** had methyl piperidine group linked with the nitrate group that might slow down the release of nitric oxide. Higher levels of nitric oxide released from alkyl attached nitrate compounds (**109** and **110**) would be another support for the hypothesis.

5.5 Nitric oxide and expression of gelatinases

As described in the Chapter 2, PMA treated HT1080 cell line produce MMP-2 and MMP-9. Nitric oxide has been reported to affect the expression of MMs. Therefore, the impact of the barbiturate-based nitrates on expression of gelatinases was investigated using PMA treated HT1080 cells. HT1080 cells were cultured until 75% confluent and split into small flasks. Each flask contained around 1 million HT1080 cells. PMA and the barbiturate nitrates were added to each flask to give 10 μM and 100 μM, except the positive control flask, which only contained 10 μM PMA. The flasks were incubated at 5% CO_2, 37°C for 24 h, after which time the supernatants of the flasks were collected. In order to make sure the same amount of proteins loaded onto the zymography gel, the supernatants were tested in the protein assay to calculate the concentration of proteins. MMP-2 and MMP-9 were in the gels separated by electrophoresis. Then the gel was washed with 2.5% tritone and incubated in zymography buffer for 48 h. The gel was dyed in the staining solution, and washed in the destaining solution, and quantified by the gel reader machine. The MMP-2 and MMP-9 activities of the supernatants were measured by density x area of the bands (Fig. 5.13).

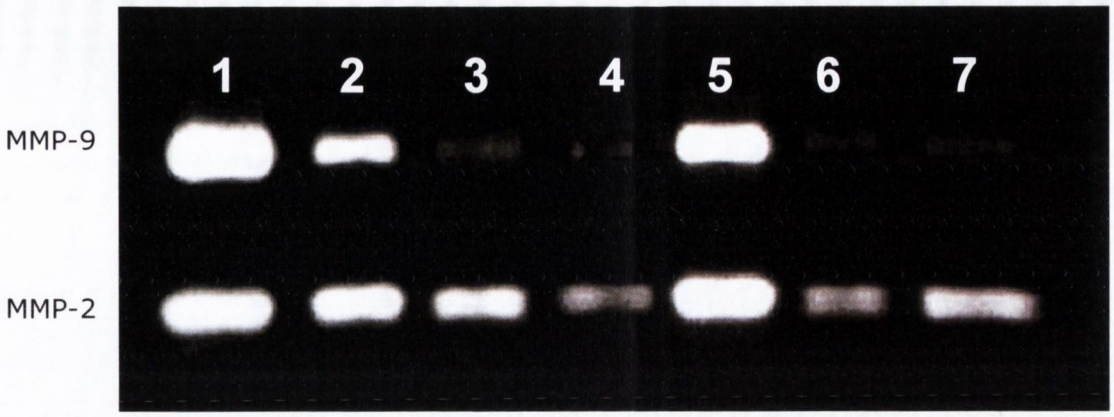


Figure 5.13. *Representative zymograph of PMA and barbiturate-based nitrate treated HT1080 cell supernatants. The two bands in line 1 were activity of MMP-9 and MMP-2 in the supernatant of the positive control flask. The two bands in line 2 to were activity of MMP-9 and MMP-2 in the supernatants of the flasks, which incubated with 10 μM PMA and 200 μM* **109**. *Line 3 was from supernatant incubated with 10 μM PMA and 100 μM* **110**. *Lines 4, 5, 6, and 7 were from supernatants incubated with 10 μM PMA and* **111**, **112**, **113**, *and* **114** *respectively.*

The zymography illustrates that MMP-2 and MMP-9 were highly expressed in PMA (10 μM) treated HT1080 cells. Compounds **109**, **110, 111**, **113** and **114** dramatically inhibited expression of MMP-9, but **112** only slightly inhibited the expression of MMP-9. Inhibition of MMP-2 expression was less dramatic than MMP-9 inhibition. Compounds **110**, **111**, **113** and **114** caused significant inhibition of MMP-2 expression. Compound **109** only marginally reduced MMP-2 expression and **112** caused little or no inhibition of MMP-2 expression.

The assay was repeated two more times and the results of inhibition of MMP-2 and MMP-9 expression for the barbiturate-based nitrates are shown in Fig. 5.14.

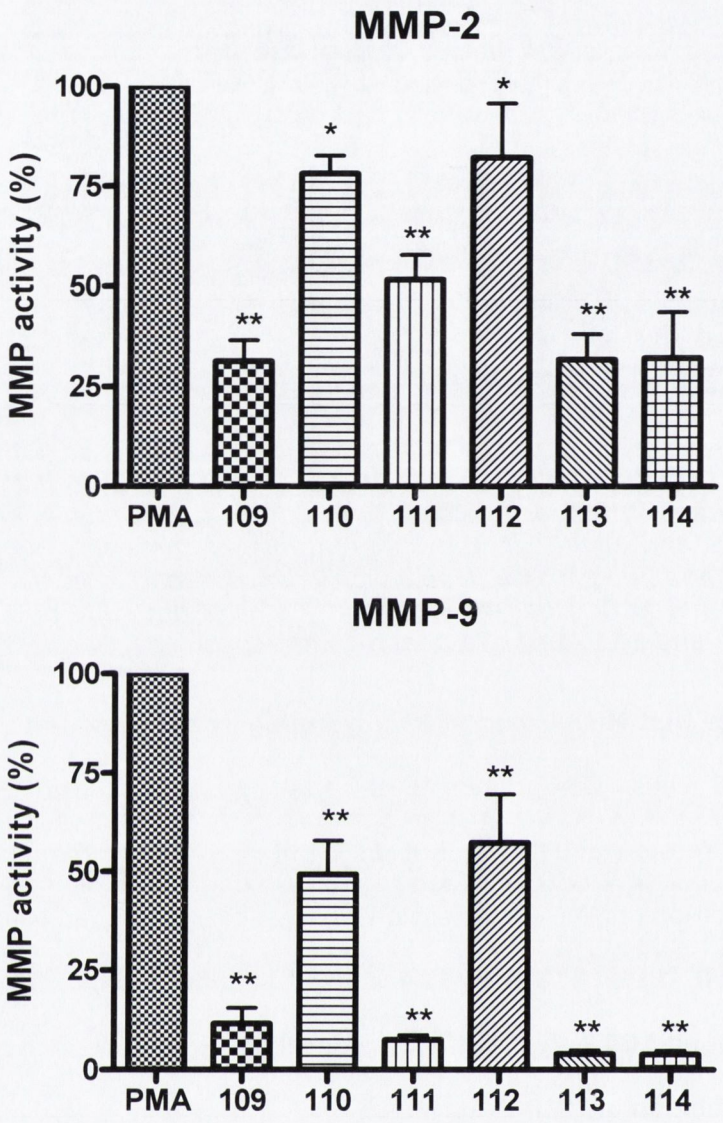


Figure 5.14. *The MMP-2 and MMP-9 activities of supernatants of HT1080 cells treated with PMA and barbiturate-based nitrates (** significantly different from control P < 0.05; * not significantly different from control P > 0.05).*

As shown in Fig. 5.11 HT1080 cells incubated with **109** and **112** retained some MMP-2 activity (78.12% and 82.10% respectively). These compounds also had least effect on MMP-9 secretion. Compound **110**, **111**, **113**, and **114** caused marked suppression of both gelatinases.

The reduced activities of MMP-2 and MMP-9 shown in the zymography results were believed to be related to the *expression* of two proteins in the PMA and the nitrate treated HT1080 cells rather than inhibition by the barbiturates because we felt that

the zymography process would lead to washout of the inhibitors. In order to validate this we repeated the experiments with phenanthroline, a non-specific MMP inhibitor. This was mixed with recombinant MMP-2 and MMP-9 at in the range 100 nM-100 μM). The mixtures were incubated at 37°C for 45 min and loaded onto the zymography gels. Meantime, a positive control containing the same amount of recombinant MMP-2 and MMP-9 as the phenanthroline mixtures was also loaded onto the gels. After electrophoresis, the gels were washed in and incubated to allow gelatine digestion for 48 h. Then the gel was stained for analysis (Fig. 5.15). There was no difference between the controls and phenathroline treated bands supporting the idea that electrophoresis causes the inhibitor to dissociate from the enzyme, and therefore proving that residual enzyme activity under these conditions can be considered an index of the cellular secretion of the two enzymes.

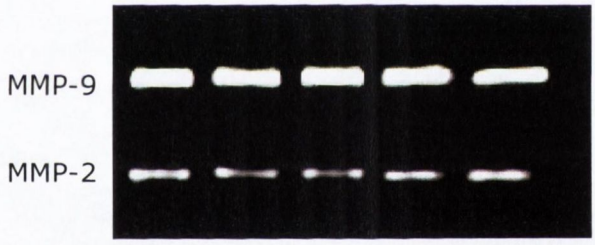


Figure 5.15. *Representative zymography of a phenanthroline loaded gel. The first column was the positive control bands, which only recombinant MMP-2 and MMP-9 were loaded. The remaining columns were loaded with recombinant MMP-2 and MMP-2 and different concentrations of phenanthroline, which 100 μM, 10 μM, 1 μM and 100 nM from the second to the fifth c*olumn in order.

Inhibition of MMP-2 and MMP-9 activities shown in the zymography of the barbiturate-based nitrates treated supernatants was caused by reduced secretion/activation of MMP-2 and MMP-9 and/or the pro-forms in the culture. Therefore, the gelatinase inhibitors with the nitric oxide release group could significantly inhibit expression of MMP-2 and MMP-9 in PMA treated HT1080 cells. In addition, these nitrates of gelatinase inhibitors had greater inhibition on expression of MMP-9 than MMP-2. Another possible explanation for the reduced MMP secretion observed in the nitrate treated suspensions was that the compounds were killing the cells. The effect of the nitrates on cell viability was assessed next.

5.6 Cytotoxicity of the barbiturate-based nitrates.

MTT assay is a standard colorimetric assay of cell viability which involves the use of the agent MTT (3(4,5-dimethylthiazol-2-yl)-2,5-dipenyltetrazolium) bromide). The assay is widely utilized to estimate cellular viability in determination of cytotoxicity of potential drugs. The principle behind the assay is that mitochondrial enzymes in cells reduce MTT, resulting in the formation of formazan crystals leading to an abrupt colour change from the pale yellow MTT to the purple formazan (Fig. 5.16) (Mosmann 1983). The absorbance of the purple solution can be quantified at 590 nm.

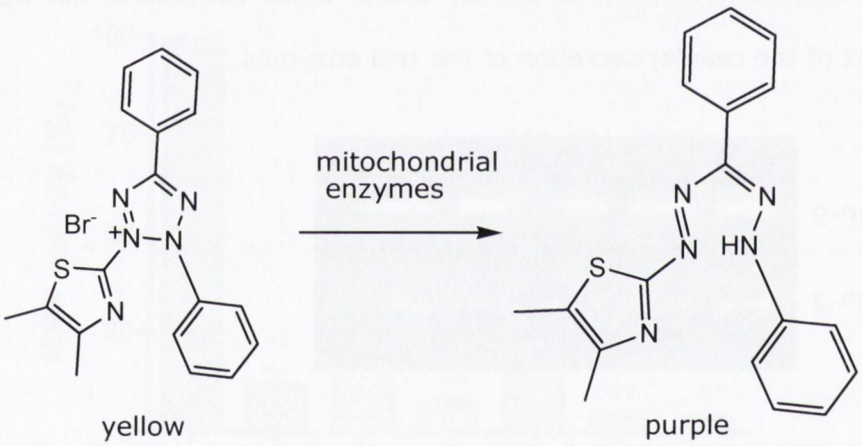


Figure 5.16. *Enzymatic cleavage of MTT by mitochondrial enzymes.*

Two cell lines (HT1080 and Caco-2) were used to evaluate cytotoxicity of the barbiturate-based nitrates. Cells were plated at a concentration of 8 x 10^4 cells/ml (HT1080) or 1.2 x 10^5 cells/ml (Caco-2) in 100 µl and incubated until 75% confluent. The medium was removed and serum free medium added. The cells were treated with 1 µl of the barbiturate-based nitrates in DMSO at various concentrations. Vehicle control wells were treated with 1 µl DMSO and the blank wells contained only medium. The plates were incubated at 37°C for 1 h and 24 h. MTT solution was added and the samples were incubated for another 3 h. The medium was gently aspirated from the wells and 100 µl of DMSO was added to each well to lyse the cells

and dissolve the purple formazan crystals in the mitchondria living cells. The plates were shaken and read at 590 nm. The blank, vehicle control, and samples were performed in triplicate. Cell survival rates were calculated by the formula 5-1 based on three independent assays. The results of survived HT1080 and Caco-2 cells incubated with the barbiturate-based nitrate for in 1 h and 24 h are shown in Fig. 5.17 and Fig. 5.18.

$$\% \text{ Cell survival} = \frac{(A_s - A_b)}{(A_v - A_b)} \times 100 \qquad 5\text{-}1$$

Where A_s is the absorbance of the barbiturate nitrates treated cells, A_b is the absorbance of medium plus MTT, A_v is the absorbance of vehicle control treated cells.

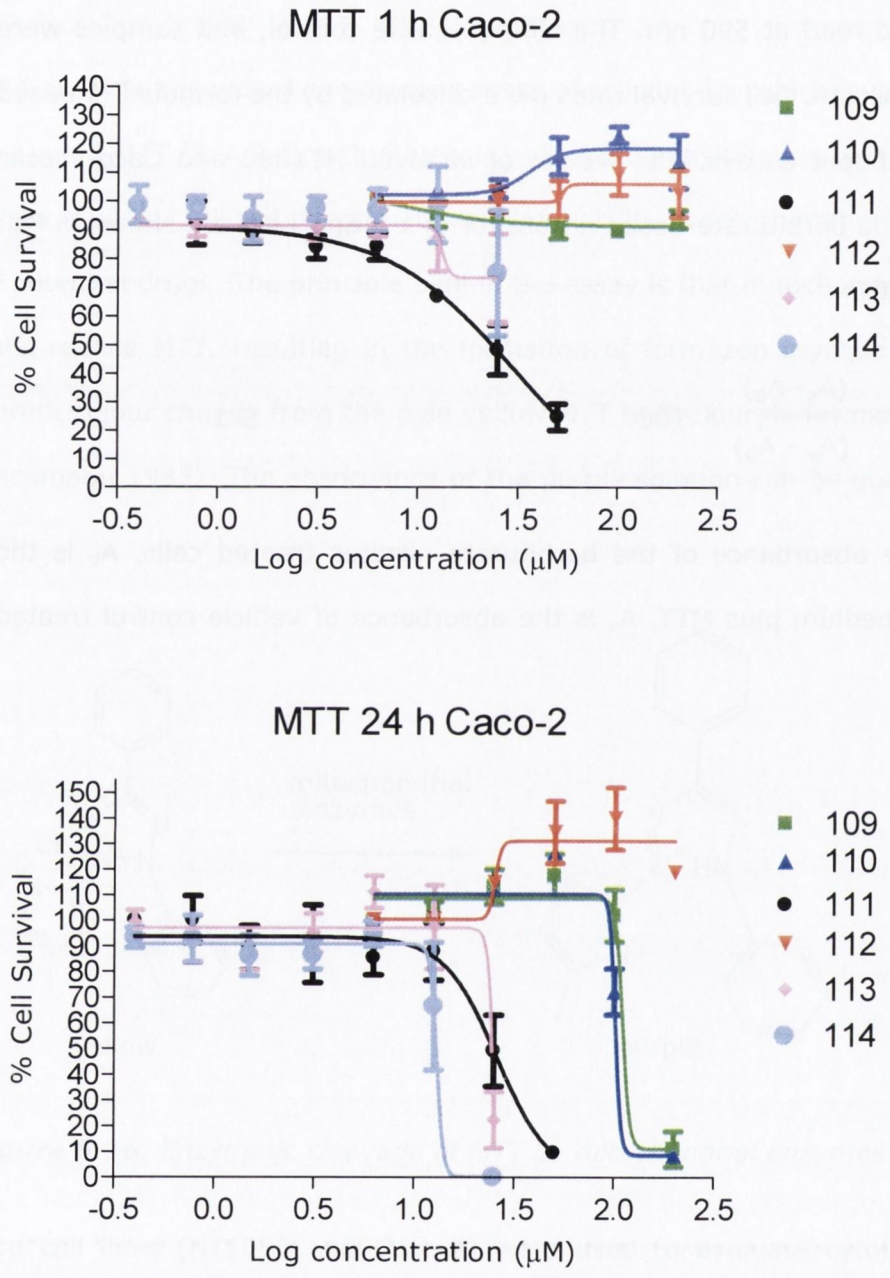


Figure 5.17. *Caco-2 cell survival incubated with relative to Log Concentration in the presence of the barbiturate-based nitrates for 1 and 24 h*

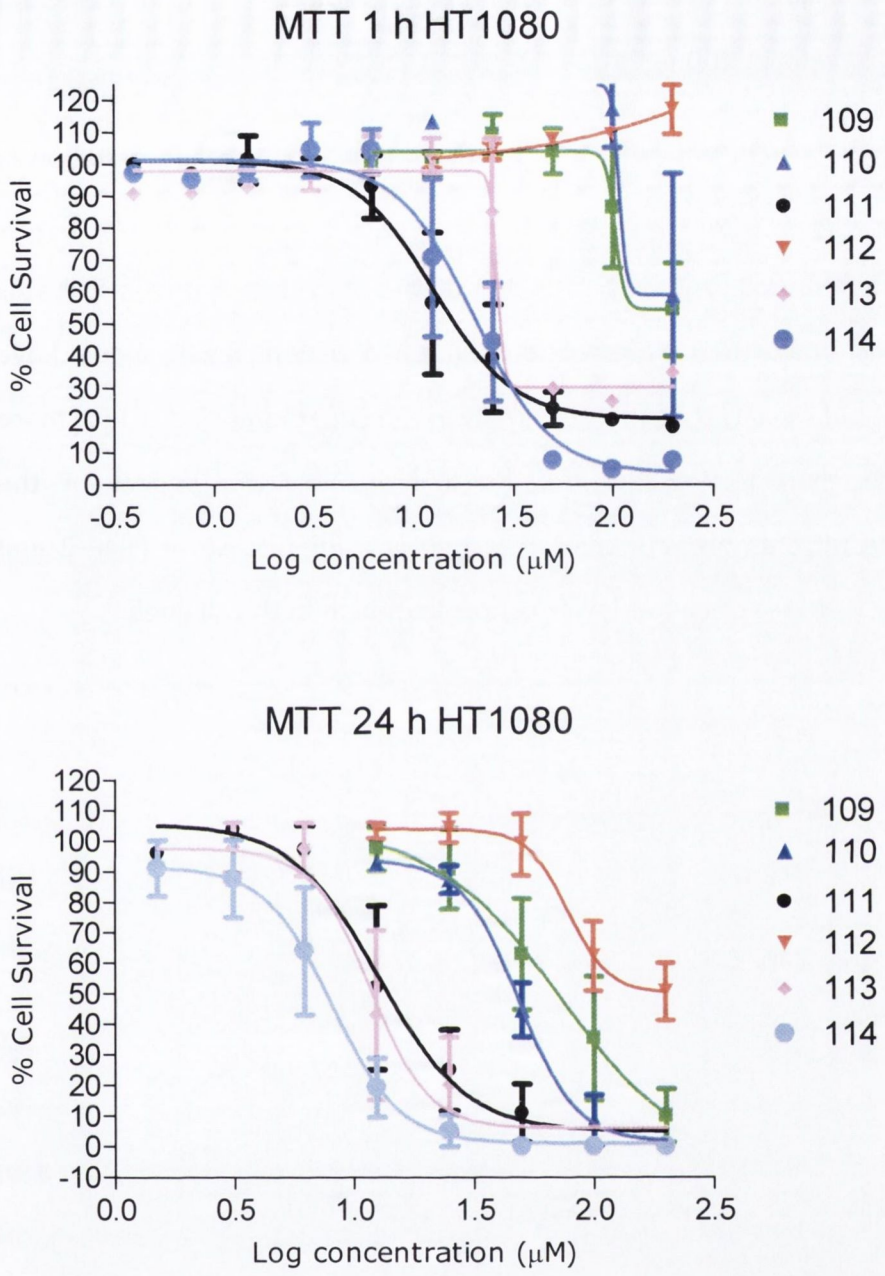


Figure 5.18. *HT1080 cell survival incubated with relative to Log Concentration in the presence of the barbiturate-based nitrates for 1 and 24 h.*

The HT1080 cells were generally more vulnerable than the Caco-2 cells. Caco-2 cell viability decreased in an abrupt manner for compounds **109**, **110**, **113**, and **114**. The threshold concentration of compounds **113** and **114** were around 10 μM for Caco-2 cells. In addition, Caco-2 cell viability was unaffected by the present of 200 μM **112** at 24 h. **109**-**111** were in general less toxic than the other comounds.

Compound **112** was the least toxic nitrate in HT1080, with no cells in the first hour and less than 50% cells in 200 μM at 24 h.

From the MTT assay of HT1080 cells, it was difficult to judge whether inhibition of MMP-2 and MMP-9 expression observed previously was due to cytocidal activity or biochemical modulation of synthesis/secretion of the enzymes. Notably, if it was merely a cytotoxic effect, then the reduction in the two enzyme levels should have been similar; instead we saw that MMP-9 activity in the supernatant was much more strongly affected than MMP-2 activity. As a first step the impact of the barbiturate-based nitrates on PMA treated cell culture for release of MMP-2 and MMP-9 should be further studied at lower concentration in both cell lines.

5.7 Conclusion

Nitric oxide is an important messenger involved in many biological processes in both normal and pathological conditions. Extensive studies have been carried out on the impact of nitric oxide in disease especially cardiovascular diseases and cancer sometimes showing positive effects (Bonavida, Baritaki et al. 2008; Coulter, McCarthy et al. 2008; Ying, kaestle et al. 2009; Nossaman, Nossaman et al. 2010). In addition, nitric oxide has been reported to affect the expression of MMPs (Zhang, Wang et al. 2004).

Incorporation of nitric oxide releasing groups into new drug types has been intensively pursued over the past decade with a view to introducing complementary pharmacological activity, amplifying activity or decreasing side effects. Several novel nitrate-gelatinase inhibitors were prepared based on the structure of phenoxyphenyl substituted scaffold with the nitrate group introduced at P2′. The strategy was vindicated because all of the compounds had some intrinsic ability to inhibit gelatinase activity of the recombinant enzymes.

The nitrate hybrids inhibited Caco-2 cell invasion at least as well as expected with some suggestion of a contribution from nitric oxide release. This requires further work for confirmation comparing directly nitrate and non-nitrate analogs with similar potency. The ability of the barbiturate-based nitrates to release nitric oxide in Caco-2 cells was determined by incubation of Caco-2 cells with the nitrates using the Griess method. There was ample evidence of nitric oxide metabolites. The results suggested that the longer alkyl chain attached nitrates might release nitric oxide more readily.

In PMA treated cell suspensions, MMP-inhibitory nitrates **110**, **111**, **113**, and **114** significantly depressed the production/secretion of MMP-2 and MMP-9, the latter more markedly than the former. The effect of the compounds on cell viability was assessed using two colonic cancer cell lines, CACO-2 and HT1080. In general, the

Caco-2 cell line showed better viability than HT1080 cells. The compounds induced substantial amounts of cell death at 24 h except in the case of **112**. Compound **110** may have ideal characteristics as a hybrid in producing substantial amounts of nitrate/nitrite, exhibiting low toxicity and yet profound inhibition of MMP-9 secretion. The effects of the compounds on cell invasion and on MMP expression as measured by zymography need to be viewed in light of this. However, the compounds were designed as anti-cancer candidates and induction of cell toxicity might be seen as advantageous in this context or even related to the other pharmacological modalities of MMP inhibition and NO-release. These interesting compounds merit further work exploring the interplay of these factors.

Chapter 6

Experimental

6.1 Chemistry

6.1.1 General methods

All chemicals were purchased from Sigma-Aldrich (Ireland), except where stated. All the reactions were monitored using TLC. Uncorrected melting points were measured on a Stuart Apparatus. Infra-red (IR) spectra were performed on a Perkin Elmer FT-IR Paragon 1000 spectrometer. ^{1}H and ^{13}C nuclear magnetic resonance (NMR) spectra were recorded at 27°C on a Brucker DPX 400 spectrometer (400.13MHz, ^{1}H; 100.61MHz, ^{13}C). Coupling constants are reported in Hertz. For ^{1}H-NMR assignments, chemical shifts are reported: shift value (number of protons, description of absorption, coupling constant(s) where applicable). Electrospray ionisation mass spectrometry (ESI-MS) was performed in the positive ion mode on a liquid chromatography time-of-flight mass spectrometer (Micromass LCT, Waters Ltd., Manchester, UK). The samples were introduced into the ion source by an LC system (Waters Alliance 2795, Waters Corporation, USA) in acetonitrile:water (60:40% v/v) at 200 µL/min. The capillary voltage of the mass spectrometer was at 3 kV. The sample cone (de-clustering) voltage was set at 40 V. For exact mass determination, the instrument was externally calibrated for the mass range m/z 100 to m/z 1000. A lock (reference) mass (m/z 556.2771) was used. Mass measurement accuracies of $<\pm 5$ ppm were obtained. Compound purity/homogeneity was confirmed using a combination of NMR, TLC and HPLC.

6.1.2 Synthesis

Dimethyl 2-phenylmalonate (2)

A suspension of NaH (60% suspension in paraffin oil (paraffin oil was removed by repeated washings with hexane)) (80 mg, 20 mmol) and dimethyl carbonate (5.4 ml, 64 mmol) in 64 ml dry THF was heated to 100°C, and a solution of methyl 2-phenylacetate (1.50 g, 10 mmol) in 20 ml THF was added dropwise over a period of 1 h. After being refluxed for 5 h, the mixture was poured onto ice water and

extracted with methylene chloride (50 ml×3). The combined organic layers were washed with water and brine, dried (Na_2SO_4), and concentrated. The crude products were purified by flash column chromatography using hexane and ethyl acetate to yield the pure compounds (1.82 g, 87.5%) as off-white solids. mp: 47–49°C. MS: Calculated for $C_{11}H_{12}O_4Na$ = 231.0633 , found $(M+Na)^+$ = 231.0628. ^1H NMR ($CDCl_3$) δ ppm: 3.78 (s, 6H, CH_3), 4.68 (s, 1H, CH), 7.36–7.44 (m, 5H, Ar-H). ^{13}C NMR ($CDCl_3$) δ ppm: 52.5; 57.2; 128.0; 128.3; 128.9; 132.2; 168.2. IR (KBr): v (cm-1): 2957, 1749, 1730.

5-phenylpyrimidine-2,4,6(1H,3H,5H,)-trione (3)

Sodium (460 mg, 20 mmol) was dissolved in 60 ml ethanol (HPLC grade), and urea (1.02 g, 17 mmol) was added to this solution. A solution of dimethyl 2-phenylmalonate (**2**) (2.08 g, 10 mmol) in ethanol was added dropwise, and the reaction mixture was heated to reflux for 7 h. After being cooled to ambient temperature, the mixture was poured onto ice water and adjusted to pH 2, using dilute hydrochloric acid. The precipitate was collected by suction filtration and dried *in vacuo* to afford the off-white solids (1.47 g, 72.0%). mp: 249–252°C. MS: Calculated for $C_{10}H_8N_2O_3Na$ = 227.0433. $(M+Na)^+$ = 227.0462 found. ^1H NMR (DMSO) δ ppm: 4.82 (s, 1H, CH), 7.26–7.37 (m, 5H, Ar-H), 10.78 (s, 2H, NH). ^{13}C NMR (DMSO) δ ppm: 55.1; 127.8; 129.3; 134.5; 151.0; 169.3. IR (KBr): v (cm-1): 3054, 1699, 1627.

5-bromo-5-phenylpyrimidine-2,4,6(1H,3H,5H,)-trione (4)

A suspension of 5-phenylpyrimidine-2,4,6(1H,3H,5H,)-trione (817 mg, 4 mmol) in 20 ml water was cooled to 0-5°C, and a mixture of 48% HBr (764 μl, 7.1 mmol) and bromine (328 μl, 6.4 mmol) was added dropwise. After stirring for 4-5h at 0-10 °C the precipitate was collected by filtration and dried *in vacuo* to afford the

off-white solids (997 mg, 88.0%). mp: 212-215°C. ^{1}H NMR (DMSO) δ ppm: 7.37–7.43 (m, 5H, Ar-H), 11.57 (s, 2H, NH). ^{13}C NMR (DMSO) δ ppm: 76.1; 125.0; 128.8; 128.9; 138.3; 150.0; 170.9. IR (KBr): v (cm^{-1}): 3055, 1768, 1740, 1687.

5-(4-cyclohexylpiperazin-1-yl)-5-phenylpyrimidine-2,4,6(1H,3H,5H,)-trione (5)

A solution of 5-bromo-5-phenylpyrimidine-2,4,6(1*H*,3*H*,5*H*,)-trione (283 mg, 1.0 mmol) in methanol (5 ml) was treated with 1-cyclohexylpiperazine (336.6 mg, 2 mmol) and stirred for 24 h at ambient temperature. The precipitate was collected by filtration and dried *in vacuo* to afford the off-white solids (227 mg, 61.3%). mp: 226–230°C (decomposition) MS: Calculated for $C_{20}H_{27}N_4O_3$ = 371.2083. $(M+H)^+$ = 371.2087 found. ^{1}H NMR (DMSO) δ ppm: 1.02-1.08 (m, 1H, CH_2), 1.14–1.31 (m, 4H, CH_2), 1.54–1.57 (m, 1H, CH_2), 1.74–1.78 (m, 2H, CH_2), 1.94–1.96 (m, 4H, CH_2), 2.61-2.98 (m, 9H), 7.40-7.47 (m, 5H, Ar-H), 11.73 (s, 2H, NH). ^{13}C NMR (DMSO) δ ppm: 24.5; 24.7; 26.4; 45.1; 48.9; 64.0; 74.5; 126.1; 127.4; 129.2; 129.6; 134.7; 149.4; 169.8. IR (KBr): v (cm^{-1}): 3054, 2936, 1737, 1710, 1687, 1615.

5-(4-isopropylpiperazin-1-yl)-5-phenylpyrimidine-2,4,6(1H,3H,5H,)-trione (6)

A solution of 5-bromo-5-phenylpyrimidine-2,4,6(1*H*,3*H*,5*H*,)-trione (283 mg, 1.0 mmol) in methanol (5 ml) was treated with 1-isopropylpiperazine (256.5 mg, 2 mmol) and stirred for 24 h at ambient temperature. The reaction mixture was dried and purified by flash column chromatography to yield the pure compounds (176 mg, 53.3%) as off-white solids. mp: 237–240°C. MS: Calculated for $C_{17}H_{23}N_4O_3$ = 331.1770. $(M+H)^+$ = 331.1774 found. ^{1}H NMR (DMSO) δ ppm: 1.04–1.06 (d, *J* = 6.02, 6H, CH_3), 2.69 (s, 8H, CH_2), 2.85–2.93(m, 1H, CH),

7.39–7.43 (m, 5H, Ar-H), 11.58 (s, 2H, NH). ^{13}C NMR (DMSO) δ ppm: 17.6; 46.7; 48.6; 54.7; 74.5; 127.7; 128.9; 129.2; 135.1; 149.5; 169.9. IR (KBr): ν (cm^{-1}): 3061, 1736, 1708, 1610.

5-(4-(cyclopropylmethyl)piperazin-1-yl)-5-phenylpyrimidine-2,4,6 (1H,3H,5H,)-trione (7)

A solution of 5-bromo-5-phenylpyrimidine-2,4,6(1*H*,3*H*,5*H*,)-trione (283 mg, 1.0 mmol) in methanol (5 ml) was treated with 1-isopropylmethylpiperazine (280.5 mg, 2 mmol) and stirred for 24 h at ambient temperature. The reaction mixture was dried and purified by flash column chromatography to yield the pure compounds (172 mg, 50.2%) as off-white solids. mp: 211–215°C. MS: Calculated for $C_{18}H_{23}N_4O_3$ = 343.1770. $(M+H)^+$ = 343.1763 found. ^{1}H NMR (DMSO) δ ppm: 0.20–0.23 (m, 2H, CH_2), 0.50–0.55 (m, 2H, CH_2), 0.87–0.97 (m, 1H, CH), 2.59 (s, broad, 2H, CH_2), 2.76–2.84 (m, 8H, CH_2), 7.40–7.47 (m, 5H, Ar-H), 11.63 (s, 2H, NH). ^{13}C NMR (DMSO) δ ppm: 3.9; 46.0; 48.6; 52.4; 61.4; 74.6; 127.6; 129.0; 129.4; 135.0; 149.4; 169.9. IR (KBr): ν (cm^{-1}): 3061, 1752, 1740, 1699, 1601.

5-(4-(cyclopropylcarbonyl)piperazin-1-yl)-5-phenylpyrimidine-2,4,6 (1H,3H,5H,)-trione (8)

A solution of 5-bromo-5-phenylpyrimidine-2,4,6(1*H*,3*H*,5*H*,)-trione (283 mg, 1.0 mmol) in methanol (5 ml) was treated with 1-cyclopropylcarbonyl piperazine (308.4 mg, 2 mmol) and stirred for 24h at ambient temperature. The reaction mixture was dried and purified by flash column chromatography to yield the pure compounds (182 mg, 51.1%) as off-white solids. mp: 155–157°C. MS: Calculated for $C_{18}H_{20}N_4O_4Na$ = 379.1382. $(M+Na)^+$ = 379.1389 found. ^{1}H NMR (DMSO) δ ppm: 0.65–0.74 (m, 4H, CH_2), 1.89–1.96 (m, 1H, CH), 2.55–2.63 (m, 4H, CH_2), 3.45 (s, broad, 2H, CH_2), 3.65 (s, broad, 2H, CH_2), 7.42–7.46 (m, 5H, Ar-H), 11.67 (s, 2H, NH). ^{13}C NMR (DMSO) δ ppm: 7.0; 10.1; 42.3; 45.7; 47.7; 48.3;

74.8; 127.7; 129.0; 129.3; 135.0; 149.4; 170.0; 170.9. IR (KBr): v (cm^{-1}): 3066, 1754, 1734, 1705, 1609.

5-(4-methyl-1,4-diazepan-1-yl)-5-phenylpyrimidine-2,4,6(1H,3H,5H,)-trione (9)

A solution of 5-bromo-5-phenylpyrimidine-2,4,6(1*H*,3*H*,5*H*,)-trione (283 mg, 1.0 mmol) in methanol (5 ml) was treated with 1-methyl-1,4-diazepane (228.4 mg, 2 mmol) and stirred for 24 h at ambient temperature. The reaction mixture was dried and purified by flash column chromatography to yield the pure compounds (180 mg, 56.9%) as off-white solids. mp: 241–244°C. MS: Calculated for $C_{16}H_{21}N_4O_3$ = 317.1614. $(M+H)^+$ = 317.1606 found. ^1H NMR (DMSO) δ ppm: 1.87–1.92 (m, 4H, CH_2), 2.56 (s, 3H, CH_3), 3.01–3.07 (m, 4H, CH_2), 3.17–3.22 (m, 4H, CH_2), 7.13–7.16 (m, 3H, Ar-H), 7.65 (s, broad, 2H, Ar-H), 9.56 (s, 2H, NH). ^{13}C NMR (DMSO) δ ppm:21.6; 41.3;44.0; 48.6; 51.8; 55.2; 87.8; 122.6; 126.4; 129.9; 137.8; 151.5; 164.1. IR (KBr): v (cm^{-1}): 3054, 1734, 1680, 1583.

5-(4-2(-2-hydroxyethoxy)ethyl)piperazin-1-yl)-5-phenylpyrimidine-2,4,6(1H,3H,5H,)-trione (10)

A solution of 5-bromo-5-phenylpyrimidine-2,4,6(1*H*,3*H*,5*H*,)-trione (283 mg, 1.0 mmol) in methanol (5 ml) was treated with 1-2(-2-hydroxyethoxy)ethyl)piperazine (348.5 mg, 2 mmol) and stirred for 24 h at ambient temperature. The precipitate was collected by filtration and dried *in vacuo* to afford the off-white solids (234 mg, 62.6%). mp: 230–234°C. MS: Calculated for $C_{18}H_{25}N_4O_5$ = 377.1825. $(M+H)^+$ = 377.1815 found. ^1H NMR (DMSO) δ ppm: 2.41–2.46 (m, 4H, CH_2), 2.49–2.51 (t, *J* = 1.75, 2H, CH_2), 2.55–2.58 (m, 4H, CH_2), 3.36–3.39 (t, *J* = 5.27, 2H, CH_2), 3.44–3.48 (m, 4H, CH_2), 7.37–7.42 (m, 5H, Ar-H), 11.57 (s, 2H, NH). ^{13}C NMR (DMSO) δ ppm: 47.4; 53.8;

57.2; 60.2; 68.1; 72.2; 74.5; 127.8; 128.7; 129.0; 135.3; 149.5; 170.0. IR (KBr): v (cm^{-1}): 3245, 2836, 1733, 1666, 1605.

5-(4-((tetrahydrofuran-2-yl)methyl)piperazin-1-yl)-5-phenylpyrimidine-2,4,6(1H,3H,5H,)-trione (11)

A solution of 5-bromo-5-phenylpyrimidine-2,4,6(1*H*,3*H*,5*H*,)-trione (283 mg, 1.0 mmol) in methanol (5 ml) was treated with 1-((tetrahydrofuran-2-yl)methyl) piperazine (340.5 mg, 2 mmol) and stirred for 24 h at ambient temperature. The precipitate was collected by filtration and dried *in vacuo* to afford the off-white solids (192 mg, 51.6%). mp: 247–250°C. MS: Calculated for $C_{19}H_{25}N_4O_4$ = 373.1876. $(M+H)^+$ = 373.1866 found. ^1H NMR (DMSO) δ ppm: 1.38–1.47 (m, 1H, CH_2), 1.69–1.79 (m, 2H, CH_2), 1.84–1.91 (m, 1H, CH_2), 2.33–2.34 (d, *J* = 5.78, 2H, CH_2), 2.41–2.46 (m, 4H, CH_2), 2.56–2.58 (m, 4H, CH_2), 3.54–3.59 (m, 1H, CH_2), 3.67–3.72 (m, 1H, CH_2), 3.84–3.91 (m, 4H, CH_2), 7.37–7.42 (m, 5H, Ar-H), 11.63 (s, 2H, NH). ^{13}C NMR (DMSO) δ ppm: 25.0; 29.8; 47.4; 54.0; 62.3; 67.1; 74.5; 76.5; 127.8; 128.7; 129.0; 135.3; 149.5; 170.0. IR (KBr): v (cm^{-1}): 3066, 1747, 1715, 1691, 1600, 1075, 917, 757, 692.

5-(4-benzylpiperazin-1-yl)-5-phenylpyrimidine-2,4,6(1H,3H,5H,)-trione (12)

A solution of 5-bromo-5-phenylpyrimidine-2,4,6(1*H*,3*H*,5*H*,)-trione (283 mg, 1.0 mmol) in methanol (5 ml) was treated with 1-benzylpiperazine (352.5 mg, 2 mmol) and stirred for 24 h at ambient temperature. The precipitate was collected by filtration and dried *in vacuo* to afford the off-white solids (265 mg, 70.0%). mp: 250–252°C. MS: Calculated for $C_{21}H_{23}N_4O_3$ = 379.1770. $(M+H)^+$ = 379.1756 found. ^1H NMR (DMSO) δ ppm: 2.36 (s, broad, 4H, CH_2), 2.58–2.60 (m, 4H, CH_2), 3.45 (s, 2H, CH_2), 7.21–7.32 (m, 5H, Ar–H), 7.37–7.42 (m, 5H, Ar–H), 11.61 (s,

2H, NH). ^{13}C NMR (DMSO) δ ppm: 47.4; 53.1; 62.0; 74.6; 126.9; 127.8; 128.2; 128.7; 128.9; 129.1; 135.3; 138.0; 149.5; 170.0. IR (KBr): v (cm^{-1}): 3062, 1751, 1732, 1694, 1604.

5-(4-butylpiperazin-1-yl)-5-phenylpyrimidine-2,4,6(1H,3H,5H,)-trione (13)

A solution of 5-bromo-5-phenylpyrimidine-2,4,6(1*H*,3*H*,5*H*,)-trione (283 mg, 1.0 mmol) in methanol (5 ml) was treated with 1-butylpiperazine (284.5 mg, 2 mmol) and stirred for 24 h at ambient temperature. The precipitate was collected by filtration and dried *in vacuo* to afford the off-white solids (200.8 mg, 58.3%). mp: 231–235°C. MS: Calculated for $C_{18}H_{25}N_4O_3$ = 345.1927. $(M+H)^+$ = 345.1937 found. ^1H NMR (DMSO) δ ppm: 0.83–0.87 (t, *J* = 7.27, 3H, CH_3), 1.20–1.29 (m, 2H, CH_2), 1.32–1.39 (m, 4H, CH_2), 2.21–2.25 (m, 4H, CH_2), 2.34 (s, broad, 4H, CH_2), 2.56–2.58 (m, 4H, CH_2), 7.37–7.42 (m, 5H, Ar-H), 11.63 (s, 2H, NH). ^{13}C NMR (DMSO) δ ppm:13.9; 20.1; 28.4; 47.4; 53.4; 57.5; 74.5; 127.8; 128.7; 129.0; 135.3; 149.5; 170.0. IR (KBr): v (cm^{-1}): 3065, 1747, 1706, 1687, 1612.

Methyl 2-(4-(benzyloxy)phenyl)acetate (15)

A solution of methyl 4-hydroxyphenylacetate (5 g, 30 mmol) and benzyl bromide (5.4 ml, 45 mmol) in 50 ml dry acetone was treated with potassium carbonate (8.3 g, 60 mmol). After being heated at 60 °C for 5 h, the reaction mixture was poured onto ice water and exacted with DCM (100 ml×3). The combined organic layers were washed with brine and dried (Na_2SO_4). The solvent was removed under reduced pressure to provide the crude products. These brownish oily residues were treated with hexane to yield the pure compounds (6.5 g, 84.6%) as off-white solids. mp: 72–74°C. MS: Calculated for $C_{16}H_{16}O_3Na$ = 279.0997. $(M+Na)^+$ = 279.0992 found. ^1H NMR ($CDCl_3$) δ ppm: 3.60 (s, 2H, CH_2), 3.72 (s,

3H, CH_3), 5.08 (s, 2H, Ar-CH_2), 6.96–6.98 (d, *J* = 8.53, 2H, Ar-H), 7.22–7.24 (d, *J* = 8.54, 2H, Ar-H), 7.35–7.47 (m, 5H, Ar-H). ^{13}C NMR ($CDCl_3$) δ ppm: 40.3; 52.0; 67.0; 114.9; 126.3; 127.4; 127.9; 128.6; 130.3; 136.9; 157.9; 172.3. IR (KBr): v (cm^{-1}): 2959, 1726, 1607, 1510.

Dimethyl 2-(4-(benzyloxy)phenyl)malonate (16)

A suspension of NaH (60% suspension in paraffin oil (paraffin oil was removed by repeated washings with hexane)) (80 mg, 20 mmol) and dimethyl carbonate (5.4 ml, 64 mmol) in 64 ml dry THF was heated to 100°C, and a solution of methyl 2-(4-(benzyloxy)phenyl)acetate (2.56 g, 10 mmol) in 20 ml THF was added dropwise over a period of 1 h. After being refluxed for 5 h, the mixture was poured onto ice water and extracted with methylene chloride (50 ml×3). The combined organic layers were washed with water and brine, dried (Na_2SO_4), and concentrated. The crude products were purified by flash column chromatography using hexane and ethyl acetate to yield the pure compounds (2.7 g, 85.9%) as off-white solids. mp: 87–88°C. MS: Calculated for $C_{18}H_{18}O_5Na$ = 337.1052. $(M+Na)^+$ = 337.1045 found.^{1}H NMR ($CDCl_3$) δ ppm: 3.78 (s, 6H, CH_3), 4.63 (s, 1H, CH), 5.08 (s, 2H, Ar-CH_2), 7.0–7.02 (d, *J* = 9.03, 2H, Ar-H), 7.28–7.31 (d, *J* = 9.03, 2H, Ar-H), 7.34–7.47 (m, 5H, Ar-H). ^{13}C NMR ($CDCl_3$) δ ppm: 52.8; 56.7; 70.0; 115.0; 124.8; 127.4; 128.0; 128.6; 130.4; 136.8; 158.8; 168.8. IR (KBr): v (cm^{-1}): 2956, 1742, 1611, 1515.

5-(4-(benzyloxy)phenyl)pyrimidine-2,4,6(1H,3H,5H,)-trione (17)

Sodium (460 g, 20 mmol) was dissolved in 60 ml ethanol (HPLC grade), and urea (1.02 g, 17 mmol) was added to this solution. A solution of dimethyl 2-(4-benzyloxy)phenyl)malonate (3.14 g, 10 mmol) in ethanol was added dropwise, and the reaction mixture was heated to reflux for 7 h. After being cooled to

ambient temperature, the mixture was poured onto ice water and adjusted to pH 2, using dilute hydrochloric acid. The precipitate was collected by suction filtration and dried *in vacuo* to afford the off-white solids (2.24g, 72.2%). mp: 251–253°C. MS: Calculated for $C_{17}H_{15}N_2O_4$ = 311.1032. $(M+H)^+$ = 311.1022 found. ^{1}H NMR (DMSO) δ ppm: 4.74 (s, 1H, CH), 5.11 (s, 2H, Ar-CH_2), 6.98–7.00 (d, *J* = 8.53, 2H, Ar-H), 7.17–7.19 (d, *J* = 8.53, 2H, Ar-H), 7.33–7.46 (m, 5H, Ar-H), 11.36 (s, 2H, NH). ^{13}C NMR (DMSO) δ ppm: 54.4; 69.4; 115.1; 126.9; 127.9; 128.1; 128.7; 130.6; 137.2; 151.2; 158.1; 169.6. IR (KBr): ν (cm^{-1}): 2967, 1795, 1770, 1643, 1520.

5-(4-(benzyloxy)phenyl)-5-bromopyrimidine-2,4,6(1H,3H,5H,)-trione (18)

A suspension of 5-(4-(benzyloxy)phenyl)pyrimidine-2,4,6(1H,3H,5H,)-trione (1.24 g, 4 mmol) in 20 ml water was cooled to 0-5°C, and a mixture of 48% HBr (764 μl, 7.1 mmol) and bromine (328 μl, 6.4 mmol) was added dropwise. After stirring for 4-5 h at 0-10°C the precipitate was collected by filtration and dried *in vacuo* to afford the off-white solids (1.36 g, 87.4%). mp: 161–163°C. ^{1}H NMR (DMSO) δ ppm: 5.10 (s, 2H, Ar-CH_2), 7.03–7.05 (d, *J* = 8.53, 2H, Ar-H), 7.31–7.33 (m, 2H, Ar-H), 7.36–7.44 (m, 5H, Ar-H), 11.51 (s, 2H, NH). ^{13}C NMR (DMSO) δ ppm: 69.5; 79.2; 115.2; 126.8; 128.0; 128.2; 128.7; 130.7; 137.1; 150.2; 158.9; 171.3. IR (KBr): ν (cm^{-1}): 2868, 1766, 1735, 1696, 1599.

5-(4-benzyloxy)phenyl)-5-(4-cyclohexylpiperazin-1-yl)pyrimidine-2,4,6(1H,3H,5,H)-trione (19)

A solution of 5-(4-(benzyloxy)phenyl)-5-bromopyrimidine-2,4,6(1*H*,3*H*,5*H*,)-trione (389 mg, 1 mmol) in the mixture of methanol (5 ml) and ethyl acetate (1 ml) was treated with 1-cyclohexylpiperazine (336.6 mg, 2 mmol) and stirred for

24 h at ambient temperature. The precipitate was collected by filtration and dried *in vacuo* to afford the off-white solids (321 mg, 67.4%). mp: 249–251°C. MS: Calculated for $C_{27}H_{33}N_4O_4$ = 477.2502. $(M+H)^+$ = 477.2516 found. ^1H NMR (DMSO) δ ppm: 1.06–1.17 (m, 6H, CH_2), 1.70–1.73 (m, 4H, CH_2) 2.47–2.56 (m, 9H), 5.10 (s, 2H, Ar-CH_2), 7.04–7.06 (d, *J* = 9.03, 2H, Ar-H), 7.31–7.36 (m, 3H, Ar-H), 7.38–7.46 (m, 4H, Ar-H), 11.58 (s, 2H, NH). ^{13}C NMR (DMSO) δ ppm: 25.3; 25.9; 28.3; 47.7; 49.0; 62.5; 69,3; 74.0; 114.8; 127.2; 127.8; 127.9; 128.5; 129.2; 136,8; 149.5; 158.7; 170.2. IR (KBr): v (cm^{-1}): 2936, 1735, 1708, 1670, 1608.

5-(4-benzyloxy)phenyl)-5-(4-isopropylpiperazin-1-yl)pyrimidine-2,4,6(1H,3H,5,H)-trione (20)

A solution of 5-(4-(benzyloxy)phenyl)-5-bromopyrimidine-2,4,6(1*H*,3*H*,5*H*,)-trione (389 mg, 1 mmol) in the mixture of methanol (5 ml) and ethyl acetate (1 ml) was treated with1-isopropylpiperazine (256.5 mg, 2 mmol) and stirred for 24 h at ambient temperature. The precipitate was collected by filtration and dried *in vacuo* to afford the off-white solids (258 mg, 59.1%). mp: 238–240°C (decomposition). MS: Calculated for $C_{24}H_{29}N_4O_4$ = 437.2189. $(M+H)^+$ = 437.2198 found. ^1H NMR (DMSO) δ ppm: 0.94–0.95 (d, *J* = 6.53, 6H, CH_3), 2.41–2.57 (m, 9H), 5.10 (s, 2H, Ar-CH_2), 7.04–7.07 (d, *J* = 8.53, 2H, Ar-H), 7.34–7.46 (m, 7H, Ar-H), 11.57 (s, 2H, NH). ^{13}C NMR (DMSO) δ ppm: 18.2; 47.6; 48.6; 53.6; 69.3; 74.0; 114.8; 127.2; 127.8; 127.9; 128.5; 129.1; 136.8; 149.5; 158.7; 170.2. IR (KBr): v (cm^{-1}): 3058, 1735, 1712, 1675, 1604.

5-((4-benzyloxy)phenyl)-5-(4-(cyclopropylmethyl)piperazin-1-yl) pyrimidine-2,4,6(1H,3H,5,H)-trione (21)

A solution of 5-(4-(benzyloxy)phenyl)-5-bromopyrimidine-2,4,6(1*H*,3*H*,5*H*,)-trione (389 mg, 1 mmol) in the mixture of methanol (5 ml) and ethyl acetate (1 ml) was treated with1-cyclopropylmethylpiperazine (280.5 mg, 2 mmol) and

stirred for 24 h at ambient temperature. The precipitate was collected by filtration and dried *in vacuo* to afford the off-white solids (286 mg, 63.8%). mp: 241–244°C. MS: Calculated for $C_{25}H_{29}N_4O_4$ = 449.2189. $(M+H)^+$ = 449.2201 found. ^1H NMR (DMSO) δ ppm: 0.03–0.06 (m, 2H, CH_2), 0.41–0.45 (m, 2H, CH_2), 0.74–.084 (m, 1H, CH), 2.15–2.16 (d, *J* = 6.52, 2H, N-CH_2), 2.42–2.58 (m, 8H) 5.10 (s, 2H, Ar–CH_2), 7.04–7.07 (d, *J* = 8.54, 2H, Ar-H), 7.34–7.46 (m, 7H, Ar-H), 11.57 (s, 2H, NH). ^{13}C NMR (DMSO) δ ppm: 3.7; 8.1; 47.2; 53.3; 62.8; 69.3; 74.1; 114.9; 127.2; 127.8; 127.9; 128.5; 129.1; 136.8; 149.5; 158.7; 170.3. IR (KBr): v (cm^{-1}): 3029, 1708, 1607.

5-((4-benzyloxy)phenyl)-5-(4-(cyclopropylcarbonyl)piperazin-1-yl) pyrimidine-2,4,6(1H,3H,5,H)-trione (22)

A solution of 5-(4-(benzyloxy)phenyl)-5-bromopyrimidine-2,4,6(1*H*,3*H*,5*H*,)-trione (389 mg, 1 mmol) in the mixture of methanol (5 ml) and ethyl acetate (1 ml) was treated with 1-cyclopropylcarbonyl piperazine (308.4 mg, 2 mmol) and stirred for 24 h at ambient temperature. The reaction mixture was dried and purified by flash column chromatography to yield the pure compounds (214 mg, 46.3%) as off-white solids. mp: 194–197°C. MS: Calculated for $C_{25}H_{27}N_4O_5Na$ = 485.1801. $(M+Na)^+$ = 485.1820 found. ^1H NMR (DMSO) δ ppm: 0.67–0.72 (m, 4H, CH_2), 1.89–1.96 (m, 1H, CH), 2.55–2.63 (m, 4H, CH_2), 2.73 (m, 2H, CH_2), 2.89 (m, 2H, CH_2), 5.10 (s, 2H, Ar-CH_2), 7.08–7.10 (d, *J* = 9.04, 2H, Ar-H), 7.34–7.46 (m, 7H, Ar-H), 11.62 (s, 2H, NH). ^{13}C NMR (DMSO) δ ppm: 7.0; 10.0; 42.3; 45.7; 47.5; 48.2; 69.4; 74.3; 115.1; 126.8; 127.8; 128.0; 128.5; 129.1; 136.7; 149.4; 158.9; 170.2; 170.9. IR (KBr): v (cm^{-1}): 3010, 1752, 1737, 1703, 1606.

5-(4-benzyloxy)phenyl)-5-(4-methyl-1,4-diazepan-1-yl)pyrimidine-2,4,6(1H,3H,5,H)-trione (23)

A solution of 5-(4-(benzyloxy)phenyl)-5-bromopyrimidine-2,4,6(1*H*,3*H*,5*H*,)-trione (389 mg, 1 mmol) in the mixture of methanol (5 ml) and ethyl acetate (1 ml) was treated with 1-methyl-1,4-diazepane (228.4 mg, 2 mmol) and stirred for 24 h at ambient temperature. The precipitate was collected by filtration and dried *in vacuo* to afford the off-white solids (273 mg, 64.6%). mp: 243–247°C. MS: Calculated for $C_{23}H_{27}N_4O_4$ = 423.2032. $(M+H)^+$ = 423.2038 found. ^{1}H NMR (DMSO) δ ppm: 1.62–1.68 (m, 2H, CH_2), 2.26 (s, 3H, CH_3), 2.42–2.44 (m, 2H, CH_2), 2.61–2.64 (t, *J* = 5.52, 2H, CH_2), 2.68–2.72 (t, *J* = 6.02, 2H, CH_2), 5.09 (s, 2H, Ar-CH_2), 7.06–7.08 (d, *J* = 9.04, 2H, Ar-H), 7.34–7.46 (m, 7H, Ar-H). ^{13}C NMR (DMSO) δ ppm: 28.0; 46.0; 49.6; 50.5; 55.3; 59.6; 63.4; 76.4; 114.9; 127.8; 128.0; 128.5; 128.6; 128.9; 136.7; 149.7; 158.8; 171.2. IR (KBr): v (cm^{-1}): 3063, 1732, 1706, 1674, 1594.

5-(4-2(-2-hydroxyethoxy)ethyl)piperazin-1-yl)-5-(4-(benzylxoy)phenyl) pyrimidine-2,4,6(1H,3H,5,H)-trione (24)

A solution of 5-(4-(benzyloxy)phenyl)-5-bromopyrimidine-2,4,6(1*H*,3*H*,5*H*,)-trione (389 mg, 1 mmol) in the mixture of methanol (5 ml) and ethyl acetate (1 ml) was treated with 1-2(-2-hydroxyethoxy)ethyl)piperazine (348.5 mg, 2 mmol) and stirred for 24 h at ambient temperature. The reaction mixture was dried and purified by flash column chromatography to yield the pure compounds (194mg, 40.2%) as off-white solids. mp: 162–164°C. MS: Calculated for $C_{25}H_{31}N_4O_6$ = 483.2244. $(M+H)^+$ = 483.2241 found. ^{1}H NMR (DMSO) δ ppm: 2.41–2.47 (m, 6H, CH_2), 2.57–2.60 (m, 2H, CH_2), 3.38–3.41 (t, *J* = 5.02, 2H, CH_2), 3.47–3.49 (t, *J* = 5.02, 4H, CH_2), 5.10 (s, 2H, Ar-CH_2), 7.05–7.07(d, *J* = 9.04, 2H, Ar-H), 7.33–7.46 (m, 7H, Ar-H). ^{13}C NMR (DMSO) δ ppm: 47.2; 53.8; 57.8; 60.3; 68.1; 69.4; 72.2; 74.1; 114.9; 127.2; 127.8; 128.0; 128.5; 129.2; 136.8; 149.7; 158.8;

170.4. IR (KBr): v (cm^{-1}): 3062, 1732, 1696, 1606, 1581.

5-(4-benzyloxy)phenyl)-5-(4-((tetrahydrofuran-2-yl)methyl)piperazin-1-yl)pyrimidine-2,4,6(1H,3H,5,H)-trione (25)

A solution of 5-(4-(benzyloxy)phenyl)-5-bromopyrimidine-2,4,6(1*H*,3*H*,5*H*,)-trione (389 mg, 1 mmol) in the mixture of methanol (5 ml) and ethyl acetate (1 ml) was treated with 1-((tetrahydrofuran-2-yl)methyl)piperazine (340.5 mg, 2 mmol) and stirred for 24 h at ambient temperature. The reaction mixture was dried and purified by flash column chromatography to yield the pure compounds (174 mg, 36.4%) as light yellow solids. mp: 165–167°C. MS: Calculated for $C_{26}H_{31}N_4O_5$= 479.2294. $(M+H)^+$ = 479.2286 found. H NMR (DMSO) δ ppm: 1.44–1.53 (m, 1H, CH_2), 1.77–1.88 (m, 2H, CH_2), 1.96–2.04 (m, 1H, CH_2), 2.51–3.04 (m, 10H, CH_2), 3.67–3.73 (m, 1H, CH_2), 3.77–3.82 (m, 1H, CH_2), 4.17–4.23 (m, 1H, CH_2), 5.10 (s, 2H, Ar-CH_2), 7.09–7.12 (d, *J* = 9.04, 2H, Ar-H), 7.31–7.36 (m, 2H, Ar-H), 7.38–7.46 (m, 2H, Ar-H), 11.64 (s, 2H, NH). ^{13}C NMR (DMSO) δ ppm: 24.2; 28.8; 44.3; 52.5; 59.9; 67.6; 69.1; 72.2; 74.3; 114.6; 125.4; 126.6; 127.1; 127.6; 128.3; 136.2; 148.7; 159.4; 169.7. IR (KBr): v (cm^{-1}): 3033, 1737, 1703, 1605,

5-(4-benzyloxy)phenyl)-5-(4-benzylpiperazin-1-yl)pyrimidine-2,4,6 (1H,3H,5,H)-trione (26)

A solution of 5-(4-(benzyloxy)phenyl)-5-bromopyrimidine-2,4,6(1*H*,3*H*,5*H*,)-trione (389 mg, 1 mmol) in the mixture of methanol (5 ml) and ethyl acetate (1 ml) was treated with 1-benzylpiperazine (352.5 mg, 2 mmol) and stirred for 24 h at ambient temperature. The precipitate was collected by filtration and dried *in vacuo* to afford the off-white solids (319 mg, 65.8%). mp: 230–232°C. MS: Calculated for $C_{28}H_{29}N_4O_4$ = 485.2189. $(M+H)^+$ = 485.2206 found. ^1H NMR

(DMSO) δ ppm: 2.35 (s, broad, 4H, CH_2), 2.58–2.60 (m, 4H, CH_2), 3.46(s, 2H, Ar-CH_2), 5.10 (s, 2H, Ar-CH_2), 7.04–7.06 (d, *J* = 9.04, 2H, Ar-H), 7.24–7.35 (m, 8H, Ar-H), 7.38–7.45 (m, 4H, Ar-H) , 11.57 (s, 2H, NH). ^{13}C NMR (DMSO) δ ppm: 47.3; 53.1; 62.0; 69.3; 74.1; 114.9; 126.9; 127.1; 127.8; 127.9; 128.1; 128.5; 128.9; 129.1; 136.8; 138.0; 149.5; 158.7; 170.2. IR (KBr): v (cm^{-1}): 3062, 1732, 1703, 1608.

5-(4-benzyloxy)phenyl)-5-(4-butylpiperazin-1-yl)pyrimidine-2,4,6 (1H,3H,5,H)-trione (27)

A solution of 5-(4-(benzyloxy)phenyl)-5-bromopyrimidine-2,4,6(1*H*,3*H*,5*H*,)-trione (389 mg, 1 mmol) in the mixture of methanol (5 ml) and ethyl acetate (1 ml) was treated with 1-butylpiperazine (284.5 mg, 2 mmol) and stirred for 24 h at ambient temperature. The reaction mixture was dried and purified by flash column chromatography to yield the pure compounds (255 mg, 56.6%) as off-white solids. mp: 146–148°C. MS: Calculated for $C_{25}H_{31}N_4O_4$ = 451.2345. $(M+H)^+$ = 451.2325 found. ^{1}H NMR (DMSO) δ ppm: 0.84–0.88 (t, *J*= 7.33, 3H, CH_3), 1.25–1.29 (m, 2H, CH_2), 1.33–1.40 (m, 2H, CH_2), 2.21–2.25 (t, *J*= 7.33, 2H, CH_2), 2.51–2.57 (m, 8H, CH_2), 5.10 (s, 2H, Ar-CH_2), 7.04–7.07 (d, *J* = 9.03, 2H, Ar-H), 7.31–7.46 (m, 7H, Ar-H), 11.58 (s, 2H, NH). ^{13}C NMR (DMSO) δ ppm: 13.9; 20.1; 28.4; 47.2; 54.4; 57.5; 69.3; 74.0; 114.8; 127.2; 127.8; 127.9; 128.5; 129.1; 136.8; 149.5; 15.7; 170.2. IR (KBr): v (cm^{-1}): 3034, 1735, 1703, 1605.

Methyl 2-(4-phenoxyphenyl)acetate (28)

Methyl 4-hydroxyphenylacetate (3.32 g, 20 mmol), copper (II) acetate (3.58 g, 20 mmol), phenylboronic acid (4.88 g, 40 mmol), powered 4 Å molecular sieves and 8 ml pyridine were added into 100 ml DCM. The reaction mixture was stirred at room temperature for 20 h. The resulting mixture was filtered and diethyl ether

(50 mlx3) was used to extract the compound and purified by column chromatography to afford the pure compounds as the yellow oil (1.55 g, 32.0%). MS: Calculated for $C_{15}H_{14}O_3Na$ = 265.0841. $(M+Na)^+$ = 265.0835 found. ^1H NMR ($CDCl_3$) δ ppm: 3.68 (s, 2H, CH_2), 3.76 (s, 3H, CH_3), 7.03–7.09 (m, 4H, Ar-H), 7.14–7.18 (t, *J* = 7.53, 1H, Ar-H), 7.30–7.32 (d, *J* = 8.53, 2H, Ar-H), 7.37–7.41 (m, *J* = 7.53, 2H, Ar-H). ^{13}C NMR ($CDCl_3$) δ ppm: 40.2; 51.9; 115.2; 118.7; 123.1; 128.5; 129.6; 130.5; 156.2; 156.9; 172.2; IR (CH_2Cl_2): v (cm^{-1}): 3063, 1731, 1613, 1589.

Dimethyl 2-(4-phenoxyphenyl)malonate (29)

A suspension of NaH (60% suspension in paraffin oil (paraffin oil was removed by repeated washings with hexane)) (80 mg, 20 mmol) and dimethyl carbonate (5.4 ml, 64 mmol) in 64 ml dry THF was heated to 100°C, and a solution of Methyl 2-(4-phenoxyphenyl) (2.42 g, 10 mmol) acetate in 20 ml THF was added dropwise over a period of 1 h. After being refluxed for 5 h, the mixture was poured onto ice water and extracted with methylene chloride (50 ml × 3). The combined organic layers were washed with water and brine, dried (Na_2SO_4), and concentrated. The crude products were purified by flash column chromatography using hexane and ethyl acetate to yield the pure compounds (2.57 g, 85.8%) as yellow solid. mp: 43–45°C. MS: Calculated for $C_{17}H_{16}O_5Na$ = 323.0895. $(M+Na)^+$ = 323.0888 found. ^1H NMR ($CDCl_3$) δ ppm: 3.79 (s, 6H, CH_3), 4.68 (s, 1H, CH), 7.01–7.07 (m, 4H, Ar-H), 7.13–7.17 (t, *J* = 7.53, 1H, Ar-H), 7.35–7.41 (m, 4H, Ar-H). ^{13}C NMR ($CDCl_3$) δ ppm: 52.8; 56.6; 118.4; 119.2; 123.5; 126.9; 129.7; 130.6; 156.5; 157.4; 168.5. IR (KBr): v (cm^{-1}): 3064, 1734, 1611, 1590.

5-(4-phenoxyphenyl)pyrimidine-2,4,6(1H,3H,5H)-trione (30)

Sodium (460 mg, 2 0mmol) was dissolved in 60 ml ethanol (HPLC grade), and

urea (1.02 g, 17 mmol) was added to this solution. A solution of dimethyl 2-(4-phenoxyphenyl)malonate (3.00 g, 10 mmol) in ethanol was added dropwise, and the reaction mixture was heated to reflux for 7 h. After being cooled to ambient temperature, the mixture was poured onto ice water and adjusted to pH 2, using dilute hydrochloric acid. The precipitate was collected by suction filtration and dried *in vacuo* to afford the off-white solids (2.31 g, 78.0%). mp: 250–253°C. MS: Calculated for $C_{16}H_{12}N_2O_4Na$ = 319.0695. $(M+Na)^+$ = 319.0684 found. ^1H NMR (DMSO) δ ppm: 4.84 (s, 1H, CH), 6.95–6.97 (d, 2H, *J* = 8.56, Ar-H), 7.01–7.03 (m, 2H, Ar-H), 7.13–7.16 (t, 1H, *J* = 6.85, Ar-H), 7.26–7.28 (d, 2H, *J* = 8.07, Ar-H), 7.37–7.41 (t, 2H, *J* = 7.58, Ar-H) 11.4 (s, 2H, NH). ^{13}C NMR (DMSO) δ ppm: 54.4; 118.5; 119.1; 123.9; 129.3; 130.2; 131.2; 151.1; 156.4; 156.5; 169.4. IR (KBr): v (cm^{-1}): 3063, 1788, 1761, 1720, 1572.

5-bromo-5-(4-phenoxyphenyl)pyrimidine-2,4,6(1H,3H,5H)-trione (31)

A suspension of 5-(4-phenyoxyphenyl)pyrimidine-2,4,6(1H,3H,5H,)-trione (1.185 g, 4 mmol) in 20 ml water was cooled to 0-5°C, and a mixture of 48% HBr (764 μl, 7.1 mmol) and bromine (328 μl, 6.4 mmol) was added dropwise. After stirring for 4-5 h at 0-10°C the precipitate was collected by filtration and dried *in vacuo* to afford the off-white solids (1.22 g, 81.9%). mp: 111–113°C. ^1H NMR (DMSO) ppm: 6.98–7.08 (m, 4H, Ar-H), 7.15–7.18 (t, 2H, *J* =7.53, Ar-H), 7.38–7.45 (m, 3H, Ar-H), 7.55–7.57 (d, 2H, *J* = 9.04, Ar-H), 11.56(s, 1H, NH), 11.57 (s, 1H, NH). ^{13}C NMR (DMSO) ppm: 115.6; 118.4; 118.8; 119.1; 121.1; 124.0; 127.1; 127.2; 130.2; 133.0; 149.9; 156.0; 157.3; 170.9. IR (KBr): v (cm^{-1}): 3078, 1737, 1718, 1607.

5-(4-cyclohexylpiperazin-1-yl)-5-(4-phenoxyphenyl)pyrimidine-2,4,6(1H,3H,5H)-trione (32)

A solution of 5-bromo-5-(4-phenoxyphenyl)pyrimidine-2,4,6(1*H*,3*H*,5*H)*-trione (375 mg, 1.0 mmol) in methanol (5 ml) was treated with 1-cyclohexylpiperazine (336.6 mg, 2 mmol) and stirred for 24 h at ambient temperature. The precipitate was collected by filtration and dried *in vacuo* to afford the off-white solids (292 mg, 63.1%). mp: > 252°C. MS: Calculated for $C_{26}H_{31}N_4O_4$ = 463.2345. $(M+H)^+$ = 463.2350 found. ^{1}H NMR (DMSO) ppm: 1.03–1.19 (m, 6H, CH_2), 2.18–2.25 (m, 1H, CH), 2.51–2.57 (m, 8H, CH_2), 7.00–7.06 (m, 4H, Ar-H), 7.16–7.20 (t, *J* = 7.53, 1H, Ar-H), 7.38–7.43 (m, 3H, Ar-H), 7.55–7.58 (m, 1H, Ar-H),11.61 (s, 2H, NH). ^{13}C NMR (DMSO) ppm: 25.3; 25.9; 28.2; 47.7; 49.0; 62.5; 73.9; 115.8; 118.0; 118.4; 119.3; 121.3; 124.1; 129.7; 129.8; 130.2; 133.0; 149.5; 155.8; 157.4; 170.0. IR (KBr): v (cm^{-1}): 2933, 1711, 1737, 1614.

5-(4-isopropylpiperazin-1-yl)-5-(4-phenoxyphenyl)pyrimidine-2,4,6 (1H,3H,5H)-trione (33)

A solution of 5-bromo-5-(4-phenoxyphenyl)pyrimidine-2,4,6(1*H*,3*H*,5*H)*-trione (375 mg, 1.0 mmol) in methanol (5 ml) was treated with 1-isopropylpiperazine (256.5 mg, 2 mmol) and stirred for 24 h at ambient temperature. The precipitate was collected by filtration and dried *in vacuo* to afford the off-white solids (240 mg, 56.8%). mp: > 252°C. MS: Calculated for $C_{23}H_{27}N_4O_4$ = 423.2032. $(M+H)^+$ = 423.2032 found. ^{1}H NMR (DMSO) ppm: 0.95–0.97 (d, *J* = 6.52, 6H, CH_3), 2.47–2.51 (m, 4H, CH_2), 2.58–2.60 (m, 4H, CH_2), 2.64–2.69 (m, 1H, CH), 7.00–7.06 (m, 4H, Ar-H), 7.16–7.20 (t, *J* = 7.53, 1H, Ar-H), 7.39–7.43 (m, 3H, Ar-H), 7.55–7.59 (m, 1H, Ar-H),11.61 (s, 2H, NH). ^{13}C NMR (DMSO) ppm 18.0; 47.5; 48.6; 53.9; 73.9; 115.8; 118.1; 118.4; 119.3; 121.3; 124.1; 129.7; 129.8;130.2; 133.0;149.5; 155.8; 157.4; 170.0. IR (KBr): v (cm^{-1}): 3066, 1735, 1717, 1608.

5-(4-(cyclopropylmethyl)piperazin-1-yl)-5-(4-phenoxyphenyl) pyrimidine-2,4,6 (1H,3H,5H)-trione (34)

A solution of 5-bromo-5-(4-phenoxyphenyl)pyrimidine-2,4,6(1*H*,3*H*,5*H)*-trione (375 mg, 1.0 mmol) in methanol (5 ml) was treated with 1-cyclopropylmethylpiperazine (280.5 mg, 2 mmol) and stirred for 24 h at ambient temperature. The precipitate was collected by filtration and dried *in vacuo* to afford the off-white solids (256 mg, 58.9%). mp: = 242–246°C. MS: Calculated for $C_{23}H_{27}N_4O_4$ = 435.2032. $(M+H)^+$ = 435.2032 found. ^1H NMR (DMSO) ppm: 0.02–0.05 (m, 2H, CH_2), 0.40–0.44 (m, 2H, CH_2), 0.73–0.83 (m, 1H, CH), 2.14–2.16 (d, *J* = 6.53, 2H, CH_2), 2.43 (s, broad, 2H, CH_2), 2.59 (s, broad, 2H, CH_2), 7.00–7.06 (m, 4H, Ar-H), 7.15–7.20 (t, *J* = 7.53, 1H, Ar-H), 7.38–7.43 (m, 3H, Ar-H), 7.55–7.58 (m, 1H, Ar-H). ^{13}C NMR (DMSO) ppm: 3.1; 8.1; 47.3; 53.2; 62.8; 73.9; 118.1; 118.4; 119.3; 121.3; 124.1; 129.7; 129.8; 130.2; 129.8; 149.5; 155.8; 157.4; 170.0. IR (KBr): v (cm^{-1}): 3000, 1735, 1709, 1607.

5-(4-(cyclopropylcarbonyl)piperazin-1-yl)-5-(4-phenoxyphenyl)pyrimidine -2,4,6(1H,3H,5H)-trione (35)

A solution of 5-bromo-5-(4-phenoxyphenyl)pyrimidine-2,4,6(1*H*,3*H*,5*H)*-trione (375 mg, 1.0 mmol) in methanol (5 ml) was treated with 1-cyclopropylcarbonyl piperazine (308.4 mg, 2 mmol) and stirred for 24 h at ambient temperature. The reaction mixture was dried and purified by flash column chromatography to yield the pure compounds (170 mg, 37.9%) as off-white solids. mp: 148–150°C. MS: Calculated for $C_{25}H_{27}N_4O_5Na$ = 471.1644. $(M+Na)^+$ = 471.1651 found. ^1H NMR (Acetone-D_6) ppm: 0.67–0.72 (m, 2H, CH_2), 0.81–0.85 (m, 2H, CH_2), 1.89–1.93 (m, H, CH), 2.72–2.81 (m, 4H, CH_2); 3.58–3.74 (m, 4H, CH_2); 7.04–7.10 (m, 4H, Ar-H), 7.18–7.12 (t, *J* = 7.53, 1H, Ar-H), 7.41–7.45 (m, 1H, Ar-H), 7.57–7.64 (m, 3H, Ar-H) 10.49 (s, 2H, NH). ^{13}C NMR (Acetone-D_6) ppm: 7.1; 10.7; 43.1; 46.5; 48.4; 48.9; 75.6; 116.5; 118.6; 119.0; 120.0; 121.9; 124.6; 129.9; 130.4; 130.6; 149.1; 156.7; 159.0; 170.2; 171.8. IR (KBr): v (cm^{-1}): 3010, 1751, 1737,

1708, 1608.

5-(4-methyl-1,4-diazepan-1-yl)-5-(4-phenoxyphenyl)pyrimidine-2,4,6 (1H,3H,5H)-trione (36)

A solution of 5-bromo-5-(4-phenoxyphenyl)pyrimidine-2,4,6(1*H*,3*H*,5*H)*-trione (375 mg, 1.0 mmol) in methanol (5 ml) was treated with 1-methyl-1,4-diazepane (228.4 mg, 2 mmol) and stirred for 24 h at ambient temperature. The precipitate was collected by filtration and dried *in vacuo* to afford the off-white solids (198 mg, 48.5%). mp: 249–251°C. MS: Calculated for $C_{22}H_{25}N_4O_4$ = 409.1876. $(M+H)^+$ = 409.1873 found. ^1H NMR (DMSO) ppm: 1.62–1.68 (m, 2H, CH_2), 2.24 (s, 3H, CH_3), 2.42–2.44 (m, 2H, CH_2), 2.59–2.62 (m, 2H, CH_2), 2.68–2.72 (m, 4H, CH_2), 7.00–7.06 (m, 4H, Ar-H), 7.16–7.20 (t, *J* = 7.53, 1H, Ar-H), 7.38–7.44 (m, 3H, Ar-H), 7.55–7.58 (m, 1H, Ar-H). ^{13}C NMR (DMSO) ppm: 28.0; 46.1; 46.7; 50.6; 55.4; 59.5; 76.2; 118.1; 118.4; 119.4; 121.4; 124.2; 129.5; 130.2; 131.1; 133.0; 149.8; 155.7; 157.5; 171.1. IR (KBr): v (cm^{-1}): 3062, 1732, 1682, 1592.

5-(4-2(-2-hydroxyethoxy)ethyl)piperazin-1-yl)-5-(4-phenoxyphenyl) pyrimidine-2,4,6(1H,3H,5H)-trione (37)

A solution of 5-bromo-5-(4-phenoxyphenyl)pyrimidine-2,4,6(1*H*,3*H*,5*H)*-trione (375 mg, 1.0 mmol) in methanol (5 ml) was treated with 1-2(-2-hydroxyethoxy)ethyl)piperazine (348.5 mg, 2 mmol) and stirred for 24 h at ambient temperature. The reaction mixture was dried and purified by flash column chromatography to yield the pure compounds (226 mg, 48.6%) as off-white solids. mp: = 156–160°C. MS: Calculated for $C_{24}H_{29}N_4O_6$ = 469.2087. $(M+H)^+$ = 469.2088 found. ^1H NMR (DMSO) ppm: 2.42–2.47 (m, 6H, CH_2), 2.56–2.59 (m, 4H, CH_2), 3.36–2.50 (m, 6H, CH_2), 7.00–7.06 (m, 4H, Ar-H), 7.15–7.19 (t, *J* = 7.53, 1H, Ar-H), 7.37–7.43 (m, 3H, Ar-H), 7.54–7.57 (m, 1H, Ar-H), 11.62

(s, 2H, NH). ^{13}C NMR (DMSO) ppm: 47.3; 53.7; 51.2; 62.6; 72.2; 74.0; 115.8; 118.1; 118.4; 119.3; 121.4; 124.1; 129.7; 130.2; 133.0; 149.5; 155.8; 157.4; 170.2. IR (KBr): v (cm^{-1}): 3066, 1737, 1708, 1605..

5-(4-((tetrahydrofuran-2-yl)methyl)piperazin-1-yl)-5-(4-phenoxyphenyl) pyrimidine-2,4,6(1H,3H,5H)-trione (38)

A solution of 5-bromo-5-(4-phenoxyphenyl)pyrimidine-2,4,6(1*H*,3*H*,5*H)*-trione (375 mg, 1.0 mmol) in methanol (5 ml) was treated with 1-((tetrahydrofuran-2-yl)methyl)piperazine (340.5 mg, 2 mmol) and stirred for 24 h at ambient temperature. The precipitate was collected by filtration and dried *in vacuo* to afford the off-white solids (239 mg, 51.5%). mp: = 248–250°C. MS: Calculated for $C_{25}H_{29}N_4O_5$ = 465.2138. $(M+H)^+$ = 465.2143 found. ^1H NMR (DMSO) ppm: 1.30–1.39 (m, 1H, CH_2), 1.61–1.71 (m, 2H, CH_2), 1.76–1.82 (m, 1H, CH_2), 1.61–1.71 (d, *J* = 5.52, 2H, CH_2), 2.32–2.48 (m, 6H, CH_2), 3.46–3.51 (m, 2H, CH_2), 3.59–3.64 (m, 1H, CH_2), 3.76–3.82 (m, 1H, CH_2), 6.92–6.98 (m, 4H, Ar-H), 7.07–7.11 (t, *J* = 7.53, 1H, Ar-H), 7.30–7.34 (t, *J* = 7.53, 3H, Ar-H), 7.46–7.49 (m, 1H, Ar-H), 11.50 (s, 2H, NH). ^{13}C NMR (DMSO) ppm: 25.0; 29.8; 47.3; 54.0; 62.3; 67.1; 73.9; 76.5; 115.7; 118.1; 118.4; 119.3; 121.3; 124.1; 129.7; 130.2; 133.0; 149.5; 155.8; 157.4; 170.0. IR (KBr): v (cm^{-1}): 3088, 1750, 1718, 1692.

5-(4-benzylpiperazin-1-yl-5-(4-phenoxyphenyl)pyrimidine-2,4,6(1H,3H,5H) -trione (39)

A solution of 5-bromo-5-(4-phenoxyphenyl)pyrimidine-2,4,6(1*H*,3*H*,5*H)*-trione (375 mg, 1.0 mmol) in methanol (5 ml) was treated with 1-benzylpiperazine (352.5 mg, 2 mmol) and stirred for 24 h at ambient temperature. The precipitate was collected by filtration and dried *in vacuo* to afford the off-white solids (269 mg, 57.2%). mp: = 206–208°C. MS: Calculated for $C_{27}H_{27}N_4O_4$ = 471.2032.

$(M+H)^+$ = 471.2048 found. ^1H NMR (DMSO) ppm: 2.36 (s, broad, 4H, CH_2), 2.58–2.61 (m, 4H, CH_2), 7.00–7.06 (m, 4H, Ar-H), 7.16–7.20 (t, *J* = 7.53, 1H, Ar-H), 7.22–7.33 (m, 5H, Ar-H), 7.39–7.43 (t, *J* = 7.53, 3H, Ar-H), 7.55–7.58 (m, 1H, Ar-H), 11.55 (s, 2H, NH). ^{13}C NMR (DMSO) ppm: 47.4; 53.1; 62.0; 73.9; 115.7; 118.1; 118.4; 119.3; 121.3; 124.1; 126.9; 128.2; 128.9; 129.7; 130.2; 133.0; 149.5; 155.8; 157.4; 170.0. IR (KBr): v (cm^{-1}): 3064, 1731, 1708, 1609.

5-(4-butylpiperazin-1-yl)-5-(4-phenoxyphenyl)pyrimidine-2,4,6(1H,3H,5H)-trione (40)

A solution of 5-bromo-5-(4-phenoxyphenyl)pyrimidine-2,4,6(1*H*,3*H*,5*H)*-trione (375 mg, 1.0 mmol) in methanol (5 ml) was treated with 1-butylpiperazine (284.5 mg, 2 mmol) and stirred for 24 h at ambient temperature. The reaction mixture was dried and purified by flash column chromatography to yield the pure compounds (169 mg, 38.7%) as off-white solids. mp: = 196–198°C. MS: Calculated for $C_{24}H_{29}N_4O_4$ = 437.2189. $(M+H)^+$ = 437.2177 found. ^1H NMR (DMSO) ppm: 0.83–0.87 (t, *J* = 7.28, 3H, CH_3), 1.22–1.29 (m, 2H, CH_2), 1.34–1.41 (m, 2H, CH_2), 2.29–2.32 (t, *J* = 7.03, 2H, CH_2), 2.41 (s, broad, 4H, CH_2), 2.58–2.61 (m, 4H, CH_2), 7.00–7.06 (m, 4H, Ar-H), 7.15–7.19 (t, *J* =7.53, 1H, Ar-H), 7.38–7.43 (m, 3H, Ar-H), 7.55–7.57 (m, 1H, Ar-H). ^{13}C NMR (DMSO) ppm: 13.9; 20.0; 28.1; 47.1; 53.3; 57.3; 73.9; 118.1; 118.4; 119.3; 121.3; 124.1; 129.6; 129.7; 130.2; 133.0; 149.5; 155.8; 157.4; 170.0. IR (KBr): v (cm^{-1}): 3057, 1734, 1705, 1605.

5-(4-methyl-piperazin-1-yl)-5-(4-phenoxyphenyl)pyrimidine-2,4,6(1H,3H,5H)-trione (41)

A solution of 5-bromo-5-(4-phenoxyphenyl)pyrimidine-2,4,6(1*H*,3*H*,5*H)*-trione (375 mg, 1.0 mmol) in methanol (5 ml) was treated with 1-methylpiperazine (200.4 mg, 2 mmol) and stirred for 24 h at ambient temperature. The reaction mixture was dried and purified by flash column chromatography to yield the pure

compounds (151 mg, 38.3%) as off-white solids. mp: 270–272°C. MS: Calculated for $C_{21}H_{23}N_4O_4$ = 395.1719; found $(M+H)^+$ = 395.1706. ^1H NMR (DMSO) ppm: 2.16 (s, 3H, CH_3), 2.29–2.35 (m, 4H, CH_2), 2.57–2.61 (m, 4H, CH_2), 7.02–7.08 (m, 4H, Ar-H), 7.17–7.21 (t, *J* = 7.53, 1H, Ar-H), 7.41–7.44 (t, *J* = 7.53, 3H, Ar-H), 7.57–7.59 (m, 3H, Ar-H), 11.65 (s, 2H, NH). ^{13}C NMR (DMSO) ppm: 45.6; 47.2; 55.2; 73.8; 118.1; 118.4; 119.4; 121.4; 124.0; 129.7; 130.2; 132.9; 149.4; 155.8; 157.4; 169.9. IR (KBr): v (cm^{-1}): 2960; 1730; 1715; 1608.

5-(4-acetyl-piperazin-1-yl)-5-(4-phenoxyphenyl)pyrimidine-2,4,6 (1H,3H,5H)-trione (42)

A solution of 5-bromo-5-(4-phenoxyphenyl)pyrimidine-2,4,6(1*H*,3*H*,5*H)*-trione (375 mg, 1.0 mmol) in methanol (5 ml) was treated with 1-methylpiperazine (256.4 mg, 2 mmol) and stirred for 24 h at ambient temperature. The reaction mixture was dried and purified by flash column chromatography to yield the pure compounds (191 mg, 45.2%) of as off-white solids. mp: 176–179°C. MS: Calculated for $C_{22}H_{23}N_4O_5$ = 423.1668; found $(M+H)^+$ = 423.1617. ^1H NMR (MeOD) ppm: 2.08 (s, 3H, CH_3), 2.69–2.71 (m, 2H, CH_2), 2.76–2.78 (m, 2H, CH_2), 3.51–3.53 (m, 2H, CH_2), 3.57–3.59 (m, 2H, CH_2), 6.96–7.05 (m, 4H, Ar-H), 7.16–7.20 (t, *J* = 7.53, 1H, Ar-H), 7.37–7.41 (t, *J* = 7.53, 3H, Ar-H), 7.50–7.55 (m, 3H, Ar-H). ^{13}C NMR (MeOD) ppm: 21.1; 43.3; 48.2; 76.3; 119.3; 119.6; 120.8; 122.4; 125.3; 130.1; 131.1; 134.1; 150.7; 156.9; 157.4; 171.6; 171.8. IR (KBr): v (cm^{-1}): 2961; 1739; 1709; 1614.

5-(4-phenoxyphenyl)-5-(piperazin-1-yl)pyrimidine-2,4,6(*1H,3H,5H*)-trione (43)

A solution of 5-bromo-5-(4-phenoxyphenyl)pyrimidine-2,4,6(1*H*,3*H*,5*H)*-trione (375 mg, 1.0 mmol) in methanol (5 ml) was treated with piperazine (177.2 mg, 2 mmol) and stirred for 24 h at ambient temperature. The precipitate was collected by filtration and dried *in vacuo* to afford the off-white solids (161 mg, 53.6%). mp: 246–248°C. MS: Calculated for $C_{20}H_{21}N_4O_4$ = 381.1563; $(M+H)^+$ = 381.1582

found. ^{1}H NMR (DMSO) ppm: 2.54–2.58 (m, 4H, CH_2), 2.70–2.73 (m, 4H, CH_2), 7.16–7.19 (t, *J* = 7.53, 2H, Ar-H), 7.39–7.43 (m, 3H, Ar-H), 7.56–7.58 (m, 1H, Ar-H). ^{13}C NMR (DMSO) ppm: 46.1; 48.6; 74.4; 118.2; 119.4; 121.4; 124.2; 130.2; 130.4; 150.6; 156.1; 157.4; 170.8. IR (KBr): v (cm^{-1}): 3065, 1705, 1665 1631.

5-(4-(thiophene-2-carbonyl)piperazin-1-yl)-5-(4-phenoxyphenyl) pyrimidine-2,4,6(1H,3H,5H)-trione (44)

A suspension of 5-(4-phenoxyphenyl)-5-(piperazin-1-yl)pyrimidine-2,4,6 (*1H,3H,5H*)-trione (380 mg, 1 mmol) in 10 ml THF was cooled to -70°C and triethylamine (101.2 mg, 1 mmol) was added. A solution of thiophene-2-carbonyl chloride (146.6 mg, 1 mmol) was added to the suspension dropwise. After stirring for 2 h at -70°C, the reaction mixture was dried and purified by flash column chromatography to yield the pure compounds (203mg, 35.3%) as off-white solids. mp: 142–144°C. MS: Calculated for $C_{25}H_{23}N_4O_5$ = 491.1389; found $(M+H)^+$ = 491.1377. ^{1}H NMR ($CDCl_3$) ppm: 2.77–2.82 (m, 4H, CH_2), 3.77–3.79 (m, 4H, CH_2), 6.94–6.96 (d, *J* = 8.53, 2H, Ar-H), 6.89–7.04 (m, 3H, Ar-H&CH), 7.16–7.19 (t, *J* = 7.53, 1H, Ar-H), 7.35–7.39 (t, *J* = 7.53, 2H, Ar-H), 7.42–7.48 (m, 4H, Ar-H&CH), 9.63 (s, 1H, NH), 9.68 (s, 1H, NH). ^{13}C NMR ($CDCl_3$) ppm: 47.6; 67.5; 75.1; 117.9; 119.4; 121.0; 123.9; 128.6; 129.0; 129.3; 129.6; 132.6; 136.1; 148.6; 154.7; 155.4; 158.6; 163.5; 169.1; 169.2. IR (KBr): v (cm^{-1}): 2959, 1738, 1711, 1608.

5-(4-(4-cyanobenzoyl))piperazin-1-yl)-5-(4-phenoxyphenyl)pyrimidine-2,4,6(1*H*,3*H*,5*H*)-trione (45)

A suspension of 5-(4-phenoxyphenyl)-5-(piperazin-1-yl)pyrimidine-2,4,6 (*1H,3H,5H*)-trione (380 mg, 1 mmol) in 10 ml THF was cooled to -70°C and

triethylamine (101.2 mg, 1 mmol) was added. A solution of 4-cyanobenzoyl chloride (165.6 mg, 1 mmol) was added to the suspension dropwise. After stirring for 2 h at -70°C, the reaction mixture was dried and purified by flash column chromatography to yield the pure compounds (202mg, 39.7%) as light yellow solids. mp: 146–148°C. MS: Calculated for $C_{28}H_{24}N_5O_5$ = 510.1777; found $(M+H)^+$ = 510.1765. ^1H NMR ($CDCl_3$) ppm: 2.71–2.83 (m, 4H, CH_2), 3.78–3.81 (m, 4H, CH_2), 6.94–6.96 (d, *J* = 8.53, 2H, Ar-H), 7.00–7.03 (m, 2H, Ar-H), 7.17–7.21 (t, *J* = 7.53, 1H, Ar-H), 7.36–7.38 (d, *J* = 8.03, 1H, Ar-H), 7.40–7.46 (m, 3H, Ar-H), 7.51–7.53 (d, *J* = 7.53H, Ar-H), 7.68–7.70 (d, *J* = 7.53, 2H, Ar-H), 9.63 (s, 2H, NH). ^{13}C NMR ($CDCl_3$) ppm: 47.5; 67.5; 75.2; 117.6; 117.9; 119.5; 121.1; 124.1; 126.7; 127.5; 129.1; 129.7; 132.0; 132.6; 135.4; 139.2; 148.3; 155.2; 158.8; 168.1; 169.2. IR (KBr): v (cm^{-1}): 2959, 2231, 1738, 1711,1608.

5-(4-(6-chloropyridine-3-carbonyl)piperazin-1-yl)-5-(4-phenoxyphenyl) pyrimidine-2,4,6(1H,3H,5H)-trione (46)

A suspension of 5-(4-phenoxyphenyl)-5-(piperazin-1-yl)pyrimidine-2,4,6 (*1H,3H,5H*)-trione (380 mg, 1 mmol) in 10 ml THF was cooled to -70°C and triethylamine (101.2 mg, 1 mmol) was added. A solution of 6-chloropyridine-3-carbonyl chloride (176.0 mg, 1 mmol) was added to the suspension dropwise. After stirring for 2 h at -70°C, the reaction mixture was dried and purified by flash column chromatography to yield the pure compounds (220 mg, 42.4%) as off-white solids. mp: 203–206°C. MS: $(M+H)^+$ = 520.1390. Calculated for $C_{26}H_{23}ClN_5O_5$ = 520.1388. ^1H NMR ($CDCl_3$) ppm: 2.78–2.87 (m, 4H, CH_2), 3.78–3.81 (m, 4H, CH_2), 6.96–7.09 (m, 4H, Ar-H), 7.17–7.21 (t, 1H, *J* =7.53, Ar-H), 7.33–7.36 (m, 1H, Ar-H), 7.41–7.47 (m, 3H, Ar-H), 7.75–7.80 (m, 1H, Ar-H), 8.46–8.49 (m, 1H, Ar-H), 8.49–8.50 (d, 1H, *J* = 5.02, Ar-H), ^{13}C NMR ($CDCl_3$) ppm: 47.5; 67.5; 75.2; 117.6; 117.9; 119.5; 121.1; 124.1; 126.7; 127.5; 129.1; 129.7; 132.0; 132.6; 135.4; 139.2; 148.3; 155.2; 158.8; 168.1; 169.2. IR (KBr):

v (cm^{-1}): 2956, 1739, 1706, 1614.

Tert-butyl 4-(cyclopropylmethyl)-1,4-diazepane-1-carboxylate (48)

A solution of Boc-homopiperazine (400.6 mg, 2 mmol) and triethylamine (202.4 mg, 2 mmol) in methanol was treated with (bromomethyl)cyclopropane (270 mg, 2 mmol) and stirred for 24 h at room temperature. After reaction finished, the solvent was removed and the residue was purified by flash column chromatography to yield the pure oil compound (328 mg, 64.4%). MS: Calculated for $C_{14}H_{27}N_2O_2$ = 255.2073. $(M+H)^+$ = 255.2060 found. ^1H NMR ($CDCl_3$) ppm: 0.12–0.14 (m, 2H, CH_2), 0.49–0.51 (m, 2H, CH_2), 0.88–0.96 (m, 1H, CH), 1.34 (s, 9H, CH_3), 1.95–2.02 (m, 2H, CH_2), 2.50–2.55 (m, 2H, CH_2), 2.82–2.85 (m, 2H, CH_2), 2.87–2.90 (m, 2H, CH_2), 3.35–3.41 (m, 2H, CH_2), 3.49–3.52 (m, 1H, CH_2), 3.57–3.60 (m, 1H, CH_2). ^{13}C NMR ($CDCl_3$) ppm: 3.8; 7.1; 25.4; 27.8; 42.9; 43.9; 53.7; 55.2; 62.0; 79.2; 154.8. IR (CH_2Cl_2): v (cm^{-1}): 2974, 1701, 1699, 1590.

5-(4-acetyl-1,4-diazepan-1-yl)--5-(4-phenoxyphenyl)pyrimidine-2,4,6 (1H,3H,5H)-trione (49)

A solution of 5-bromo-5-(4-phenoxyphenyl)pyrimidine-2,4,6(1*H*,3*H*,5*H*)-trione (375 mg, 1.0 mmol) in methanol (5 ml) was treated with 1-(1,4-diazepan-1-yl)ethanone (284.4 mg, 2 mmol) and stirred for 24 h at ambient temperature. The reaction mixture was dried and purified by flash column chromatography to yield the pure compounds (222 mg, 50.9%) as off-white solids. mp: 136–139°C. MS: Calculated for $C_{23}H_{24}N_4O_5$ = 4459.1644. $(M+Na)^+$ = 459.1625 found. ^1H NMR (Acetone-D_6) ppm: 1.59–1.65 (m, 1H, CH_2), 1.72–1.78 (m, 1H, CH_2), 2.06–2.10 (m, 5H, CH_2+CH_3), 2.78–2.82 (m, 1H, CH_2), 2.92–2.94 (m, 1H, CH_2), 3.46–3.50 (m, 2H, CH_2), 4.04–4.09 (m, 2H, CH_2), 7.03–7.08 (m, 4H, Ar-H), 7.18–7.21 (t, *J* = 7.53, 1H, Ar-H), 7.40–7.44 (t, *J* = 7.33, 1H, Ar-H), 7.56–7.62 (m, 3H, Ar-H).

^{13}C NMR (Acetone-D_6) ppm: 21.2; 28.4; 48.1; 50.4; 52.5; 53.8; 78.1; 116.5; 118.9; 120.0; 121.9; 124.6; 130.0; 130.5; 133.4; 149.2; 156.6; 158.9; 170.1; 170.9. IR (KBr): v (cm^{-1}): 3067, 1737, 1706, 1608.

5-(4-benzyl-1,4-diazepan-1-yl)-5-(4-phenoxyphenyl)pyrimidine-2,4,6 (1H,3H,5H)-trione (50)

A solution of 5-bromo-5-(4-phenoxyphenyl)pyrimidine-2,4,6(1*H*,3*H*,5*H)*-trione (375 mg, 1.0 mmol) in methanol (5 ml) was treated with 1-benzyl-1,4-diazepane (380.6 mg, 2 mmol) and stirred for 24 h at ambient temperature. The reaction mixture was dried and purified by flash column chromatography to yield the pure compounds (304 mg, 62.7%) as off-white solids. mp: 123–125°C. MS: Calculated for $C_{28}H_{29}N_4O_4$ = 485.2189, $(M+H)^+$ = 485.2202 found. ^{1}H NMR (Acetone-D_6): ppm: 1.80–1.86 (m, 2H, CH_2), 2.07–2.10 (m, 2H, CH_2), 2.75 (s, broad, 2H, CH_2), 2.90–2.94 (m,4H, CH_2), 3.86 (s, 2H, CH_2), 7.02–7.08 (m, 4H, Ar-H), 7.18–7.21 (t, 1H, *J* = 7.33, Ar-H), 7.24–7.27 (t, *J* = 7.33,1H, Ar-H), 7.30–7.34 (t, 2H, *J* =7.33, Ar-H), 7.40–7.48 (m, 3H, Ar-H), 7.56–7.62 (m, 3H, Ar-H). ^{13}C NMR (Acetone-D_6) ppm: 28.3; 50.3; 51.1; 53.5; 57.6; 61.5; 77.6; 116.5; 118.9; 120.0; 121.9; 124.6; 127.8; 128.7; 129.7; 130.2; 130.4; 130.6; 131.4; 133.5; 149.3; 156.7; 158.9; 171.1. IR (KBr): v (cm^{-1}): 3062, 1736, 1708, 1604.

5-(4-phenoxyphenyl)-5-(cyclopropylmethyl)-1,4-diazepan-1-l)pyrimidine-2,4,6(1*H*,3*H*,5*H)*-trione (51)

A solution of 5-bromo-5-(4-phenoxyphenyl)pyrimidine-2,4,6(1*H*,3*H*,5*H)*-trione (375 mg, 1.0 mmol) in methanol (5 ml) was treated with *tert*-butyl 4-(cyclopropylmethyl)-1,4-diazepane-1-carboxylate (509 mg, 2 mmol) and stirred for 24 h at ambient temperature. The reaction mixture was dried and purified by flash column chromatography to yield the pure compounds (184 mg, 41.1%) as

off-white solids. mp: 201–204°C. MS: Calculated for $C_{25}H_{29}N_4O_4$ = 449.2189; found $(M+H)^+$ = 449.2186. ^{1}H NMR (MeOD) ppm: 0.47–0.49 (m, 2H, CH_2), 0.77–0.79 (m, 2H, CH_2), 1.16–1.19 (m, 1H, CH), 1.47–1.52 (m, 2H, CH_2), 2.01–2.10 (m, 2H, CH_2), 2.87–2.93 (m, 2H, CH_2), 3.41–3.46 (m, 2H, CH_2), 3.55–3.58 (m, 1H, CH_2), 3.62–3.66 (m, 1H, CH_2), 7.00–7.09 (m, 4H, Ar-H), 7.19–7.23 (t, *J* = 7.53, 1H, Ar-H), 7.40–7.44 (t, *J* = 7.53, 1H, Ar-H), 7.52–7.58 (m, 3H, Ar-H). ^{13}C NMR (MeOD) ppm: 4.9; 9.2; 26.2; 47.8; 51.0; 53.7; 56.8; 63.2; 78.5; 119.4; 119.8; 120.9; 122.6; 125.5; 130.6; 130.7; 131.2; 131.3; 150.6; 156.7; 157.2; 171.9. IR (KBr): v (cm^{-1}): 2962; 1768; 1711; 1604.

5-(1,4-diazepan-1-yl)-5-(4-phenoxyphenyl)pyrimidine-2,4,6(1H,3H,5H)-trione (52)

A solution of 5-bromo-5-(4-phenoxyphenyl)pyrimidine-2,4,6(1*H*,3*H*,5*H)*-trione (375 mg, 1.0 mmol) in methanol (5 ml) was treated with 1,4-diazepane (200.3 mg, 2 mmol) and stirred for 24 h at ambient temperature. The precipitate was collected by filtration and dried *in vacuo* to afford the off-white solids (229 mg, 58.0%). mp: 240–244°C. MS: Calculated for $C_{21}H_{23}N_4O_4$ = 395.1719. $(M+H)^+$ = 395.1704 found. ^{1}H NMR (DMSO) ppm: 1.52–1.58 (m, 2H, CH_2), 2.66–2.68 (m, 4H, CH_2), 2.69–2.71 (m, 2H, CH_2), 2.87–2.90 (m, 2H, CH_2), 6.99–7.06 (m, 4H, Ar-H), 7.16–7.19 (t, *J* = 7.53, 1H, Ar-H), 7.38–7.47 (m, 3H, Ar-H), 7.55–7.58 (m, 1H, Ar-H). ^{13}C NMR (DMSO) ppm: 29.8; 45.7; 49.6; 50.7; 53.0; 76.3; 115.7; 118.0; 119.3; 121.3; 124.0; 129.4; 130.2; 150.6; 155.8; 157.3; 172.1. IR (KBr): v (cm^{-1}): 3065, 1702, 1665, 1625.

5-(4-phenoxyphenyl)-5-(4-(cyclopropylcarbonyl)-1,4-diazepan-1-yl) pyrimidine-2,4,6(1H,3H,5H)-trione (53)

A suspension of 5-(1,4-diazepan-1-yl)-5-(4-phenoxyphenyl)pyrimidine-2,4,6(1*H*,3*H*, 5*H)*-trione (394 mg, 1 mmol) in 10 ml THF was cooled to -70°C and triethylamine (101.2 mg, 1 mmol) was added. A solution of cyclopropanecarbonyl

chloride (104.5 mg, 1 mmol) was added to the suspension dropwise. After stirring for 2 h at -70°C, the reaction mixture was dried and purified by flash column chromatography to yield the pure compounds (172 mg, 37.2%) as off-white solids. mp: = 147–149°C. MS: Calculated for $C_{25}H_{36}N_4O_5$ = 485.1801. $(M+H)^+$ = 485.1796 found. ^1H NMR ($CDCl_3$): ppm: 0.71–0.76 (m, 2H, CH_2), 1.00–1.03 (m, 2H, CH_2), 1.58–1.67 (m, 1H, CH), 1.70–1.77 (m, 2H, CH_2), 2.71–2.82 (m, 4H, CH_2), 3.57–3.63 (m, 2H, CH_2), 3.69–3.72 (m,1H, CH_2), 3.82–3.85 (m, 1H, CH_2), 6.90–7.03 (m, 4H, Ar-H), 7.14–7.17 (t, 1H, *J* = 7.53, Ar-H), 7.34–7.38 (t, *J* = 7.53,1H, Ar-H), 7.44–7.51 (m, 3H, Ar-H), 10.03 (s, 2H, NH). ^{13}C NMR ($CDCl_3$): 7.5; 11.0; 29.1; 46.7; 50.3; 51.1; 53.1; 77.8; 116.6; 118.2; 119.6; 121.2; 124.1; 129.3; 129.8; 132.8; 149.1; 155.5; 158.6; 170.5; 173.0. IR (KBr): v (cm^{-1}): 3000, 1734, 1709, 1607, 1587.

5-(4-phenoxyphenyl)-5-(4-(thiophene-2-carbonyl)-1,4-diazepan-1-yl) pyrimidine-2,4,6(1H,3H,5H)-trione (54)

A suspension of 5-(1,4-diazepan-1-yl)-5-(4-phenoxyphenyl)pyrimidine-2,4,6(1*H*,3*H*, 5*H)*-trione (394 mg, 1 mmol) in 10 ml THF was cooled to -70°C and triethylamine (101.2 mg, 1 mmol) was added. A solution of thiophene-2-carbonyl chloride (146.6 mg, 1 mmol) was added to the suspension dropwise. After stirring for 2 h at -70°C, the reaction mixture was dried and purified by flash column chromatography to yield the pure compounds (178 mg, 35.3%) as off-white solids. mp: 110–113°C. MS: Calculated for $C_{26}H_{25}N_4O_5S$ = 527.1365. $(M+H)^+$ = 527.1342 found. ^1H NMR ($CDCl_3$): ppm: 1.76–1.86 (m, 2H, CH_2), 2.79–2.90 (m, 4H, CH_2), 3.60–3.69 (m, 2H, CH_2), 3.80–3.85 (m, 2H, CH_2), 6.87–7.01 (m, 5H, CH), 7.13–7.17 (t, 1H, *J* = 7.53, Ar-H), 7.33–7.46 (m, *6*H, CH), 9.57 (s, 2H, NH). ^{13}C NMR ($CDCl_3$): 30.0; 45.6; 49.2; 50.7; 53.4 77.7; 117.8; 119.4; 121.0; 123.9; 128.6; 129.0; 129.3; 129.6; 132.6; 136.1 148.7; 154.6; 155.3; 158.6; 164.4; 169.9; 171.0. IR (KBr): v (cm^{-1}): 3067, 1736, 1708, 1605, 1587.

5-(4-phenoxyphenyl)-5-(4-(4-cyanobenzoyl)-1,4-diazepan-1-yl) pyrimidine-2,4,6(1H,3H,5H)-trione (55)

A suspension of 5-(1,4-diazepan-1-yl)-5-(4-phenoxyphenyl)pyrimidine-2,4,6(1*H*,3*H*, 5*H)*-trione (394 mg, 1 mmol) in 10 ml THF was cooled to -70°C and triethylamine (101.2 mg, 1 mmol) was added. A solution of 4-cyanobenzoyl chloride (165.6 mg, 1 mmol) was added to the suspension dropwise. After stirring for 2 h at -70°C, the reaction mixture was dried and purified by flash column chromatography to yield the pure compounds (163 mg, 31.1%) as yellow solids. 220–224°C. MS: Calculated for $C_{29}H_{26}N_5O_5$ = 524.1934, $(M+H)^+$ = 524.1934 found. ^{1}H NMR ($CDCl_3$): ppm: 1.83–1.87 (m, 2H, CH_2), 2.76–2.84 (m, 3H, CH_2), 3.21–3.25 (m, 1H, CH_2), 3.41–3.45 (m, 1H, CH_2), 3.67–3.70 (m, 1H, CH_2), 3.74–3.78 (m, 1H, CH_2), 3.82–3.86 (m, 1H, CH_2), 6.84–7.00 (m, 4H, Ar-H), 7.15–7.19 (t, 1H, *J* = 7.53, Ar-H), 7.34–7.40 (m, 2H, Ar-H), 7.44–7.48 (m, 2H, Ar-H), 7.53–7.57 (m, 2H, Ar-H), 7.66–7.72 (m, 2H, Ar-H), 10.11 (s, 2H, NH). ^{13}C NMR ($CDCl_3$): 29.7; 44.7; 48.2; 50.6; 51.6; 77.6; 112.9; 116.7; 116.8; 118.2; 119.8; 121.3; 124.2; 127.1; 127.4; 129.2; 130.0; 132.3; 132.8; 135.7; 140.9; 149.0; 154.7; 158.9; 169.8; 170.5. IR (KBr): v (cm^{-1}): 3068, 2230, 1737, 1709, 1606, 1582.

5-(4-phenoxyphenyl)-5-(4-(6-chloropyridine-3-carbonyl)-1,4-diazepan-1-yl)pyrimidine-2,4,6(1H,3H,5H)-trione (56)

A suspension of 5-(1,4-diazepan-1-yl)-5-(4-phenoxyphenyl)pyrimidine-2,4,6(1*H*,3*H*, 5*H)*-trione (394 mg, 1 mmol) in 10 ml THF was cooled to -70°C and triethylamine (101.2 mg, 1 mmol) was added. A solution of 6-chloropyridine-3-carbonyl chloride (176.0 mg, 1 mmol) was added to the suspension dropwise. After stirring for 2 h at -70°C, the reaction mixture was dried and purified by flash column chromatography to yield the pure compounds (172 mg, 32.2%) as

off-white solids. mp: 246–248°C. MS: Calculated for $C_{24}H_{25}ClN_5O_5$ = 534.1544, $(M+H)^+$ = 534.1569 found. ^{1}H NMR (DMSO): ppm: 1.48–1.54 (m, 1H, CH_2), 1.62–1.68 (m, 1H, CH_2), 2.73–2.85 (m, 4H, CH_2), 3.19–3.23 (m, 1H, CH_2), 3.40–3.43 (m, 1H, CH_2), 3.54–3.47 (m, 1H, CH_2), 3.67–3.70 (m, 1H, CH_2), 6.96–7.09 (m, 4H, Ar-H), 7.15–7.19 (t, 1H, *J* =7.53, Ar-H), 7.33–7.36 (m, 1H, Ar-H), 7.40–7.47 (m, 3H, Ar-H), 7.57–7.62 (m, 1H, Ar-H), 7.91–7.96 (t, 1H, *J* = 8.03, Ar-H), 8.49–8.50 (d, 1H, *J* = 5.02, Ar-H), 11.50 (s, 2H, NH). ^{13}C NMR (DMSO): 29.5; 43.9; 47.8; 50.7; 52.6; 76.8; 116.0; 118.3; 119.5; 121.6; 124.3; 124.9; 128.0; 129.1; 129.4; 130.2; 132.2; 133.0; 138.2; 139.2; 147.8; 149.4; 150.5; 155.0; 157.7; 170.7; 170.8. IR (KBr): v (cm^{-1}): 3068, 1736, 1708, 1609, 1586.

5-(4-phenoxyphenyl)-5-(4-(cyclobutanecarbonyl)-1,4-diazepan-1-yl) pyrimidine-2,4,6(1H,3H,5H)-trione (57)

A suspension of 5-(1,4-diazepan-1-yl)-5-(4-phenoxyphenyl)pyrimidine-2,4,6(1*H*,3*H*, 5*H)*-trione (394 mg, 1 mmol) in 10 ml THF was cooled to -70°C and triethylamine (101.2 mg, 1 mmol) was added. A solution of cyclobutanecarbonyl chloride (118.6 mg, 1 mmol) was added to the suspension dropwise. After stirring for 2 h at -70°C, the reaction mixture was dried and purified by flash column chromatography to yield the pure compounds (165 mg, 34.6%) as off-white solids. mp: 142–145°C. MS: Calculated for $C_{26}H_{29}N_4O_5$ = 477.2138. $(M+H)^+$ = 477.2133 found. ^{1}H NMR ($CDCl_3$): ppm: 1.68–1.74 (m, 2H, CH_2), 1.82–2.01 (m, 2H, CH_2), 2.05–2.15 (m, 2H, CH_2), 2.30–2.45 (m, 2H, CH_2), 2.71–2.84 (m, 4H, CH_2), 3.23–3.31 (m, 1H, CH), 3.52–3.60 (m, 2H, CH_2), 3.69–3.72 (m,1H, CH_2), 3.77–3.80 (m, 1H, CH_2), 6.91–7.05 (m, 4H, Ar-H), 7.15–7.20 (t, 1H, *J* = 7.53, Ar-H), 7.36–7.40 (t, *J* = 7.53,1H, Ar-H), 7.44–7.49 (m, 3H, Ar-H), 9.55 (s, 2H, NH). ^{13}C NMR ($CDCl_3$): 17.7; 24.9; 29.2; 36.7; 45.8; 49.4; 50.2; 53.4; 77.6; 116.5; 118.1; 119.5; 121.0; 124.0; 129.2; 129.6; 132.6; 148.7; 154.7; 158.5; 170.0; 174.5. IR (KBr): v (cm^{-1}): 3068, 1754, 1736, 1708, 1608.

5-(4-phenoxyphenyl)-5-(4-(2-(phenylthio)acetyl)-1,4-diazepan-1-yl) pyrimidine-2,4,6(1H,3H,5H)-trione (58)

A suspension of 5-(1,4-diazepan-1-yl)-5-(4-phenoxyphenyl)pyrimidine-2,4,6(1*H*,3*H*, 5*H)*-trione (394 mg, 1 mmol) in 10 ml THF was cooled to -70°C and triethylamine (101.2 mg, 1 mmol) was added. A solution of 2-(phenylthio)acetyl chloride (186.7 mg, 1 mmol) was added to the suspension dropwise. After stirring for 2 h at -70°C, the reaction mixture was dried and purified by flash column chromatography to yield the pure compounds (207 mg, 38.0%) as off-white solids. mp: 100–103°C. MS: Calculated for $C_{29}H_{29}N_4O_5S$ = 545.1869, $(M+H)^+$ = 545.1840 found. ^{1}H NMR ($CDCl_3$): ppm: 1.67–1.74 (m, 2H, CH_2), 2.71–2.80 (m, 3H, CH_2), 2.88–2.91 (m, 1H, CH_2), 3.42–3.45 (m, 1H, CH_2), 3.58–3.64 (m, 2H, CH_2), 3.67–3.70 (m, 1H, CH_2), 3.82 (s, 2H, CH_2), 6.88–6.92 (m, 4H, Ar-H), 7.01–7.03 (d, 1H, *J* = 8.53, Ar-H), 7.15–7.20 (m, 2H, Ar-H), 7.23–7.29 (m, 2H, Ar-H), 7.35–7.39 (t, 1H, *J* = 7.53, Ar-H), 7.41–7.49 (m, 5H, Ar-H), 9.75 (s, 2H, NH). ^{13}C NMR ($CDCl_3$): 29.3; 36.7; 47.2; 50.7; 52.2; 53.1; 77.9; 116.8; 118.3; 119.8; 121.4; 124.3; 125.4; 126.9; 128.9; 129.5; 129.9; 130.3; 132.9; 135.0; 149.1; 154.9; 158.3; 170.3; 170.4. IR (KBr): v (cm^{-1}): 3064, 1736, 1708, 1611.

5-(4-phenoxyphenyl)-5-(4-(3,5-diethoxybenzoyl)-1,4-diazepan-1-yl) pyrimidine-2,4,6(1H,3H,5H)-trione (59)

A suspension of 5-(1,4-diazepan-1-yl)-5-(4-phenoxyphenyl)pyrimidine-2,4,6(1*H*,3*H*, 5*H)*-trione (394 mg, 1 mmol) in 10 ml THF was cooled to -70°C and triethylamine (101.2 mg, 1 mmol) was added. A solution of 3,5-diethoxybenzoyl chloride (228.7 mg, 1 mmol) was added to the suspension dropwise. After stirring for 2 h at -70°C, the reaction mixture was dried and purified by flash column chromatography to yield the pure compounds (195 mg, 33.2%) as off-white solids. mp: 213–217°C. MS: Calculated for $C_{32}H_{35}N_4O_7$ = 587.2506, $(M+H)^+$ =

587.2488 found. ^{1}H NMR (DMSO): ppm: 1.27–1.33 (dt, *J* = 7.53, 6H, CH_3), 1.50–1.56 (m, 1H, CH_2), 1.65–1.71 (m, 1H, CH_2), 2.70–2.73 (m, 3H, CH_2), 2.83–2.86 (m, 1H, CH_2), 3.10–3.13 (m, 1H, CH_2), 3.34–3.40 (m, 1H, CH_2), 3.51–3.64 (m, 1H, CH_2), 3.63–3.66 (m, 1H, CH_2), 3.95–4.06 (m, 4H, CH_2), 6.44–6.50 (m, 3H, Ar-H), 6.87–6.92 (m, 1H, Ar-H), 7.01–7.10 (m, 3H, Ar-H), 7.20–7.23 (m, 1H, Ar-H), 7.35–7.47 (m, 3H, Ar-H), 7.57–7.60 (m, 1H, Ar-H), 11.57 (s, 2H, NH). ^{13}C NMR (DMSO): 14.6; 29.7; 47.7; 50.7; 52.6; 53.7; 63.3; 76.7; 101.1; 104.6; 116.0; 118.1; 119.5; 121.6; 124.2; 124.9; 129.1; 130.2; 133.0; 139.2; 149.4; 155.4; 157.8; 159.5; 169.9; 170.6. IR (KBr): v (cm^{-1}): 3063, 2851, 1736, 1706, 1590.

5-(4-phenoxyphenyl)-5-(4-(4-(trifluoromethoxy)benzoyl)-1,4-diazepan-1-yl)pyrimidine-2,4,6(1H,3H,5H)-trione (60)

A suspension of 5-(1,4-diazepan-1-yl)-5-(4-phenoxyphenyl)pyrimidine-2,4,6(1*H*,3*H*, 5*H)*-trione (394 mg, 1 mmol) in 10 ml THF was cooled to -70°C and triethylamine (101.2 mg, 1 mmol) was added. A solution of 4-(trifluoromethoxy)benzoyl chloride (224.6 mg, 1 mmol) was added to the suspension dropwise. After stirring for 2 h at -70°C, the reaction mixture was dried and purified by flash column chromatography to yield the pure compounds (186 mg, 31.9%) as off-white solids. mp: 183–187°C. MS: Calculated for $C_{29}H_{26}F_3N_4O_6$ = 583.1804, $(M+H)^+$ = 583.1823 found.^{1}H NMR (MeOD): ppm: 1.61–1.67 (m, 1H, CH_2), 1.81–1.87 (m, 1H, CH_2), 2.84–2.87 (m, 3H, CH_2), 3.00–3.02 (m, 1H, CH_2), 3.27–3.30 (m, 1H, CH_2), 3.52–3.55 (m, 1H, CH_2), 3.68–3.71 (m, 1H, CH_2), 3.81–3.84 (m, 1H, CH_2), 6.84–6.89 (m, 1H, Ar-H), 6.92–6.95 (m, 1H, Ar-H), 6.98–7.02 (m, 1H, Ar-H), 7.03–7.07 (m, 1H, Ar-H), 7.17–7.21 (t, 1H, *J* = 7.53, Ar-H), 7.37–7.46 (m, 4H, Ar-H), 7.51–7.54 (m, 1H, Ar-H), 7.55–7.57 (m, 1H, Ar-H), 7.58–7.63 (m, 2H, Ar-H). ^{13}C NMR (MeOD): ppm: 28.8; 48.4; 51.4; 52.6; 53.7; 78.7; 117.4; 118.8; 119.2; 120.5; 122.0; 122.3; 125.1; 125.9;

129.4; 129.9; 130.9; 136.8; 150.9; 156.7; 159.4; 160.0; 172.1; 172.4. IR (KBr): v (cm^{-1}): 3067, 2852, 1752, 1732, 1708, 1603.

5-(4-phenoxyphenyl)-5-(4-(3-cyclopentylpropanoyl)-1,4-diazepan-1-yl)pyrimidine-2,4,6(1*H*,3*H*,5*H*)-trione (61)

A suspension of 5-(1,4-diazepan-1-yl)-5-(4-phenoxyphenyl)pyrimidine-2,4,6(1*H*,3*H*, 5*H*)-trione (394 mg, 1 mmol) in 10 ml THF was cooled to -70°C and triethylamine (101.2 mg, 1 mmol) was added. A solution of 3-cyclopentylpropanoyl chloride (160.6 mg, 1 mmol) was added to the suspension dropwise. After stirring for 2 h at -70°C, the reaction mixture was dried and purified by flash column chromatography to yield the pure compounds (196 mg, 38.1%) as off-white solids. mp: 139–141°C. MS: Calculated for $C_{29}H_{35}N_4O_5$ = 519.2607, $(M+H)^+$ = 19.2609 found. ^1H NMR ($CDCl_3$) δ ppm: 1.50–1.52 (m, 2H, CH_2), 1.58–1.61 (m, 2H, CH_2), 1.65–1.69 (m, 2H, CH_2), 1.71–1.77 (m, 5H, CH_2+CH), 1.86–1.90 (m, 2H, CH_2), 2.33–2.39 (m, 2H, CH_2), 2.73–2.80 (m, 3H, CH_2), 3.40–3.43 (m, 1H, CH_2), 3.59–3.62 (m, 1H, CH_2), 3.64–6.67 (m, 1H, CH_2), 3.70–3.73 (m, 1H, CH_2), 3.77–3.80 (m, 1H, CH_2), 6.92–7.01 (m, 4H, Ar-H), 7.04–7.06 (d, *J* = 7.53, 1H, Ar-H), 7.37–7.41 (t, *J* = 8.53, 1H, Ar-H), 7.46–7.49 (m, 3H, Ar-H), 9.36–9.54 (d, 2H, NH). ^{13}C NMR ($CDCl_3$) δ ppm: 25.1; 29.6; 31.5; 32.3; 32.7; 34.1; 39.8; 44.6; 46.9; 50.4; 52.3; 52.7; 77.8; 118.2; 118.4; 121.4; 124.3; 129.5; 129.9; 148.8; 155.0; 158.3; 170.2; 170.3; 173.4. IR (KBr): v (cm^{-1}): 3065, 1750, 1731, 1697, 1598.

5-(4-phenoxyphenyl)-5-(4-(2,5-diethoxybenzoyl)-1,4-diazepan-1-yl) pyrimidine-2,4,6(1H,3H,5H)-trione (62)

A suspension of 5-(1,4-diazepan-1-yl)-5-(4-phenoxyphenyl)pyrimidine-2,4,6(1*H*,3*H*, 5*H*)-trione (394 mg, 1 mmol) in 10 ml THF was cooled to -70°C and

triethylamine (101.2 mg, 1 mmol) was added. A solution of 2,5-diethoxybenzoyl chloride (228.7 mg, 1 mmol) was added to the suspension dropwise. After stirring for 2 h at -70°C, the reaction mixture was dried and purified by flash column chromatography to yield the pure compounds (208 mg, 35.4%) as off-white solids. mp: 117–119°C. MS: Calculated for $C_{32}H_{35}N_4O_7$ = 587.2506, $(M+H)^+$ = 587.2507 found. ^1H NMR ($CDCl_3$): ppm: 1.35–1.38 (m, 6H, CH_3), 1.86–1.91 (m, 2H, CH_2), 2.66–2.73(m, 1H, CH_2), 2.82–2.93 (m, 3H, CH_2), 3.14–3.25 (m, 1H, CH_2), 3.43–3.51 (m, 1H, CH_2), 3.79–3.89 (m, 2H, CH_2), 3.96–4.00 (m, 4H, CH_2), 6.78–6.87 (m, 5H, Ar-H), 6.95–6.97 (d, *J* = 8.03, 1H, Ar-H), 7.01–7.05 (m, 2H, Ar-H), 7.17–7.21 (t, 1H, *J* = 7.53, Ar-H), 7.36–7.40 (t , *J* = 7.28, 2H, Ar-H), 7.51–7.54 (4, *J* = 7.03,1H, Ar-H). ^{13}C NMR ($CDCl_3$): 14.9; 29.4; 47.7; 50.9; 52.3; 53.1; 64.0; 64.8; 77.8; 113.7; 113.9; 116.0; 118.2; 118.4; 119.8; 121.4; 124.3; 124.9; 127.4; 129.2; 130.0; 132.9; 148.4; 152.9; 155.6; 158.9; 169.1; 169.9. IR (KBr): v (cm^{-1}): 3069, 2845, 1738, 1710, 1606, 1588.

5-(4-phenoxyphenyl)-5-(4-(2-chloro-6-methylpyridine-4-carbonyl)-1,4-diazepan-1-yl)pyrimidine-2,4,6(1H,3H,5H)-trione (63)

A suspension of 5-(1,4-diazepan-1-yl)-5-(4-phenoxyphenyl)pyrimidine-2,4,6(1*H*,3*H*, 5*H)*-trione (394 mg, 1 mmol) in 10 ml THF was cooled to -70°C and triethylamine (101.2 mg, 1 mmol) was added. A solution of 2-chloro-6-methylpyridine-4-carbonyl chloride (190 mg, 1 mmol) was added to the suspension dropwise. After stirring for 2 h at -70°C, the reaction mixture was dried and purified by flash column chromatography to yield the pure compounds (137 mg, 25.0%) as off-white solids. mp: 116–119°C. MS: Calculated for $C_{28}H_{27}ClN_5O_5$ = 548.1701, $(M+H)^+$ = 548.1712 found. ^1H NMR ($CDCl_3$) ppm: 1.86–1.88 (m, 2H, CH_2), 2.52–2.55 (d, 3H, CH_3), 2.82–2.94 (m, 4H, CH_2), 3.19–3.24 (m, 1H, CH_2), 3.42–3.46 (m, 1H, CH_2), 3.66–3.70 (m, 1H, CH_2), 3.78–3.84 (m, 1H, CH_2), 6.89–6.91 (d, *J* = 8.03, 2H, Ar-H), 6.94–6.96 (d, *J* = 8.03, 1H, Ar-

H), 6.99–7.03 (t, *J* = 7.53, 1H, Ar-H), 7.13–7.22 (m, 3H, Ar-H), 7.35–7.39 (t, 2H, *J* = 7.53, Ar-H), 7.43–7.47 (m , 2H, Ar-H), 9.69–9.73 (m, 2H, NH). ^{13}C NMR ($CDCl_3$): 24.0; 29.7; 48.1; 50.8; 52.5; 54.1; 77.8; 116.9; 118.1; 119.0; 119.3; 119.8; 121.4; 124.4; 129.2; 129.9; 132.9; 147.3; 148.9; 154.8; 159.0; 160.2; 168.1; 170.1. IR (KBr): v (cm^{-1}): 3074, 2959, 2849, 1738, 1710, 1608.

5-(4-phenoxyphenyl)-5-(4-(2-oxoimidazolidine-1-carbonyl)-1,4-diazepan-1-yl)pyrimidine-2,4,6(1H,3H,5H)-trione (64)

A suspension of 5-(1,4-diazepan-1-yl)-5-(4-phenoxyphenyl)pyrimidine-2,4,6(1*H*,3*H*, 5*H)*-trione (394 mg, 1 mmol) in 10 ml THF was cooled to -70°C and triethylamine (101.2 mg, 1 mmol) was added. A solution of 2-oxoimidazolidine-1-carbonyl chloride (148.5 mg, 1 mmol) was added to the suspension dropwise. After stirring for 2 h at -70°C, the reaction mixture was dried and purified by flash column chromatography to yield the pure compounds (176 mg, 34.7%) as off-white solids. mp: 186–190°C. MS: Calculated for $C_{25}H_{27}N_6O_6$ = 529.1838, $(M+H)^+$ = 529.1812 found. ^1H NMR (MeOD) ppm: 1.76–1.82 (m, 2H, CH_2), 2.80–2.83 (m, 2H, CH_2), 2.91–2.94 (m, 2H, CH_2), 3.46–3.50 (m, 4H, CH_2), 3.62–3.68 (m, 2H, CH_2), 3.84–3.87 (m, 2H, CH_2), 5.51 (s, 1H, NH), 6.99–7.01 (d, *J* = 8.04, 2H, Ar-H), 7.05–7.07 (d, *J* = 8.03, 2H, Ar-H), 7.18–7.21 (t, *J* = 7.53, 1H, Ar-H), 7.40–7.43 (t, *J* = 8.03, 2H, Ar-H), 7.50–7.53 (m, 2H, Ar-H). ^{13}C NMR (MeOD) ppm: 29.4; 30.7; 38.9; 48.5; 51.8; 53.4; 54.8; 78.8; 118.5; 119.1; 120.8; 125.3; 130.6; 131.1; 150.9; 155.8; 157.5; 157.8; 160.4; 172.5. IR (KBr): v (cm^{-1}): 3068, 2958, 1735, 1641, 1588.

5-(4-phenoxyphenyl)-5-(4-(3-methylbenzofuran-2-carbonyl)-1,4-diazepan-1-yl)pyrimidine-2,4,6(1H,3H,5H)-trione (65)

A suspension of 5-(1,4-diazepan-1-yl)-5-(4-phenoxyphenyl)pyrimidine-

2,4,6(1*H*,3*H*, 5*H*)-trione (394 mg, 1 mmol) in 10 ml THF was cooled to -70°C and triethylamine (101.2 mg, 1 mmol) was added. A solution of 4-methylbenzofuran-2-carbonyl chloride (194.6 mg, 1 mmol) was added to the suspension dropwise. After stirring for 2 h at -70°C, the reaction mixture was dried and purified by flash column chromatography to yield the pure compounds (160 mg, 28.9%) as off-white solids. mp: 134–137°C. MS: Calculated for $C_{31}H_{29}N_4O_6$ = 533.2093, $(M+H)^+$ = 533.2087 found. ^{1}H NMR (MeOD) ppm: 1.76–1.82 (m, 2H, CH_2), 2.43 (s, 3H, CH_3), 2.79–2.83 (m, 1H, CH_2), 2.90–2.94 (m, 1H, CH_2), 3.45–3.48 (m, 1H, CH_2), 3.58–3.63 (m, 1H, CH_2), 3.70–3.73 (m, 1H, CH_2), 3.79–3.85 (m, 2H, CH_2), 3.95–3.98 (m, 2H, CH_2), 6.88–7.02 (m, 3H, Ar-H), 7.14–7.17 (t, *J* = 7.53, 1H, Ar-H), 7.23–7.26 (t, *J* = 7.53, 1H, Ar-H), 7.30–7.37 (m, 3H, Ar-H), 7.41–7.44 (m, 1H, Ar-H), 7.47–7.54 (m, 2H, Ar-H), 7.58–7.60 (m, 1H, Ar-H), 7.63–7.65 (m, 1H, Ar-H). ^{13}C NMR (MeOD) ppm: 8.8; 28.6; 48.7; 51.9; 52.8; 54.3; 78.9; 112.4; 119.0; 119.2; 120.7; 121.3; 121.5; 122.4; 125.3; 130.5; 131.1; 134.1; 145.8; 150.9; 155.0; 157.3; 159.4; 160.3; 172.4. IR (KBr): v (cm^{-1}): 3065, 2954, 2846, 1737, 1711, 1608, 1588.

5-(4-phenoxyphenyl)-5-(4-(3-chloro-6-fluorobenzo[b]-thiophene-2-carbonyl)-1,4-diazepan-1-yl)pyrimidine-2,4,6(1H,3H,5H)-trione (66)

A suspension of 5-(1,4-diazepan-1-yl)-5-(4-phenoxyphenyl)pyrimidine-2,4,6(1*H*,3*H*, 5*H*)-trione (394 mg, 1 mmol) in 10 ml THF was cooled to -70°C and triethylamine (101.2 mg, 1 mmol) was added. A solution of 3-chloro-6-fluorobenzo[b]-thiophene-2-carbonyl chloride (247.9 mg, 1 mmol) was added to the suspension dropwise. After stirring for 2 h at -70°C, the reaction mixture was dried and purified by flash column chromatography to yield the pure compounds (163 mg, 26.9%) as off-white solids. mp: 138–142°C. MS: Calculated for $C_{30}H_{24}ClFN_4O_5SNa$ = 629.1609, $(M+Na)^+$ = 629.1601 found. ^{1}H NMR ($CDCl_3$) ppm: 1.70–1.76 (m, 1H, CH_2), 1.92–1.98 (m, 1H, CH_2), 2.85–2.91 (m, 3H, CH_2), 3.00–

3.05 (m, 1H, CH_2), 3.43–3.46 (m, 1H, CH_2), 3.68–3.72(m, 1H, CH_2), 3.80–3.85 (m, 1H, CH_2), 3.93–3.98 (m, 1H, CH_2), 6.84–6.90 (t, *J* = 8.03, 1H, Ar-H), 6.95–7.13 (m, 3H, Ar-H), 7.23–7.34 (m, 2H, Ar-H), 7.40–7.57 (m, 5H, Ar-H), 7.77–7.88 (m, 1H, Ar-H), 9.45–9.57 (m, 2H, NH). ^{13}C NMR ($CDCl_3$): 29.4; 47.8; 50.5; 52.3; 53.4; 77.6; 108.6; 114.5; 116.6; 117.9; 118.3; 119.5; 121.1; 123.5; 124.1; 128.4; 129.4; 131.7; 137.9; 148.7; 154.3; 155.0; 158.1; 158.7; 162.4; 169.9. IR (KBr): v (cm^{-1}): 3071, 2953, 1736, 1708, 1606, 1588.

5-(4-phenoxyphenyl)-5-(4-(2,5-dimethylfuran-3-carbonyl)-1,4-diazepan-1-yl)pyrimidine-2,4,6(1H,3H,5H)-trione (67)

A suspension of 5-(1,4-diazepan-1-yl)-5-(4-phenoxyphenyl)pyrimidine-2,4,6(1*H*,3*H*, 5*H)*-trione (394 mg, 1 mmol) in 10 ml THF was cooled to -70°C and triethylamine (101.2 mg, 1 mmol) was added. A solution of 2,5-dimethylfuran-3-carbonyl chloride (158.6 mg, 1 mmol) was added to the suspension dropwise. After stirring for 2 h at -70°C, the reaction mixture was dried and purified by flash column chromatography to yield the pure compounds (193 mg, 37.4%) as off-white solids. mp: 122–126°C. MS: Calculated for $C_{28}H_{28}N_4O_6Na$ = 539.1923, $(M+Na)^+$ = 539.1907 found. ^1H NMR ($CDCl_3$) ppm: 1.78–1.82 (m, 1H, CH_2), 1.93–1.99 (m, 1H, CH_2), 2.28–2.33 (d, 3H, CH_3), 2.39–2.44 (d, 3H, CH_3), 2.86–2.91 (m, 3H, CH_2), 2.99–3.04 (m, 1H, CH_2), 3.51–3.55 (m, 1H, CH_2), 3.72–3.78(m, 2H, CH_2), 3.85–3.89 (m, 1H, CH_2), 6.03–6.06 (d, 1H, CH), 7.01–7.03 (m, 4H, Ar-H), , 7.26–7.31 (t, *J* = 7.53, 1H, Ar-H), 7.49–7.58 (m, 4H, Ar-H), 9.33–9.48 (m, 2H, NH). ^{13}C NMR ($CDCl_3$): 12.8; 13.2; 27.5; 47.8; 51.4; 52.7; 53.5; 77.7; 105.8; 116.6; 118.2; 119.8; 121.4; 124.3; 129.4; 130.0; 149.6; 150.9; 155.6;158.0; 158.9; 166.9; 170.1. IR (KBr): v (cm^{-1}): 3068, 2952, 1737, 1708, 1588.

5-(4-phenoxyphenyl)-5-(4-(quinoxaline-2-carbonyl)-1,4-diazepan-1-yl)pyrimidine-2,4,6(1H,3H,5H)-trione (68)

A suspension of 5-(1,4-diazepan-1-yl)-5-(4-phenoxyphenyl)pyrimidine-2,4,6(1*H*,3*H*, 5*H)*-trione (394 mg, 1 mmol) in 10 ml THF was cooled to -70°C and triethylamine (101.2 mg, 1 mmol) was added. A solution of quinoxaline-2-carbonyl chloride (192.6 mg, 1 mmol) was added to the suspension dropwise. After stirring for 2 h at -70°C, the reaction mixture was dried and purified by flash column chromatography to yield the pure compounds (233 mg, 42.3%) as yellow solids. mp: 186–188°C. MS: Calculated for $C_{30}H_{26}N_6O_5Na$ = 573.1862, $(M+Na)^+$ = 578.7877 found. ^1H NMR ($CDCl_3$) δ ppm: 1.86–1.89 (m, 2H, CH_2), 2.89–2.92 (m, 2H, CH_2), 2.93–2.96 (m, 1H, CH_2), 3.01–3.04 (m, 1H, CH_2), 3.60–3.63 (m, 1H, CH_2), 3.80–3.83 (m, 2H, CH_2), 3.96–3.99 (m, 1H, CH_2), 6.85–6.87 (d, *J* = 8.53, 1H, Ar-H), 6.93–6.98 (m, 2H, Ar-H), 7.03–7.05 (d, *J* = 8.53, 1H, Ar-H), 7.15–7.18 (t, *J* = 8.03, 1H, Ar-H), 7.34–7.37 (m, 1H, Ar-H), 7.42–7.45 (m, 2H, Ar-H), 7.50–7.52 (d, *J* = 8.03, 1H, Ar-H), 7.79–7.85 (m, 2H, Ar-H), 8.05–8.09 (t, *J* = 7.53, 1H, Ar-H), 8.17–8.22 (t, *J* = 8.03, 1H, Ar-H), 9.27 (s, 1H, Ar-H), 9.38 (s, 1H, NH), 9.46 (s, 1H, NH). ^{13}C NMR ($CDCl_3$) δ ppm: 29.7; 48.8; 51.1; 51.9; 53.3; 77.7; 117.8; 117.9. 119.6. 121.1; 124.0; 125.2; 128.6; 128.8; 129.1; 129.3; 129.6; 130.3; 130.8; 132.6; 140.0; 141.8; 144.6; 148.5; 155.3; 158.7; 166.7; 169.8; 169.9. IR (KBr): ν (cm^{-1}): 3066, 2953, 1729, 169, 1578.

5-(4-phenoxyphenyl)-5-(4-(2-(thiophen-2-yl)acetyl)-1,4-diazepan-1-yl) pyrimidine-2,4,6(1*H*,3*H*,5*H)*-trione (69)

A suspension of 5-(1,4-diazepan-1-yl)-5-(4-phenoxyphenyl)pyrimidine-2,4,6(1*H*,3*H*, 5*H)*-trione (394 mg, 1 mmol) in 10 ml THF was cooled to -70°C and triethylamine (101.2 mg, 1 mmol) was added. A solution of 2-(thiophen-2-yl)acetyl chloride (160.6 mg, 1 mmol) was added to the suspension dropwise. After stirring for 2 h at -70°C, the reaction mixture was dried and purified by

flash column chromatography to yield the pure compounds (163 mg, 31.5%) as off-white solids. mp: 107–109°C. MS: Calculated for $C_{27}H_{27}N_4O_5S$ = 519.1702, $(M+H)^+$ = 519.1721 found. ^1H NMR ($CDCl_3$) δ ppm: 1.63–1.68 (m, 1H, CH_2), 1.73–1.77 (m, 1H, CH_2), 2.70–2.73 (m, 1H, CH_2), 2.74–2.77 (m, 1H, CH_2), 2.80–2.84 (m, 2H, CH_2), 3.40–3.43 (m, 1H, CH_2), 3.61–3.63 (m, 1H, CH_2), 3.67–3.70 (m, 1H, CH_2), 3.72–3.75 (m, 1H, CH_2), 3.93 (s, 1H, CH_2), 3.95 (s, 1H, CH_2), 6.90–6.95 (m, 4H, Ar-H), 7.01–7.05 (t, *J* = 7.53, 2H, Ar-H), 7.136–7.19 (m, 2H, Ar-H), 7.36–7.40 (m, 2H, Ar-H), 7.42–7.48 (m, 2H, Ar-H), 9.44 (s, 1H, NH), 9.51 (s, 1H, NH). ^{13}C NMR ($CDCl_3$) δ ppm: 29.8; 36.5; 45.8; 49.2; 51.0; 53.2; 77.8; 117.8; 119.4; 121.2; 123.9; 124.3; 125.4; 126.1; 129.0; 129.3; 129.6; 130.3; 139.1; 148.7; 155.3; 158.6; 159.3; 169.9. IR (KBr): ν (cm^{-1}): 3068, 2957, 2766, 1730, 1706, 1601.

2-(4-(2,4,6,-trioxo-5-(4-phenoxyphenyl)hexanhydropyrimidin-5-yl)-1,4-diazepane-1-carbonyl)benzyl benzoate (70)

A suspension of 5-(1,4-diazepan-1-yl)-5-(4-phenoxyphenyl)pyrimidine-2,4,6(1*H*,3*H*, 5*H)*-trione (394 mg, 1 mmol) in 10 ml THF was cooled to -70°C and triethylamine (101.2 mg, 1 mmol) was added. A solution of 2-(chlorocarbonyl)benzyl benzoate (274.7 mg, 1 mmol) was added to the suspension dropwise. After stirring for 2 h at -70°C, the reaction mixture was dried and purified by flash column chromatography to yield the pure compounds (230 mg, 36.3%) as off-white solids. mp: 120–123°C. MS: Calculated for $C_{36}H_{33}N_4O_7$ = 633.2349, $(M+H)^+$ = 633.2344 found. ^1H NMR ($CDCl_3$) δ ppm: 1.87–1.90 (m, 2H, CH_2), 2.71–2.74 (m, 2H, CH_2), 2.78–2.81 (m, 1H, CH_2), 2.92–2.96 (m, 1H, CH_2), 3.18–3.27 (m, 1H, CH_2), 3.35–3.40 (m, 1H, CH_2), 3.55–3.61 (m, 2H, CH_2), 3.78–3.81 (m, 1H, CH_2), 5.47 (s, 2H, CH_2), 6.83–6.85 (d, *J* = 8.53, 1H, Ar-H), 6.89–6.94 (t, *J* = 8.53, 1H, Ar-H), 6.99–7.03 (t, *J* = 8.53, 2H, Ar-H), 7.17–7.21(m, 2H, Ar-H), 7.35–7.46 (m, 9H, Ar-H), 7.52–7.56 (m, 2H, Ar-H),

8.04–8.06 (d, *J* = 8.33, 2H, Ar-H), 9.49–9.54 (d, 2H, NH). ^{13}C NMR ($CDCl_3$): 29.6; 47.8; 50.9; 52.5; 53.4; 64.1; 77.8; 118.0; 118.2; 119.8; 121.4; 124.3; 125.5; 126.5; 128.0; 128.3; 128.4; 128.9; 129.0; 129.2; 129.4; 129.6; 129.8; 129.9; 132.9; 133.1; 136.0; 148.9; 155.8; 158.9; 166.2; 170.2; 170.4; 170.6. . IR (KBr): v (cm^{-1}): 3065, 2953, 1738, 1708, 1607, 1588

5-(4-phenoxyphenyl)-5-(4-(6-(trifluoromethyl)nicotinoyl)-1,4-diazepan-1-yl)pyrimidine-2,4,6(1*H*,3*H*,5*H*)-trione (71)

A suspension of 5-(1,4-diazepan-1-yl)-5-(4-phenoxyphenyl)pyrimidine-2,4,6(1*H*,3*H*, 5*H*)-trione (394 mg, 1 mmol) in 10 ml THF was cooled to -70°C and triethylamine (101.2 mg, 1 mmol) was added. A solution of 6-(trifluoromethyl)nicotinoyl chloride (209.6 mg, 1 mmol) was added to the suspension dropwise. After stirring for 2 h at -70°C, the reaction mixture was dried and purified by flash column chromatography to yield the pure compounds (178 mg, 31.3%) as light yellow solids. mp: 162–165°C. MS: Calculated for $C_{28}H_{24}F_3N_5O_5Na$ = 590.1627, $(M+Na)^+$ = 590.1622 found. ^{1}H NMR ($CDCl_3$) δ ppm: 1.87–1.90 (m, 2H, CH_2), 2.83–2.90 (m, 2H, CH_2), 3.03–3.05 (m, 1H, CH_2), 3.31–3.35 (m, 1H, CH_2), 3.50–3.54 (m, 1H, CH_2), 3.77–3.81 (m, 2H, CH_2), 3.88–3.92 (m, 1H, CH_2), 6.92–6.94 (d, *J* = 8.53, 2H, Ar-H), 6.96–7.06 (m, 2H, Ar-H), 7.20–7.23 (t, *J* = 7.53, 1H, Ar-H), 7.39–7.43 (m, 2H, Ar-H), 7.48–7.51 (t, *J* = 7.53, 1H, Ar-H), 7.75–7.81(t, *J* = 7.53, 1H, Ar-H), 8.01–8.03 (d, *J* = 7.53, 2H, Ar-H), 8.34–8.36 (d, *J* = 7.53, 2H, Ar-H), 8.84 (s, 1H,Ar-H), ^{13}C NMR ($CDCl_3$): 29.6; 48.5; 51.6.52.3; 52.9; 78.1; 118.2; 118.4; 119.8; 120.0; 120.3; 121.6; 124.6; 125.5; 128.2; 129.1; 129.5; 130.0; 133.0; 138.8; 143.3; 147.9; 151.5; 155.5; 159.4; 167.7; 169.9. IR (KBr): v (cm^{-1}): 3090, 2954, 1730, 1702, 1610, 1588

5-(4-phenoxyphenyl)-5-(4-(4-methylbenzoyl)-1,4-diazepan-1-yl) pyrimidine-2,4,6(1*H*,3*H*,5*H*)-trione (72)

A suspension of 5-(1,4-diazepan-1-yl)-5-(4-phenoxyphenyl)pyrimidine-

2,4,6(1*H*,3*H*, 5*H)*-trione (394 mg, 1 mmol) in 10 ml THF was cooled to -70°C and triethylamine (101.2 mg, 1 mmol) was added. A solution of 4-methylbenzoyl chloride (154.6 mg, 1 mmol) was added to the suspension dropwise. After stirring for 2 h at -70°C, the reaction mixture was dried and purified by flash column chromatography to yield the pure compounds (193mg, 37.7%) as off-white solids. mp: 206–210°C. MS: Calculated for $C_{29}H_{29}N_4O_5$ = 513.2137, $(M+H)^+$ = 513.2138 found. ^{1}H NMR (DMSO) ppm: 1.48–1.53 (m, 1H, CH_2) 1.67–1.71 (m, 1H, CH_2), 2.27 (s, 3H, CH_3), 2.69–2.74 (m, 3H, CH_2), 2.83–2.87 (m, 1H, CH_2), 3.17–3.20 (m, 1H, CH_2), 3.37–3.43 (m, 1H, CH_2), 3.52–3.55 (m, 1H, CH_2), 3.65–3.69 (m, 1H, CH_2), 6.84–6.88 (m, 1H, Ar-H), 7.00–7.09 (m, 3H, Ar-H), 7.21–7.28 (m, 5H, Ar-H), 7.33–7.35 (d, *J* = 7.35, 1H, Ar-H), 7.40–7.47 (m, 2H, Ar-H), 7.57–7.59 (d, *J* = 7.53, 1H, Ar-H), 11.56 (s, 1H, NH), 11.62 (s, 1H, NH). ^{13}C NMR (DMSO) ppm: 20.8; 29.7; 47.6; 50.9; 52.8; 53.6; 76.7; 117.9; 119.5; 121.6; 124.2; 124.9; 126.3; 128.7; 129.1; 130.2; 133.0; 138.4; 149.4; 155.5; 157.7; 170.5; 170.7. IR (KBr): v (cm^{-1}): 3068, 2952, 3068, 2952, 1736, 1709, 1597.

5-(4-phenoxyphenyl)-5-(4-(4-bromobenzoyl)-1,4-diazepan-1-yl) pyrimidine-2,4,6(1*H*,3*H*,5*H)*-trione (73)

A suspension of 5-(1,4-diazepan-1-yl)-5-(4-phenoxyphenyl)pyrimidine-2,4,6(1*H*,3*H*, 5*H)*-trione (394 mg, 1 mmol) in 10 ml THF was cooled to -70°C and triethylamine (101.2 mg, 1 mmol) was added. A solution of 4-bromobenzoyl chloride (219 mg, 1 mmol) was added to the suspension dropwise. After stirring for 2 h at -70°C, the reaction mixture was dried and purified by flash column chromatography to yield the pure compounds (247 mg, 42.8%) as off-white solids. mp: 258–260°C. MS: Calculated for $C_{28}H_{25}BrN_4O_5Na$ = 599.0906, $(M+Na)^+$ = 599.0880 found. ^{1}H NMR (DMSO) ppm: 1.49–1.53 (m, 1H, CH_2) 1.68–1.72 (m, 1H, CH_2), 2.68–2.74 (m, 3H, CH_2), 2.82–2.87 (m, 1H, CH_2), 3.17–3.20 (m, 1H, CH_2), 3.35–3.41 (m, 1H, CH_2), 3.50–3.54 (m, 1H, CH_2), 3.65–3.69 (m, 1H, CH_2),

6.91–6.94 (m, 2H, Ar-H), 7.00–7.09 (m, 2H, Ar-H), 7.19–7.23 (t, *J* = 7.53, 1H, Ar-H), 7.27–7.32 (m, 4H, Ar-H), 7.45–7.49 (m, 2H, Ar-H), 7.59–7.61 (d, *J* = 7.53, 2H, Ar-H). ^{13}C NMR (DMSO) ppm: 29.6; 47.7; 50.9; 52.7; 53.8; 76.9; 118.0; 118.4; 119.3; 121.3; 124.5; 128.5; 128.9; 129.1; 129.6; 129.8; 130.2; 131.5; 131.6; 135.4; 150.3; 155.7; 168.9; 170.7. IR (KBr): v (cm^{-1}): 3086, 2956, 1738, 1709, 1588.

5-(4-phenoxyphenyl)-5-(4-(2,6-dichlorobenzoyl)-1,4-diazepan-1-yl) pyrimidine-2,4,6(1*H*,3*H*,5*H*)-trione (74)

A suspension of 5-(1,4-diazepan-1-yl)-5-(4-phenoxyphenyl)pyrimidine-2,4,6(1*H*,3*H*, 5*H*)-trione (394 mg, 1 mmol) in 10 ml THF was cooled to -70°C and triethylamine (101.2 mg, 1 mmol) was added. A solution of 2,6-dichlorobenzoyl chloride (209.5 mg, 1 mmol) was added to the suspension dropwise. After stirring for 2 h at -70°C, the reaction mixture was dried and purified by flash column chromatography to yield the pure compounds (230 mg, 40.5%) as off-white solids. mp: 158–160 °C. MS: Calculated for $C_{28}H_{25}Cl_2N_4O_5Na$ = 589.1021, $(M+Na)^+$ = 589.1019 found. ^{1}H NMR ($CDCl_3$) δ ppm: 1.88–1.92 (m, 2H, CH_2), 2.86–2.90 (m, 2H, CH_2), 2.96–2.98 (m, 1H, CH_2), 3.15–3.18 (m, 1H, CH_2), 3.41–3.44 (m, 1H, CH_2), 3.78–3.81 (m, 2H, CH_2), 3.97–3.99 (m, 1H, CH_2), 6.89–6.91 (d, *J* = 8.03, 2H, Ar-H), 6.95–6.97 (d, *J* = 8.03, 1H, Ar-H), 7.00–7.05 (t, *J* = 8.03, 1H, Ar-H), 7.16–7.25 (m, 2H, Ar-H), 7.27–7.33 (m, 2H, Ar-H), 7.36–7.39 (m, 2H, Ar-H), 7.46–7.49 (m, 2H, Ar-H), 9.49–9.54 (d, 2H, NH). ^{13}C NMR ($CDCl_3$): 28.9; 47.3; 50.3; 52.1;52.8; 77.9; 116.8; 118.4; 119.8; 121.4; 124.3; 127.9; 128.1; 128.2; 129.0; 129.3; 131.6; 132.9; 135.3; 135.6; 148.9; 154.9; 155.6; 158.9; 165.3; 170.2. IR (KBr): v (cm^{-1}): 3105, 2958, 1728, 1702, 1579.

5-(4-phenoxyphenyl)-5-(4-(3-phenylpropanoyl)-1,4-diazepan-1-yl) pyrimidine-2,4,6(1*H*,3*H*,5*H*)-trione (75)

A suspension of 5-(1,4-diazepan-1-yl)-5-(4-phenoxyphenyl)pyrimidine-2,4,6(1*H*,3*H*, 5*H*)-trione (394 mg, 1 mmol) in 10 ml THF was cooled to -70°C and triethylamine (101.2 mg, 1 mmol) was added. A solution of 3-phenylpropanoyl chloride (168.6 mg, 1 mmol) was added to the suspension dropwise. After stirring for 2 h at -70°C, the reaction mixture was dried and purified by flash column chromatography to yield the pure compounds (236 mg, 44.8%) as off-white solids. mp: 121–124°C. MS: Calculated for $C_{30}H_{30}N_4O_5Na$ = 549.2114, $(M+Na)^+$ = 549.2110 found. ^1H NMR ($CDCl_3$) δ ppm: 1.61–1.67 (m, 1H, CH_2), 1.70–1.76 (m, 1H, CH_2), 2.71–2.76 (m, 2H, CH_2), 2.80–2.84 (m, 2H, CH_2), 2.99–3.04 (m, 2H, CH_2), 3.35–3.38 (m, 1H, CH_2), 3.57–3.60 (m, 1H, CH_2), 3.61–3.64 (m, 1H, CH_2), 3.71–3.74 (m, 1H, CH_2), 6.92–6.96 (m, 2H, Ar-H), 7.02–7.05 (m, 2H, Ar-H), 7.19–7.29 (m, 6H, Ar-H), 7.36–7.40 (t, *J* = 7.53, 2H, Ar-H), 7.44–7.48 (m, 2H, CH_2), 9.36 (s, 1H, NH), 9.50 (s, 1H, NH). ^{13}C NMR ($CDCl_3$) δ ppm: 29.0; 31.4; 34.1; 48.3; 50.7; 52.2; 53.4; 77.8; 118.2; 119.8; 121.5; 124.3; 126.1; 128.4; 128.6; 129.1; 129.3; 129.9; 130.0; 141.4; 148.9; 155.6; 158.9; 170.2; 172.5. IR (KBr): v (cm^{-1}): 3068, 2955, 1730, 1711, 1590.

5-(4-phenoxyphenyl)-5-(4-(2-(4-chlorophenyl)acetyl)-1,4-diazepan-1-yl) pyrimidine-2,4,6(1*H*,3*H*,5*H*)-trione (76)

A suspension of 5-(1,4-diazepan-1-yl)-5-(4-phenoxyphenyl)pyrimidine-2,4,6(1*H*,3*H*, 5*H*)-trione (394 mg, 1 mmol) in 10 ml THF was cooled to -70°C and triethylamine (101.2 mg, 1 mmol) was added. A solution of 2-(4-chlorophenyl)acetyl chloride (189.0 mg, 1 mmol) was added to the suspension dropwise. After stirring for 2 h at -70°C, the reaction mixture was dried and purified by flash column chromatography to yield the pure compounds (173 mg, 31.6%) as off-white solids. mp: 138–140°C. MS: Calculated for $C_{29}H_{27}ClN_4O_5Na$ =

569.1568, $(M+Na)^+$ = 569.1571 found. ^1H NMR (MeOD) δ ppm: 1.55–1.59 (m, 1H, CH_2), 1.66–1.72 (m, 1H, CH_2), 2.67–2.73 (m, 2H, CH_2), 2.85–2.89 (m, 1H, CH_2), 2.94–2.98 (m, 1H, CH_2), 3.33–3.39 (m, 1H, CH_2), 3.52–3.55 (m, 1H, CH_2), 3.60–3.63 (m, 1H, CH_2), 3.71–3.74 (m, 1H, CH_2), 3.89–3.93 (m, 1H, CH_2), 3.99–4.02(m, 1H, CH_2), 6.85–6.91 (m, 1H, Ar-H), 6.93–6.97(m, 2H, Ar-H), 7.01–7.05 (m, 1 H, Ar-H), 7.18–7.25 (m, 2H, Ar-H), 7.28–7.3 (m, 1H, Ar-H), 7.33–7.38 (m, 3H, Ar-H), 7.41–7.45 (m, 1H, Ar-H), 7.49–7.57 (m, 2H, Ar-H). ^{13}C NMR (MeOD) δ ppm: 30.8; 45.4; 51.4; 52.3; 53.7; 54.8; 78.7; 119.0; 119.5; 120.7; 121.0l 122.7; 125.5; 129.4; 129.9; 130.4; 130.6; 130.7; 130.9; 131.1; 131.2; 134.0; 134.4; 150.8; 156.1; 159.2; 160.4; 170.3. IR (KBr): v (cm^{-1}): 3096, 2956, 1738, 1710, 1588.

5-(4-phenoxyphenyl)-5-(4-(2-cyclohexylacetyl)-1,4-diazepan-1-yl) pyrimidine-2,4,6(1*H*,3*H*,5*H*)-trione (77)

A suspension of 5-(1,4-diazepan-1-yl)-5-(4-phenoxyphenyl)pyrimidine-2,4,6(1*H*,3*H*, 5*H*)-trione (394 mg, 1 mmol) in 10 ml THF was cooled to -70°C and triethylamine (101.2 mg, 1 mmol) was added. A solution of 2-cyclohexylacetyl chloride (160.6 mg, 1 mmol) was added to the suspension dropwise. After stirring for 2 h at -70°C, the reaction mixture was dried and purified by flash column chromatography to yield the pure compounds (179 mg, 34.5%) as off-white solids. mp: 121–124°C. MS: Calculated for $C_{29}H_{35}N_4O_5$ = 519.2607, $(M+H)^+$ = 519.2597 found. ^1H NMR ($CDCl_3$) δ ppm: 1.22–1.25 (m, 2H, CH_2), 1.28–1.32 (m, 2H, CH_2), 1.66–1.70 (m, 4H, CH_2), 1.74–1.79 (m, 3H, CH_2+CH), 1.86–1.91 (m, 2H, CH_2), 2.20–2.22 (d, *J* = 6.84, 1H, CH_2), 2.24–2.26 (d, *J* = 6.84, 1H, CH_2), 2.73–2.76 (m, 1H, CH_2), 2.79–2.82 (m, 2H, CH_2), 2.86–2.89 (m, 1H, CH_2), 3.41–3.44 (m, 1H, CH_2), 3.60–3.63 (m, 1H, CH_2), 3.64–3.67 (m, 1H, CH_2), 3.71–3.74 (m, 1H, CH_2), 3.78–3.81 (m, 1H, CH_2), 6.94–6.97 (m, 2H, Ar-H), 7.04–7.06 (d, *J* = 8.03, 2H, Ar-H), 7.16–7.20 (t, *J* = 7.53, 1H, Ar-H), 7.37–7.40 (t, *J* = 7.53, 1H,

Ar-H), 7.47–7.51 (m, 3H, Ar-H), 9.60 (s, 2H, NH). ^{13}C NMR ($CDCl_3$) δ ppm: 25.8; 27.4; 29.0; 33.0; 34.6; 40.5; 48.0; 50.3; 52.4; 53.1; 77.5; 117.9. 118.1; 119.4; 119.5; 121.0; 127.9; 128.9; 129.0; 129.2; 129.6; 148.8; 151.1; 155.4; 158.5; 169.9; 170.0. IR (KBr): ν (cm^{-1}): 3066, 2956, 1730, 1711, 1590.

5-(4-phenoxyphenyl)-5-(4-(2,6-dichloro-5-fluoronicotinoyl)-1,4-diazepan-1-yl)pyrimidine-2,4,6(1*H*,3*H*,5*H*)-trione (78)

A suspension of 5-(1,4-diazepan-1-yl)-5-(4-phenoxyphenyl)pyrimidine-2,4,6(1*H*,3*H*, 5*H*)-trione (394 mg, 1 mmol) in 10 ml THF was cooled to -70°C and triethylamine (101.2 mg, 1 mmol) was added. A solution of 2,6-dichloro-5-fluoronicotinoyl chloride (228.4 mg, 1 mmol) was added to the suspension dropwise. After stirring for 2 h at -70°C, the reaction mixture was dried and purified by flash column chromatography to yield the pure compounds (190 mg, 32.4%) as off-white solids. mp: 154–156°C. MS: Calculated for $C_{27}H_{22}ClN_5O_5Na$ = 608.0880, $(M+Na)^+$ = 608.0881 found. ^{1}H NMR ($CDCl_3$) δ ppm: 1.87–1.90 (m, 2H, CH_2), 2.75–2.81 (m, 1H, CH_2), 2.83–2.87 (m, 1H, CH_2), 2.96–2.98 (m, 1H, CH_2), 3.18–3.23 (m, 1H, CH_2), 3.43–3.46 (m, 1H, CH_2), 3.78–3.81 (m, 1H, CH_2), 3.95–3.99 (m, 1H, CH_2), 6.91–6.94 (m, 2H, Ar–H), 6.96–6.98 (m, 1H, Ar-H), 7.04–7.06 (m, 1H, Ar-H), 7.19–7.23 (t, *J* = 7.53, 1H, Ar-H), 7.37–7.41 (m, 2H, Ar-H), 7.43–7.45 (d, *J* = 8.03, 1H, Ar-H), 7.48–7.51 (m, 1H, Ar-H), 9.13 (s, 1H, Ar–H), 9.24 (s, 1H, NH), 9.28 (s, 1H, NH). ^{13}C NMR ($CDCl_3$) δ ppm: 29.5; 48.0; 50.5; 50.7; 52.6; 78.1; 118.1; 118.2; 120.0; 121.6; 124.6; 125.7; 128.2; 129.1; 129.3; 130.0; 132.6; 133.0; 148.5; 148.7; 152.7; 155.3; 159.2; 164.6; 170.2. IR (KBr): ν (cm^{-1}): 3066, 2958, 1735, 1640, 1588.

5-(4-phenoxyphenyl)-5-(4-(morpholine-4-carbonyl)-1,4-diazepan-1-yl) pyrimidine-2,4,6(1*H*,3*H*,5*H*)-trione (79)

A suspension of 5-(1,4-diazepan-1-yl)-5-(4-phenoxyphenyl)pyrimidine-2,4,6(1*H*,3*H*, 5*H*)-trione (394 mg, 1 mmol) in 10 ml THF was cooled to -70°C and

triethylamine (101.2 mg, 1 mmol) was added. A solution of morpholine-4-carbonyl chloride (149.6 mg, 1 mmol) was added to the suspension dropwise. After stirring for 2 h at -70°C, the reaction mixture was dried and purified by flash column chromatography to yield the pure compounds (210 mg, 41.4%) as off-white solids. mp: 135–138°C. MS: Calculated for $C_{26}H_{29}N_5O_6Na$ = 530.2016, $(M+Na)^+$ = 530.1994 found. ^1H NMR ($CDCl_3$) δ ppm: 1.79–1.83 (m, 1H, CH_2), 1.86–1.89 (m, 1H, CH_2), 2.76–2.78 (m, 2H, CH_2), 2.87–2.90 (m, 1H, CH_2), 3.22–3.24 (m, 4H, Ar–H), 3.36–3.39 (m, 2H, CH_2), 3.48–3.52 (m, 2H, CH_2), 3.3.67–3.69 (m, 4H CH_2), 3.78–3.80 (m, 1H, CH_2), 6.91–6.96 (m, 3H, Ar-H), 7.00–7.04 (m, 1H, Ar-H), 7.15–7.19 (t, *J* = 7.53, 1H, Ar-H), 7.35–7.39 (m, 1H, Ar-H), 7.46–7.50 (m, 3H, Ar-H) 9.81 (s, 1H, NH), 9.87 (s, 1H, NH). ^{13}C NMR ($CDCl_3$) δ ppm: 29.2; 47.4; 47.6; 50.6; 51.1; 52.2; 66.6; 77.2; 118.1; 118.3; 119.7; 121.3; 124.4; 128.2; 129.3; 129.4; 130.0; 149.2; 155.7; 158.7; 164.2; 170.3; 170.4. IR (KBr): v (cm^{-1}): 3065, 2978, 1711, 1610, 1580.

5-(4-phenoxyphenyl)-5-(4-((8-(dimethylamino)napththalen-4-yl)sulfonyl) -1,4-diazepan-1-yl)pyrimidine-2,4,6(1*H*,3*H*,5*H*)-trione (80)

A suspension of 5-(1,4-diazepan-1-yl)-5-(4-phenoxyphenyl)pyrimidine-2,4,6(1*H*,3*H*, 5*H*)-trione (394 mg, 1 mmol) in 10 ml THF was cooled to -70°C and triethylamine (101.2 mg, 1 mmol) was added. A solution of (8-(dimethylamino)napththalen-4-yl)sulfonyl chloride (285.8 mg, 1 mmol) was added to the suspension dropwise. After stirring for 2 h at -70°C, the reaction mixture was dried and purified by flash column chromatography to yield the pure compounds (328 mg, 52.3%) as yellow solids. mp: 138–140 °C. MS: Calculated for $C_{33}H_{34}N_5O_6S$ = 628.2230, $(M+H)^+$ = 628.2249 found. ^1H NMR ($CDCl_3$) ppm: 1.75–1.78 (m, 2H, CH_2), 2.86–2.89 (m, 4H, CH_2), 2.91 (s, 6H, CH_3), 3.34–3.38 (m, 2H, CH_2), 3.63–3.66 (m, 2H, CH_2), 6.89–6.92 (m, 3H, Ar-H), 7.02–7.04 (d, *J* = 7.53, 1H, Ar-H), 7.16–7.22 (t, *J* = 7.53, 2H, Ar-H), 7.36–7.43 (m, 4H, Ar-H),

7.51–7.59 (m, 2H, Ar-H), 8.16–8.18 (d, *J* = 7.53, 1H, Ar-H), 8.34–8.36 (d, *J* = 7.03, 1H, Ar-H), 8.54–8.56 (m, 1H, Ar-H), 8.86 (s, 1H, N-H), 8.90 (s, 1H, N-H). ^{13}C NMR ($CDCl_3$) ppm: 29.6; 46.7; 50.0; 50.8; 51.6; 53.8; 78.1; 118.2; 118.3; 119.9; 121.4; 123.2. 123.4; 128.0; 128.8; 129.0; 129.2; 129.4; 130.0; 132.9; 144.3; 148.5; 151.3; 155.5; 159.1; 169.9; 170.0. IR (KBr): v (cm^{-1}): 3170, 1736, 1713, 1609, 1588.

5-(4-phenoxyphenyl)-5-(4-(4-(methylthio)benzoyl)-1,4-diazepan-1-yl)pyrimidine-2,4,6(1*H*,3*H*,5*H*)-trione (81)

A suspension of 5-(1,4-diazepan-1-yl)-5-(4-phenoxyphenyl)pyrimidine-2,4,6(1*H*,3*H*, 5*H*)-trione (394 mg, 1 mmol) in 10 ml THF was cooled to -70°C and triethylamine (101.2 mg, 1 mmol) was added. A solution of 4-(methylthio)benzoyl chloride (186.7 mg, 1 mmol) was added to the suspension dropwise. After stirring for 2 h at -70°C, the reaction mixture was dried and purified by flash column chromatography to yield the pure compounds (176 mg, 32.3%) as off-white solids. mp: 240–244°C. MS: Calculated for $C_{29}H_{29}N_4O_5S$ = 545.1841, $(M+H)^+$ = 545.1859 found. ^1H NMR (DMSO) ppm: 1.48–1.55 (m, 1H, CH_2) 1.64–1.70 (m, 1H, CH_2), 2.46 (s, 3H, CH_3), 2.68–2.73 (m, 3H, CH_2), 3.19–3.23 (m, 1H, CH_2), 3.41–3.41 (m, 1H, CH_2), 3.51–3.54 (m, 1H, CH_2), 3.64–3.68 (m, 1H, CH_2), 6.90–6.95 (m, 1H, Ar-H), 7.00–7.03 (m, 3H, Ar-H), 7.18–7.21 (t, *J* = 7.53, 1H, Ar-H), 7.27–7.35 (m, 5H, Ar-H), 7.39–7.47 (m, 2H, Ar-H), 7.56–7.58 (m, 1H, Ar-H), 11.57 (s, 2H, NH). ^{13}C NMR (DMSO) ppm: 14.3; 29.8; 47.7; 50.8; 52.9; 53.5; 76.7; 118.0; 119.4; 121.5; 124.2; 125.1; 127.0; 127.4; 129.0; 129.4; 130.0; 133.0; 133.3; 139.6; 149.5; 155.5; 157.6; 170.0; 170.7. IR (KBr): v (cm^{-1}): 3058, 2951, 2763, 1729, 1708, 1589.

5-(4-phenoxyphenyl)-5-(4-(1-methyl-1*H*-indazole-3-carbonyl)-1,4-diazepan-1-yl)pyrimidine-2,4,6(1*H*,3*H*,5*H*)-trione (82)

To a solution of 5-(1,4-diazepan-1-yl)-5-(4-phenoxyphenyl)pyrimidine-2,4,6(1*H*,3*H*, 5*H*)-trione (394 mg, 1 mmol) in 10 ml THF was added DCC (206 mg, 1 mmol), DMAP (132 mg, 1 mmol) and 1-methyl-1*H*-indazole-3-carboxylic acid (176 mg, 1 mmol). The mixture was stirred at room temperature for 24 h before filtering. The solvents of the filtrate were removed *in vacuo* and the resulting crude products purified by flash column chromatography to yield pure products (268 mg, 48.6%) as off-white solids. mp: 185–187°C. MS: Calculated for $C_{30}H_{29}N_6O_6$ = 553.2199. $(M+H)^+$ = 553.2193 found. ^{1}H NMR (DMSO) δ ppm: 1.76–1.78 (m, 2H, CH_2), 2.71–2.75 (m, 2H, CH_2), 2.82–2.88 (m, 2H, CH_2), 3.60–3.63 (m, 2H, CH_2), 3.77–3.80 (m, 2H, CH_2), 4.11 (s, 3H, CH_2), 7.03–7.10 (m, 3H, Ar-H), 7.21–7.26 (m, 2H, Ar-H), 7.30–7.34 (t, *J* = 7.53, 1H, Ar-H), 7.41–7.49 (m, 4H, Ar-H), 7.59–7.62 (m, 1H, Ar-H), 7.70–7.72 (d, *J* = 8.53, 1H, Ar-H), 8.00–8.03 (d, *J* = 8.03, 1H, Ar-H), 11.55 (s, 2H, NH). ^{13}C NMR (DMSO) δ ppm: 29.9; 35.8; 48.4; 51.2; 52.1; 53.3; 76.7; 110.0; 117.6; 118.5; 119.6; 121.4; 123.4; 124.9; 126.4; 128.0; 129.1; 129.3; 130.2; 133.0; 139.2; 140.0; 149.4; 155.4; 157.7; 162.8; 170.7. IR (KBr): ν (cm^{-1}): 2929, 1737, 1710, 1625.

5-(4-phenoxyphenyl)-5-(4-(2-(2,3-dihydrobenzo[*b*][1,4]dioxine-6-sulfonamido)3-methylbutyryl)-1,4-diazepan-1-yl)pyrimidine-2,4,6(1*H*,3*H*,5*H*)-trione (83)

To a solution of 5-(1,4-diazepan-1-yl)-5-(4-phenoxyphenyl)pyrimidine-2,4,6(1*H*,3*H*, 5*H*)-trione (394 mg, 1 mmol) in 10 ml THF was added DCC (206 mg, 1 mmol), DMAP (132 mg, 1 mmol) and 4-(2-(2,3-dihydrobenzo[*b*][1,4]dioxine-6-sulfonamido)3-methylbutyric acid (315 mg, 1 mmol). The mixture was stirred at room temperature for 24 h before filtering. The solvents of the filtrate were removed *in vacuo* and the resulting crude products purified by flash column

chromatography to yield pure products (217 mg, 31.4%) as off-white solids. mp: 143–146°C. MS: Calculated for $C_{34}H_{38}N_5O_9S$ = 692.2390, $(M+H)^+$ = 692.2383 found. ^1H NMR ($CDCl_3$) δ ppm: 0.84–0.89 (m, 3H, CH_3), 1.01–1.04 (m, 3H, CH_3), 1.88–1.93 (m, 2H, CH_2), 2.39–2.43 (m, 1H, CH), 2.68–2.74 (m, 2H, CH_2), 2.82–2.84 (m, 1H, CH_2), 3.24–3.26 (m, 1H, CH_2), 3.51–3.54 (m, 2H, CH_2+CH), 3.76–3.80 (m, 1H, CH_2), 3.84–3.87 (m, 1H, CH_2), 3.92–3.94 (m, 1H, CH_2), 4.27–4.31 (m, 4H, CH_2), 6.91–7.00 (m, 6H, Ar-H), 7.04–7.07 (t, *J* = 7.53, 1H, Ar-H), 7.18–7.22 (m, 1H, CH), 7.29-7.32 (m, 3H, Ar–H), 7.37-7.47 (m, 1H, Ar–H), 7.47-7.51 (m, 2H, Ar–H), 8.87 (s, 1H, NH), 9.07 (s, 1H, NH). ^{13}C NMR ($CDCl_3$) δ ppm: 19.5; 29.0; 30.8; 46.1; 49.6; 50.1; 51.5; 53.2; 57.5; 77.7; 116.4; 116.8; 117.4; 117.9; 118.1; 119.6; 120.6; 121.2; 124.2; 128.9; 129.1; 129.7; 132.0; 146.9; 151.2; 154.5; 155.2; 158.3; 169.4; 170.5. IR (KBr): v (cm^{-1}): 2929, 1736, 1710, 1615.

5-(4-phenoxyphenyl)-5-(4-(3-(benzo[*d*]thiazol-2-yl)-2-methyl-2-phenylpropanoyl)-1,4-diazepan-1-yl)pyrimidine-2,4,6(1*H*,3*H*,5*H*)-trione (84)

To a solution of 5-(1,4-diazepan-1-yl)-5-(4-phenoxyphenyl)pyrimidine-2,4,6(1*H*,3*H*, 5*H*)-trione (394 mg, 1 mmol) in 10 ml THF was added DCC (206 mg, 1 mmol), DMAP (132 mg, 1 mmol) and 3-(benzo[*d*]thiazol-2-yl)-2-methyl-2-phenylpropanoic acid (297 mg, 1 mmol). The mixture was stirred at room temperature for 24 h before filtering. The solvents of the filtrate were removed *in vacuo* and the resulting crude products purified by flash column chromatography to yield pure products (209 mg, 32.8%) as off-white solids. mp: 141–144°C. MS: Calculated for $C_{38}H_{36}N_5O_5S$ = 674.2437, $(M+H)^+$ = 674.2426 found. ^1H NMR (MeOD) δ ppm: 1.82–7.89 (m, 2H, CH_2), 2.24 (s, 3H, CH_3), 2.93–2.96 (m, 3H, CH_2), 3.32–3.35 (m, 2H, CH_2), 3.45–3.51 (m, 2H, CH_2), 3.73–3.76 (m, 2H, CH_2), 6.93–6.97 (m, 6H, Ar–H), 6.99–7.02 (m, 2H, Ar-H), 7.14–7.18 (t, *J* = 7.53, 1H,

Ar-H), 7.35–7.39 (m, 2H, Ar-H), 7.48–7.52 (m, 3H, Ar-H), 7.54–7.57 (m, 2H, Ar-H), 7.80–7.82 (d, *J* = 8.53, 1H, Ar-H), 7.87–7.89 (d, *J* = 8.53, 1H, Ar-H). ^{13}C NMR (MeOD) δ ppm: 21.4; 29.0; 39.7; 47.3; 48.4; 52.3; 55.7; 78.7; 117.4; 119.1; 119.4; 120.7; 122.3; 122.5; 122.9; 125.2; 126.1; 127.0; 129.5; 130.3; 130.4; 130.7; 130.9; 131.1; 133.0; 139.1; 150.9; 154.0; 157.0; 159.2; 170.4; 172.6; 178.7. IR (KBr): v (cm^{-1}): 2929, 1736, 1710, 1615.

5-(4-phenoxyphenyl)-5-(4-(3-(*N*-(5-methylisoxazol-3-yl)sulfamoyl)benzoyl)-1,4-diazepan-1-yl)pyrimidine-2,4,6(1*H*,3*H*,5*H*)-trione (85)

To a solution of 5-(1,4-diazepan-1-yl)-5-(4-phenoxyphenyl)pyrimidine-2,4,6(1*H*,3*H*, 5*H*)-trione (394 mg, 1 mmol) in 10 ml THF was added DCC (206 mg, 1 mmol), DMAP (132 mg, 1 mmol) and 3-(*N*-(5-methylisoxazol-3-yl)sulfamoyl)benzoic acid (282 mg, 1 mmol). The mixture was stirred at room temperature for 24 h before filtering. The solvents of the filtrate were removed *in vacuo* and the resulting crude products purified by flash column chromatography to yield pure products (235 mg, 35.7%) as off-white solids. mp: 145–147°C. MS: Calculated for $C_{32}H_{31}N_6O_8S$ = 659.1924, $(M+H)^+$ = 659.1931 found. ^1H NMR (MeOD) δ ppm: 1.83–1.88 (m, 2H, CH_2), 2.24 (s, 3H, CH_3), 2.81–2.85 (m, 3H, CH_2), 2.98–3.00 (m, 1H, CH_2), 3.18–3.21 (m, 1H, CH_2), 3.42–3.45 (m, 1H, CH_2), 3.68–3.71(m, 1H, CH_2), 3.81–3.83 (m, 1H, CH_2), 6.2 (s, 1H, CH), 6.80–6.83 (d, *J* = 8.53, 1H, Ar-H), 6.94–6.95 (m, 1H, Ar-H), 6.97–7.00 (m, 1H, Ar-H), 7.03–7.06 (m, 1H, Ar-H), 7.18–7.21 (t, *J* = 7.03, 1H, Ar-H), 7.36–7.41 (m, 1H, Ar-H), 7.51–7.55 (m, 1H, Ar-H), 7.56–7.59 (m, 1H, Ar-H), 7.63–7.68 (m, 1H, Ar-H), 7.74–7.76 (m, 1H, Ar-H), 7.96–7.98 (m, 1H, Ar-H), 8.01–8.03 (m, 2H, Ar-H). ^{13}C NMR (MeOD) δ ppm: 12.3; 28.9; 45.6; 51.6; 52.4; 54.3; 78.8; 96.5; 117.7; 119.0; 119.3; 119.6; 120.9; 122.6; 125.4; 129.2; 129.5; 130.3; 130.5; 130.8; 131.1; 132.2; 136.2; 141.3; 150.8; 152.8; 156.7; 158.9; 171.8; 172.1; 172.5. IR (KBr):

v (cm^{-1}): 2929, 1738, 1712, 1613.

5-(4-phenoxyphenyl)-5-(4-(5-fluoro-2-(methylsulfonamido)benzoyl)-1,4-diazepan-1-yl)pyrimidine-2,4,6(1*H*,3*H*,5*H*)-trione (86)

To a solution of 5-(1,4-diazepan-1-yl)-5-(4-phenoxyphenyl)pyrimidine-2,4,6(1*H*,3*H*, 5*H*)-trione (394 mg, 1 mmol) in 10 ml THF was added DCC (206 mg, 1 mmol), DMAP (132 mg, 1 mmol) and 5-fluoro-2-(methylsulfonamido)benzoic acid (233 mg, 1 mmol). The mixture was stirred at room temperature for 24 h before filtering. The solvents of the filtrate were removed *in vacuo* and the resulting crude products purified by flash column chromatography to yield pure products (233 mg, 38.2 %) as off-white solids. mp: 200–204°C. MS: Calculated for $C_{29}H_{29}N_5O_7S$ = 610.1772, $(M+H)^+$ = 610.1799 found. ^{1}H NMR (MeOD) δ ppm: 1.82–1.89 (m, 2H, CH_2), 2.85–2.90 (m, 3H, CH_2), 3.00–3.03 (m, 1H, CH_2), 3.06 (s, 3H, CH_3), 3.21–3.24 (m, 1H, CH_2), 3.44–3.50 (m, 1H, CH_2), 3.68–3.71 (m, 1H, CH_2), 3.81–3.85 (m, 1H, CH_2), 6.87–6.91 (m, 1H, Ar-H), 6.93–6.96 (m, 2H, Ar-H), 7.00–7.06 (m, 2H, Ar-H), 7.17–7.22 (m, 1H, Ar-H), 7.25–7.28 (m, 1H, Ar-H), 7.34–7.39 (m, 1H, Ar-H), 7.74–7.44 (m, 1H, Ar-H), 7.45–7.50 (m, 1H, Ar-H), 7.51–7.55 (m, 2H, Ar-H). ^{13}C NMR (MeOD) δ ppm: 29.4; 41.0; 45.7; 51.1; 52.5; 53.6; 79.0; 113.5; 115.6; 116.3; 117.9; 118.1; 119.2; 119.6; 120.8; 122.5; 129.5; 130.4; 130.6; 130.9; 131.1; 139.2; 150.8; 152.3; 156.8; 159.6; 169.8; 172.4. IR (KBr): v (cm^{-1}): 2931, 1738, 1712, 1613.

5-(4-phenoxyphenyl)-5-(4-(3-(*N*-(4-methoxyphenyl)sulfamoyl)-4-methylbenzoyl)-1,4-diazepan-1-yl)pyrimidine-2,4,6(1*H*,3*H*,5*H*)-trione (87)

To a solution of 5-(1,4-diazepan-1-yl)-5-(4-phenoxyphenyl)pyrimidine-2,4,6(1*H*,3*H*, 5*H*)-trione (394 mg, 1 mmol) in 10 ml THF was added DCC (206 mg, 1 mmol), DMAP (132 mg, 1 mmol) and 3-(*N*-(4-methoxyphenyl)sulfamoyl)-4-

methylbenzoic acid (321 mg, 1 mmol). The mixture was stirred at room temperature for 24 h before filtering. The solvents of the filtrate were removed *in vacuo* and the resulting crude products purified by flash column chromatography to yield pure products (179 mg, 25.7) as off-white solids. mp: 147–149°C. MS: Calculated for $C_{36}H_{26}N_5O_8S$ = 698.2285, $(M+H)^+$ = 698.2290 found. ^1H NMR (MeOD) δ ppm: 1.70–1.76 (m, 2H, CH_2), 2.67 (s, 3H, CH_3) 2.70–2.73 (m, 1H, CH_2), 2.75–2.78 (m, 2H, CH_2), 2.91–2.96 (m, 1H, CH_2), 3.33 (s, 3H, CH_3), 3.47–3.50 (m, 1H, CH_2), 3.56–3.58 (m, 1H, CH_2), 3.63–3.65 (m, 1H, CH_2), 3.70–3.73 (m, 1H, CH_2), 6.53–6.55 (d, *J* = 8.53, 1H, Ar-H), 6.70–6.73 (d, *J* = 8.53, 1H, Ar-H), 6.77–6.80 (m, 2H, Ar-H), 6.90–6.94 (m, 2H, Ar-H), 6.97–7.03 (m, 2H, Ar-H), 7.20–7.23 (t, *J* = 7.03, 1H, Ar-H), 7.32–7.37 (m, 1H, Ar-H), 7.40–7.46 (m, 2H, Ar-H), 7.52–7.55 (m, 1H, Ar-H), 7.59–7.61 (d, *J* = 8.03, 1H, Ar-H), 7.66–7.68 (d, *J* = 8.03, 1H, Ar-H), 8.11 (s, 1H, Ar-H). ^{13}C NMR (MeOD) δ ppm: 20.5; 28.9; 45.5; 51.2; 52.7; 53.8; 55.9; 78.9; 115.3; 115.4; 118.8; 119.1; 119.5; 119.7; 120.8; 121.0; 122.7; 124.3; 125.5; 125.7; 129.5; 129.6; 130.4; 130.5; 130.6; 130.7; 130.8; 135.4; 138.5; 139.2; 150.9; 152.9; 155.8; 157.2; 169.4; 172.2. IR (KBr): ν (cm^{-1}): 2932, 1731, 1708, 1607.

5-(4-phenoxyphenyl)-5-(4-(4-methyl-2-(methylsulfonamido)benzoyl)-1,4-diazepan-1-yl)pyrimidine-2,4,6(1*H*,3*H*,5*H*)-trione (88)

To a solution of 5-(1,4-diazepan-1-yl)-5-(4-phenoxyphenyl)pyrimidine-2,4,6(1*H*,3*H*, 5*H*)-trione (394 mg, 1 mmol) in 10 ml THF was added DCC (206 mg, 1 mmol), DMAP (132 mg, 1 mmol) and 4-methyl-2-(methylsulfonamido)benzoic acid (229 mg, 1 mmol). The mixture was stirred at room temperature for 24 h before filtering. The solvents of the filtrate were removed *in vacuo* and the resulting crude products purified by flash column chromatography to yield pure products (241 mg, 39.8%) as off-white solids. mp: 203–206°C. MS: Calculated for $C_{30}H_{31}N_5O_7SNa$ = 628.1842, $(M+Na)^+$ = 628.1821 found. ^1H NMR (DMSO) δ

ppm: 1.64–1.70 (m, 2H, CH_2), 2.27 (s, 3H, CH_3), 2.70–2.75 (m, 2H, CH_2), 2.84–2.87 (m, 1H, CH_2), 2.98 (s, 3H, CH_3), 3.09–3.13(m, 1H, CH_2), 3.31–3.36 (m, 2H, CH_2), 3.70–3.73 (m, 1H, CH_2), 6.88 (s, 1H, Ar–H), 6.94–6.96 (d, *J* = 8.03, 1H, Ar-H), 7.02–7.04 (d, *J* = 8.53, 1H, Ar-H), 7.06–7.09 (m, 1H, Ar-H), 7.16–7.23 (m, 2H, Ar-H), 7.23–7.31 (m, 2H, Ar-H), 7.34–7.39 (m, 2H, Ar-H), 7.42–7.44 (m, 1H, Ar-H), 7.57–7.59 (d, *J* = 7.53, 1H, Ar-H). ^{13}C NMR (DMSO) δ ppm: 21.0; 29.4; 42.3; 47.3; 50.5; 50.9; 52.3; 76.7; 116.0; 117.7; 118.2; 118.5; 119.5; 119.6; 121.7; 127.9; 128.4; 129.4; 129.9; 130.1; 130.6; 139.2; 141.1; 149.4; 151.5; 155.2; 157.3; 168.1; 170.7. IR (KBr): v (cm^{-1}): 2933, 1744, 1706, 1602.

5-(4-phenoxyphenyl)-5-(4-(2-(4-oxo-2-(phenylimino)thizolidin-5-yl)acetyl)-)-1,4-diazepan-1-yl)pyrimidine-2,4,6(1*H*,3*H*,5*H*)-trione (89)

To a solution of 5-(1,4-diazepan-1-yl)-5-(4-phenoxyphenyl)pyrimidine-2,4,6(1*H*,3*H*, 5*H*)-trione (394 mg, 1 mmol) in 10 ml THF was added DCC (206 mg, 1 mmol), DMAP (132 mg, 1 mmol) and 2-(4-oxo-2-(phenylimino)thizolidin-5-yl)acetic acid (315 mg, 1 mmol). The mixture was stirred at room temperature for 24 h before filtering. The solvents of the filtrate were removed *in vacuo* and the resulting crude products purified by flash column chromatography to yield pure products (214 mg, 34.1%) as off-white solids. mp: 167–169°C. MS: Calculated for $C_{32}H_{30}N_6O_6SNa$ = 649.1845, $(M+Na)^+$ = 649.1827 found.^1H NMR (MeOD) δ ppm: 1.82–7.89 (m, 2H, CH_2), 2.75–2.79 (m, 2H, CH_2), 2.83–2.86 (m, 1H, CH_2), 2.90–2.94 (m, 2H, CH_2), 3.42–3.47 (m, 2H, CH_2), 3.50–3.55 (m, 1H, CH_2), 3.61–3.67 (m, 2H, CH_2), 4.53–4.55 (m, 1H, CH_2), 6.91–6.97 (m, 3H, Ar-H), 7.01–7.02 (d, *J* = 7.53, 2H, Ar-H), 7.15–7.19 (t, *J* = 7.03, 2H, Ar-H), 7.30–7.32 (m, 1H, Ar-H), 7.34–7.37 (t, *J* = 7.03, 2H, Ar-H), 7.46–7.54 (m, 4H, Ar-H). ^{13}C NMR (MeOD) δ ppm: 29.0; 35.7; 46.3; 47.7; 50.4; 52.5; 53.6; 79.0; 117.5; 119.3; 119.8; 120.7; 122.2; 122.4; 122.5; 127.2; 129.5; 130.0; 130.5; 130.8; 131.1; 150.8; 152.3; 156.9; 157.4; 159.5; 171.6; 172.4; 178.0. IR (KBr): v (cm^{-}

^{1}): 2930, 1737, 1710, 1618.

5-(4-phenoxyphenyl)-5-(4-((4*S*)-4-((3*S*,5R,7R,13S,17S)-3,7-dihydroxy-10,13-dimethylhexadecahydro-1*H*-cyclopenta[*a*]phenanthren-17-yl)pentanoyl)-1,4-diazepan-1-yl)pyrimidine-2,4,6(1*H*,3*H*,5*H*)-trione (90)

To a solution of 5-(1,4-diazepan-1-yl)-5-(4-phenoxyphenyl)pyrimidine-2,4,6(1*H*,3*H*, 5*H*)-trione (394 mg, 1 mmol) in 10 ml THF was added DCC (206 mg, 1 mmol), DMAP (132 mg, 1 mmol) and ursodeoxycholic acid (392 mg, 1 mmol). The mixture was stirred at room temperature for 24 h before filtering. The solvents of the filtrate were removed *in vacuo* and the resulting crude products purified by flash column chromatography to yield pure products (317 mg, 41.2%) as off-white solids. mp: 167–170°C. MS: Calculated for $C_{45}H_{61}N_4O_7$ = 769.4540, $(M+H)^+$ = 769.4565 found. ^{1}H NMR (MeOD) δ ppm: 0.99 (s, 6H, CH_3), 1.01–1.03 (d, *J* = 6.53, 3H, CH_3), 1.20–1.22 (m, 1H, CH_2), 1.25–1.29 (m, 2H, CH_2), 1.31–1.34 (m, 2H, CH_2), 1.35–1.37 (m, 2H, CH_2), 1.38–1.40 (m, 1H, CH_2), 1.44–1.46 (m, 2H, CH_2), 1.47–1.52 (m, 5H, CH_2+CH), 1.55–1.57 (m, 1H, CH_2), 1.58–1.61 (m, 1H, CH_2), 1.62–1.64 (m, 2H, CH_2), 1.66–1.68 (m, 3H, CH_2), 1.77–1.80 (m, 1H, CH), 1.82–1.83 (m, 1H, CH_2), 1.85–1.86 (m, 1H, CH_2), 1.88–1.90 (m, 1H, CH_2), 1.91–1.94 (m, 2H, CH_2), 2.77–2.81 (m, 2H, CH_2), 2.83–2.86 (m, 1H, CH_2), 2.93–2.96 (m, 1H, CH_2), 3.49–3.54 (m, 4H, CH_2+CH), 3.67–3.72 (m, 2H, CH_2), 6.98–7.01 (m, 2H, Ar-H), 7.05–7.07 (d, *J* = 8.53, 2H, Ar-H), 7.17–7.21 (t, *J* = 7.53, 1H, Ar-H), 7.39–7.43 (t, *J* = 7.53, 1H, Ar-H), 7.51–7.56 (m, 3H, Ar-H). ^{13}C NMR (MeOD) δ ppm: 12.7; 19.2; 22.4; 28.0; 29.1; 29.7; 31.2; 32.8; 33.1; 35.2; 36.1; 37.0; 38.0; 38.6; 40.7; 41.644.0; 44.5; 44.8; 48.1; 49.7; 51.4; 52.6; 53.4; 56.5; 71.9; 72.1; 79.0; 119.2; 119.6; 120.8; 122.5; 125.4; 129.6; 130.6; 131.2; 131.7; 150.9; 156.9; 157.5; 172.5; 176.1. IR (KBr): v (cm^{-1}): 2934, 2864, 1737, 1711, 1618.

5,5'-(4,4'-terepthaloylbis(1,4-diazepane-4,1-diyl))bis(5-(4-phenoxyphenyl) pyrimidine-2,4,6(1*H*,3*H*,5*H*)-trione) (91)

A suspension of 5-(1,4-diazepan-1-yl)-5-(4-phenoxyphenyl)pyrimidine-2,4,6(1*H*,3*H*, 5*H*)-trione (788 mg, 2 mmol) in 10 ml THF was cooled to -70°C and triethylamine (202 mg, 2 mmol) was added. A solution of terephthaloyl chloride (203 mg, 1 mmol) was added to the suspension dropwise. After stirring for 8 h at -70°C, the reaction mixture was dried and purified by flash column chromatography to yield the pure compounds (216 mg, 23.5%) as light yellow solids. mp: 208–210°C. MS: Calculated for $C_{50}H_{47}N_8O_{10}$ = 941.3235; $(M+H)^+$ = 941.3270 found. ^{1}H NMR (MeOD) ppm: 1.83–1.87 (m, 4H, CH_2), 2.82–2.88 (m, 6H, CH_2), 2.97–2.01 (m, 2H, CH_2), 3.26–3.29 (m, 2H, CH_2), 3.48–3.52 (m, 2H, CH_2), 3.66–3.70 (m, 2H, CH_2), 3.79–3.84 (m, 2H, CH_2), 6.97–6.99 (d, *J* = 8.54, 4H, Ar-H), 7.00–7.05 (m, 8.54, 4H, Ar-H), 7.14–7.18 (t, *J* = 7.53, 2H, Ar-H), 7.35–7.39 (t, *J* = 8.03, 2H, Ar-H), 7.42–7.49 (m, 6H, Ar-H) 7.58 (s, 2H, Ar-H), 7.59 (s, 2H, Ar-H). ^{13}C NMR (MeOD) ppm: 29.2; 51.6; 52.8; 53.8; 54.2; 78.9; 119.2; 119.6; 120.8; 122.5; 125.3; 127.8; 128.2; 129.5; 130.6; 131.1; 138.0; 150.8; 157.4; 160.3; 172.3; 173.2. IR (KBr): v (cm^{-1}): 2966, 1731, 1708, 1612.

5,5'-(4,4'-succinylbis(1,4-diazepane-4,1-diyl))bis(5-(4-phenoxyphenyl) pyrimidine-2,4,6(1*H*,3*H*,5*H*)-trione) (92)

A suspension of 5-(1,4-diazepan-1-yl)-5-(4-phenoxyphenyl)pyrimidine-2,4,6(1*H*,3*H*, 5*H*)-trione (788 mg, 2 mmol) in 10 ml THF was cooled to -70°C and triethylamine (202 mg, 2 mmol) was added. A solution of succinyl chloride (155 mg, 1 mmol) was added to the suspension dropwise. After stirring for 8 h at -70°C, the reaction mixture was dried and purified by flash column chromatography to yield the pure compounds (189 mg, 21.7%) as off-white solids. mp: 218–220°C. MS: Calculated for $C_{46}H_{46}N_8O_{10}Na$ = 893.3235; $(M+Na)^+$

= 893.3226 found. ^{1}H NMR (MeOD) ppm: 1.61–1.65 (m, 2H, CH_2), 1.76–1.79 (m, 2H, CH_2), 2.74–2.77 (m, 4H, CH_2), 2.78–2.83 (m, 6H, CH_2), 2.92–2.95 (m, 2H, CH_2), 3.50–3.55 (m, 4H, CH_2), 3.64–3.67 (m, 2H, CH_2), 3.73–3.76 (m, 2H, CH_2), 6.94–6.96 (d, *J* = 8.03, 4H, Ar-H), 6.98–7.02 (m, 4H, Ar-H), 7.14–7.18 (t, *J* = 7.53, 2H, Ar-H), 7.36–7.39 (t, *J* = 8.03, 2H, Ar-H), 7.49–7.55 (m, 6H, Ar-H). ^{13}C NMR (MeOD) ppm: 29.4; 30.1; 51.1; 52.7; 53.2; 54.0; 79.0; 119.2; 119.5; 120.8; 122.5; 125.3; 129.5; 130.7; 131.1; 150.9; 156.9; 160.2; 172.4; 174.1. IR (KBr): v (cm^{-1}): 2954, 1732, 1710, 1618.

5,5′-(4,4′-glutaroylbis(1,4-diazepane-4,1-diyl))bis(5-(4-phenoxyphenyl) pyrimidine-2,4,6(1*H*,3*H*,5*H*)-trione) (93)

A suspension of 5-(1,4-diazepan-1-yl)-5-(4-phenoxyphenyl)pyrimidine-2,4,6(1*H*,3*H*, 5*H*)-trione (788 mg, 2 mmol) in 10 ml THF was cooled to -70°C and triethylamine (202 mg, 2 mmol) was added. A solution of glutaroyl chloride (169 mg, 1 mmol) was added to the suspension dropwise. After stirring for 8 h at -70°C, the reaction mixture was dried and purified by flash column chromatography to yield the pure compounds (242 mg, 27.3%) as off-white solids. mp: 162–164°C. MS: Calculated for $C_{47}H_{49}N_8O_{10}$ = 885.3572; $(M+H)^+$ = 885.3561 found.^{1}H NMR (MeOD) ppm: 1.63–1.66 (m, 2H, CH_2), 1.72–1.76 (m, 2H, CH_2), 1.87–1.90 (m, 6H, CH_2), 2.48–2.56 (m, 4H, CH_2), 2.74–2.79 (m, 4H, CH_2), 2.81–2.85 (m, 2H, CH_2), 2.89–2.93 (m, 2H, CH_2), 3.49–3.53 (m, 4H, CH_2), 3.65–3.70 (m, 4H, CH_2), 6.97–6.99 (d, *J* = 8.03, 4H, Ar-H), 7.02–7.05 (m, 4H, Ar-H), 7.16–7.20 (t, *J* = 7.53, 2H, Ar-H), 7.38–7.42 (t, *J* = 8.03, 2H, Ar-H), 7.49–7.54 (m, 6H, Ar-H). ^{13}C NMR (MeOD) ppm: 26.5; 29.1; 39.6.3; 50.2; 51.1; 52.8; 54.2; 78.9; 119.2; 120.8; 122.5; 125.3; 129.6; 130.6; 131.1; 150.9; 157.5; 160.2; 172.5; 174.8. IR (KBr): v (cm^{-1}): 2933, 1741, 1712, 1618.

5,5'-(4,4'-adipoylbis(1,4-diazepane-4,1-diyl))bis(5-(4-phenoxyphenyl) pyrimidine-2,4,6(1*H*,3*H*,5*H*)-trione) (94)

A suspension of 5-(1,4-diazepan-1-yl)-5-(4-phenoxyphenyl)pyrimidine-2,4,6(1*H*,3*H*, 5*H*)-trione (788 mg, 2 mmol) in 10 ml THF was cooled to -70°C and triethylamine (202 mg, 2 mmol) was added. A solution of adipoyl chloride (183 mg, 1 mmol) was added to the suspension dropwise. After stirring for 8 h at -70°C, the reaction mixture was dried and purified by flash column chromatography to yield the pure compounds (280 mg, 31.1%) as off-white solids. mp: 138–140°C. MS: Calculated for $C_{48}H_{50}N_8O_{10}Na$ = 921.3548; $(M+Na)^+$ = 921.3539 found. ^1H NMR (MeOD) ppm: 1.62–1.65 (m, 2H, CH_2), 1.72–1.74 (m, 4H, CH_2),1.76–1.78 (m, 2H, CH_2), 2.44–2.47 (m, 4H, CH_2), 2.75–2.78 (m, 4H, CH_2), 2.81–2.84 (m, 2H, CH_2), 2.90–2.93 (m, 2H, CH_2), 3.48–3.52 (m, 4H, CH_2), 3.64–3.68 (m, 2H, CH_2), 6.96–6.98 (d, *J* = 8.03, 4H, Ar-H), 6.99–7.03 (m, 4H, Ar-H), 7.15–7.18 (t, *J* = 7.53, 2H, Ar-H), 7.36–7.39 (t, *J* = 8.03, 2H, Ar-H), 7.48–7.54 (m, 6H, Ar-H). ^{13}C NMR (MeOD) ppm: 29.0; 29.1.1; 34.2; 51.1; 52.6; 53.3; 54.3; 78.9; 119.2; 119.6; 120.8; 122.5; 125.3; 129.5; 130.6; 131.1; 150.9; 156.9; 160.2; 172.5; 175.0. IR (KBr): v (cm^{-1}): 2936, 1732, 1710, 1611.

5,5'-(4,4'-heptanedioylbis(1,4-diazepane-4,1-diyl))bis(5-(4-phenoxyphenyl)pyrimidine-2,4,6(1*H*,3*H*,5*H*)-trione) (95)

A suspension of 5-(1,4-diazepan-1-yl)-5-(4-phenoxyphenyl)pyrimidine-2,4,6(1*H*,3*H*, 5*H*)-trione (788 mg, 2 mmol) in 10 ml THF was cooled to -70°C and triethylamine (202 mg, 2 mmol) was added. A solution of heptanedioyl chloride (197 mg, 1 mmol) was added to the suspension dropwise. After stirring for 8 h at -70°C, the reaction mixture was dried and purified by flash column chromatography to yield the pure compounds (205 mg, 22.4%) as off-white solids. mp: 135–137°C. MS: Calculated for $C_{49}H_{53}N_8O_{10}$ = 935.3704; $(M+H)^+$ = 935.3707 found. ^1H NMR (MeOD) ppm: 1.45–1.47 (m, 4H, CH_2), 1.62–1.66 (m, 4H, CH_2), 1.69–1.74 (m, 4H, CH_2), 2.39–2.46 (m, 4H, CH_2), 2.74–2.79 (m, 4H,

CH_2), 2.82–2.85 (m, 2H, CH_2), 2.89–2.92 (m, 2H, CH_2), 3.47–3.53 (m, 4H, CH_2), 3.64–3.67 (m, 4H, CH_2), 6.97–6.99 (d, *J* = 8.54, 4H, Ar-H), 7.00–7.05 (m, 8.54, 4H, Ar-H), 7.14–7.18 (t, *J* = 7.53, 2H, Ar-H), 7.35–7.39 (t, *J* = 8.03, 2H, Ar-H), 7.42–7.54 (m, 6H, Ar-H). ^{13}C NMR (MeOD) ppm: 27.9; 29.1; 30.1; 39.9; 51.2; 52.5; 53.3; 54.3; 78.9; 119.2; 119.6; 120.8; 122.5; 125.4; 129.5; 130.7; 131.1; 150.8; 156.8; 160.2; 172.4; 175.3. IR (KBr): v (cm^{-1}): 2962, 1734, 1709, 1607.

5,5′-(4,4′-octanedioylbis(1,4-diazepane-4,1-diyl))bis(5-(4-phenoxyphenyl)pyrimidine-2,4,6(1*H*,3*H*,5*H*)-trione) (96)

A suspension of 5-(1,4-diazepan-1-yl)-5-(4-phenoxyphenyl)pyrimidine-2,4,6(1*H*,3*H*, 5*H*)-trione (788 mg, 2 mmol) in 10 ml THF was cooled to -70°C and triethyl amine (202 mg, 2 mmol) was added. A solution of octanedioyl chloride (211 mg, 1 mmol) was added to the suspension dropwise. After stirring for 8 h at -70°C, the reaction mixture was dried and purified by flash column chromatography to yield the pure compounds (181 mg, 19.6%) as off-white solids. mp: 145–148°C. MS: Calculated for $C_{50}H_{55}N_8O_{10}$ = 927.4041; $(M+H)^+$ = 927.4033 found. ^{1}H NMR (MeOD) ppm: 1.42–1.43 (m, 4H, CH_2), 1.63–1.66 (m, 4H, CH_2), 1.68–1.74 (m, 4H, CH_2), 2.39–2.45 (m, 4H, CH_2), 2.74–2.78 (m, 4H, CH_2), 2.81–2.84 (m, 2H, CH_2), 2.89–2.92 (m, 2H, CH_2), 3.48–3.53 (m, 4H, CH_2), 3.65–3.70 (m, 4H, CH_2), 6.97–6.99 (d, *J* = 8.54, 4H, Ar-H), 7.00–7.05 (m, 8.54, 4H, Ar-H), 7.16–7.19 (t, *J* = 7.53, 2H, Ar-H), 7.37–7.41 (t, *J* = 8.03, 2H, Ar-H), 7.48–7.53 (m, 6H, Ar-H). ^{13}C NMR (MeOD) ppm: 29.1; 30.2; 33.6; 39.2; 51.6; 52.6; 54.1; 78.9; 119.2; 119.6; 120.8; 122.5; 125.8; 130.5; 130.7; 130.8; 131.1; 150.8; 157.5; 160.2; 172.4; 173.0. IR (KBr): v (cm^{-1}): 2952, 1730, 1716, 1586.

Bis-(2-nitrooxy-ethyl)-amine (99)

To a stirring solution of DCM (10 ml) and fuming nitric acid (1.5 ml) cooled to -

10°C, was added a solution of diethanolamine (420 mg, 4 mmol) in DCM (2 ml) dropwise over 20 min. After stirring for 30 min, the solution was treated with acetic anhydride (2 ml) and the solution was stirred for a further 15 min, after which time product precipitate out as white crystalline solids. (375 mg, 48.1%). mp: 110–112°C. MS: Calculated for $C_4H_{10}N_3O_6$ = 196.0570; found $(M+H)^+$ = 196.0573. ^1H NMR (D_2O) ppm: 3.45–3.47 (t, *J* = 5.02, 4H, CH_2), 4.74–4.76 (m, *J* = 5.02, 4H, CH_2). ^{13}C NMR (D_2O) ppm: 44.6; 67.5. IR (KBr): v (cm^{-1}): 1648, 1283, 925.

Methyl-(2-nitrooxy-ethyl)-amine (100)

To a stirring solution of DCM (10 ml) and fuming nitric acid (1.5 ml) cooled to -10°C, was added a solution of methylaminoethanol (451 mg, 4 mmol) in DCM (2 ml) dropwise over 20 min. After stirring for 30 min, the solution was treated with acetic anhydride (2 ml) and the solution was stirred for a further 15 min, after which time product precipitate out as white crystalline solids. (413 mg, 57.3%). mp: 58–60°C. MS: Calculated for $C_3H_9N_2O_3$ = 121.0613; found $(M+H)^+$ = 121.0611. ^1H NMR (D_2O) ppm: 2.79 (s, 3H, CH_3), 3.49–3.51 (t, *J* = 5.02, 4H, CH_2), 4.85–4.87 (m, *J* = 5.02, 4H, CH_2). ^{13}C NMR (D_2O) ppm: 35.1; 48.2; 70.1. IR (KBr): v (cm^{-1}): 1646, 1280, 912.

(2-nitrooxy-ethyl)-piperazine (105)

To a stirring solution of DCM (10 ml) and fuming nitric acid (1.5 ml) cooled to -10°C, was added a solution of 2-(piperazin-1-yl)ethanol (521 mg, 4 mmol) in DCM (2 ml) dropwise over 20 min. After stirring for 30 min, the solution was treated with acetic anhydride (2 ml) and the solution was stirred for a further 15 min, after which time the solution was adjusted to pH 14 by adding 7 M NaOH. The mixture was transferred into a separating funnel and extracted with DCM (20

ml x 3). The combined organic layers were washed with water and brine, dried (Na_2SO_4). The solvents were removed *in vacuo* to yield product as light yellow oil (324 mg, 46.2%). MS: Calculated for $C_6H_{14}N_3O_3$ = 176.1035; found $(M+H)^+$ = 176.1030. ^1H NMR ($CDCl_3$) ppm: 2.37–2.41 (m, 4H, CH_2); 2.50–2.53 (m, 2H, CH_2); 2.62–2.68 (m, 4H, CH_2); 4.04–4.07 (m, 2H, CH_2). ^{13}C NMR ($CDCl_3$) ppm: 46.3; 53.0; 57.3; 70.7. IR (film) v (cm^{-1}): 1641; 1280; 936.

4-(1-nitrooxy-methyl)-piperidine (106)

To a stirring solution of DCM (10 ml) and fuming nitric acid (1.5 ml) cooled to -10°C, was added a solution of piperidin-4-ylmethanol (461 mg, 4 mmol) in DCM (2 ml) dropwise over 20 min. After stirring for 30 min, the solution was treated with acetic anhydride (2 ml) and the solution was stirred for a further 15 min, after which time the solution was adjusted to pH 14 by adding 7 M NaOH. The mixture was transferred into a separating funnel and extracted with DCM (20 mlx3). The combined organic layers were washed with water and brine, dried (Na_2SO_4). The solvents were removed *in vacuo* to yield product as yellow oil (285 mg, 44.5%). MS: Calculated for $C_6H_{13}N_2O_3$ = 161.0926; found $(M+H)^+$ = 161.0921. ^1H NMR ($CDCl_3$) ppm: 1.10–1.21 (m, 2H, CH_2), 1.63–1.71 (m, 3H, $CH+CH_2$), 2.40–2.47 (m, 2H, CH_2), 2.92–2.97 (m, 2H, CH_2), 4.49–4.52 (m, 2H, CH_2). ^{13}C NMR ($CDCl_3$) ppm: 29.4; 34.6; 46.2; 76.2. IR (film) v (cm^{-1}): 1640, 1282, 910

4-(2-nitrooxy-ethyl)-piperidine (107)

To a stirring solution of DCM (10 ml) and fuming nitric acid (1.5 ml) cooled to -10°C, was added a solution of 2-(piperidin-4-yl)ethanol (517 mg, 4 mmol) in DCM (2 ml) dropwise over 20 min. After stirring for 30 min, the solution was treated with acetic anhydride (2 ml) and the solution was stirred for a further 15 min, after which time the solution was adjusted to pH 14 by adding 7 M NaOH. The

mixture was transferred into a separating funnel and extracted with DCM (20 mlx3). The combined organic layers were washed with water and brine, dried (Na_2SO_4). The solvents were removed *in vacuo* to yield product as yellow oil (328 mg, 47.1%). MS: Calculated for $C_7H_{15}N_2O_3$ = 175.1083; found $(M+H)^+$ = 175.1077. ^1H NMR ($CDCl_3$) ppm: 1.08–1.18 (m, 2H, CH_2), 1.71–1.78 (m, 5H, $CH+CH_2$), 2.48–2.55 (m, 2H, CH_2), 2.99–3.06 (m, 2H, CH_2), 3.48–3.52 (m, 2H, CH_2), 4.57–4.61 (m, 2H, CH_2). ^{13}C NMR ($CDCl_3$) ppm: 21.4; 32.3; 33.9; 46.3; 70.7. IR (film) v (cm^{-1}): 1652, 1281, 915

3-(1-nitrooxy-methyl)-piperidine (108)

To a stirring solution of DCM (10 ml) and fuming nitric acid (1.5 ml) cooled to -10°C, was added a solution of 1-(piperidin-3-yl)methanol (461 mg, 4 mmol) in DCM (2 ml) dropwise over 20 min. After stirring for 30 min, the solution was treated with acetic anhydride (2 ml) and the solution was stirred for a further 15 min, after which time the solution was adjusted to pH 14 by adding 7 M NaOH. The mixture was transferred into a separating funnel and and extracted with DCM (20 mlx3). The combined organic layers were washed with water and brine, dried (Na_2SO_4). The solvents were removed *in vacuo* to yield product as yellow oil (342 mg, 53.4%). MS: Calculated for $C_6H_{13}N_2O_3$ = 161.0926; found $(M+H)^+$ = 161.0924. ^1H NMR ($CDCl_3$) ppm: 1.07–1.17 (m, 1H, CH_2), 1.37–1.47 (m, 1H, CH_2), 1.58–1.62 (m, 1H, CH_2), 1.86–1.92 (m, 1H, CH), 2.32–2.37 (m, 1H, CH_2), 2.45–2.52 (m, 1H, CH_2), 2.90–2.94 (m, 1H, CH_2), 3.02–3.04 (m, 1H, CH_2), 4.18–4.25 (m, 2H, CH_2). ^{13}C NMR ($CDCl_3$) ppm: 24.5; 26.8; 34.2; 33.9; 45.7; 48.4; 75.2. IR (film) v (cm^{-1}): 1641, 1277, 910

5-(4-phenoxyphenyl)-5-(bis-(2-nitrooxy-ethyl)-amino)pyrimidine-2,4,6(1*H*,3*H*,5*H*)-trione (109)

A solution of 5-bromo-5-(4-phenoxyphenyl)pyrimidine-2,4,6(1*H*,3*H*,5*H*)-trione (375 mg, 1.0 mmol) in methanol (5 ml) was treated with bis-(2-nitrooxy-ethyl)-amine (293 mg, 1.5 mmol) and tirethylamine (0.5 ml). After stirring 24 h at ambient temperature, the solvents were removed *in vacuo*. The resulting crude products were purified by flash column chromatography to yield products as off-white solids (194 mg, 39.6%). mp: 184–186°C. Calculated for $C_{20}H_{19}N_5O_{10}Na$ = 512.1182; found $(M+Na)^+$ = 512.1168. ^1H NMR (MeOH) ppm: 2.84–2.87 (m, 4H, CH_2), 4.64–4.67 (m, 4H, CH_2), 6.91–7.01 (m, 4H, Ar-H), 7.12–7.15 (t, *J* = 7.53, 1H, Ar-H), 7.34–7.38 (t, *J* = 7.53, 2H, Ar-H), 7.46–7.51 (m, 2H, Ar-H). ^{13}C NMR (MeOH) ppm: 46.7; 70.7; 84.0; 119.3; 120.6; 121.2; 124.2; 128.7; 131.1; 150.6; 157.6; 160.2; 170.5. IR (KBr) ν (cm^{-1}): 3068; 1728; 1706; 1648; 1281; 849.

5-(4-phenoxyphenyl)-5-(methyl-(2-nitrooxy-ethyl)-amino)pyrimidine-2,4,6(1*H*,3*H*,5*H*)-trione (110)

A solution of 5-bromo-5-(4-phenoxyphenyl)pyrimidine-2,4,6(1*H*,3*H*,5*H*)-trione (375 mg, 1.0 mmol) in methanol (5 ml) was treated with Methyl-(2-nitrooxy-ethyl)-amine (180 mg, 1.5 mmol) and tirethylamine (0.5 ml). After stirring 24 h at ambient temperature, the solvents were removed *in vacuo*. The resulting crude products were purified by flash column chromatography to yield products as off-white solids (134 mg, 32.3%). mp: 143–145°C. Calculated for $C_{19}H_{18}N_4O_7Na$ = 437.1073; found $(M+Na)^+$ = 437.1078. ^1H NMR ($CDCl_3$) ppm: 2.41 (s, 3H, CH_3), 2.91–2.96 (m, 2H, CH_2), 4.37–4.42 (m, 2H, CH_2), 6.90–6.92 (d, *J* = 8.03, 2H, Ar-H), 7.00–7.02 (d, *J* = 8.03, 2H, Ar-H), 7.15–7.18 (t, *J* = 7.53, 1H, Ar-H), 7.34–7.38 (t, *J* = 7.53, 2H, Ar-H), 7.40–7.46 (d, *J* = 8.03, 2H, Ar-H). ^{13}C NMR ($CDCl_3$) ppm: 38.2; 49.8; 70.8; 76.1; 118.3; 119.8; 121.4; 124.6; 129.5; 130.0; 150.8; 155.6; 159.1; 171.2. IR (KBr) ν (cm^{-1}): 3066; 1720; 1698; 1644; 1280; 842.

5-(4-phenoxyphenyl)-5-(4-(2-nitrooxy-ethyl)piperazin-1-yl)pyrimidine-2,4,6(1*H*,3*H*,5*H*)-trione (111)

A solution of 5-bromo-5-(4-phenoxyphenyl)pyrimidine-2,4,6(1*H*,3*H*,5*H*)-trione (375 mg, 1.0 mmol) in methanol (5 ml) was treated with (2-nitrooxy-ethyl)-piperazine (262 mg, 1.5 mmol) and tirethylamine (0.5 ml). After stirring 24 h at ambient temperature, the solvents were removed *in vacuo*. The resulting crude products were purified by flash column chromatography to yield products as off-white solids (197 mg, 42.0%). mp: 206–208°C. Calculated for $C_{22}H_{24}N_5O_7$ = 470.1676; found $(M+H)^+$ = 470.1679. ^{1}H NMR (DMSO) ppm: 2.40-2.48(s, 6H, CH_2); 2.62–2.68 (m, 4H, CH_2); 4.04-4.07 (s, 2H, CH_2); 7.02–7.07 (m, 4H, Ar-H); 7.17–7.21 (t, *J* = 7.53, 1H, Ar-H); 7.40–7.43 (m, 4H, Ar-H). ^{13}C NMR (DMSO) ppm: 47.8; 52.8; 57.3; 71.0; 74.0; 118.2; 118.4; 119.2; 121.4; 124.2; 129.6; 130.2; 150.2; 155.9; 159.3. 170.1. IR (KBr) v (cm^{-1}): 3066; 1710; 1684; 1640; 1281; 849.

5-(4-phenoxyphenyl)-5-(4-(1-nitrooxy-methyl)piperidin-1-yl)pyrimidine-2,4,6(1*H*,3*H*,5*H*)-trione (112)

A solution of 5-bromo-5-(4-phenoxyphenyl)pyrimidine-2,4,6(1*H*,3*H*,5*H*)-trione (375 mg, 1.0 mmol) in methanol (5 ml) was treated with 4-(1-nitrooxy-methyl)-piperidine (240 mg, 1.5 mmol) and tirethylamine (0.5 ml). After stirring 24 h at ambient temperature, the solvents were removed *in vacuo*. The resulting crude products were purified by flash column chromatography to yield products as off-white solids (158 mg, 34.8%). mp: 190–192°C. Calculated for $C_{22}H_{23}N_4O_7$ = 455.1561; found $(M+H)^+$ = 455.1567. ^{1}H NMR ($CDCl_3$) ppm: 1.16–1.27 (m, 2H, CH_2) 1.47–1.58 (m, 3H, CH_2+CH), 2.32–2.37 (m, 2H, CH_2), 2.77–2.83 (m, 2H, CH_2), 4.84–4.90 (m, 2H, CH_2), 6.92–6.95 (d, *J* = 8.53, 1H, Ar-H), 6.97–6.99 (d, *J* = 8.53, 2H, Ar-H), 7.01–7.03 (d, *J* = 8.53, 1H, Ar-H), 7.15–7.18 (t, *J* = 7.53, 1H, Ar-H), 7.37–7.40 (t, *J* = 7.53, 2H, Ar-H), 7.43–7.48 (m, 2H, Ar-H). ^{13}C NMR

($CDCl_3$) ppm: 27.4; 34.2; 49.1; 75.7; 76.1; 118.4; 119.8; 121.3; 124.3; 129.6; 130.2; 150.7; 155.9; 159.4; 170.6. IR (KBr) ν (cm^{-1}): 3068; 1732; 1694; 1642; 1286; 849.

5-(4-phenoxyphenyl)-5-(4-(2-nitrooxy-ethyl)piperidin-1-yl)pyrimidine-2,4,6(1*H*,3*H*,5*H*)-trione (113)

A solution of 5-bromo-5-(4-phenoxyphenyl)pyrimidine-2,4,6(1*H*,3*H*,5*H*)-trione (375 mg, 1.0 mmol) in methanol (5 ml) was treated with 4-(2-nitrooxy-ethyl)-piperidine (261 mg, 1.5 mmol) and tirethylamine (0.5 ml). After stirring 24 h at ambient temperature, the solvents were removed *in vacuo*. The resulting crude products were purified by flash column chromatography to yield products as off-white solids (145 mg, 30.9%). mp: 201–203°C. Calculated for $C_{23}H_{25}N_4O_7$ = 469.1723; found $(M+H)^+$ = 469.1723. ^1H NMR ($CDCl_3$) ppm: 1.33–1.39 (m, 2H, CH_2) 1.42–1.46 (m, 2H, CH_2), 1.48–1.51 (m, 1H, CH),1.73–1.78 (m, 2H, CH_2), 2.57–2.64 (m, 2H, CH_2), 2.76–2.79 (m, 2H, CH_2), 4.78–4.82 (m, 2H, CH_2), 6.92–6.94 (d, *J* = 8.53, 1H, Ar-H), 6.96–6.98 (d, *J* = 8.53, 2H, Ar-H), 7.03–7.05 (d, *J* = 8.53, 1H, Ar-H), 7.16–7.19 (t, *J* = 7.53, 1H, Ar-H), 7.36–7.40 (t, *J* = 7.53, 2H, Ar-H), 7.45–7.49 (m, 2H, Ar-H), 8.99 (s, 2H, NH). ^{13}C NMR ($CDCl_3$) ppm: 21.4; 32.2; 32.6; 48.1; 70.5; 76.0; 118.2; 119.7; 121.2; 124.2; 129.5; 129.9; 148.7; 155.8; 158.1; 169.8 IR (KBr) ν (cm^{-1}): 3068; 1732; 1704; 1633; 1285; 849.

5-(4-phenoxyphenyl)-5-(3-(1-nitrooxy-methyl)piperidin-1-yl)pyrimidine-2,4,6(1*H*,3*H*,5*H*)-trione (114)

A solution of 5-bromo-5-(4-phenoxyphenyl)pyrimidine-2,4,6(1*H*,3*H*,5*H*)-trione (375 mg, 1.0 mmol) in methanol (5 ml) was treated with 3-(1-nitrooxy-methyl)-piperidine (240 mg, 1.5 mmol) and tirethylamine (0.5 ml). After stirring 24 h at ambient temperature, the solvents were removed *in vacuo*. The resulting crude products were purified by flash column chromatography to yield products as off-white solids (181 mg, 39.8%). mp: 190–192°C. Calculated for $C_{22}H_{23}N_4O_7$ = 455.1568; found $(M+H)^+$ = 455.1567. ^1H NMR ($CDCl_3$) ppm: 1.28–1.30 (m, 1H,

CH_2), 1.36–1.40 (m, 1H, CH_2), 1.56–1.59 (m, 1H, CH_2), 1.64–1.68 (m, 1H, CH_2), 1.71–1.76 (m, 1H, CH), 2.08–2.13 (m, 1H, CH_2), 2.51–2.57 (m, 1H, CH_2), 2.61–2.68 (m, 1H, CH_2), 2.71–2.75 (m, 1H, CH_2), 4.37–4.41 (m, 1H, CH_2), 4.52–4.57 (m, 1H, CH_2), 6.92–6.94 (d, *J* = 8.53, 1H, Ar-H), 6.96–6.99 (d, *J* = 8.53, 1H, Ar-H), 7.04–7.06 (d, *J* = 8.53, 1H, Ar-H), 7.16–7.20 (t, *J* = 7.53, 1H, Ar-H), 7.36–7.40 (t, *J* = 7.53, 2H, Ar-H), 7.45-7.49 (m, 2H, Ar–H), 9.15 (s, 1H, NH), 9.16 (s, 1H, NH). ^{13}C NMR ($CDCl_3$) ppm: 26.6; 34.2; 48.8; 50.7; 53.7; 73.7; 74.6. 118.5; 119.7; 121.3; 124.2;129.4; 129.9; 148.9; 155.7; 158.9; 170.0. IR (KBr) v (cm^{-1}): 3066; 1723; 1688; 1640; 1281; 853.

6.2 Biological Methods

6.2.1. Cell culture

Human HT-1080 cells (Sigma-Aldrich, Ireland) were cultivated in Eagle's minimal essential medium (EMEM) containing 10% fetal bovine serum (FBS), 100 IU/ml penicillin, 50 µg/ml streptomycin, and 50 µg/ml gentamycin. The cultures were incubated at 37°C in a humidified 5% CO_2 atmosphere until confluence.

Caco-2 cells (Sigma-Aldrich, Ireland) were cultivated in Dulbecco's modified Eagle's medium (DMEM) containing 10% FBS, 1 X nonessential amino acids, 2 mM L-glutamine, 100 IU/ml penicillin, and 50 µg/ml streptomycin

6.2.2 Gelatinases secretion

Confluent HT1080 cells were washed twice with serum-free medium and incubated under serum-free conditions for 6 h. The cells were treated with 12-*O*-tetradecanoylphorbol-13-acetate (PMA) at final concentration of 10 µM. After incubation for 24 h, the supernatants were collected, which contained MMP-2 and MMP-9.

6.2.3 Zymography

The enzymatic activities of MMP-2 and MMP-9 were assayed by gelatin zymography in the absence of serum. Cell supernatants were electrophoresed on an 8% SDS–PAGE containing gelatin (Liabakk, Talbot et al. 1996). The gels were washed with 2.5% triton three times for 20 min. The gels were washed twice for 30 min in zymography buffer and were then incubated in the zymography buffer (0.15 M NaCl, 5 mM $CaCl_2$, 0.05% NaN_3 and 50 mM Tris-HCl buffer, pH 7.5) at 37 ^{o}C for 48 h in the presence of the inhibitors at 10 μM or 0.5 μM. The control bands were incubated in the same conditions but without the inhibitors. After incubation, the gels were stained with 0.25% Coomassie Brilliant Blue G250, and then destained with acetic acid, methanol and water. The procedure was repeated three times. The remaining enzymatic activity was measured by the intensity of digestion (white bands in blue gels) using the gel reader (Bio-Rad universaly hood II). The inhibition was calculated by comparing the intensity of bands incubated with inhibitors to the bands incubated without inhibitors.

6.2.4 MMP-2 and MMP-9 Fluorogenic Assay

Recombinant MMP-2 and MMP-9 (R & D Systems, Ireland) was activated by APMA (*p*-aminophenylmercuric acetate) at 37 °C for 1 h and 24 h, respectively (Breyholz, Schäfers et al. 2005; Whitlock, Dack et al. 2007). The synthetic broad-spectrum fluorogenic substrate (7-methoxycoumarin-4-yl)-acetyl-pro-Leu-Gly-Leu-(3-(2,4-dinitrophenyl)-L-2,3-diaminopropionyl)-Ala-Arg-NH_2 (R & D Systems, UK) was used to assay MMP-2 and MMP-9 activity. The inhibition of human active MMP-2 and MMP-9 was assayed by preincubating MMP-2 (2 nM) or MMP-9 (2 nM) and the inhibitory compounds at varying concentrations (10 pM to 10 μM) in 50 mM Tris-HCl, pH 7.5, containing 0.2 M NaCl, 5 mM $CaCl_2$, 20 μM $ZnSO_4$, and 0.05% Brij 35, at 37 °C for 30–45 min. An aliquot of substrate (10 μL of a 50 μM solution) was then added to 90 μl of the preincubated MMP/inhibitor mixture, and the activity was determined at 37 °C by following product release with time. The

fluorescence changes were monitored using a plate reader machine (Fluostar OPTIMA, BMG LABTECH) with excitation and emission wavelengths set to 330 and 405 nm, respectively. Reaction rates were measured from the initial 10 min of the reaction profile where product release was linear with time and plotted as a function of inhibitor dose. From the resulting inhibition curves, the IC_{50} value for each inhibitor was calculated by nonlinear regression analysis using the *Prism 4.0* programme.

6.2.5 Invasion assay

Caco-2 cells were cultured until 80% confluence and removed from flask using DPBS-EDTA. The cells were collected in serum-free medium and were counted in a cell-counting machine (Z1 coulter® Particle counter). The inserts contained matrigel membranes with 8.0 μm pore (BD Bioscience, UK) were treated with 500 μl serum-free medium. After incubation for 2 h, the blank inserts were treated with 250,000 Caco-2 cells and the positive control inserts contained 250,000 Caco-2 cells and 75 ng HGF (Kermorgant, Aparicio et al. 2001). All the remaining inserts were treated with 250,000 Caco-2 cells, 75 ng HGF, and the tested inhibitors (with finial concentrations at 10 μM and/or 100 nM). Medium with 2% FCS was added to each inserts to make the total volume 1 ml. The inserts were then transferred to the assay chambers containing 750 ml of 20% FCS medium and left in cell culture incubator for 48 h. After incubation, supernatants were taken out and the non-migratory cells on the upper surface of the membranes were removed with serum-free medium using cotton swabs. The inserts were treated with the Diff-Quik kit (BD Bioscience, USA) for fixing and staining the invade cells on the membranes. The inserts were left for drying and the migrated cells were counted under the microscopy (Zeiss Axiovert 200 M). The inhibition of cell invasion induced by the test inhibitors were calculated by the formula 3-1.

6.2.6 Griess assay

A series of nitrite and nitrate standard solutions were prepared by sodium nitrite

and sodium nitrate at the concentration from 3 μM to 200 μM. 200 μl of each nitrite standard solutions and 200 μl of water were added to a 96-well plate (Miranda, Espey et al. 2001). As for measure of nitrate standard solution, 200 μl of 4°C saturated solution of VCl_3 was added instead of water. The blank wells contained only 400 μl of water. All the wells were treated with 100 μl of 4°C SULF (2% w/v) and 100 μl of NED (0.1 w/v). The plate was shaken for 45 min and the absorbance was measured in the plate reader machine at 540 nM. The linear regression formulae of relationships between nitrite and nitrate concentrations and absorbance were established. The supernatants of the barbiturate-based nitrate treated Caco-2 cells were tested in similar manners with those of nitrite and nitrate standard solutions. The resulting absorbance of the supernatants were applied to the linear regression formulae for calculation of concentrations of nitrite and nitrate of the supernatants

6.2.7 MTT assay

Cells were plated into 96 well plates at a concentration of 8×10^4 cells/ml (HT1080) or 1.2×10^5 cells/ml (Caco-2) in 100 μl volume. After incubated for 24 h, the medium was removed carefully and the cells were treated with 1 μl of the barbiturate-based nitrates in DMSO at indicated concentrations in supplement free medium. The final concentration of DMSO in Cell never exceeded 1%. Vehicle control wells were treated with 1 μl DMSO and the blank wells contained only medium. The plates were incubated at 37°C for 1 h or 24 h. After incubation, 20 μl of MTT solution (0.5 mg MTT in 1 ml PBS) were added to each well and incubated for another 3 h at 37°C (Mosmann 1983). The medium was gently aspirated from the wells and 100 μl of DMSO was added to each well to lyse the cells. The plates were covered with tinfoil, shaken for 15 min, and then read plate reader machine at a wavelength of 590 nm. Cell survival rates were calculated by the formula 5-1.

6.3 Molecular modelling

The crystal structure of MMP-2 (PDB code 1QIB) was used for the study. Since this is a co-crystallised structure complexed with a hydroxamate inhibitor, the hydroxamate inhibitor was removed. The structure of MMP-9 (PDB code 2VOX) used was an MMP-9 active site mutant with barbiturate inhibitor, so the barbiturate inhibitor was removed. In addition water molecules were removed. Docking calculations were carried out using AutoDock version 4.0, with the Lamarckian genetic algorithm (LGA). The molecular models of each inhibitor were built using the builder function of MOE and minimized with MOPAC 7 (AM1 method) interfaced to MOE. The zinc parameters were changed to zinc radius: 0.87 Å; well depth: 0.35 kcal/mol; and zinc charges: +0.95 e (Hu and Shelver 2003). The 3D affinity grid box was designed to include the full active site and possible residues. The setting of the center of grid boxes was based on the value of active zinc atom. Docking calculations were set to 100 runs. 25000000 energy evaluations were allowed as a maximum in each run. At the end of the calculation, AutoDock performed cluster analysis. Docking solutions with ligand all-atom root mean square deviation (RMSD) within 2.0 Å of each other were clustered together and ranked by the lowest energy representative.

6.4 Stability studies

A gradient reverse High performance liquid chromatography (HPLC) method was employed for analysis the stability, which involved elution on a Waters Xbridge C18 5 µm column (4.6 x 250 mm) with a binary mixture of methanol and water at 1 ml/min in gradient mode. HPLC was performed using a system consisting of a Waters 600 pump and controller, Waters 717 Autosampler and a Waters 996 photodiode Array Detector controlled by Epower programme.

6.5 Statistical analysis

All date are presented as group of means + standard error of the mean of $n \geq 3$. Statistical analysis of the mean difference between multiple groups was

determined by one-way ANOVA followed by Tukey-Kramer multiple comparison post test. A P value < 0.05 is considered to be statistically significant. All statiscial analysis were performed using GraphPad Prism version 4.0 for Windows.

References

Ahokas, K., J. Lohi, et al. (2002). "Matrix metalloproteinase-21, the human orthologue for XMMP, is expressed during fetal development and in cancer." Gene **301**(1-2): 31-41.

Ahokas, K., T. Skoog, et al. (2005). "Matrilysin-2 (matrix metalloproteinase-26) is upregulated in keratinocytes during wound repair and early skin carcinogenesis." J. Invest. Dermatol. **124**(4): 849-856.

Allan, J. A., A. J. P. Docherty, et al. (1995). "Binding of gelatinases A and B to type-I collagen and other matrix components." Biochem. J. **309**(1): 299-306.

Alonso, D. and M. W. Radomski (2003). "Nitric oxide, platelet function, myocardial infraction and reperfusion therapies." Heart Fail Rev. **8**: 47-54.

Amour, A., C. G. Knight, et al. (2000). "The in vitro activity of ADMA-10 as inhibited by TIMP-1 and TIMP-3." FEBS Lett. **473**: 257-259.

Andrade, S. P., I. R. Hart, et al. (1992). "Inhibitors of nitric oxide synthase selectively reduce flow in tumor-assoicated neovasculature." Br. J. Pharmacol. **107**(4): 1092-1095.

Angel, P., I. Baumann, et al. (1987). "12-Otetradecanoyl-phorbol-13-acetate induction of human collagense gene is mediated by and inducible enhancer element located in the 5'-flanking region." Mol. Cell Biol. **7**: 2256-2266.

Atkinson, J. J., K. Holmbeck, et al. (2005). "Membrane-type 1 matrix metalloproteinase is required for normal alveolar development." Dev. Dyn. **232**(4): 1079-1090.

Bailey, C. J., R. M. Hembry, et al. (1999). "Distribution of matrix metalloproteinases stromelysin, gelatinases A and B, and collagenase in Crohn's disease and normal intestine." J. Clin. Pathol. **47**: 113-116.

Baker, E. A. and D. J. Leaper (2002). "Measuring gelatinase activity in colorectal cancer." Eur. J. Surg. Oncol. **28**(1): 24-29.

Balbin, M., A. Fueyo, et al. (1998). "Collagenase 2 (MMP-8) expression in murine tissue-remodeling processes. Analysis of its potential role in postpartum involution of the uterus." J. Bio. Chem. **273**: 23959-23968.

Bandarage, U. K., T. Wang, et al. (2008). "Novel thiol-based TACE inhibitors. Part 2: Rational design, synthesis, and SAR of thiol-containing aryl sulfones." Bioorg. Med. Chem. Lett. **18**: 44-48.

Barrett, A. J. (1981). "α2-Macroglobulin." Methods Enzymol. **80**: 737-754.

Bartlett, J. D., E. Beniash, et al. (2004). "Decreased mineral content in MMP-20 null mouse enamel is prominent during the maturation stage." J. Dent. Res. **83**(12): 909-913.

Bartlett, J. D., J. P. Simmer, et al. (1996). "Molecular cloning and mRNA tissue distribution of a novel matrix metalloproteinase isolated from porcine enamel organ." Gene **183**(1-2): 123-128.

Barvian, N. C., M. Ann Arbor, et al. (2002). Biphenyl sulfonamides useful as matrix metalloproteinase inhibitors. EP 1233016A1. W.-L. Company. German, Tesch, Rudolf.

Bassed, P., J. P. Bellocq, et al. (1990). "A novel metalloproteinase gene specifically expressed in stromal cells of breast carcinomas." Nature **348**(6303): 699-704.

Baugh, M. D., M. J. Perry, et al. (1999). "Matrix metalloproteinase levels are elevated in inflammatory bowel diseases." Gastroenterology **117**: 814-822.

Benbow, U. and C. E. Brinckerhoff (1997). "The AP-1 site and MMP gene regulation: What is all the fuss about?" Matrix Biol. **15**(8-9): 519-526.

Bergers, G. and L. E. Benjamin (2003). "Tumorigeneisis and the angiogenic switch." Nat. Rev. Cancer. **3**: 401-410.

Bergers, G., R. Brekken, et al. (2000). "Matrix metalloproteinase-9 triggers the angiogenic switch during carcinogensis." Nat. Cell Biol. **2**(10): 737-744.

Bergers, G. and L. M. Coussens (2000). "Extrinsic regulators of epithelial tumor progression: metalloproteinases." Curr. Opin. Genet. Dev. **10**(1): 120-127.

Berndt, G., N. Grosser, et al. (2005). "AZD3582 increases heme oxygenase-1 expression and antioxidant activity in vascular endothelial and gastric mucosal cells." Eur. J. Pharm. Sci. **25**(2-3): 229-235.

Bidlinmery, B. A. (1992). Pratical HPLC methodlogy and applications. New York, Wiley Interscience.

Bidlinmeyer, B. A. (1992). Pratical HPLC methdology and Applications. New York, Wiley Interscience.

Bister, v., M. T. Salmela, et al. (2005). "Matrilysins-1 and -2 (MMP-7 and -26) and metalloelastase (MMP-12), unlike MMP-19, are up-regulated in necrotizing enterocolitis." J. Pediatr. Gastroenterol Nutr. **40**: 60-66.

Bjorklund, M. and E. Koivunen (2005). "Gelatinase-mediated migration and invasion of cancer cells." Biochim. Biophys. Acta. **1755**: 37-69.

Blagg, J. A., M. C. Noe, et al. (2005). "Potent pyrimidinetrione-based inhibitors of MMP-13 with enhanced selectivity over MMP-14." Bioorg. Med. Chem. Lett. **15**: 1807-1810.

Bloomston, M., E. E. Zervos, et al. (2002). "Matrix metalloproteinases and their role in pancreatic cancer: A review of preclincial studies and clinical trials." Ann. Surg. Oncol. **9**: 668-674.

Bogdan, C. (2001). "Nitric oxide and the immue response." Nat. Immunol. **2**: 907-916.

Boire, A., L. Covic, et al. (2005). "PAR1 is a matrix metalloproteases receptor that promotes in invasion and tumorigensis of brease cancer cells." Cell **120**(3): 303-313.

Bonavida, B., S. Baritaki, et al. (2008). "Novel therapeutic applications of nitric oxide donors in cancer: roles in chemo- and immunosensitization to poptosis and inhibition of metastases." Nitric Oxide **19**: 152-157.

Brandstetter, H., F. Grams, et al. (2001). "The 1.8-A° Crystal Structure of a Matrix Metalloproteinase 8-Barbiturate Inhibitor Complex Reveals a Previously Unobserved Mechanism for Collagenase Substrate Recognition." J. Bio. Chem. **276**(20): 17405-17412.

Breyholz, H., M. Schafers, et al. (2005). "C-5-disubstituted barbiturates as potential molecular probes for noninvasive matrix metalloproteinases imaging." J. Med. Chem. **48**: 3400-3409.

Brooijmans, N. and I. D. Kuntz (2003). "Molecular recognition and docking algorithms." Annu. Rev. Biophys. Biomol. Struct. **32**: 335-373.

Brown, D. J. (1994). The Chemistry of Heterocyclic Compounds, The Pyrimidines. New York, John Wiley & Sons, Inc.

Brown, D. L., M. S. Hibbs, et al. (1995). "Identification of 92-kD gelatinase in human coronary atherosclerotic lesions: Association of active enzyme sythesis with unstable angina." Circulation **91**(8): 2125-2131.

Burke, S. G., C. L. Wainwright, et al. (2006). "The effect of NCX4016 [2-acetoxy-benzoate 2-(2-nitroxymethyl)-phenyl ester] on the consequences of ischemia and reperfusion in the streptozotocin diabetic rat." J. Pharmacol. Exp. Ther. **316**(3): 1107-1114.

Burrage, P. S., K. S. Mix, et al. (2006). "Matrix metalloproteinases: Role in arthritis." Front Biosci. **11**(1 P.447-888): 529-543.

Burrow, J. W., J. A. Koch, et al. (2007). "Nitric oxide donors selectively reduce the expression of matrix metalloproteinase-8 and -9 by human diabetic skin fibroblasts." J. Surg. Res. **140**: 90-98.

Butler, T. C., J. M. Ruth, et al. (1954). "The second ionization of 5,5-disubstituted derivatives of barbituric acid." J. Am. Chem. Soc. **77**: 1486-1488.

Cao, J. and S. Zucker. (2004). "Biology and chemistry of matrix metalloproteinases (MMPs)." Introduction to the MMP and TIMP families (structures, substrates) and overview of diseases where MMPs have been incriminated Retrieved 25th Aug., 2010, from http://www.abcam.com/index.html?pageconfig=resource&rid=11034.

Castaneda, F. E., B. Walia, et al. (2005). "Targeted deletion of Metalloproteinase 9 attenuates experimental colitisin mice: central role of epithelia-derived MMP." Gastroenterology **129**: 1991-2008.

Cataldo, D. D., K. G. Tournoy, et al. (2002). "Matrix metalloproteinase-9 deficiency impairs cellular infiltration and bronchial hyperresponsiveness during allergen-induced airway inflammation." Am. J. Pathol. **161**(2): 491-498.

Cha, H., E. Kopetzki, et al. (2002). "Structural basis of the adaptive molecular recognition by MMP-9." J. Mol. Biol. **320**: 1065-1079.

Chakrabarti, S. and K. Patel (2005). "Matrix metalloproteinase-2 (MMP-2) and MMP-9 in pulmonary pathology." Exp. Lung. Res. **31**(6): 599-621.

Chen, L., H. Xu, et al. (2004). "Synthesis and biological activity of tonghaosu analogs containing phenoxy-phenyl moiety." Chinese Journal of Chemistry **22**(9): 984-989.

Cheng, M., B. De, et al. (1999). "Design, synthesis, and biological evaluation of matrix metalloproteinase inihibitors derived from a modified proline scaffold." J. Med. Chem. **42**: 5426-5436.

Cheng, M., B. De, et al. (2000). "Design and Synthesis of Piperazine-Based Matrix Metalloproteinase Inhibitors." J. Med. Chem. **43**(3): 369-380.

Cherr, G. S., S. J. Motew, et al. (2002). "Metalloproteinase inhibition and the response to angioplasty and stenting in atherosclerotic primates." Arterioscler. Thromb. Vasc. Biol. **22**: 161-166.

Chicoine, E., P. O. Estève, et al. (2002). "Evidence for the role of promoter methylation in the regulation of MMP-9 gene expression." Biochem. Biophys. Res. Commun. **297**(4): 765-772.

CHOI, W.-S., O.-H. JEON, et al. (2008). "MMP-2 regulates human platelet activiation by interacting with with integrin $\alpha_{IIb}\beta_3$ " J. Thromb. Haemost. **6**(3): 517-523.

Chung, L., D. Dinakarpandian, et al. (2004). "Collagenase unwinds triple-helical collagen prior to peptide bond hydrolysis." EMBO J **23**(15): 3020-3030.

Close, D. (2001). "Matrix metalloproteinase inhibitors in rheumatic diseases." Ann. Rheum. Dis. **60**(Suppl 3): 62-67.

Couillard, J., M. Demers, et al. (2006). "The role of DNA hypomethylation in the control of stromelysin gene expression." Biochem. Biophys. Res. Commun. **342**(4): 1233-1239.

Coulter, J. A., H. O. McCarthy, et al. (2008). "Nitric oxide--a novel therapeutic for cancer." Nitric Oxide **19**: 192-198.

Crawford, H. C. and L. M. Matrisian (1994). "Tumor and stromal expression of metalloproteinases and their role in tumor progression." Invasion and Metastasis **14**: 234-245.

Curry TE Jr and O. KG (2003). "The matrix metalloproteinase system: changes, regulation, and impact throughout the ovarian and uterine reproductive cycle." Endocr. Rev. **24**: 428-465.

D'Armiento, J., S. S. Dalal, et al. (1992). "Collagenase expression in the lungs of transgenic mice causes pulmonary emphysema." Cell **71**(6): 955-961.

Dasgupta, S., M. Bhattachaya-Chatterjee, et al. (2006). "Tumor metastasis in an orthotopic murine model of head and neck cancer: possible role of TGF-beta 1 secreted by the tumor cells." J. Cell Biochem. **97**: 1036-1051.

De, B., M. G. Natchus, et al. (1999). "The next generation of MMP inhibitors. Design and synthesis." Ann. N. Y. Acad. Sci. **878**: 40-60.

De Smet, B. J., D. De Kleijn, et al. (2000). "Metalloproteinase inhibiton reduces constrictive arterial remodeling after balloon angioplasty: a study in the atherosclerotic Yucatan micropig." Circulation **101**: 2962-2967.

Deryugina, E. I., G. X. Luo, et al. (1997). "Tumor cell invasion through matrigel is regulated by activated matrix metalloproteinas-2." Anticancer Rev. **17**(5A): 3201-3210.

Deryugina, E. I. and J. P. Quigley (2006). "Matrix metalloproteinases and tumor metastasis." Cancer metastasis Rev. **25**: 9-34.

Dhanaraj, V., M. G. William, et al. (1999). "X-ray structure of gelatinase A catalytic domain complexed with a hydroxamate inhibitor." Croatica Chemic. Acta. **72**(575-591).

Di sebastiano, P., F. F. Di Mola, et al. (2001). "Beneficial effects of Batimastat (BB-94), a matrix metalloproteinase inhibitor, in rat experimental colitis." Digestion **63**(234-239).

Dong, Z., J. A. Nemeth, et al. (2001). "Differental regulation of matrix metalloproteinase-9, tissue inhibitor of metalloproteinase-1 (TIMP-1) and TIMP-2 expression in co-cultures of prostate cancer and stromal cells." Int. J. Cancer **93**: 507-515.

Dong, Z., A. H. Starosesky, et al. (1994). "Inverse corelation between expression of inducible ntric oxide synthase activity and production of metastasis in K-1735 murine melanoma cells." Cancer Res. **54**: 789-793.

Drummond, A. H., P. Beckett, et al. (1999). "Preclincial and clinical studies of MMP inhibitors in cancer." Ann. N. Y. Acad. Sci. **228-235**.

Duan, J. J., L. Chen, et al. (2002). "Discovery of γ-lactam hydroxamic acids as selective inhibitors of tumor necrosis factor α converting enzyme: design,

synthesis, and structure-activity relationships." J. Med. Chem. **45**: 4954-4957.

Duan, J. J., Z. H. Lu, et al. (2005). "Non-hydroxamate 5-phenylpyriminde-2,4,6,-trione derivatives as selective inhibitors of tumor necrosis factor-α converting enzyme." Bioorg. Med. Chem. Lett. **15**: 2970-2973.

Dubois, B., S. Masure, et al. (1999). "Resistance of young gelatinase B-deficient mice to experimental autoimmune encephalomyelitis and necrotizing tail lesions." J. Clin. Invest. **104**(11): 1507-1515.

Ducharme, A., S. Frantz, et al. (2000). "Targeted deletion of matrix metalloproteinase-9 attenuates left ventricular enlargement and collagen accumulation after experimental myocardial infarction." J. Clin. Invest. **106**(1): 55-62.

Egan, l. J. and W. L. Sandborn (2005). Clinical pharmacologiy in inflammatory bowel disease: optimizing current medical therapy. Inflammatory Bowel disease: from bench to bedside. S. R. Targan, F. Shanahan and L. C. Karp. New York, Springer**:** 495-521.

Egeblad, M. and Z. Werb (2002). "New functions for the matrix metalloproteinases in cancer progression." Nat. Rev. Cancer. **2**(3): 161-174.

Emmert-Buck, M. R., M. J. Roth, et al. (1994). "Increased gelatinase A (MMP-2) and cathepsin B activity in invasive tumor regions of human colon cancer samples." Am. J. Pathol. **145**(6): 1285-1290.

Evans, D. A., J. L. Katz, et al. (1998). "Synthesis of diaryl ethers through the copper-promoted arylation of phenols with arylboronic acids. An expedient synthesis of thyroxine." Tetrahedron Lett. **39**(19): 2937-2940.

Evgenov, O. V., P. Pacher, et al. (2006). "NO-independent stimulators and activators of soluble guanylate cyclase: discovery and therapeutic potential." Nat. Rev. Drug. Discov. **5**(9): 755-768.

Faber, H. R., C. R. Groom, et al. (1995). "1.8 A crystal structure of the C-terminal domain of rabbit serum haemopexin." Structure **3**(6): 551-559.

Fata, J. E., K. J. Leco, et al. (2001). "Accelerated apoptosis in the Timp-3-deficient mammary gland." J. Clin. Invest. **108**: 831-841.

Faveeuw, C., G. Preece, et al. (2001). "Transendothelial migration of lymphocytes across high endothelia venules into lymph nodes is affected by metalloproteinases." Blood **98**(3): 688-695.

Fernandez-Catalan, C., W. Bode, et al. (1998). "Crystal structure of the complex formed by the membrane type 1-matrix metalloproteinase with the tissue

inhibitor of metalloproteinases-2, the soluble progelatinase A receptor." EMBO J **17**: 5238-5248.

Fernandez-Catalan, C., M. A. Martinz-Cuesta, et al. (1999). "Differential regulation of platalet aggregation by matrix metalloproteinase -9 and -2." Thromb. Haemost. **86**: 1562-1783.

Fernandez-Catalan, C., K. G. Stewart, et al. (2000). "Vasculaar matrix metalloproteinase-2-dependent cleavage of calcitonin gene-related peptide promotes vasoconstriction." Circ. Res. **87**: 670-676.

Fernandez-Patron, C., C. Zouki, et al. (2001). "Matrix metalloproteinases regulate neutrophil-endothelial cell adhesion through generation of endothelin-1[1-32]." FASEB J. **15**(12): 2230-2240.

Filippin, L. I., A. J. Moreira, et al. (2009). "Nitric oxide and repair of skeletal muscle injury." Nitric Oxide **21**: 157-163.

Fink, C. A., J. E. Carlson, et al. (1995). "Design and synthesis of thiol containing inhibitors of matrix metalloproteinases." Bioorg. Med. Chem. Lett. **9**: 195-200.

Foley, L. H., R. Palermo, et al. (2001). "Novel 5,5-disubstitutedpyrimidine-2,4,6-triones as selective MMP inhibitors." Bioorg. Med. Chem. Lett. **11**(8): 969-972.

Freije, J. M., I. Diez-Itza, et al. (1994). "Molecular cloning and expression of collagenases, a novel human matrix metalloproteinase produced by breast carcinomas." J. Bio. Chem. **269**(24): 16766-16773.

Freskos, J. N., B. V. Mischke, et al. (1999). "Discovery of a novel series of selective MMP inhibitors: identification of the γ-sulfone-thiols." Bioorg. Med. Chem. Lett. **9**: 943-948.

Fridman, R., T. R. Fuerst, et al. (1992). "Domain structure of human 72-kDa gelatinase/type IV collagenase: Characterization of proteolytic activity and identification of the tissue inhibitor of metalloproteinase-2 (TIMP-2) binding regions." J. Bio. Chem. **267** (22): 15398-15405.

Friedl, P. and E. B. Brocker (2000). "The biology of cell locomotion within three dimensional extracellular matrix." Cell Mo.l Life Sci. **57**: 41-64.

Friedl, P. and K. wolf (2003). "Tumor-cell invasion and migration: diversit and escape mechanisms." Nat. Rev. Cancer. **3**: 362-374.

Galis, Z. S. and J. J. Khatri (2002). "Matrix metalloproteinases in vascular remodeling and atherogenesis: The good, the bad, and the ugly." Circ. Res. **90**(3): 251-262.

Garg, P., M. Rojas, et al. (2006). "Selective ablation of matrix metalloproteinase-2 exacerbates experimental colitis: contrasting role of gelatinases in pathogenesis of colitis." J. Immunol. **177**: 4103-4112.

Gearing, A. J. H., P. Beckett, et al. (1994). "Processing of tumour necrosis factor-α precursor by metalloproteinases." Nature **370**(6490): 555-557.

Gianneli, G., J. Flak-Marziller, et al. (1997). "Induction of cell migration by matrix metalloprotease-2 cleavage of laminin-5." Science **277**: 225-228.

Gilmer, J. F., M. N. Lally, et al. (2005). "Noevel isosorbide-based substrates for human butyrylcholinesterase." Chem. Biol. Interact. **157-158**: 317-319.

Goldberg, G. I., A. Strongin, et al. (1992). "Interaction of 92-kDa type IV collagenase with the tiussue inhibitor of metalloproteinases prevents dimerization, complex formation iwth intestinal collagenase, and activation of the proenzyme with stromelysin." J. Bio. Chem. **267**: 4583-4591.

Goodall, S., M. Crowther, et al. (2001). "Ubiquitous elevation of matrix metalloproteinase-2 expression in the vasculature of patients with abdominal aneurysms." Circulation **104**(3): 304-309.

Goodman, L. S., A. Gilman, et al. (2006). Goodman and Gilman's the pharmacological basis of therapeutics. New York, McGraw-Hill.

Goss, K. J. H., P. D. Brown, et al. (1998). "Differing effects of endogenous and synthetic inhibitors of metalloproteinases on intestinal tumorigenesis." Int. J. Cancer **78**: 629-635.

Gough, P. J., I. G. Gomez, et al. (2006). "Macrophage expression of active MMP-9 induces acute plaque disruption in apoE-deficient mice." J. Clin. Invest. **116**(1): 59-69.

Gram, F., P. Reinemer, et al. (1995). "X-ray structure of human eutrophil collagenase complexed with peptide hydromate and peptide thiol inhibitors. Implications for substrate binding and rational drug design." Eur. J. Biochem. **228**: 830-841.

Granger, D. L., R. R. Taintor, et al. (1996). "Measurement of nitrate and nitrite in biological samples using nitrate reductase and Griess reaction." Methods Enzymol. **268**: 142-151.

Gross, J. and C. M. Lapiere (1962). "Collagenolytic activity in amphibian tissues: A tissue culture assay. ." Proc. Natl. Acad. Sci. U.S.A. **48**(6): 1041-1022.

Gu, Z., M. Kual, et al. (2002). "S-nitrosylation of matrix metalloproteinases: singaling pathway to neuronal cell death." Science **1297**: 1186-1190.

Guevara, L., J. Iwanejko, et al. (1998). "Determination of nitite/nitrate in human biolgocial material b the simple Griess reaction." Clin. Chim. Acta. **27**: 177-188.

Gujar, M. V., R. Sharma, V.,, et al. (1999). "eNOs Gene trasfer inhibits smooth muscle cell migration and MMP-2 and MMP-9 activity." Arterioscler. Thromb. Vasc. Biol. **19**: 2871-2899.

Gutman, S. I. and C. A. Hollywood (1992). "Simple, rapid method fro dermining nitrates and nitrites in biological fluids." Clin. Chem. **38**: 2152.

Hägglund, A. C., A. Ny, et al. (1999). "Regulation and localization of matrix metalloproteinases and tissue inhibitors of metalloproteinases in the mouse ovary during gonadotropin-induced ovulation." Endocrinology **140**(9): 4351-4358.

Hanessian, S., N. Moitessier, et al. (2001). "N-Aryl sulfonyl homocysteine hydroxamate inhibitors of matrix metalloproteinases: further probing of the S1, S1', and S2' pockets." J. Med. Chem. **44**: 3066-3073.

Haro, H., H. C. Crawford, et al. (2000). "Matrix metalloproteinase-3-dependent generation of a macrophage chemoattractant in a model of herniated disc resorption." J. Clin. Invest. **105**(2): 133-141.

Hautamaki, R. D., D. K. Kobayashi, et al. (1997). "Requirement for macrophage elastase for cigarette smoke-induced emphysema in mice." Science **277**(5334): 2002-2004.

He, M. M., A. S. Smith, et al. (2005). "small molecule inhibition of TNF-α." Science **310**: 1022-1025.

Heissig, B., K. Hattori, et al. (2002). "Recruitment of stem and progenitor cells from the bone marrow niche requires MMP-9 mediated release of Kit-ligand." Cell **109**(5): 625-637.

Heldin, C. H. (1995). "Dimerization of cell surface receptors in singal transduction." Cell **80**: 213-223.

Heniksen, M., J. Jahnsen, et al. (2007). "Clincial course in Crohn's disease: resutls of a five-year population-baed follow-up study (the IBSEN study)." Scand. J. Gastroenterol. **42**: 602-610.

Herman, M. P., G. K. Sukhova, et al. (2001). "Tissue factor pathway inhibitor-2 is a novel inhibitor of matrix metalloproteinases with implications for atherosclerosis." J. Clin. Invest. **107**: 1117-1126.

Herman, M. P., G. K. Sukhova, et al. (2001). "Expression of neutrophil collagenase (matrix metalloproteinase-8) in human atheroma: A novel collagenolytic pathway suggested by transcriptional profiling." Circulation **104**(16): 1899-1904.

Holmbeck, K., P. Bianco, et al. (1999). "MT1-MMP-deficient mice develop dwarfism, osteopenia, arthritis, and connective tissue disease due to inadequate collagen turnover." Cell **99**(1): 81-92.

Hori, Y., F. Watanabe, et al. (2000). MMP-12 inhibitors. WO2001083431. L. Shionogi & Co. Japan.

Hu, J., P. E. Van den Steen, et al. (2007). "Matrix metalloproteinase inhibitors as therapy for inflammatory and vascular diseases." Nat. Rev. Drug. Discov. **6**(6): 480-498.

Hu, X. and W. H. Shelver (2003). "Docking studies of matrix metalloproteinase inhibitors: zinc parameter optimization to improve the binding free energy prediction." J. Mol. Graph. Model **22**(2): 115-126.

Hudson, M. P., P. W. Armstrong, et al. (2006). "Effects of selective matrix metalloproteinases inhibitor (PG-116800) to prevent ventricular remodeling after myocardial infarction: results of the PERMIER (Prevention of Myocardial Infarction Early remodeling) trial." J. Am. Coll. Cardiol. **48**(1): 15-20.

Hurst, D. R., M. A. Schwartz, et al. (2005). "Inhibition of enzyme activity of and cell mediated substrate cleavage by membrane type 1 matrix metalloproteinase by newly developed mercaptosulphide inhibitors." Biochem. J. **392**: 527-536.

Hwang, Y. S. and J. Chemielewski (2005). "Development of low molecular weight HIV-1 protease dimmerization inhibitors." J. Med. Chem. **48**: 2239-2242.

Ii, M., H. Yamamoto, et al. (2006). "Role of Matrix metalloproteinase-7 (Matrilysin) in human cancer invasion, apoptosis, growth and angiogenesis." Exp. Biol. Med. **231**: 20-27.

Imai, K., S. S. Dalal, et al. (2001). "Human collagenase (matrix metalloproteinase-1) epxression in the lungs of patients with emphysema." Am. J. Respir. Crit. Care Med. **163**: 786-791.

Imai, K., A. Hiramatsu, et al. (1997). "Degradation of decorin by matrix metalloproteinases: identification of the cleavage sites, kinetic analyses and transforming growth factor-b1 release." Biochem. J. **322**: 809-814.

Ingvarsen, S., D. H. Madsen, et al. (2008). "Dimerization of endogenous MT1-MMP is a regulatory step in the activation of the 72-kDa gelatinase MMP-2 on fibroblast and fibrosarcoma cells." Biol. Chem. **389**: 943-953.

Ito, A., A. Mukaiyama, et al. (1996). "Degradation of interleukin 1β by matrix metalloproteinases." J. Biol. Chem. **271**(25): 14657-14660.

Itoh, Y., M. Kajita, et al. (1999). "Membrane type 4 matrix metalloproteinase (MT4-MMP, MMP-17) is a glycosylphosphatidylinositol-anchored proteinase." J. Biol. Chem. **274**(48): 34260-34266.

Jaworski, D. M., P. Soloway, et al. (2006). "Tissue inhibitor of metalloproteinase-2 (TIMP-2)-deficient mice display motor deficits." J. Neurobiol. **66**(1): 82-94.

Jean-Louis, S., S. Akare, et al. (2006). "Deoxycholic acid induces intracellular signalling through membrane perturbations." J. Biol. Chem. **281**: 14948-14960.

Jeffrey, J. J., C. P. William, et al. (1998). Interstitial Collagenases. Matrix Metalloproteinases. San Diego, Academic Press**:** 15-42.

Jenkins, G. M., M. T. Grow, et al. (1998). "Increased expression of membrane-type matrix metalloproteinase and preferential localizationof matrix metalloproteinase-2 to the neointima of balloon injured rat carotid arteries." Circulation **97**: 82-90.

Jezierska, A. and T. Motyl (2009). "Matrix metalloproteinase-2 involvement in breast cancer progression: a mini-review." Med. Sci. Monit. **15**: RA32-40.

Jeziorska, M., N. Y. Haboubi, et al. (1994). "Distribution of gelatinase B (MMP-9) and type IV collagen in colorectal carcinoma." Int. J. Colorectal. Dis. **9**(3): 141-148.

Jin, X., M. Yagi, et al. (2006). "Matriptase activates stromelysin (MMP-3) and promotes tumor growth and angiogensis." Cancer Science **97**(2): 1327-1334.

Johnson, J. L., S. J. George, et al. (2005). "Divergent effects of matrix metalloproteinases 3, 7, 9, and 12 on atherosclerotic plaque stability in mouse brachiocephalic arteries." Proc. Natl. Acad. Sci. U.S.A. **102**(43): 15575-15580.

Jones, C. B., D. C. Sane, et al. (2003). "Matrix metalloproteinases: A review of their structure and role in acute coronary syndrome." Cardiovasc. Res. **2003**: 812-823.

Jones, M. K., K. Tsugawa, et al. (2004). "Dual actions of nitric oxide on angiogenesis: possible roles of PKC, ERK, and AP-1." Biochem. Biophys. Res. Commun. **318**: 520-528.

Jurasz, P., D. Alonso-Escolan, et al. (2004). "Platelet-cancer interactions: mechanisms and pharmacology of tumour cell-induced platelet agrregation." Br. J. Pharmacol. **143**: 819-826.

Kar, A. (2006). Medicinal Chemistry. Kent, Anshan Ltd. .

Kashiwagi, A., M. Tortorella, et al. (2001). "TIMP-3 is a potent inhibitor of aggrecanse 1 (ADAM-TS4) and Aggrecanase 2 (ADAM-TS5)." J. Bio. Chem. **276**: 12501-12504.

kelly, E. and N. Jarjour (2003). "Role of matrix metalloproteinses in asthma." Curr. Opin. Pulm. Med. **9**: 28-33.

Kelm, M. (1999). "Nitric oxide metabolsim and breakdown." Biochim. Biophys. Acta. **1411**: 273-289.

Kermorgant, S., T. Aparicio, et al. (2001). "Hepatocyte growth factor induces colonic cancer cell invasiveness via enhanced motility and protease overproduction. Evidence for PI3 kinase and PKC involvement." Carcinogenesis **22**(7): 1035-1042.

Ketchen, D. B., H. Decornez, et al. (2004). "Docking and scoring in vitrual screening for drug discovery methods and applications." Nat. Rev. Drug. Discov. **3**: 935-949.

Kido, A., M. Tsutsumi, et al. (1999). "Overexpression of matrix metalloproteinase (MMP)-9 correlates with metastatic potency of spontateous and 4-hdroxyaminoquinolin 1-oxide (4-HAQO)-induced transplantable osteosarcomas in rats." Cancer Lett. **137**: 209-216.

Kim, H. E., S. S. Dalal, et al. (2000). "Disruption of the myocardial extracellular matrix leads to cardiac dysfunction." J. Clin. Invest. **106**(7): 857-866.

Kim, S. H., A. T. Pudzianowski, et al. (2005). "Structure-based design of potent and selective inhibitors of collagenase-3 (MMP-13)." Bioorg. Med. Chem. Lett. **15**(4): 1101-1106.

Kirkegaard, T., A. Hansen, et al. (2004). "Expression and localisation of matrix metalloproteinases and their natural inhibitors in fistulae of patients iwth Crohn's disease." Gut **53**: 701-709.

Klein, G., E. Vellenga, et al. (2004). "The possible role of matrix metalloproteinase (MMP)-2 and MMP-9 in cancer, e.g. acute leukemia." Crit. Rev. Oncol. Hematol. **50**(2): 87-100.

Klotz, U. and M. Schwab (2005). "Topical delivery of therapeutic agents in the treatment of inflmmatory bowel disease." Adv. Drug Deliv. Rev **57**: 267-279.

Knäuper, V., C. López-Otin, et al. (1996). "Biochemical characterization of human collagenase-3." J. Biol. Chem. **271**(3): 1544-1550.

Knäuper, V., H. Will, et al. (1996). "Cellular mechanisms for human procollagenase-3 (MMP-13) activation. Evidence that MT1-MMP (MMP-14) and gelatinase A (MMP-2) are able to generate active enzyme." J. Biol. Chem. **271**(29): 17124-17131.

Knauper, V., A. J. Docherty, et al. (1997). "Analysis of the contribution of the hinge region of human neutrophil collagenase (HNC, MMP-8) to stability and collagenolytic activity by alanine scanning mutagenesis." FEBS Lett. **405**(1): 60-64.

Knauper, V. and G. Murphy (1998). "Membrane-type matrix metalloproteinases and cell surface-associated activation cascades for matrix metalloproteinases." Matrix Metalloproteinases: 199-218.

Knight, C. G., F. Willenbrock, et al. (1992). "A novel coumarin-labelled peptide for sensitive continuous assays of the matrix metalloproteinases." FEBS Lett. **296**(3): 263-266.

Knott, A. B. and E. Bossy-Wetzel (2009). "Nitric oxide in health and disease of the nervous system." Antioxid. Redox Signal. **11**: 541-554.

Kottirsch, G., G. Koch, et al. (2002). "β-Aryl-succinic acid hydroxamates as dual inhibitors of marix metalloproteinases and tumor necrosis factor alpha converting enzyme." J. Med. Chem. **45**: 2289-2293.

Kowenz-Leutz, E. and A. Leutz (1999). "A C/EBPβ isoform recruits the SWI/SNF complex to activate myeloid genes." Mol. Cell **4**(5): 735-743.

Krahl, M. E. (1940). "The effect of variation in ionic strength and temperature on the apparent dissociation constant of thirty substituted barbituric acids." J. Phys. Chem. **44**(4): 449-463.

Krampert, M., W. Bloch, et al. (2004). "Activities of the matrix metalloproteinase stromelysin-2 (MMP-10) in matrix degradation and keratinocyte organization in wounded skin." Mol. Biol. Cell. **15**: 5242-5254.

Kuntz, I. D., J. M. Blaney, et al. (1982). "A geometric approach to macromolecule-ligand interactions." J. Mol. Biol. **161**: 269-288.

Lark, M. W., E. Bayne, et al. (1999). Role of stromelysin-1 in cartilage metabolism. Metalloproteinases as targets for anti-inflammatory drugs. K. M. K. Bottomely, D. Bradshaw and J. S. Nixon. Welwyn Carden City, Birkhauser verlag.

Leco, K. J., P. Waterhouse, et al. (2001). "Spontaneous air space enlargement in the lungs of mice lacking tissue inhibitor of metalloproteinases-3 (TIMP-3)." J. Clin. Invest. **108**(6): 817-829.

Lee, M. H., M. Rapti, et al. (2003). "Unveiling the surface epitopes that render tissue inhibitor of metalloproteinase-1 inactive against membrane type 1 matrix metalloproteinase." J. Bio. Chem. **278**: 40224-40230.

Lemaitre, V. and J. D'Armiento (2006). "Matrix metalloproteinases in development and disease." Birth. Defects Res. C. Embryo. Today **78**(1): 1-10.

Leontovich, A., J. Zhang, et al. (2000). "A novel hyda matix metalloproteinase (HMMP) funcitions in extracellular matrix degradation, morphogenesis and the maintenance of differentiated cells in the foot process. ." Development **127**: 907-920.

Lepage, T. and C. Gache (1990). "Early expression of a collagenase-like hatching enzyme gene in the sea urchin embryo." EMBO J. **9**: 3003-3012.

Levin, J. I., M. T. Du, et al. (2001). "The discovery of anthranilic acid-based MMP inhibitors. Part 1: SAR of the 3 position." Bioorg. Med. Chem. Lett. **11**: 235-238.

Li, F., Q. Wang, et al. (2003). "Microwave-assisted synthesis of diaryl ethers without catalyst." Org. Lett. **5**(12): 2169-2171.

Liabakk, N. B., I. Talbot, et al. (1996). "Matrix metalloprotease 2 (MMP-2) and matrix metalloprotease 9 (MMP-9) type IV collagenases in colorectal cancer." Cancer Research **56**(1): 190-196.

Libra, M., A. Scalisi, et al. (2009). "Uterine cervical carcinoma: Role of matrix metalloproteinases." Int. J. Oncol. **34**: 897-903.

Liu, G., X. Zhang, et al. (2005). "Expression of matrix metalloproteinase-26 (MMP-26) mRNA in mouse uterus during the estrous cycle and early pregnancy." Life Sciences **77**(26): 3355-3365.

Lohi, J. and J. Keski-Oja (1995). "Calcium ionophores decrease pericellular gelatinolytic activity via inhibition of 92-kDa gelatinase expression and decrease of 72-kDa gelatinase activation." J. Bio. Chem. **270**(29): 17602-17609.

Lohi, J., C. L. Wilson, et al. (2001). "Epilysin, a novel human matrix metalloproteinase (MMP-28) expressed in testis and keratinocytes and in response to injury." J. Bio. Chem. **276**(13): 10134-10144.

Lohmander, L. S., L. A. Hoerrner, et al. (1993). "Metalloproteinases, tissue inhibitor and proteoglycan fragments in knee synovial fluid in human osteoarthritis " Arithritis Rheum. **36**: 181-189.

Lohse, M. J. (2010). "Dimerization in GPCR mobility and signaling." Curr. Opin. Pharmacol. **10**: 53-58.

Lopez-Figueroa, M. O. and M. Moller (1996). "Nitric oxide synthase in the pineal gland." Histol. Histopathol. **11**(4): 1089-1100.

Loyer, X., C. Heymes, et al. (2008). "Constitutive nitric oxide synthases in the heart from hypertrophy to failure." Clin. Exp. Pharmacol. Physiol. **35**: 483-488.

Lund, L., J. Romer, et al. (1996). "Two distinct phases of apoptosis in mammary gland involution: proteinase-independent and -dependent pathways." Development **23**: 2123-2130.

lundberg, J. O., E. Weitzberg, et al. (2008). "The nitrate-nitrite-nitric oxide pathway in physiology and therapeutics." Nat. Rev. Drug. Discov. **7**: 156-167.

Luttun, A., E. Lutgens, et al. (2004). "Loss of Matrix Metalloproteinase-9 or Matrix Metalloproteinase-12 Protects Apolipoprotein E-Deficient Mice Against Atherosclerotic Media Destruction but Differentially Affects Plaque Growth." Circulation **109**(11): 1408-1414.

Mañes, S., E. Mira, et al. (1997). "Identification of insulin-like growth factor-binding protein-1 as a potential physiological substrate for human stromelysin-3." J. Biol. Chem. **272**(41): 25706-25712.

Macpherson, L., E. K. Bayburt, et al. (1997). "Discovery of CGS27023A, a non-peptidic, ptoent, and orally active stromelysin inhibitor that blocks cartilaged degradation in rabbits." J. Med. Chem. **40**: 2525-2532.

Maidement, J., D. Moore, et al. (1999). "Matrix metalloproteinases homologues form Arabidopsis thaliana: expression and activity." J. Bio. Chem. **274**: 34706-34710.

Malemud, C. J. (2006). "Matrix metalloproteinases: role in skeltal development and growth plate disorders." Front Biosci. **11**: 1702-1715.

Malla, N., s. Sjoli, et al. (2008). "Biological patholbiolgical functions of gelatinase." Connect. Tissue Res. **49**: 180-184.

Mallei, A., S. A. Aden, et al. (2005). "The nitrosteroid NCX 1015, a prednisolone derivative, improves recovery of function in rats after spinal cord injury." Brain Res. **1062**(1-2): 16-25.

Maragos, C. M., D. Morley, et al. (1991). "Complexes of .NO with nucleophiles as agents for the controlled biological release of nitric oxide. Vasorelaxant effects." J. Med. Chem. **34**(11): 3242-3247.

Marchenko, G. N., N. D. Marchenko, et al. (2003). "The structure and regulation of the human and mouse matrix metalloproteinase-21 gene and protein." Biochem. J. **372**(Pt 2): 503-515.

Martin, M. D. and L. M. Matrisian (2007). "The other side of MMPs: protective roles in tumor progression." Cancer Metastasis Rev. **26**(3-4): 717-724.

Marzinzig, M., A. K. Nussler, et al. (1997). "Improved methods to measure end products of nitric oxide in biological fluids: nitrite, nitrate, and S-Nitrosothiols." Nitric Oxide **1**: 177-189.

Matsumura, S. I., S. Iwanaga, et al. (2005). "Targeted deletion or pharmacological inhibition of MMP-2 prevents cardiac rupture after myocardial infarction in mice." J. Clin. Invest. **115**(3): 599-609.

Matziari, M., V. Dive, et al. (2007). "Matrix metalloproteinase 11 (MMP-11; stromelysin-3) and synthetic inhibitors." Med. Res. Rev. **27**(4): 528-552.

McCallum, K. S. and W. D. Emmons (1956). "The dssociation constants and infrared spectra of some nitratoacids." J. Org. Chem. **21**: 367-368.

McMillan, W. D., N. A. Tamarina, et al. (1997). "Size matters: the relationship between MMP-9 expression and aortic diameter." Circulation **96**: 2228-2232.

Medina, C. and M. W. Radomski (2006). "Role of matrix metalloproteinases in intestinal inflammation." J. Pharmacol. Exp. Ther. **318**: 933-938.

Medina, C., S. Videla, et al. (2001). "Therapeutic effect of phenantrolin in two rat models of inflammatory bowel disease." Scand. J. Gastroenterol. **36**: 1314-1319.

Meijer, M. J., M. A. Mieremet-Ooms, et al. (2007). "Increased mucosal matrix metalloproteinase-1, -2, -3, and -9 activity in patients iwth inflammatory bowel disease and th relation iwth Crohn's disease phenotype." Dig. Liver Dis. **39**: 733-739.

Menchen, L., I. Marin-Jimenez, et al. (2009). "Matrix metalloproteinase 9 is involved in Crohn's disease-associated platelet hyperactivation through the release of soluble CD40 ligand." Gut **58**: 920-928.

Mertz, P. M., D. L. Dewitt, et al. (1994). "Inerleukin 10 suppression of monocyte prostaglandin H synthase-2. Mechanism of inhibtion of postaglandin-dependent matrix metalloproteinase production." J. Biol. Chem. **269**(33): 21322-21329.

Milar, A. W., P. D. Brown, et al. (1998). "Results of single and repeat dose studies of the oral matrix metalloproteinase inhibitor maritmastat in healthy male volunteers." Br. J. Clin. Pharmacol. **45**: 21-26.

Miranda, K. M., M. G. Espey, et al. (2001). "A rapid, simple spectrophotometric method for simulataneous detection of nitrate and nitrite." Nitric Oxide **5**: 62-71.

Mitchell, P. G., H. A. Magna, et al. (1996). "Cloning, expression, and type-II collagenolytic acitivity of matrix metalloproteinase-13 from human osteoarthritic cartilage." J. Clin. Invest. **97**: 761-768.

Moncada, S. and A. Higgs (1993). "The L-arginine-nitiric oxide pathway." N. Engl. J. Med. **329**: 2002-2012.

Monovich, L. G., R. A. Tommasi, et al. (2009). "Discovery of potent, selective, and orally active carboxylic acid based inhibitors of matrix metalloproteinase-13." J. Med. Chem. **52**: 3523-3538.

Montogery, A. M., H. Sabzevari, et al. (1993). "Production and regulation of gelatinase B by human T-cells." Biochim. Biophys. Acta. **1176**(3): 265-268.

Mook, O. R. F., W. M. Frederiks, et al. (2004). "The role of gelatinases in colorectal cancer progression and metastasis." Biochim. Biophys. Acta. **1705**: 69-89.

Morgunova, E., A. Tuuttila, et al. (1999). "Structure of Human Pro-Matrix Metalloproteinase-2: Activation Mechanism Revealed." Science **284**(5420): 1667-1670.

Morris, G. M., D. S. Goodsell, et al. (1998). "Automated docking using a Lamarckian genetic algorithm and an empirical binding free energy function." J. Comput. Chem. **19**(14): 1639-1662.

Mosmann, T. (1983). "Rapid colorimetric assay for cellular growth and survial: Application to proliferation and cytotoxicity assays." J Immunol. Methods **65**: 55-63.

Mosmann, T. (1983). "Rapid colorimetric assay for cellular growth and survival: Application to proliferation and cytotoxicity assays." Journal of Immunological Methods **65**(1-2): 55-63.

Mott, J. D., C. L. Thomas, et al. (2000). "Post-translational proteolytic processing of procollagen C-terminal proteinase enhancer releases a metalloproteinase inhibitor." J. Bio. Chem. **275**: 1384-1390.

Munaut, C., T. Salonurmi, et al. (1999). "Murine matrix metalloproteinase 9 gene. 5'-Upstream region contains cis- acting elements for expression in osteoclasts and migrating keratinocytes in transgenic mice." J. Biol. Chem. **274**(9): 5588-5596.

Murphy, A. J., A. Houbrechts, et al. (1991). "The N-terminal domain of tissue inhibitor of metalloproteinases retains metalloproteinase inhibitory activity." Biochemistry **30**: 8097-8102.

Murphy, G., J. A. Allan, et al. (1992). "The role of the C-terminal domain in collagenase and stromelysin specificity." J. Bio. Chem. **267**(14): 9612-9618.

Murphy, G. and H. Nagase (2008). "Progress in matrix metalloproteinase research." Mol. Aspects Med. **29**(5): 290-308.

Myers, G. S. and G. F. Wright (1948). "Catalysed hydrolysis of amines V. The nitration of alphatic dialkylcholoramines." Canad. J. Res., Sect. B **26**: 257-270.

Nabeshima, K., H. Iwaski, et al. (2006). "Emmprin (basigin/CD147): matrix metalloproteinase modulator and multifunctional cell recognition molecule that plays a critical role in cancer progression." Pathol. Int. **56**: 359-367.

Nagase, H. (1997). "Activation mechanisms of matrix metalloproteinases." Biol. Chem. **378**(3-4): 151-160.

Nagase, H. (1998). Stromelysin 1 and 2. Matrix metalloproteinases. W. C. Parks and R. P. Mecham. San Diego, Academic Press 43-84.

Nagase, H., J. J. Enghild, et al. (1990). "Stepwise activation mechanism of the precursor of matrix metalloproteinase 3 (stromelysin) by proteinases and (4-aminophenyl)mercuric acetate." Biochemistry **29**(24): 5783-5789.

Nagase, H., R. Visse, et al. (2006). "Structure and function of matrix metalloproteinases and TIMPs." Cardiovasc. Res. **69**: 562-573.

Nagase, H. and J. F. Woessner Jr (1999). "Matrix metalloproteinases." J. Biol. Chem. **274**(31): 21491-21494.

Naglich, J. G., M. Jure-Kunkel, et al. (2001). "Inhibition of angiogenesis and metastasis in two murine models by the matrix metalloproteinase inhibitor, BMS-275291." Cancer Res. **61**: 8480-8485.

Naito, Y. and T. Yoshikawa (2005). "Role of matrix metalloproteinases in inflammatory bowel disease." Mol. Aspects. Med. **26**: 379-390.

Nakajima, F., D. R. Welch, et al. (1993). "Serum and plasma Mr 92,000 progelatinse levels correlated with spanotaneous metastasis of rat 13762NF mammary adenocarcinoma." Cancer Res. **53**: 5802-5807.

Natchus, M. G., R. G. Bookland, et al. (2000). "Development of new hydroxamate matrix metalloproteinase inhibitors derived from functionalized 4-aminoprolines." J. Med. Chem. **43**: 4948-4963.

Natchus, M. G., R. G. Bookland, et al. (2001). "Development of new carboxylic acid-based MMP inhibitors derived from functionalized propargylglycines." J. Med. Chem. **44**: 1060-1071.

Nathan, c. f. and J. B. Hibbs (1991). "Role of nitrix oxide synthesis in macrophage antimicrobial activity." Curr. Opin. Immunol. **3**: 65-70.

Nicholson, R., G. Murphy, et al. (1989). "Human and rat malignant-tumor-associated mRNAs encode stromelysin-like metalloproteinases." Biochemistry **33**: 2089-2095.

Nicolotti, O., T. F. Miscioscia, et al. (2007). "Screening of matrix metalloproteinases available from the protein data bank: insights into bilogical functions, domain organization, and zinc binding groups." J. Chem. Inf. Model. **47**: 2439-2448.

Nikkola, J., P. Vihinen, et al. (2005). "High serum levels of matrix metalloproteinase-9 and matrix metalloproteinase-1 are associated with rapid progession in patient with metastatic melanoma." Clin. Cancer Res. **11**: 5158-5166.

Noe, V., B. Fingleton, et al. (2001). "Release of an invasion promoter E-cadherin fragemnt by matrilysin and stromelysin-1." J. Cell Sci. **114**: 111-118.

Nossaman, V. E., B. D. Nossaman, et al. (2010). "Nitrates and nitrites in the treatment of iscemic cardiac diseases." Cardiol. Rev. **18**: 190-197.

Ohuchi, E., K. Imai, et al. (1997). "Membrane type 1 matrix metalloproteinase digests interstitial collagens and other extracellular matrix macromolecules." J. Biol. Chem. **272**(4): 2446-2451.

Okada, Y., E. J. Harris, et al. (1988). "The precursor of a metalloendopeptidase from human rheumatoid synovial fibroblasts: Purification and mechanisms of activation by endopeptidases and 4-aminophenylmercuric acetate." Biochem. J. **254**(3): 731-741.

Okamoto, T., T. Akaike, et al. (1997). "Activation of hman neutrophil procollagenase by nitrogen dioxide and peroxynitrite: a novel mechanism for procollagenase activation involving nitric oxide." Arch. Biochem. Biophys. **15**: 261-274.

Oltenfreiter, R., L. Staelens, et al. (2004). "New radioiodinated carboxylic and hydroxamic matrix metalloproteinase inhibitor tracers as potential tumor imaging agents." Nucl. Med. Biol **31**: 459-468.

Opedenakker, G., P. Van den Steen, et al. (2001). "Gelatinase B: a tuner and amplifier of immune functions." Trends Immunol. **22**: 571-579.

Overall, C. M. and C. López-Otín (2002). "Strategies for MMP inhibition in cancer: Innovations for the post-trial era." Nat. Rev. Cancer. **2**(9): 657-672.

Pacher, P., R. Schutz, et al. (2005). "Nitrosative stress and pharmacological modulation of heart failure." Trends Pharmacol. Sci. **26**(6): 302-310.

Palmer, R. M. J., A. G. Ferrige, et al. (1987). "Nitric oxide release accounts for the biological activity of endothelia-derived relaxing factor." Nature **327**: 524-526.

Pang, Y. P., P. Quiram, et al. (1996). "Highly potent, selective, and low cost bis-tetrahydroaminacrine inhibitors of acetylcholinesterase. Steps forward novel drugs for treating Alzheimer's disease." J. Bio. Chem. **271**: 23646-23649.

Parks, W. and S. Shapiro (2001). "Matrix metalloproteinase in lung biology." Respir. Res. **2**: 10-19.

Parsons, S. L., S. A. Watson, et al. (1998). "Gelatinase (MMP-2 and -9) expression in gastrointestinal malignancy." Br. J. Cancer **78**(11): 1495-1502.

Patel, M. I., J. Melrose, et al. (1996). "Increased synthesis of matrix metalloproteinases by aortic smoth muscle cells is implicated in the etiophathogenesis of abdominal aortic aneurysms." J. Vasc. Surg. **24**: 82-92.

Paul-Clark, M. J., F. Roviezzo, et al. (2003). "Glucocorticoid receptor nitration leads to enhanced anti-inflammatory effects of novel steroid ligands." J. Immunol. **171**(6): 3245-3252.

Paul, S. and M. Gupta (2004). "Zinc-catalyzed Williamson ether synthesis in the absence of base." Tetrahedron Lett. **45**: 8825-8829.

Pei, D. (1999). "CA-MMP: a matrix metalloproteinase with a novel cysteine array, but without the classic cysteine switch." FEBS Lett. **457**(2): 262-270.

Pei, D. and S. J. Weiss (1995). "Furin-dependent intracellular activation of the human stromelysin-3 zymogen." Nature **375**(6528): 244-247.

Pendas, A. M., V. Knauper, et al. (1997). "Identification and characterization of a novel human matrix metalloproteinase with unique structural characteristics, chromosomal location, and tissue distribution." J. Bio. Chem. **272**(7): 4281-4286.

Pender, S. L., C. Braegger, et al. (2003). "Matrxi metalloproteinases in necrotising enterocolitis." Pediatr. Res. **54**: 160-164.

Pepine, C. J. (2009). "The impact of nitric oxide in cardiovascular medicine: untapped potential utility." Am. J. Med. **122**: S10-S15.

Pikul, S., K. L. McDow Dunham, et al. (1998). "Discovery of potent, archiral matrix metalloproteinase inhibitors." J. Med. Chem. **41**: 3568-3571.

Pikul, S., K. L. McDow Dunham, et al. (1999). "Design and snthesis of phosphinamide-based hydroxamic acids as inhibitors of matrix metalloproteinases." J. Med. Chem. **42**: 87-94.

Pikul, S., N. E. Ohler, et al. (2001). "Potent and selective carboxylic acid-based inhibitors of matrix metalloproteinases." J. Med. Chem. **44**: 2499-2502.

Pilcher, B. K., B. D. Sudbeck, et al. (1998). "Collagenase-1 and collagen in epidermal repair." Arch. Dermatol. Res. **290 Suppl**: S37-46.

Pintucci, G., P.-J. Yu, et al. (2003). "Induction of stromelysin-1 (MMP-3) by fibroblast growth factor-2 (FGF-2) in FGF-$2^{-/-}$ microvascular endothelial cells requires prolonged activation of extracellular signal-regulated kinases-1 and -2 (ERK-1/2)." J. Cell. Biochem. **90**(5): 1015-1025.

Pirard, B. (2007). "Insight into the structural determinants for selective inhibition of matrix metalloproteinases." Drug Discov. Today **12**: 640-646.

Podolsky, D. K. (2002). "Inflammatory bowel disease." N. Engl. J. Med. **347**: 417-429.

Puente, X. S., A. M. Pendas, et al. (1996). "Molecular cloning of a novel membrane-type matrix metalloproteinase from a human breast carcinoma." Cancer Res. **56**(5): 944-949.

Ra, H. and W. C. Parks (2007). "Control of matrix metalloproteinse catalytic activity." Matrix Biol. **26**: 587-596.

Radomski, M. W., R. M. J. Palmer, et al. (1990). "Characterization of the L-arginine:nitric oxide pathway in human platelets." Br. J. Pharmacol. **101**: 325-328.

Raffetto, J. D. and R. A. Khalil (2008). "Matrix metalloproteinases and their inhibitors in vascular remodeling and vascular disease." Biochem. Pharmacol. **75**(2): 346-259.

Rao, B. G. (2005). "Recent developments in the design of specific matrix metalloproteinase inhibitors aided by structural and computational studies." Curr. Pharm. Des. **11**: 295-322.

Rath, H. C., M. Schultz, et al. (2001). "Different subsets of enteric bacteria induce and perpetuate experimental colitis in rats and mice." Infect. Immun. **69**(4): 2277-2285.

Ratzinger, G., P. Stoitzner, et al. (2002). "Matrix metalloproteinase 9 and 2 are necessay for the migration of langerhans cells and dermal dendritic cells from human and murine skin." J. Immunol. **168**: 4361-4371.

Ravi, A., P. Garg, et al. (2007). "Matrix metalloproteinases in inflammatory bowel disease: Boon or a bane." Inflamm. Bowel Dis. **13**(1): 97-107.

Reel, B., G. Oktay, et al. (2009). "MMP-2 and MMP-9 alteration in response to collaring in rabbits: the effects of endothelin recptor antagonism." J. Cardiovasc. Pharmacol. Ther. **14**(4): 292-301.

Reiter, L. A., K. D. Freeman-Cook, et al. (2006). "Potent, selective pyrimidinetrione-based inhibitors of MMP-13." Bioorg. Med. Chem. Lett. **16**: 5822-5826.

Rizzo, R. C., W. D.P., et al. (2000). "Validation of a model for the compliex of HIV-1 reverse transcriptase with sustiva through computation of resistance profiles." J. Am. Chem. Soc. **122**: 12898-12900.

Roda, A., A. f. Hofmann, et al. (1983). "The influence of bile salt structure on self-association in aqueous solutions." J. Biol. Chem. **258**: 6362-6370.

Rodriguez, J. A., J. Orbe, et al. (2008). "Metalloproteinases and atherothrombosis: MMP-10 mediates vascular remodeling promoted by inflammatory stimuli." Front Biosci. **13**(2916-2921).

Romanic, A. M., S. M. Harrison, et al. (2002). "Myocardial protection from ischemia/reperfusion injury by targeted deletion of matrix metalloproteinase-9." Cardiovasc. Res. **54**: 549-558.

Rosemurgy, A., J. Harris, et al. (1999). "Marimastat in patients with advanced pancreatic cancer: a dose finding study." Am. J. Clin. Oncol. **22**: 247-252.

Rossello, A., E. Nuti, et al. (2005). "A new development of matrix metalloproteinase inhibitors: twin hydroxamic acids as potent inhibitors of MMPs." Bioorg. Med. Chem. Lett. **15**: 2311-2314.

Rudek, M. A., J. Venitz, et al. (2002). "Matrix metalloproteinase inhibitors: do they have a place in anticancer therapy?" Pharmacotherapy **22**: 705-720.

Rudolph-Owen, L. A., D. L. Hulboy, et al. (1997). "Coordinate expression of matrix metalloproteinase family members in the uterus of normal, matrilysin-deficient, and stromelysin-1-deficient mice." Endocrinology **138**(11): 4902-4911.

Ryuichi, K., Y. Tamura, et al. (1999). "Homology modeling of gelatinases catalytic domains and docking simulations of novel sulfonamide inhibitors." J. Med. Chem. **42**: 1723-1738.

Sadowski, T., S. Dietrich, et al. (2003). "Matrix Metalloproteinase 19 Regulates Insulin-like Growth Factor-mediated Proliferation, Migration, and Adhesion in Human Keratinocytes through Proteolysis of Insulin-like Growth Factor Binding Protein-3." Mol. Biol. Cell. **14**(11): 4569-4580.

Sahara, M., T. Takahashi, et al. (2006). "New insights in the treatment strategy for pulmonary arterial hypertension." Cardiovasc. Drugs Ther. **20**: 377-386.

Sang, Q. A., M. Jia, et al. (2002). "New thiol and sulfodiimine metalloproteinase inhibitors and their effect on human microvascular endothelia cell growth." Biochem. Biophys. Res. Commun. **274**: 780-786.

Santana, A., C. Medina, et al. (2006). "Attenuation of dextran sodium sulphate induced colitis in matrix metalloproteinase-9 deficient mice." World J. Gastroenterol. **12**(40): 6464-6472.

Santos-Martínez, M. J., C. Medina, et al. (2007). "Role of metalloproteinases in platelet function." Thromb. Res. **121**(4): 535-542.

Sawa, M., T. Kiyoi, et al. (2002). "New type of metalloproteinase inhibitor: design and synthesis of new phosphonamide-base hydroxamic acids." J. Med. Chem. **45**: 919-929.

Sawa, M., T. Tsukamoto, et al. (2002). "new strategy for antedrug application: development of metalloproteinase inhibitors as antipsoriatic drugs." J. Med. Chem. **45**: 930-936.

Sawicki, G., E. Salas, et al. (1997). "Release of gelatinase A during platelet activation mediates aggregation." Nature **386**: 616-619.

Schönbeck, U., F. Mach, et al. (1998). "Generation of biologically active IL-1β by matrix metalloproteinases: A novel caspase-1-independent pathway of IL-1β processing." J. Immunol. **161**(7): 3340-3346.

Schwilden, H. and H. Stoeckel (1990). "Effective therapeutic infusions produced by closed-loop feedback control of methohexital adminstration during total intravenous anesthesia with fentanyl." Anesthesiology **73**: 225-229.

Sekine-Aizawa, Y., E. Hama, et al. (2001). "Matrix metalloproteinase (MMP) system in brain: Identification and characterization of brain-specific MMP highly expressed in cerebellum." Eur. J. Neurosci. **13**(5): 935-948.

Sekine-Aizawa, Y., E. Hama, et al. (2001). "Matrix metalloproteinase (MMP) system in brain: identification and characterization of brain-specific MMP highly expressed in cerebellum." Eur. J. Neurosci. **13**(5): 935-948.

Shapiro, S. and R. M. Senior (1998). Stromelysin 1 and 2. Matrix metalloproteinases. W. C. Parks and R. P. Mecham. San Diego, Academic Press 185-197.

Shapiro, S. D., D. K. Kobayashi, et al. (1993). "Cloning and characterization of a unique elastolytic metalloproteinase produced by human alveolar macrophages." J. Biol. Chem. **268**(32): 23824-23829.

Sheu, J. R., T. H. Fong, et al. (2004). "Expression of matrix metalloproteinasee-9 in human platelets: regulation of platelet activiation in vitro and in vivo studies." Br. J. Pharmacol. **143**: 193-201.

Shiomi, T., Y. Okada, et al. (2003). "Emphysematous changes are caused by degradation of type III collagen in transgenic mice expressing MMP-1." Exp. Lung. Res. **29**(1): 1-15.

Shipley, J. M., R. L. Wesselschmidt, et al. (1996). "Metalloelastase is required for macrophage-mediated proteolysis and matrix invasion in mice." Proc. Natl. Acad. Sci. U.S.A. **93**(9): 3942-3946.

Shofuda, K. I., H. Yasumitsu, et al. (1997). "Expression of three membrane-type matrix metalloproteinases (MTMMPs) in rat vascular smooth muscle cells and characterization of MT3-MMPs with and without transmembrane domain." J. Biol. Chem. **272**(15): 9749-9754.

Silence, J., F. Lupu, et al. (2001). "Persistence of atherosclerotic plaque but reduced aneurysm formation in mice with stromelysin-1 (MMP-3) gene inactivation." Arterioscler. Thromb. Vasc. Biol. **21**(9): 1440-1445.

Skiles, J. W., N. C. Gonnella, et al. (2004). "The design, structure, and clinical update of small molecular weight matrix metalloproteinase inhibitors." Curr. Med. Chem. **11**(22): 2911-2977.

Sneddon, P. and A. Gramaham (1992). "Role of nitric oxide in autonomic innervation of smoothe muscle." J. Auton. Pharmacol. **12**: 445-456.

Sodhi, C., W. Richardson, et al. (2008). "The development of animal model for the study of necrotizing enterocolitis." Dis Model Mech **1**: 94-98.

Sorsa, T., L. Tjaderhane, et al. (2006). "Matrix metalloproteinases: Contribution to pathogenesis, diagnosis and treatment of periodontal inflammation." Ann. Med. **38**: 306-321.

Southgate, K. M., M. Fisher, et al. (1996). "Upregulation of basement membrane-degrading metalloproteinase secretion after balloon injury of pig carotid arteries." Circ. Res. **79**: 1177-1187.

Spinale, F. G. (2002). "Matrix metalloproteinases: Regulation and dysregulation in the failing heart." Circ. Res. **90**(5): 520-530.

Springman, E. B., E. L. Angleton, et al. (1990). "Multiple modes of activation of latent human fibroblast collagenase: Evidence for the role of a Cys active-site zinc complex in latency and a 'cysteine switch' mechanism for activation

" Proc. Natl. Acad. Sci. U.S.A. **87**(1): 364-368.

Ståhle-Bäckdahl, M., B. Sandstedt, et al. (1997). "Collagenase-3 (MMP-13) is expressed during human fetal ossification and re-expressed in postnatal bone remodeling and in rheumatoid arthritis." Lab. Invest. **76**(5): 717-728.

Stallmach, A., C. C. Chan, et al. (2000). "Comparable expression of matrix metalloproteinases 1 and 2 in pouchitis and ulcerative colitis." Gut **47**(3): 415-422.

Stamenkovic, I. (2000). "Matrix metalloproteinases in tumor invasion and metastasis." Semin. Cancer Biol. **10**: 415-433.

Stamenkovic, I. (2003). "Extracellular matrix remodelling: the role of matrix metalloproteinases." J. Pathol. **200**: 448-464.

Sternlicht, M. D., A. Lochtest, et al. (1999). "The stromal proteinase MMP3/stromelysin-1 promotes mammary carcinogenesis." Cell **98**(2): 137-146.

Sternlicht, M. D. and Z. Werb (2001). "How matrix metalloproteinases regulate cell behavior." Annu. Rev. Cell Dev. Biol. **17**: 463-561.

Stetler-Stevenson, W. G. (1999). "Matrix metalloproteinases in angiogenesis: a moving target for therapeutic intervention." J. Clin. Invest. **103**: 1237-1241.

Stolow, M. A., D. D. Bauzon, et al. (1996). "Identification and characterization of a novel collagenase in Xenopus laevis: possible roles during frog development." Mol. Biol. Cell. **7**(10): 1471-1483.

Stracke, J. O., A. J. Fosang, et al. (2000). "Matrix metalloproteinases 19 and 20 cleave aggrecan and cartilage oligomeric matrix protein (COMP)." FEBS Lett. **478**(1-2): 52-56.

Stracke, J. O., M. Hutton, et al. (2000). "Biochemical characterization of the catalytic domain of human matrix metalloproteinase 19. Evidence for a role as a potent basement membrane degrading enzyme." J. Biol. Chem. **275**(20): 14809-14816.

Stricklin, G. P., E. A. Bauer, et al. (1977). "Human skin collagenase: isolation of precursor and active forms from both fibroblast and organ cultures." Biochemistry **16**: 1607-1615.

Su, C. G., X. Wen, et al. (1999). "A novel therapy for colitis utilzing PPAR-gamma ligands to inhibit the epithelial inflammatory response." J. Clin. Invest. **104**: 383-389.

Sugita, H., M. Kaneki, et al. (2010). "Nitric oxide inhibits the proliferation and invasion of pancreatic cancer cells through degradation of insulin recepotr substrate-1 protein." Mol. Cancer Res. **8**: 1152-1163.

Suzuki, K., J. J. Enghild, et al. (1990). "Mechanisms of activiation of tissue procollagenase by matrix metalloproteinase 3 (stromelysin)." Biochemistry **29**: 10261-10270.

Sykes, A. P., R. Bhogal, et al. (1999). "The effect of an inhibitor of matrix metalloproteinases on colonic inflammation in a trinitrobenzensulphonic acid rat model of inflammatroy bowel disease." Aliment. Pharmacol. Ther. **13**: 1535-1542.

Takahashi, H., T. Kimura, et al. (2008). "Joint Diseases and Matrix metalloproteinases: A Role for MMP-13." Curr. Pharm. Biotechnol. **9**: 47-54.

Takehara, M., T. Nishimura, et al. (2009). "Effect of claudin expression on paracelluar permeability, migration, and invasion of colonic cancer cells." Biol. Pharm. Bull. **32**(5): 825-831.

Tam, E. M., T. B. Moore, et al. (2004). "Characterization of the distinct collagen binding, helicase and cleavage mechanisms of matrix metalloproteinase 2 and 14 (gelatinase A and MT1-MMP): The differential roles of the MMP hemopexin C domains and the MMP-2 fibronectin type II modules in collagen triple helicase activities." J. Biol. Chem. **279**(41): 43336-43344.

Tamura, Y., F. Watanabe, et al. (1998). "Highly selective and orally active inhibitors of type IV collagenase (MMP-9 and MMP-2): N-sulfonylamino acid derivatives." J. Med. Chem. **41**: 640-649.

Thomas, G. (2007). Medicinal Chemistry: an Introduction. New York, John wiley & Sons Ltd.

Thomasset, N., A. Lochter, et al. (1998). "Expression of autoactivated stromelysin-1 in mammary glands of transgenic mice leads to a reactive stroma during early development." Am. J. Pathol. **153**(2): 457-467.

Tochowicz, A., K. Maskos, et al. (2007). "Crystal Structures of MMP-9 Complexes with Five Inhibitors: Contribution of the Flexible Arg424 Side-chain to Selectivity." J. Mol. Biol. **371**(4): 989-1006.

Tsuruo, T., H. Kawabata, et al. (1986). "Tumor-induced platalet aggregation and grwoth promoting factors as dterminats for successufl tumor metastasis." Clin. Exp. Metastasis. **4**: 25-33.

Tuillis, J. S., M. J. Laufersweiler, et al. (2001). "The Development of new carboxylic acid-based MMP inhibitors derived from a cyclohexylglycine scaffold." Bioorg. Med. Chem. Lett. **11**: 1975-1979.

Turpeenniemi-Hujanen, T. (2005). "Gelatinases (MMP-2 and MMP-9) and their natureal inhibitors as prognostic indicators in solid cancers." Biochimie **87**: 287-297.

Tyagi, S. C. and M. R. Hayden (2003). "Role of nitric oxide in matrix remodeling in diabetes and heart failure " Heart Fail Rev. **8**: 23-28.

Uria, J. and C. Lopez-Otin (2000). "Matrilysin-2, a new matrix metalloproteinase expressed in human tumors and showing the minimal domain orgainization reuired for secretion, latency and activity." Cancer Res. **60**: 4745-4751.

Van Meurs, J., P. Van Lent, et al. (1999). "Active matrix metalloproteinases are present in cartilage during immune complex-mediated arthritis: A pivotal role for stromelysin-1 in cartilage destruction." J. Immunol. **163**(10): 5633-5639.

Van Wart, H. E. and H. Birkedal-Hansen (1990). "The cysteine switch: A principle of regulation of metalloproteinase activity with potential applicability to the entire matrix metalloproteinase gene family." Proc. Natl. Acad. Sci. U.S.A. **87**(14): 5578-5582.

Velasco, G., A. M. Pendas, et al. (1999). "Cloning and characterization of human MMP-23, a new matrix metalloproteinase predominantly expressed in reproductive tissues and lacking conserved domains in other family members." J. Biol. Chem. **274**(8): 4570-4576.

Verma, R. P. and C. Hansch (2007). "Matrix metalloproteinases (MMPs): Chemical-biological functions and (Q)SARs." Bioorg. Med. Chem. **15**(6): 2223-2268.

Visse, R. and H. Nagase (2003). "Matrix metalloproteinases and tissue inhibitors of metalloproteinases: Structure, function, and biochemistry." Circ. Res. **92**(8): 827-839.

Vu, T. H., J. M. Shipley, et al. (1998). "MMP-9/gelatinase B is a key regulator of growth plate angiogenesis and apoptosis of hypetrophic chondrocytes." Cell **93**(3): 411-422.

Vu, T. H. and Z. Werb (1998). Gelatinase B: Structure, Regulation, and Function. Matrix Metalloproteinases. W. C. Parks and R. P. Mecham. San Diego, Academic Press**:** 115-148.

Wang, F., R. Zhang, et al. (2007). "Inhitory effects of nitric oxide on invasion of human cancer cells." Cancer Lett. **257**: 274-282.

Westermarck, J. and V. M. Kähäri (1999). "Regulation of matrix metalloproteinase expression in tumor invasion." FASEB J. **13**(8): 781-792.

Whitlock, G. A., K. N. Dack, et al. (2007). "A novel series of highly selective inhibitors of MMP-3." Bioorg. Med. Chem. Lett. **17**: 6750-6753.

Whittaker, M., C. D. Floyd, et al. (1999). "Design and therapeutic application of matrix metalloproteinase inhibitors." Chem. Rev. **99**: 2735-2776.

Williamson, R. A., F. A. Marston, et al. (1990). "Disulphide bond assignment in human tissue inhibitor of metalloproteinases (TIMP)." Biochem. J. **268**: 267-274.

Wilson, C. L., K. J. Heppner, et al. (1997). "Intestinal tumorigenesis is suppressed in mice lacking the metalloproteinase matrilysin." Proc. Natl. Acad. Sci. U.S.A. **94**(4): 1402-1407.

Wilson, C. L. and L. M. Matrisian (1998). Matrilysin. Matrix Metalloproteinases. W. C. Parks and R. P. Mecham. San Diego, Academic Press**:** 149-184.

Wink, D. A., L. A. Ridnour, et al. (2008). "The reemergence of nitric oxide and cancer." Nitric Oxide **19**: 65-67.

Wlodawer, A., A. Miller, et al. (1989). "Conserved folding in retroviral proteases crystal structure of synthetic HIV-1 protease." Science **245**: 616-621.

Woessner, J. F. and H. Nagase (2000). Matrix Metalloproteinases and TIMPS. New York, Oxford University Press.

Wolf, C., M. P. Chenard, et al. (1992). "Breast-cancer-associated stromelysin-3 gene is expressed in basal cell carcinoma and during cutaneous wound healing." J. Invest. Dermatol. **99**(6): 870-872.

Xi, L. L., J. Du, et al. (2009). "A combined molecular modeling study on gelatinases and their potent inhibitors " J. Comput. Chem. **31**(1): 24-42.

Xie, K., Z. Dong, et al. (1996). "Activation of nitric oxide synthase gene for inhibition of cancer metastasis." J. Leukoc. Biol. **59**(6): 797-803.

Yamamoto, H., A. Vinitketkumnuen, et al. (2004). "Association of matrilysin-2 (MMP-26) expression with tumor progression and activation of MMP-9 in esophageal squamous cell carcinoma." Carcinogenesis **25**(12): 2353-2360.

Yang, M. and M. Kurkinen (1998). "Cloning and characterization of a novel matrix metalloproteinase (MMP), CMMP, from chicken embryo fibroblasts. CMMP, xenopus XMMP, and human MMP19 have a conserved unique cysteine in the catalytic domain." J. Biol. Chem. **273**(28): 17893-17900.

Yao, W., Z. R. Wasserman, et al. (2001). "Design and synthesis of a series of (2R)-N^4-hydroxy-2-(3hydroxybenzyl)-N^1-[(1S,2R)-2-hydroxy-2,3-dihydro-

1H-inden-1-yl]butanediamide dervatives as potent selective, and orally bioavailable aggrecanse inhibitors." J. Med. Chem. **44**: 3347-3350.

Ye, S. (2000). "Polymorphism in matrix metalloproteinase gene promoters: Implication in regulation of gene expression and susceptibility of various diseases." Matrix Biol. **19**(7): 623-629.

Ying, L. and L. J. Hofseth (2007). "An emerging role for endothelial nitric oxide synthase in chronic inflammation and cancer." Cancer Res. **67**(4): 1407-1410.

Ying, N., S. kaestle, et al. (2009). "Inhaled nitric oxide versus aerosolized iloporst for the treatment of pulmonary hypertension with left heart diseases." Crit. Care Med. **37**: 980-986.

Yu, A. E., A. N. Murphy, et al. (1998). 72-kDa gelatinase (gelatinase A): Structure, activation, regulation, and substrate specificity. Matrix Metalloproteinases. W. C. Parks and R. P. Mecham**:** 85-113.

Yu, Q. and I. Stamenkovic (2000). "Cell sufrace-localized matrix metalloproteinase-9 proteolytically activiates TGF-β and promotes tumor invasion and angiogenesis." Genes Dev. **14**: 163-176.

Zervos, E. E., A. E. Shafii, et al. (1999). "Matrix metalloproteinases inhibition suppresses MMP-2 activity and activation of PANC-1cells in vitro." J. Surg. Res **84**: 162-167.

Zhang, B., S. Ye, et al. (1999). "Functional polymorphism in the regulatory region of gelatinase B gene in relation to severity of coronary atherosclerosis." Circulation **99**(14): 1788-1794.

Zhang, X., H. M. Wang, et al. (2004). "Regulation of matrix metalloproteinases (MMPs) and their inhibitors (TIMPs) during mouse peri-implantation: role of nitric oxide." Placenta **25**(4): 243-252.

Zhou, Z., S. S. Apte, et al. (2000). "Impaired endochondral ossification and angiogenesis in mice deficient in membrane-type matrix metalloproteinase I." Proc. Natl. Acad. Sci. U.S.A. **97**(8): 4052-4057.

Zhu, X. W., L. A. Mulcahy, et al. (2008). "IL-17 expression by breast-caner-associated macrophages:IL-17 promotes invasiveness of breast cancer cell lines." Breast Cancer Res. **10**: R95.

Zucker, S., R. M. Lysik, et al. (1995). "Plasma assay of gelatinase B: tissue inhibitor of metalloproteinase complexes in cancer." Cancer **76**(4): 700-708.